सत्यमेव जयते

भारत मौसम विज्ञान विभाग

INDIA METEOROLOGICAL DEPARTMENT

आदित्यात् जायते वृष्टिः

Government of India
Ministry of Earth Sciences
India Meteorological Department

A Report on Numerical Weather Prediction Products For Sectoral Applications

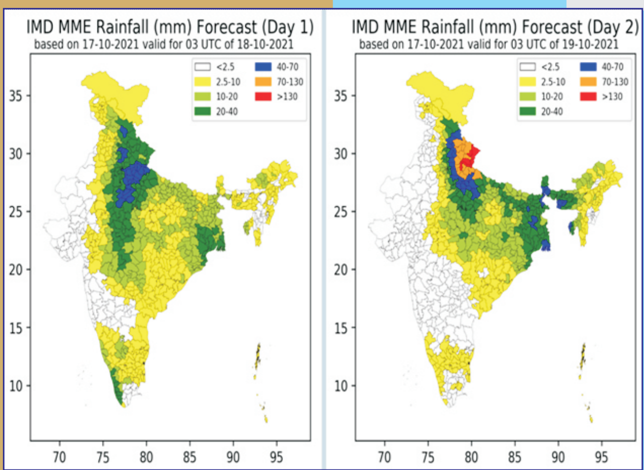

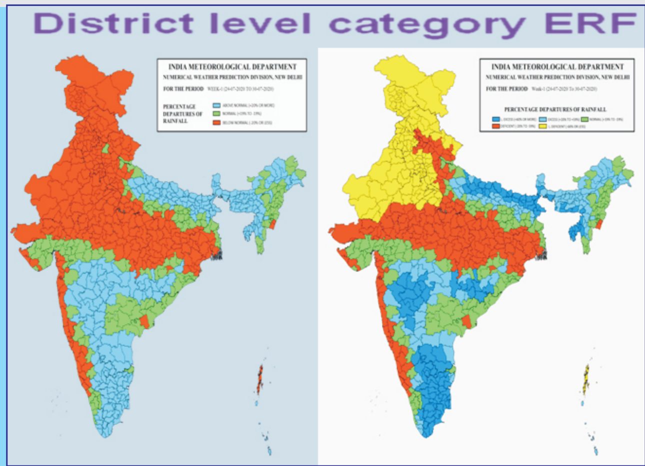

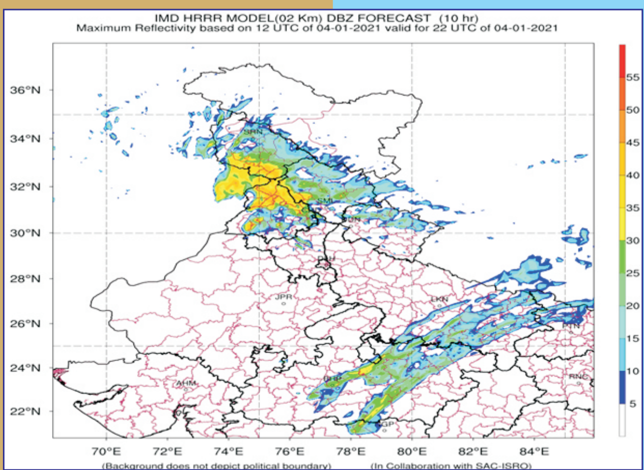

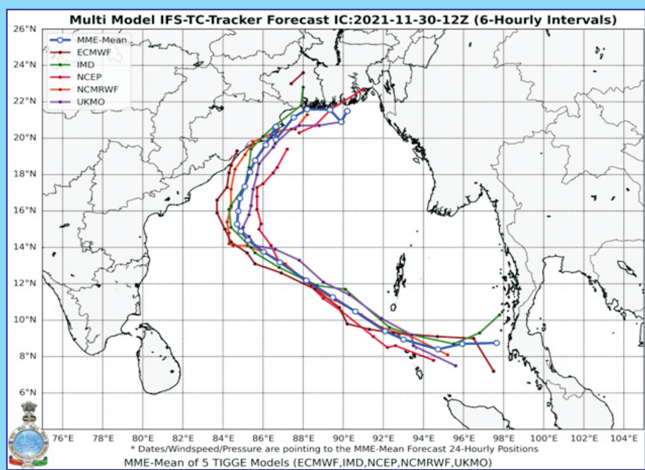

Numerical Weather Prediction Division
India Meteorological Department
New Delhi
January, 2022

Government of India
Ministry of Earth Sciences
India Meteorological Department

A Report
on
Numerical Weather Prediction Products For Sectoral Applications

Compiled & Edited by
Dr. D. R. Pattanaik

Numerical Weather Prediction Division
India Meteorological Department
New Delhi
January, 2022

PREFACE

There have been significant progress achieved in India in the field of Numerical Weather Prediction (NWP) in last one decade and a number of Operational/Research Centres and Universities/Institutions have played a significant role in different capacities in promoting NWP in India and contributing towards research and operation. With the availability of high power computing system by the Ministry of Earth Sciences (MoES), IMD is running high resolution meso-scale models, global models and coupled models for generating various NWP products in collaboration with Indian Institute of Tropical Meteorology (IITM), Pune and National Centre for Medium Range Weather Forecasting (NCMRWF) Noida for application in weather and climate services covering the time scale from Nowcasting to the extended range forecasting.

I am happy to note that the NWP division, IMD New Delhi has brought out a report highlighting various models products that are being generated operationally which includes, city forecasts, district level forecasts, forecasts for coastal and marine weather, High resolution rapid refresh (HRRR) products for Nowcasting to very short range forecasting, cyclone track and intensity forecast, meteorological subdivision level and district level extended range forecast etc for applications by users. IMD acknowledges the contributions and support provided by modelling groups from IITM Pune, NCMRW Noida, Indian National Centre for Ocean Information Services (INCOIS) in enhancing the modelling capability of IMD in running various models and generating various application products. IMD also acknowledges the support provided by SAC-Ahmedabad in implementing HRRR system at IMD.

I congratulate scientists in NWP division for bringing out this publication, which will be very useful for forecasting services of IMD.

(**Dr. M. Mohapatra**)
Director General of Meteorology
India Meteorological Department

Contents

CHAPTER 1

An Overview of the Evolution of NWP Activities of IMD Since its Beginning in 1958 till 2021

D. R. PATTANAIK

Head, Numerical Weather Prediction Division
India Meteorological Department, New Delhi – 110 003

1. Background

It is just more than a century ago, in 1904, when the Norwegian hydrodynamist V. Bjerknes suggested that the weather could be quantitatively predicted by applying a set of hydrodynamic and thermodynamic equations to carefully analysed initial atmospheric state. As analytical solutions are not feasible for the complex system of equations needed for weather prediction, we need to take recourse to numerical solutions.

The dawn of numerical weather prediction (NWP) in India Meteorological Department (IMD) may be traced back to 1958 when the first paper entitled **"Numerical prediction of the movement of Bay depressions"** was published in the Indian Journal of Meteorology and Geophysics authored by Dr. P. K. Das and his collaborator (Das and Bose, 1958). It may perhaps be mentioned that in 1957 Dr. P.K. Das himself had published a paper on application of numerical methods in forecasting. With this landmark effort, the early and mid-1970s witnessed significant developments in Objective Analysis of meteorological observations – which is a crucial component of numerical weather prediction (NWP). Short-range forecast experiments of 500 hPa flow patterns were performed over the Indian region using barotropic models, as well as the movement of wintertime western disturbances over the Asian subtropics. In addition, there were attempts to forecast the movement of monsoon depressions and tropical cyclones over the Indian Seas. Thus, the NWP related research began in India in late fifties and operationalisation of NWP got thrust in seventies. With advances in high-speed computing together with growing needs for information on both weather and climate variability on different time-scales, the scope of the NWP activities has expanded. Now in India, many operational centres, academic institutions and research laboratories are engaged in NWP for weather forecasts on different temporal and spatial scales. Besides running the model, some of the institutions are also conducting research on data assimilation based on 3Dimensional Variational Technique/ 4Dimensional Variational Technique. NWP, by regional, global and high-resolution models, has made significant progress in India in the last decade.

There has been significant progress achieved in India in the field of NWP in last sixty-five years (65) and a number of Operational/Research Centres and Universities/Institutions have played a significant role in different capacities in promoting NWP in India and contributing towards research and operationalisation. To name a few Andhra University, IIT Delhi, SAC Ahmedabad, IISc Bangalore, CMMACS Bangalore, NAL Bangalore, ISRO Bangalore, CUSAT Cochin, NIO GOA, NIOT Chennai, INCOIS Hyderabad, Indian Air Force, C-DAC Pune, SASE Chandigarh etc. are involved in NWP activities and contributed significantly for its progress. Many eminent scientists such as Late Prof. T. N. Krishnamurti, Prof. J. Shukla etc. have also helped in the growth of NWP in India. In 2008 IMD celebrated the 50 years of NWP to highlight the important landmark by bringing out a booklet on "Five Decades of NWP in India" (Tyagi and Pattanaik, 2008). The Booklet on "Five Decades of NWP in India" brought out by the IMD (Tyagi and

Pattanaik, 2008) has highlighted the role of various organizations and institutes in promoting NWP in enhancing the weather forecasting services of India.

The development of NWP activities in each of the institute has been highlighted in the book by different researchers (Tyagi and Pattanaik, 2008). During the initial period of NWP in IMD there was a major problem of availability of computer as well as the trained manpower. Dr. P. K. Das, who is known to be the father of NWP in India has nicely documented the beginning phase of NWP in the book by Tyagi and Pattanaik (2008). The main difficulty around that time was the lack of a suitable computer. The late Prof. P. C. Mahalanobis, who was then the Director of the Indian Statistical Institute at Kolkata, had acquired a computer named "Ural" from Russia. Prof. Mohalanobis was kind enough to permit Dr. Das group from IMD to try out and run Dr Das's own programmes on "Ural". At that time a number of young officers at the Meteorological Department had acquired good skill in computer programmes and were also to run these programmes by themselves. Of these young scientists, Dr. P. K. Das mentioned the names of M.C. Sinha, H. S. Bedi and B. L. Bose. They made significant contributions. Around that time a group of scientists, under Prof G. C. Asnani became interested in computer technology as applied to weather prediction. They also collaborated with the Delhi group. In this context, as mentioned by Dr. Das in his article, Dr. P. Koteswaram and Prof. P. R. Pisharoty, two senior officers of IMD along with Mr. Saradindu Basu who was then the Director General of Meteorology in India also provided valuable support to this group.

The evolution of NWP is closely linked to the development of computing infrastructure and resources. A major boost to NWP in India occurred with the establishment of the National Centre for Medium Range Weather Forecasting (NCMRWF) in 1988 after India purchased its first Super Computer CRAY-XMP14. The centre is also commemorated 20 years of NCMRWF in 2008. IMD, under its modernization programme of observational and forecasting system, has given priority for procurement of High Performance Computing System, which strengthened and enhanced NWP activities, especially in mesoscale data assimilation and high resolution local area modelling.

The NWP studies prior to the 1990s were focused mainly on short-range monsoon predictions and cyclone track predictions. However, with the advances in high-speed computing capabilities, together with growing needs for information on both weather and climate variability on different timescales, climate modelling research was initiated in the Indian Institute of Tropical Meteorology (IITM) from the early and mid-1990s onward. It is apt to mention here that, to give further thrust to this important subject, MoES has taken steps to establish a Climate Research Centre at IITM.

2. Decadal evolution of NWP in IMD (1950-2010)

The main mandates of NWP division are :

- To operationally run NWP models for different time scales (Nowcast to Extended range) on real time basis.
- Post processing & sector specific products generation for users (forecaster's) and their dissemination.
- To provide value added model guidance for weather forecasting activities.
- Research and development related to models and its post processing.
- To provide training to stake holders.

The evolution of NWP is closely linked to the development of computing infrastructure and resources. As you can see below the initial period was with lack of computer system available for NWP work in IMD.

(Migration of Computer Systems in IMD from beginning to 2015)

Decade of 1960s: First paper on NWP from India was published by Dr. P. K. Das on Application of Numerical Methods in NWP in 1957.

1961-1968 : As IMD had no computer of its own the scientists used to visit Planning commission and Delhi University, New Delhi to use the computer systems (IBM 1620 and ICL 1901)

1969-1980 : Formation of NWP group in IMD New Delhi in 1969. Acquired mainframe 3rd generation computer system IBM 360/44 with 512 KB memory was installed in IMD in 1973 and the commencement of operational NWP in IMD. This was followed by installation of a baroclinic primitive equation model. A significant development was the acquiring of a telecommunication computer in 1975, which facilitated receipt of GTS data. The NIC of Government of India had installed a Japanese NEC S-1000 computer system in their premises in CGO Complex, which was made available to IMD Scientists for research activities.

1981-1990 : A major boost to NWP in India occurred with the establishment of the NCMRWF in 1988 after India purchased its first Super Computer CRAY-XMP14.

1991-2000 : Operational implementation of Limited Area Analysis & Forecast Model (LAM) on cyber computing system and Quasi-Lagrangian Model (QLM) for cyclone track prediction on servers.

2001-2010 : Operational implementation of regional modelling system like MM5, WRF, ARPS.

2010 : IBM-P5 HPCS purchased and IMD implemented the first Global Forecast System (GFS) Model IMD-GFS (T-254) at a horizontal resolution of about 60 km. In the same time the Mesoscale model WRF is also operationally implemented.

2011 : The GFS model's resolution was increased to T382 (approximately 38 km).

3. Modern Era of NWP in India (2011-2021)

Ministry of Earth Sciences (MoES) implemented AADITYA (790 TF) in 2015. Subsequently the HPCS capability was further enhanced in 2018 with purchase of additional computing power as mentioned below.

- MoES recently installed two HPC (2018); One each at NCMRWF, Noida and IITM Pune with computing capacity of 6.8 Peta Flops.
- The MoES combined HPC capacity now is 8.0 Peta Flops and India is placed at 4th Position after Japan, UK, USA for dedicated HPC resources for Weather/Climate services.
- The NWP division at IMD, New Delhi uses these HPC capacities for its operational needs.

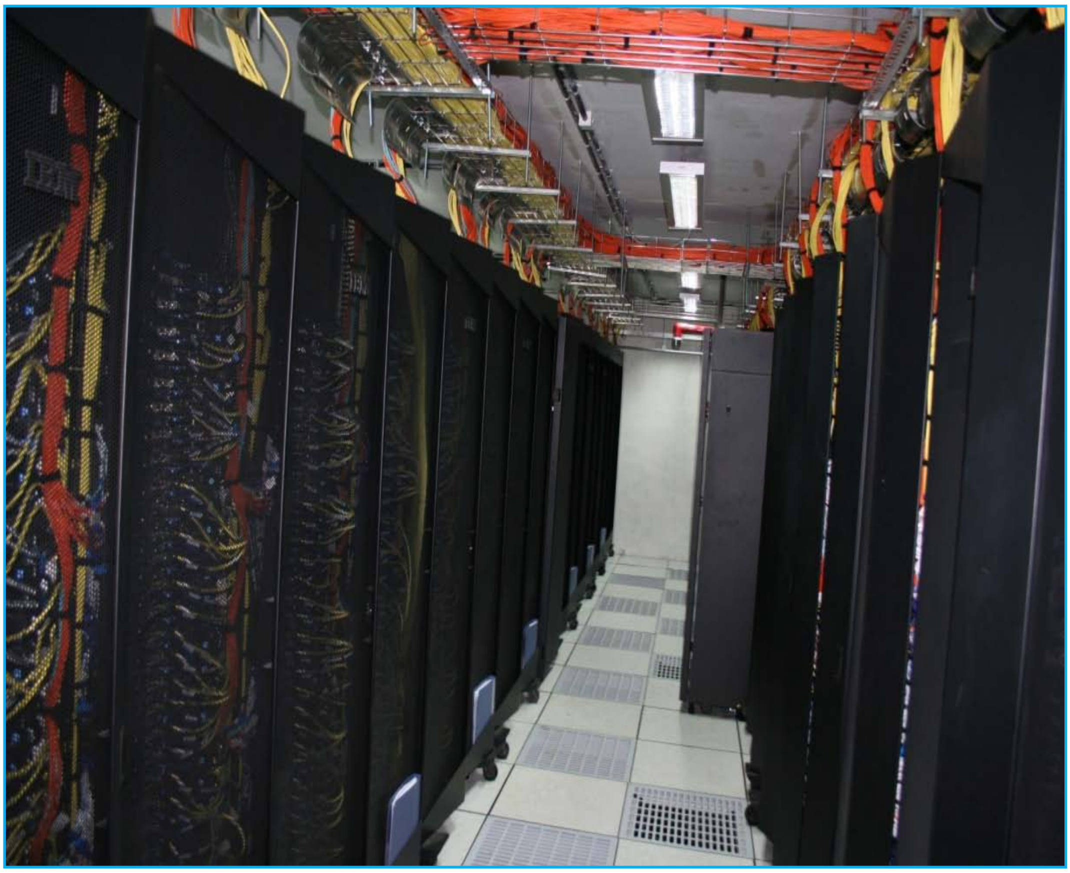

MoES AADITYA (790 TF) : 2015, IITM Pune

MIHIR HPC @NCMRWF, Noida

PRATYUSH HPC @ IITM, Pune

With the availability of high power computing resources by MoES, IMD gradually improved its modeling capability by running high resolution, regional, global and coupled models for catering the need of forecasting at different time scales.

IMD-GFS for Medium Range forecasting:-

The GFS model's resolution gradually increased from T382 running in IMD computer system to T574 (25 km) in 2012. Its resolution is further increased to T1534 (12 km) in 2016. At present the IMD-GFS global model is run with ~12 km horizontal resolution 2 times a day (00 and 12 UTC) to generate 10 days forecast and additional 2 times a day (06 and 18 UTC) up to 5 days.

IMD-GEFS for Medium Range forecasting:-

In 2018 IMD also implemented the IMD-GEFS global ensemble model (21 members) is run with ~12 km horizontal resolution 2 times a day to generate 10 days forecast. At present, it is the highest resolution global ensemble model operationally run in the world.

CFSv2 coupled model for Extended Range forecasting:-

IMD implemented CFsv2 coupled model for operational extended range forecasting in year 2016. This suite of multi-model is based on CFSv2 and GFS system. It is run operationally for 32 days based on every Wednesday initial condition with 16 ensemble members to forecast for 4 weeks.

Dynamical-Statistical modeling for Tropical Cyclone Forecasting:

The Cyclone Genesis Potential Parameter (GPP), Multi-Model Ensemble (MME) technique for cyclone track prediction and SCIP & decay models for tropical cyclone intensity forecast are run for to provide objective guidance for tropical cyclone forecasting.

IMD-HWRF-HYCOM/POM coupled model:-I

IMD-HWRF ocean coupled model is triple nested (18x6x2km) and run 4 times a day during cyclones over NIO to give 5 day forecast products for tropical cyclone predictions. It is the only regional ocean coupled modeling system being run operationally in India for Tropical Cyclone forecasting.

Regional Models for short range forecast:-

IMD-WRF model: IMD-WRF is a cloud resolving Mesoscale model, run at 3 km resolution four times a day covering the entire Indian region. Forecast products are available for next 3 days.

IMD-HRRR model for Nowcast Applications:-

The High Resolution Rapid Refresh Model is cloud resolving non- hydrostatic model which is run every hour at 2 km resolution giving forecast for next 12 hours using the observations available from Doppler Weather radars every 10-15 minutes.

Present Status (As on 2021):-

- High resolution (12 km) global model and global ensemble forecasting system for short to medium range forecast of weather.
- Coupled model for generation of operational extended range forecast.
- High resolution cloud resolving mesoscale forecasting system for nowcast/very short range.
- Specific models for tropical cyclone like HWRF Ocean coupled model,
- Multi-model ensemble/dynamical statistical model for cyclone track/intensity prediction.
- WRF-Polar model for Antarctica & WRF-HYSPLIT for trajectory forecasting.
- Generation of NWP based products for various sectoral applications.
- 2021: High Resolution Rapid Refresh (HRRR) model
- IN parallel to GFS framework Unified model frame work was adapted by NCMRWF
- All the above has been possible due to combined effort of IITM, NCMRWF and IMD

Evolution of NWP activities in IMD

1958:- Publication of first paper on NWP titled Numerical prediction of the movement of Bay depressions" by Dr. P. K. Das.

***1969:-* Initial NWP research group was setup.**

1970s:- Development of Objective Analysis of meteorological observations; crucial component of NWP.

***1980s:-* Attempts to forecast movement of monsoon depressions and tropical cyclones.**

1990s:- Operational implementation of Limited Area Analysis & Forecast Model (LAM) on cyber computing system and Quasi-Lagrangian Model (QLM) for cyclone track prediction on servers.

***2000s:-* Operational implementation of regional modeling system like MM5,WRF, ARPS.**

2010:- IBM-P5 HPCS purchased and Global Model IMD-GFS (T-254) and Mesoscale model WRF operationally implemented.

***2016:-* Operational implementation of coupled modeling system (CFSv2) with 16 ensemble members for real time extended range forecasts (upto 4 weeks).**

***2016:-* High resolution (12 km) Global Forecast System IMD-GFS model is operationalized.**

***2018:-* High resolution (12 km) Global Ensemble Forecast System IMD-GEFS model with 21 members ensemble is operationalized.**

2018:- HWRF modeling system coupled with POM-TC ocean model operationally implemented for Tropical Cyclone Forecasting.

2019: Another Ocean Model HYCOM coupled with HWRF in 2019.

2021: The High Resolution Rapid Refresh Model is cloud resolving non- hydrostatic model which is run every hour at 2 km resolution giving forecast for next 12 hours using the observations available from Doppler Weather radars every 10-15 minutes

References

Das, P. K., 1957, Experiments with numerical forecasting in India. *J. Met. Soc. of Japan*, Vol. 75th Anniversary, 275-279.

Das, P. K. and B. L. Bose, 1958, Numerical prediction of the movement of Bay depressions. *Ind. Journal of Met. Geophys*., **9**, 225-232.

Tyagi Ajit and B. R. Pattanaik, 2008, Five Decades of NWP in India. IMD, pp1-200.

CHAPTER 2

An assessment of operational GFS and GEFS Model forecasts during the south west monsoon 2021

C. J. JOHNY, V. R. DURAI, D. R. PATTANAIK and ANANDA K. DAS

Summary

Performance of GFS and GEFS model forecasts run operationally at IMD is assessed during South west monsoon season from June to September, 2021. Both models are of the resolution T1534 with 64 vertical levels. GEFS model has 21 ensemble members and ensemble mean forecast is used in this study. Model forecasts of wind, Geo-potential height and temperature at different atmospheric levels are assessed over different regions of the globe. Model forecasts of rainfall are investigated over Indian region. Models are able to forecast general characteristics of the rainfall. The ability of models to forecast extreme rainfall events is investigated separately. In the forecast of extreme rainfall events both the models show dry bias yet GFS model is able to capture more than 80 % of the extreme rainfall events in heavy rain or above category. In North East India wet bias is observed in rainfall forecasts of the both the models.

2.1. Introduction

India Meteorological Department (IMD) routinely provides forecasts in medium range scale using deterministic model Global forecast system (GFS) and ensemble model Global ensemble Forecast system (GEFS) with 21 ensemble members. GFS model is providing forecast at T1534L64 resolution for 10 days at 00 and 12 UTC and issuing forecast for 5 days at 06 and 18 UTC. GFS model initially implemented at IMD in 2010 with T382L64 resolution (Durai *et al.*, 2011). Model is subsequently upgraded to T574L64 in 2012 and upgraded to T1534L64 (~12 km) in 2016. In 2018 model upgraded from spectral based sigma framework to NOAA Environmental Modelling system (NEMS) framework with a modular structure for all NCEP models and associated changes in land surface, cumulus parameterization schemes and introduction of Near-Surface Sea Temperature (NSST) (White *et al.*, 2018). GEFS model operationally implemented at IMD in 2016 at T574L64 resolution and upgraded to T1534L64 resolution in 2018 (Deshpande *et al.*, 2020). At present GEFS model is providing forecast at T1534L64 resolution for 10 days at 00 and 12 UTC. In this ensemble system ensemble initial conditions are produced by combining Ensemble Kalman Filter (EnKF) based ensemble forecast from previous cycle and current cycle GFS analysis. Here ensemble forecast perturbations are created from EnKF ensembles and converted to analysis perturbation using Ensemble transform rescaling (ETR) techniques combining with GFS deterministic analysis from the current cycle. GEFS uses different set of EnkF ensembles in the Global data assimilation system (GDAS)at 00 and 12 UTC for computing forecast perturbations. At 00 UTC 1-20 ensemble members of GDAS system and at 12 UTC 41-60 ensemble members of GDAS system is used in creating initial condition for GEFS. The details of the GEFS system operational at IMD can be seen at Deshpande *et al.* (2020). In representing GEFS forecasts, ensemble mean of the forecasts are used.

GFS model uses initial conditions created from GDAS operational at National Centre for Medium range Forecasting (NCMRWF) in providing forecasts (Prasad *et al.*, 2021). GFS data assimilation system at NCMRWF employs hybrid 4D Ensemble Variational (EnsVar) assimilation system with 80 member EnKF ensembles. The system utilizes satellite observations and conventional observations from all major operational meteorological centers and it consist of large number of observations over India region. Observation pre-processing system at NCMRWF receives observations through different channels like EUMETCAST, GTS, DBNET and from NOAA (National Oceanographic and Atmospheric Administration), CMA (China Meteorological Administration) and KMA (Korea Meteorological Administration) through their respective data access servers and processed in near real time. GFS model version 14.1.0 operational at IMD uses two time level semi-implicit semi-Lagrangian dynamics in Gaussian grids with 3072×1536 grid points horizontally and 64 hybrid sigma pressure levels in vertical direction. Model employs near surface sea temperature (NSST) model for providing lower thermal boundary conditions during the integration of model forecasts. Model employs following schemes Zhao – Carr microphysics, Scale and Aerosol aware (SAS) deep and shallow convection, Modified rapid radiative transfer model (RRTMG) radiation, eddy diffusivity mass-flux (EDMF) based strongly unstable planetary boundary layer (PBL), eddy-diffusivity counter-gradient based weakly unstable planetary boundary layer (PBL) and NOAH land surface model for parameterizing various physical processes occurring in the sub-grid scales (Johny and Prasad, 2020).

Onset of the southwest monsoon over Kerala had taken place over Kerala on 3rd June and advanced to many parts of northern and central India by 13th June and further advanced to more parts of North Arabian Sea, Gujarat, Uttar Pradesh, Rajasthan by 19th June and there was no further advance of the system till July 11th. South west monsoon covered entire country by 13th July by advancing further to Delhi and remaining parts. In June mean rainfall over India was 110% of long period average. In June extreme rainfall events observed mostly over Konkan-Goa region and Karnataka and some extreme events are reported in Assam, Bihar, Orissa, East Uttar Pradesh and Uttarakhand. In July rainfall over the country was 93% of it's long period average (LPA). In July South peninsula received 126 % of LPA and all other regions it was below normal. In July also a number of extreme rain events occurred in Konkan-Goa region and Karnataka. There were occurrences of some extreme events in other part of country also. In August rainfall over the country was 76 % of LPA. In East and North East India rainfall was 103 % of LPA in August and it was below normal in other regions. In this month a number of extreme rainfall events occurred in East Rajasthan and West M.P region and Assam Meghalaya region. Delhi Received heavy rainfall of the amount in August 21. In September month cyclone Gulab caused heavy rainfall over coastal Andhra Pradesh, Telangana, Maharashtra and Gujarat. Depression systems also caused good amount of rainfall Odishaand Gujarat in September. In September rainfall over the country was 135 % of LPA and rainfall was above normal in all regions except in the region East and North East India. Central India received rainfall above 88 % than normal. In this study model performances in the months from June to September is investigated.

2.2. Configuration of GFS and GEFS models

GFS and GEFS model are operationally running in Mihir High Performance Computing System at NCMRWF. Both the modelsuse time step of450 seconds in dynamics computations and a time step of 225 seconds in physics computations. Models produce forecasts in NEMS format binary files in Gaussian grids and converted to grib2 format by employing post processing techniques. GFS model takes 60 minutes with 50 nodes for 10 day forecasts and GEFS takes 100 minutes with 488 nodes for 10 day forecasts. GFS based products are generated for meteorological subdivision level, state level and district level for various users. Location specific forecasts are generated for aviation sector and major cities. Probabilistic forecasts products are generated from GEFS in subdivision wise and district level and location specific EPSGRAM for major cities.

2.3. Verification of wind, temperature and Geo-potential height

Model forecasts of upper air fields at 850, 500 and 200 hPa are compared against respective analysis over different domains: (a) NH (20N-80N) (b) Tropics (20S-20N) and RSMC (30S-50N; 30-120E). Here we are presenting monthly statistics of model forecasts of temperature, wind and geo-potential height with respect to analysis for the monsoon months June, July, August and September. Table 2.1 shows RMS error of GEFS model forecasts for the month of June. It can be seen that all the three variables considered here has less error in tropics compared to the other two regions. Table 2.2 shows similar statistics for the GFS model. In GFS also model errors are less over tropics compared to other regions. Table 2.3 and 2.4 provide RMSE of GEFS and GFS forecasts for the month of July. Table 2.5 and 2.6 provide RMSE of GEFS and GFS forecasts for the month of August, Table 2.7 and 2.8 provide RMSE of GEFS and GFS forecasts for the month of September.

Table 2.1

Shows RMS error of upper air fields in GEFS model forecasts for the month of June

GEFS(JUN)	LEVEL	NH			Tropics			RSMC		
		WIND	Temp	HGT	WIND	Temp	HGT	WIND	Temp	HGT
Day1	850	2.281	0.781	5.685	1.884	0.6	3.597	2.308	0.724	5.373
	500	2.557	0.513	6.016	1.832	0.40	3.334	2.317	0.5	4.756
	200	3.224	0.657	7.525	3.84	0.457	6.04	3.807	0.53	7.477
Day3	850	3.835	1.355	13.35	2.839	0.89	6.316	3.255	1.02	8.067
	500	4.855	1.08	17.84	3.089	0.648	5.982	3.647	0.8	7.796
	200	6.305	1.535	22.08	6.141	0.719	11.46	5.852	0.91	14.77
Day5	850	5.331	2.019	24.30	3.451	1	8.059	3.892	1.25	10.75
	500	7.219	1.7	34.96	4.024	0.81	7.921	4.639	1	10.97
	200	9.733	2.44	43.49	7.74	0.825	14.70	7.584	1.15	20.57
Day8	850	6.725	2.91	37.03	4.117	1.21	9.53	4.559	1.65	13.4
	500	9.708	2.418	55.74	5.174	0.98	9.755	5.878	1.3	15.62
	200	11.33	2.82	72.8	8.373	0.916	18.22	9.27	1.5	29.64
Day10	850	7.227	3.357	43.22	4.402	1.31	10.38	4.847	1.82	16.15
	500	10.73	2.724	66.26	5.629	1.07	10.54	6.364	1.44	18.72
	200	15.65	3.712	87.9	10.19	0.928	19.63	10.10	1.64	34.23

Table 2.2

Shows RMS error of upper air fields in GFS model forecasts for the month of June

GFS(JUN)	LEVEL	NH			Tropics			RSMC		
		WIND	Temp	HGT	WIND	Temp	HGT	WIND	Temp	HGT
Day1	850	2.487	0.83	5.84	2.1	0.7	3.79	2.5	0.8	5.4
	500	2.9	0.6	6.14	2.1	0.5	3.3	2.6	0.5	4.37
	200	3.6	0.71	7.8	4.3	0.52	6.31	4.4	0.6	7.63
Day3	850	4.4	1.5	14	3.24	1	6.8	3.64	1.13	9
	500	5.6	1.2	19	3.5	0.7	6	4.1	0.9	8.1
	200	7.1	0.7	23	7	1	11	6.7	0.9	14
Day5	850	6.4	2.35	27.7	4	1.2	8.7	4.4	1.5	12.7
	500	8.7	2	39.6	4.6	0.9	8.1	5.3	1.1	12
	200	11	2.7	48.8	8.9	0.9	15	8.7	1.2	20
Day8	850	6.8	3.7	47	4.9	1.5	11	5.5	2	16.9
	500	12.43	3.1	69	6.2	1.1	10	7.1	1.5	18
	200	17.6	4.1	90	11	1	20	11	1.7	32
Day10	850	9.5	4.3	55	5.5	1.6	12.4	6	2.3	20
	500	14	3.5	84	7	1.3	12.5	7.8	1.8	22
	200	20	4.7	111	12.6	1	23	12.2	1.8	38

Table 2.3

Shows RMS error of upper air fields GEFS model forecasts for the month of July

GEFS (JULY)	LEVEL	NH			Tropics			RSMC		
		WIND	Temp	HGT	WIND	Temp	HGT	WIND	Temp	HGT
Day1	850	2.3	0.8	5.8	2	0.63	3.7	2.2	0.7	5.9
	500	2.4	0.5	6.737	1.9	0.4	3.4	2.2	0.49	5.2
	200	3.2	0.65	7.25	4.06	0.6	5.6	3.9	0.49	6.2
Day3	850	3.7	1.3	12.6	2.92	0.9	6.2	3.14	0.97	8.3
	500	4.4	1	15.9	3.3	0.64	6.1	3.5	0.78	8.1
	200	6.2	1.5	20.6	6.6	0.71	10.8	5.93	0.74	12.4
Day5	850	4.9	1.84	21	3.5	1.05	8.1	4	1.21	11
	500	6.3	1.5	28	4.24	0.81	7.8	4.3	0.98	11.6
	200	9	2.3	37	7.9	0.9	14	7.1	0.93	17
Day8	850	6.1	2.5	32	4.1	1.223	9.9	4.7	1.3	13.5
	500	8.3	2.1	46	5.3	1.03	9.7	5.3	1.2	14.6
	200	10.3	3.1	62	9.5	0.98	18.5	8.8	1	24
Day10	850	6.513	2.8	36	4.42	1.31	11.9	5.03	1.61	15.3
	500	9	2.3	53	5.9	1.114	12	5.7	1.33	17
	200	13.5	3.4	73	10.21	1.04	20	9.6	1.164	29.4

Table 2.4

Shows RMS error of upper air fields GFS model forecasts for the month of July

GEFS (JULY)	LEVEL	NH			Tropics			RSMC		
		WIND	Temp	HGT	WIND	Temp	HGT	WIND	Temp	HGT
Day1	850	2.4	0.83	6	2.1	0.7	3.9	2.5	0.7	5.8
	500	2.7	0.5	5.8	2.2	0.45	3.5	2.7	0.54	4.6
	200	3.6	0.7	7.6	4.6	0.5	6	4.8	0.6	6.6
Day3	850	4.3	1.5	13.9	3.2	1	6.8	3.8	1.1	9.4
	500	5.1	1.1	17	3.7	0.71	6.2	4.3	0.9	8.2
	200	7.1	1.6	22	7.5	0.77	10.6	7.4	0.84	12.5
Day5	850	5.9	2.1	24	4	1.2	8.6	4.5	1.4	13.2
	500	7.5	1.7	33	4.8	0.9	8	5.5	1	12
	200	10.5	2.5	42	9.1	0.9	14.4	8.6	1	18
Day8	850	7.8	3.1	39.7	4.8	1.4	10.7	5.4	1.7	16.1
	500	10.5	2.6	57	6.2	1.2	10.7	6.9	1.43	16.6
	200	15.6	3.7	77	11.3	1.1	20	10.6	1.3	27
Day10	850	8.6	3.7	47	5.4	1.6	13	5.9	2	18
	500	11.8	2.9	70	7.1	1.3	14	7.5	1.6	20
	200	17.65	4.2	95	12.51	1.2	23	12.2	1.4	35

Table 2.5

Shows RMS error of upper air fields GEFS model forecasts for the month of August

GEFS (AUG)	LEVEL	NH			Tropics			RSMC		
		WIND	Temp	HGT	WIND	Temp	HGT	WIND	Temp	HGT
Day1	850	2.19	0.74	5.57	1.93	0.62	3.67	2.23	0.67	5.55
	500	2.34	0.49	5.48	1.86	0.38	3.31	2.23	0.47	4.94
	200	3.15	0.65	7.23	3.97	0.43	5.12	3.94	0.45	6.05
Day3	850	3.65	1.24	12.64	2.95	0.9	6.66	3.22	0.95	8.22
	500	4.31	1	15.59	3.16	0.6	6.4	3.64	0.76	8.37
	200	6.24	1.5	21.27	6.43	0.64	9.3	6.14	0.7	11.97
Day5	850	5.03	1.79	22.1	3.59	1.06	8.14	3.78	1.15	9.86
	500	6.41	1.55	29.75	4.1	0.74	8.04	4.53	0.96	10.27
	200	9.7	2.37	41.21	7.75	0.75	12.33	7.25	0.86	17.77
Day8	850	6.44	2.58	35.04	4.23	1.26	9.49	4.36	1.46	13.15
	500	8.6	2.15	49.24	5.07	0.9	9.46	5.64	1.22	14.3
	200	13.26	3.18	69.3	8.96	0.85	15.32	8.95	1.1	20.2
Day10	850	6.86	2.9	39.77	4.49	1.35	10.74	4.66	1.65	15.42
	500	9.3	2.36	57.06	5.46	0.97	10.79	5.9	1.32	16.96
	200	14.54	3.44	80.76	9.5	0.89	16.99	9.6	1.14	32.96

Table 2.6

Shows RMS error of GFS model forecasts for the month of August

GFS (AUG)	LEVEL	NH			Tropics			RSMC		
		WIND	Temp	HGT	WIND	Temp	HGT	WIND	Temp	HGT
Day1	850	2.4	0.79	5.8	2.1	0.7	3.9	2.3	0.7	5.5
	500	2.6	0.53	5.5	2.1	0.43	3.4	2.5	0.5	4.4
	200	3.5	0.7	7.4	4.5	0.5	5.5	4.5	0.52	8.2
Day3	850	4.2	1.4	13	3.4	1	7.4	3.6	1	9.7
	500	5	1.1	16	3.6	0.7	6.6	4.1	0.8	8.6
	200	7	1.6	22	7.4	0.7	9.4	7	0.8	11.9
Day5	850	6	2.1	24	4.1	1.2	8.9	4.2	1.3	11.7
	500	7.6	1.8	33	4.7	0.85	8.5	5.1	1.1	11.1
	200	11	2.7	46	8.9	0.85	13	8.5	1	20
Day8	850	8.1	3.1	42	5	1.5	10	5.1	1.7	16
	500	10.8	2.7	60	6.1	1.1	10.9	6.6	1.4	16.3
	200	16.6	3.8	85	10.6	0.97	17	10.8	1.3	32
Day10	850	8.8	3.7	49	5.5	1.7	12	5.7	2	19
	500	12	3.1	72	6.9	1.2	12.8	7.3	1.6	20.3
	200	18.7	4.2	103	11.7	1	19.6	11.9	1.4	39.2

Table 2.7

Shows RMS error of GEFS model forecasts for the month of September

GEFS (SEP)	LEVEL	NH			Tropics			RSMC		
		WIND	Temp	HGT	WIND	Temp	HGT	WIND	Temp	HGT
Day1	850	2.137	0.695	5.46	1.94	0.6	3.79	2.15	0.654	5.15
	500	2.363	0.497	5.672	1.846	0.398	3.323	2.188	0.462	4.38
	200	3.147	0.624	7.23	3.803	0.424	5.348	3.846	0.446	5.82
Day3	850	3.676	1.205	12.98	2.96	0.859	6.8	3.145	0.909	8.2
	500	4.516	1.055	16.34	3.074	0.618	6.3	3.451	0.725	7.725
	200	6.21	1.391	22.01	6.01	0.725	9.9	5.93	0.692	11.40
Day5	850	5.23	1.82	24	3.566	1.01	8.7	3.836	1.145	10.8
	500	6.89	1.687	32.6	3.9	0.759	7.7	4.32	0.926	10.5
	200	9.29	2.211	43.6	7.4	0.766	13.44	7.06	0.845	16.48
Day8	850	6.79	2.663	38	4.2	1.225	9.9	4.45	1.1587	13
	500	9.4	2.436	54	4.9	0.935	8.86	5.3	1.176	13.77
	200	14	3.089	74	9.27	0.868	17.4	8.8	1.040	26
Day10	850	7.357	2.962	44	4.52	1.347	11.5	4.865	1.764	15.27
	500	10.36	2.72	63	5.4	1.007	10	5.739	1.32	15
	200	15.54	3.46	86	9.903	0.919	19	9.65	1.17	32

Table 2.8

Shows RMS error of GFS model forecasts for the month of July to September

GFS (SEP)	LEVEL	NH			Tropics			RSMC		
		WIND	Temp	HGT	WIND	Temp	HGT	WIND	Temp	HGT
Day1	850	2.3	0.72	5.6	2.16	0.67	4	2.3	0.67	5
	500	2.6	0.54	5.6	2.1	0.45	3.4	2.4	0.5	3.8
	200	3.5	0.664	7.5	4.3	0.49	5.7	4.3	0.5	6.2
Day3	850	4.2	1.34	14	3.36	0.9	7.6	3.5	1	9
	500	5.2	1.18	17	3.5	0.7	6.4	3.9	0.8	7.75
	200	7	1.5	23.38	6.9	0.715	9.5	6.8	0.754	11.46
Day5	850	6.3	2.1	27.9	4	1.2	9.5	4.3	1.3	12.4
	500	8.3	2	37	4.5	0.9	8	4.9	1	11
	200	11.6	2.5	49.5	8.5	0.84	13.3	8.2	0.9	16.7
Day8	850	8.3	3.2	44.6	4.9	1.5	11.8	5.2	1.8	15.6
	500	11.2	2.9	62	5.8	1.1	10	6.1	1.3	15
	200	16.6	3.6	84	11	0.97	19	10.5	1.2	28
Day10	850	9.3	3.7	54	5.4	1.6	12.9	5.8	2.1	17.9
	500	12.9	3.4	77	6.6	1.2	17	7	1.6	18.7
	200	19.6	4	107	11.9	1	22.6	11.9	1.3	36

In all the months errors are less in tropics and error in RSMC region is less than that in NH region. In all the fields forecast errors are increasing with lead time and GEFS model shows less error compared to GFS. There is not much monthly variation is observed in mean error characteristics. Observed error characteristics are in comparable range with the values reported for NCEP GFS.

In the lower atmosphere RMS error of wind forecasts in models vary between 2.5 m/s in day 1 forecast to 6 m/s in day 10 forecasts. In middle atmosphere RMSE in wind forecasts vary in the range 2.9 m/s (day1) to 14 m/s (day 10). In upper atmospheric wind forecasts RMSE vary between 4.8 m/s (day 1) to 20 m/s (day 10). In lower atmosphere RMSE in temperature forecasts vary from 0.8 K (day 1) to 2.3 K (day 10). In middle atmosphere RMS errors in temperature forecasts vary between 0.6 K in day 1 forecasts to 3.5 k in day10 forecasts. In upper atmosphere RMS error in temperature forecasts vary between 0.7 K in day1 forecasts to 4.7 K in day 10 forecasts. In lower atmosphere, error characteristics of temperature forecasts are similar all the regions in day 1 forecasts. It can be seen that error characteristics over NHX region show more increase compared to other regions with longer lead time. In day 10 forecast RMSE in NHX region is almost twice as that in RSMC region.

In the geo-potential height field more variation is observed in forecast errors characteristics between different regions, especially in forecasts of longer lead time in NHX region. In lower atmospheric levels RMSE varies between 6 m in day 1 forecast to 54 m in day 10 forecasts in NHX region, over tropics it varies between 3.9 m (day 1) to 13 m (day 10) and 5.9 m (day 1) to 20 m (day 10) over RSMC region. In middle atmosphere RMS errors of geo-potential height forecasts are in the range 6 m (day 1) to 84 m (day 10) in NHX region, vary between 3.5 m (day 1) -14m (day 10) in tropics and vary between 5.2 m to 22 m in RSMC region. In upper atmosphere NHX region RMSE vary in the range 7.5 m (day 1) -111 m (day 10) while tropics it vary in the range 6.3 m(day 1) -23 m (day 10) and in RSMC region in the range 8.2 m to 39m.

2.4. Rainfall Verification

Rainfall forecasts over Indian region is investigated with respect to 0.25degree gridded rainfall combining IMD rain gauge observations and satellite derived rainfall (Mitra *et al.*, 2009). Figure 2.1 shows cumulative rainfall for the month of June in observations and GFS model forecasts of lead times from day1 to day5. In this month major rainfall activity is seen over west coast of India, central India, north east region, Himalayan foothills region, Bihar and Bengal. In west coast cumulative rainfall in the range 100-150 cm is observed along Maharashtra coast. Cumulative rainfall in the range 30-50 cm is observed in the central parts of India. It can be seen that in day1 forecasts GFS rainfall over central India is mostly missing while better represented in forecasts of longer lead times. Rainfall over East U.P., Bihar and Bengal is not represented in model forecasts which are more evident in shorter lead times. Figure 2.2 shows mean difference between observation and GFS model forecasts (observation – model). Positive mean difference indicates regions where model under estimates and vice versa. It can be seen that model under estimates rainfall forecast in most of the region except in north east India and sea region of west coast. Figure 2.3 show root mean square error (RMSE) of GFS forecasts with respect to observations. It can be seen that RMS error shows same pattern in forecasts of all lead times while RMSE values are less over central India in 24hour forecasts. RMS error of 80-100 cm can be seen over Northern Bay of Bengal (BOB) in day1 to day 5 forecasts. Figure 2.4 shows cumulative rainfall in GEFS model forecasts and observations over Indian region. Model is able to represent general characteristics of rainfall over all regions. It can be seen that in GEFS rainfall forecast over East U.P., Bihar and Bengal are represented better on comparison to GFS. Rainfall over north east region is over estimated in both GFS and GEFS forecasts. Mean difference between rainfall observation and GEFS forecasts is given in Figure 2.5 and RMSE is shown in Figure 2.6 respectively. It can be seen that RMSE over central India is comparatively less in GEFS forecasts in comparison with GFS.

Cumulative rainfall observations for the month of July and corresponding GFS model forecasts are shown in Figure 2.7. It can be seen that in July month main rainfall activity is occurred over west coast, central India, Foot hills of Himalayas, east and north east part of India. In west coast especially over coastal

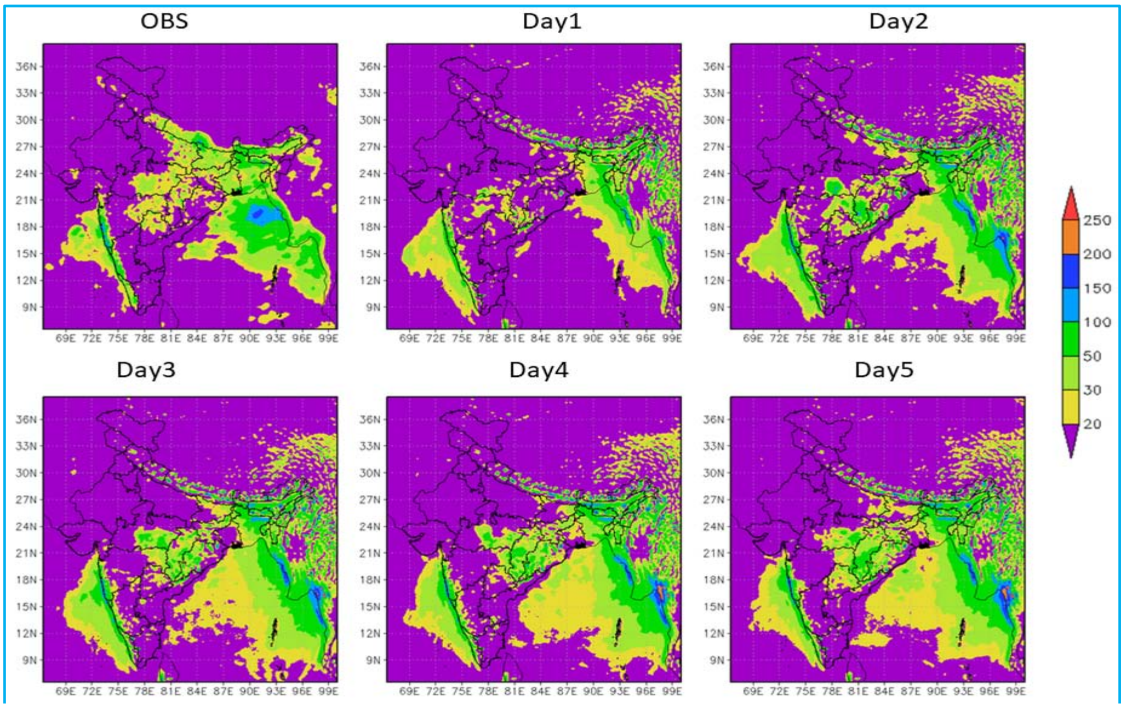

Fig. 2.1. Cumulative rainfall observed and GFS forecast for the month of June

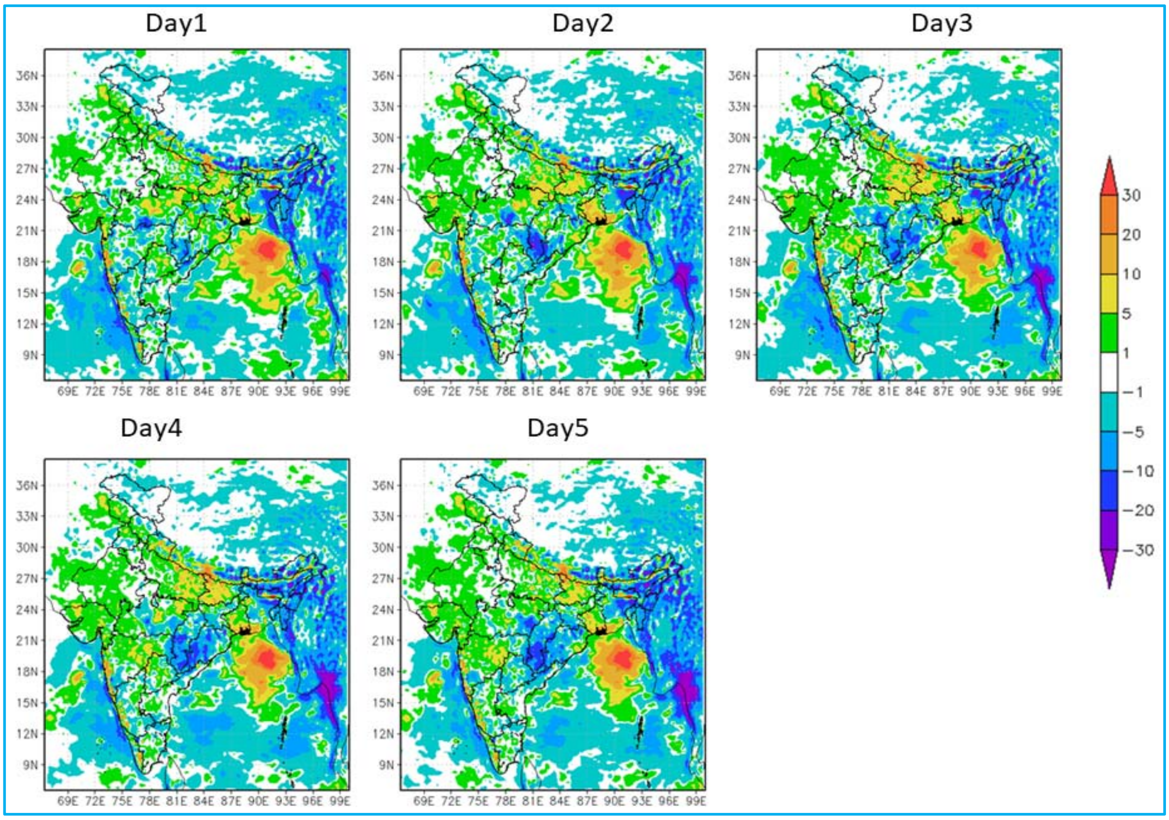

Fig.2.2. Mean difference between observed rainfall and GFS forecast (observed-model) for the month of June

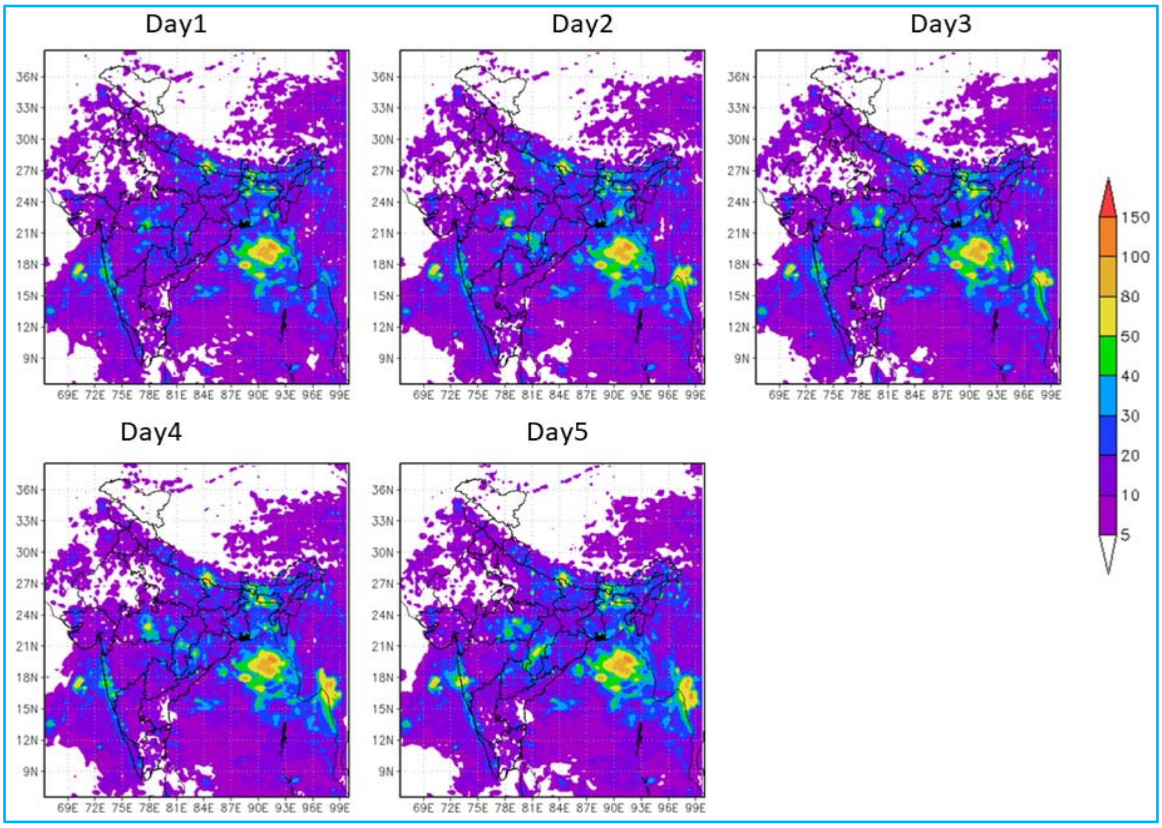

Fig. 2.3. RMS error in GFS forecasts with respect to observed rainfall

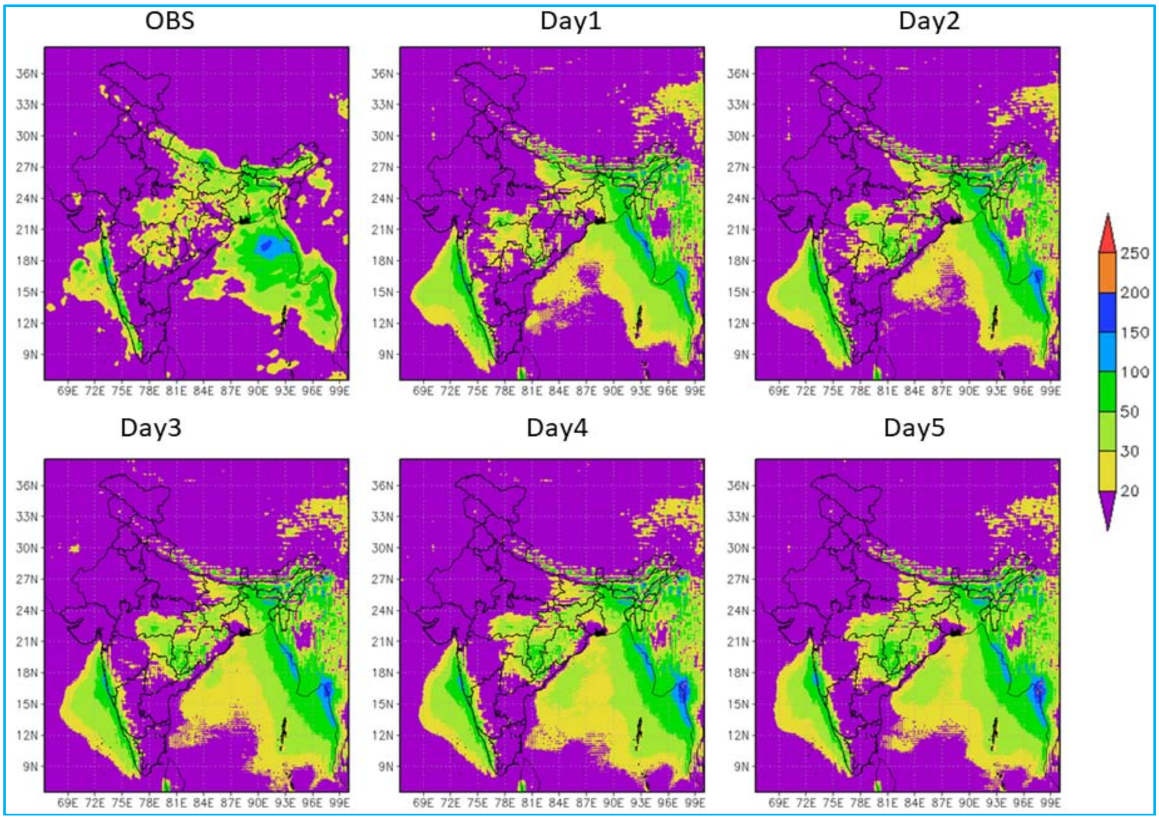

Fig. 2.4. Cumulative rainfall observed and GEFS forecast for the month of June

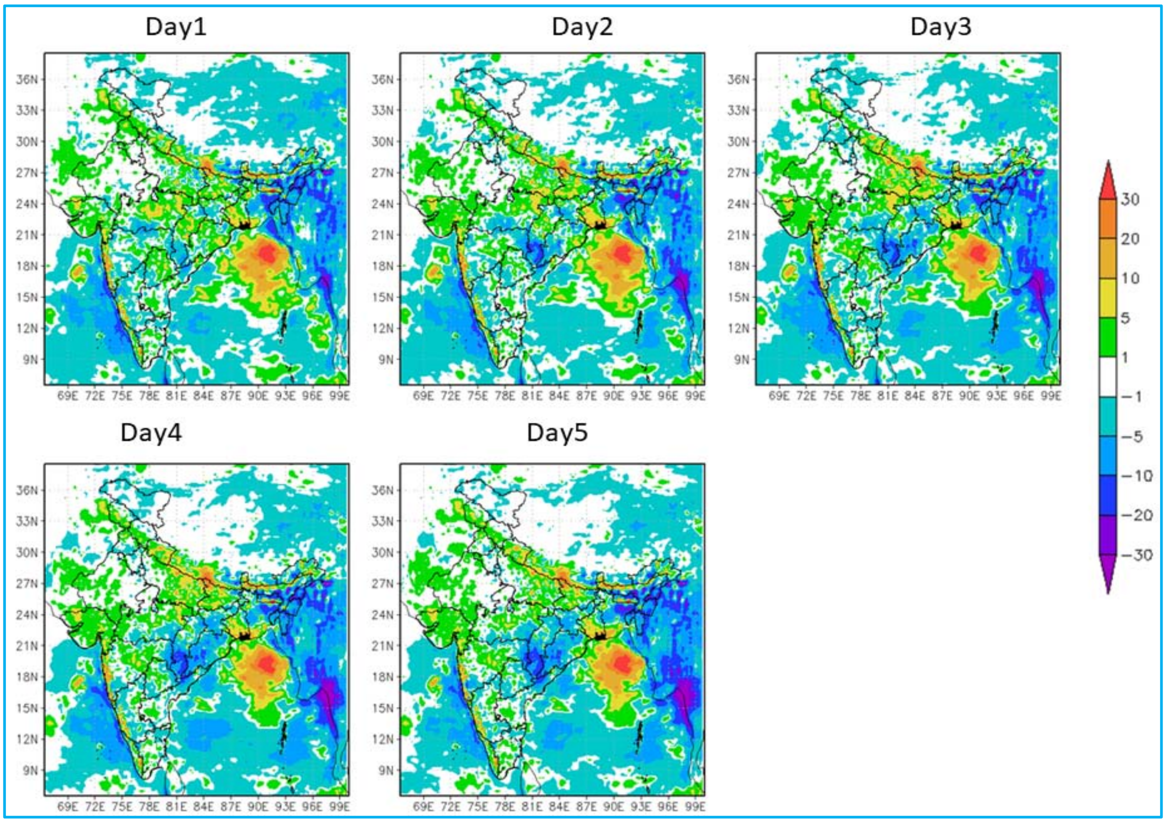

Fig. 2.5. Mean difference between observed rainfall and GEFS (observed-model) forecast for the month of June

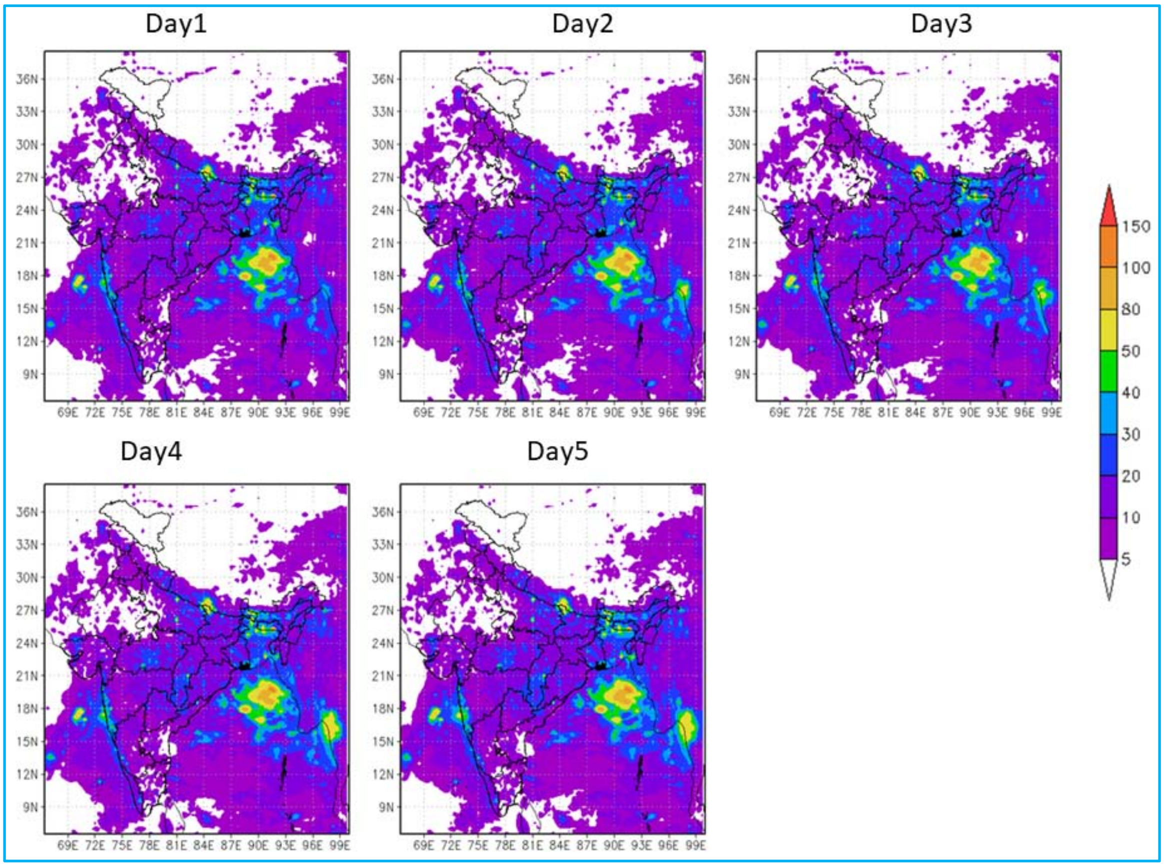

Fig. 2.6. RMS error in GEFS forecasts with respect to observed rainfall June

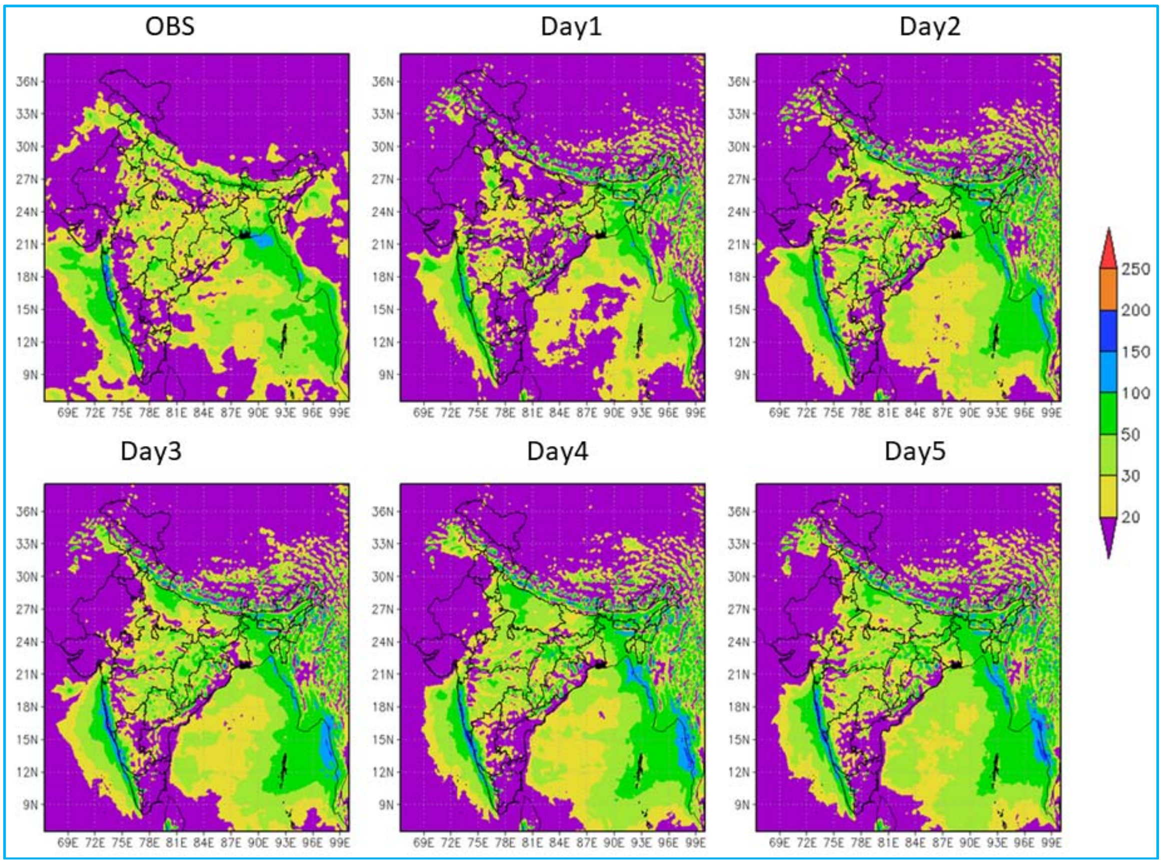

Fig. 2.7. Cumulative rainfall observed and GFS forecast for the month of July

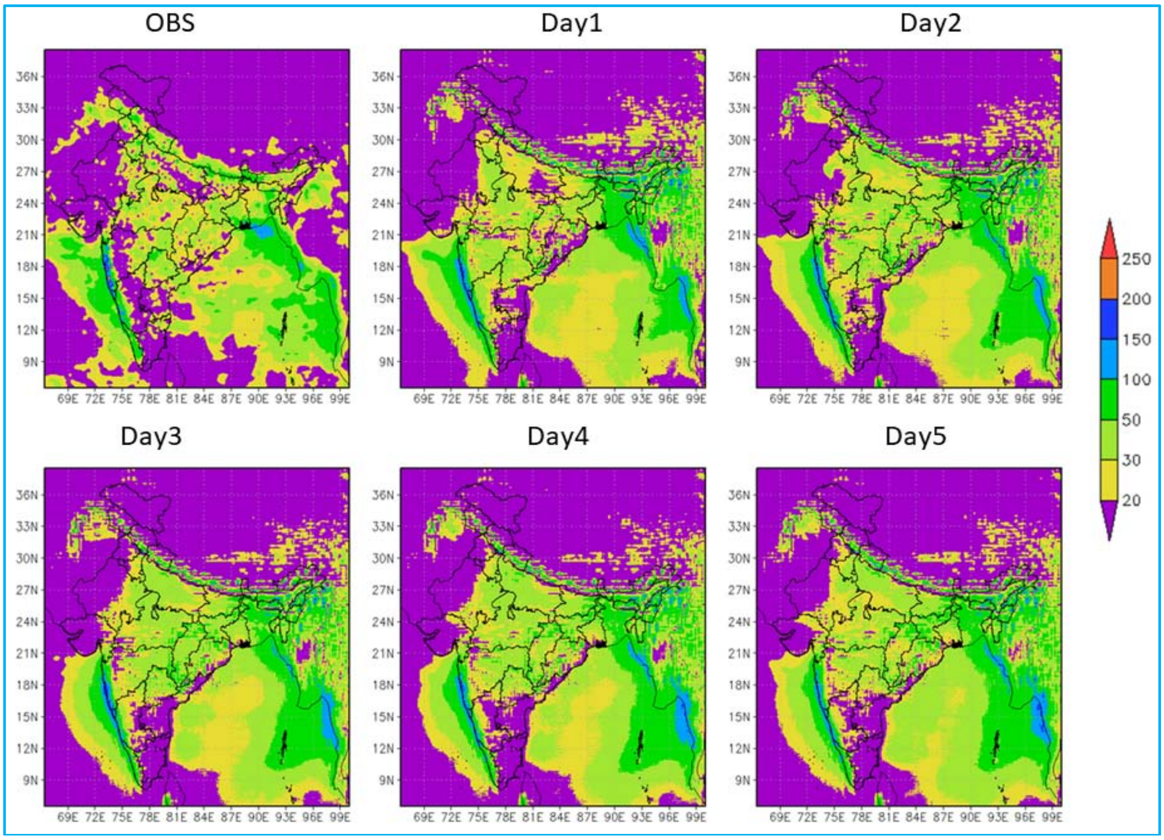

Fig. 2.8. Cumulative rainfall observed and GEFS forecast for the month of July

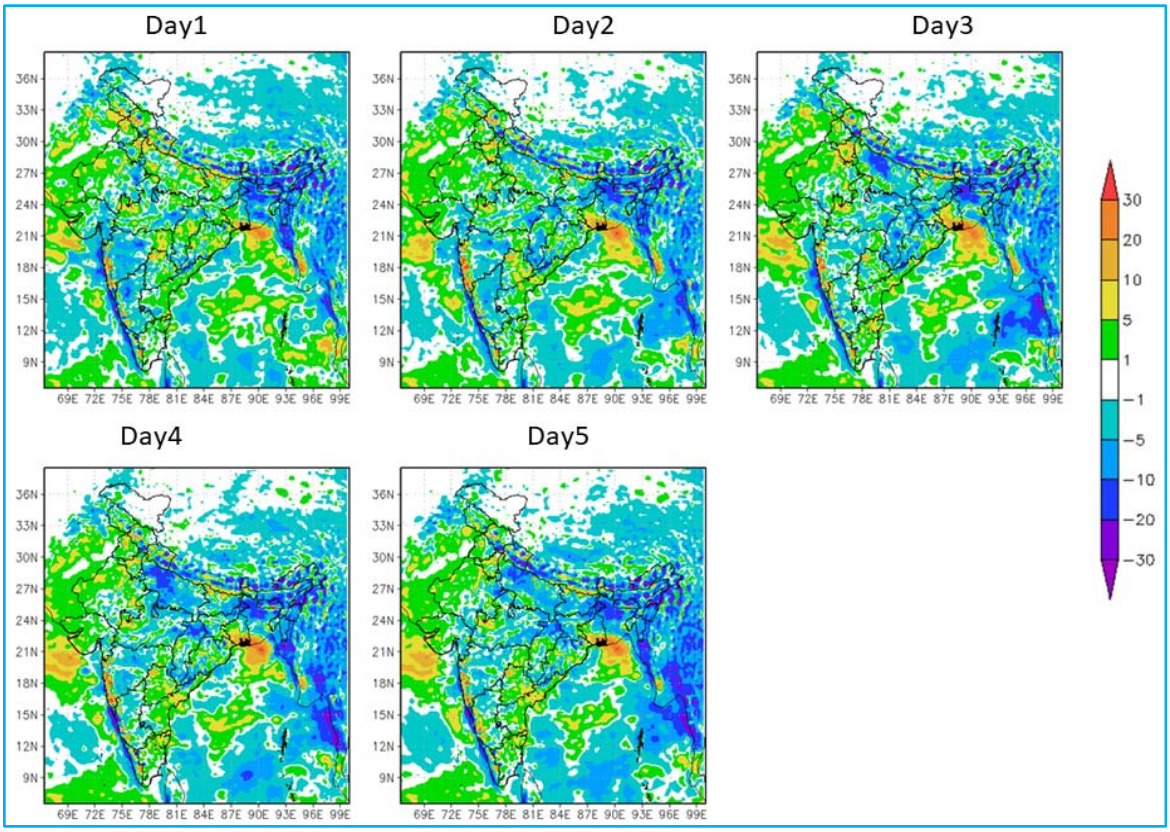

Fig. 2.9. Mean difference between observed rainfall and GFS forecast (observed-model) for the month of July

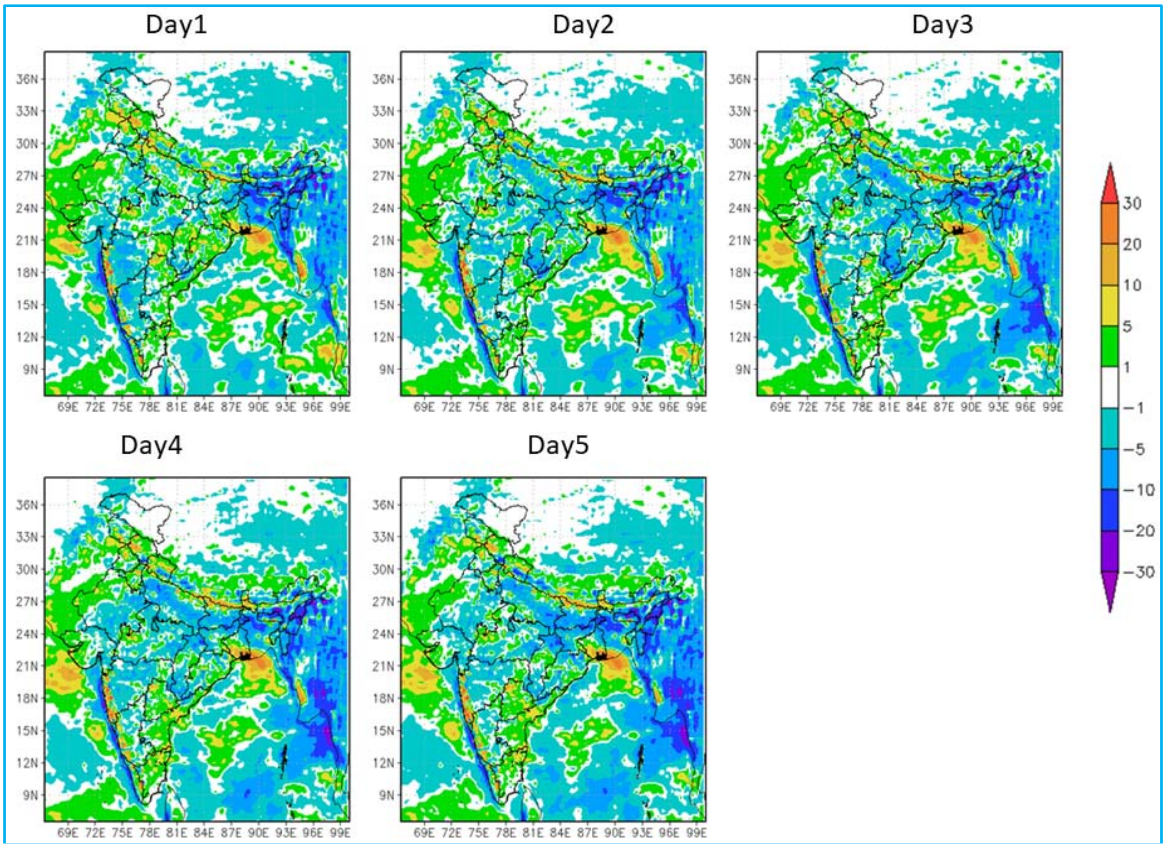

Fig. 2.10. Mean difference between observed rainfall and GEFS forecast (observed-model) for the month of July

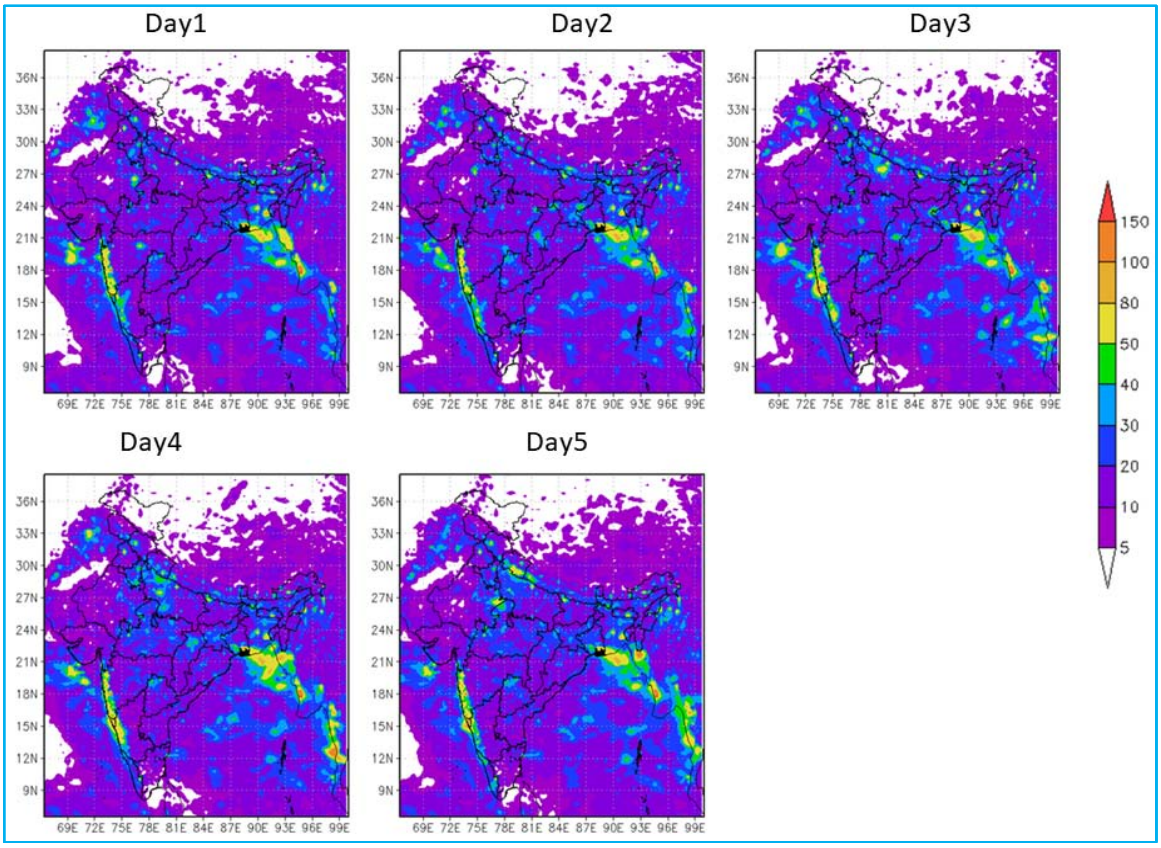

Fig. 2.11. RMS error in GFS forecasts with respect to observed rainfall July

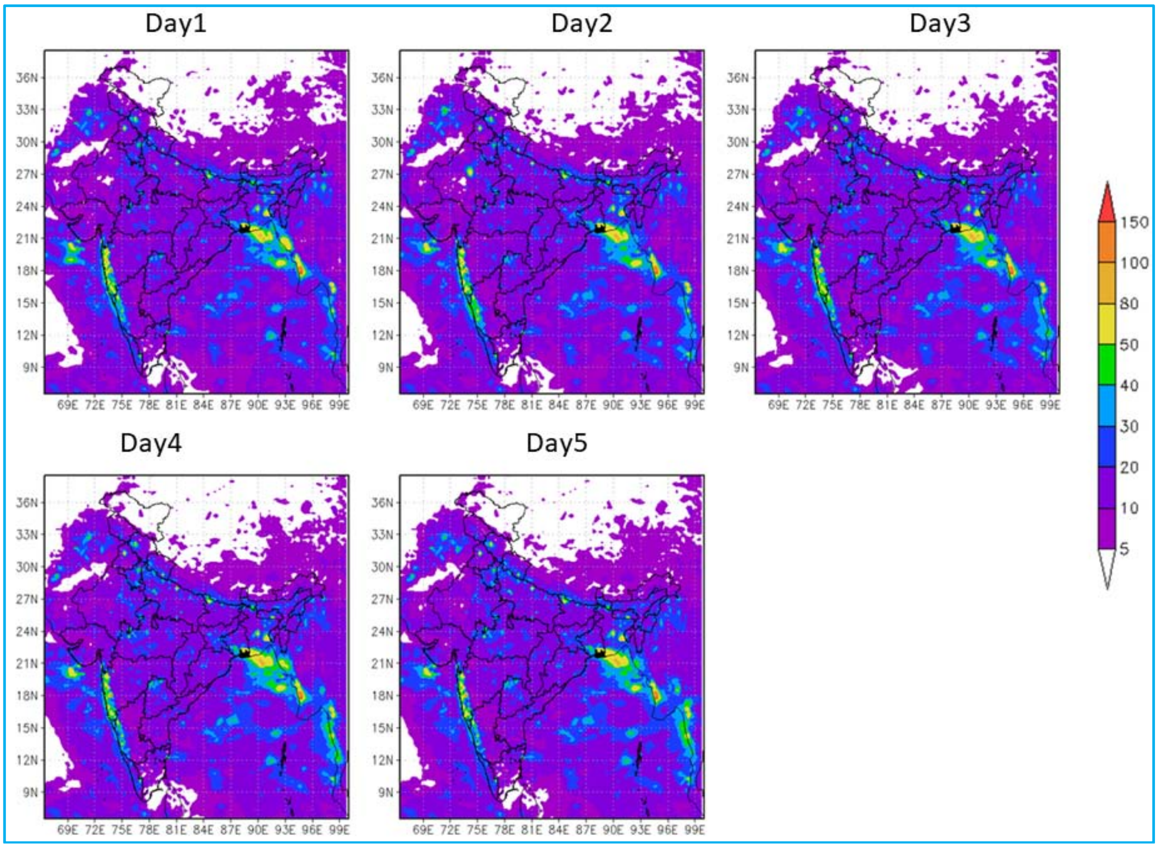

Fig. 2.12. RMS error in GEFS forecasts with respect to observed rainfall in July

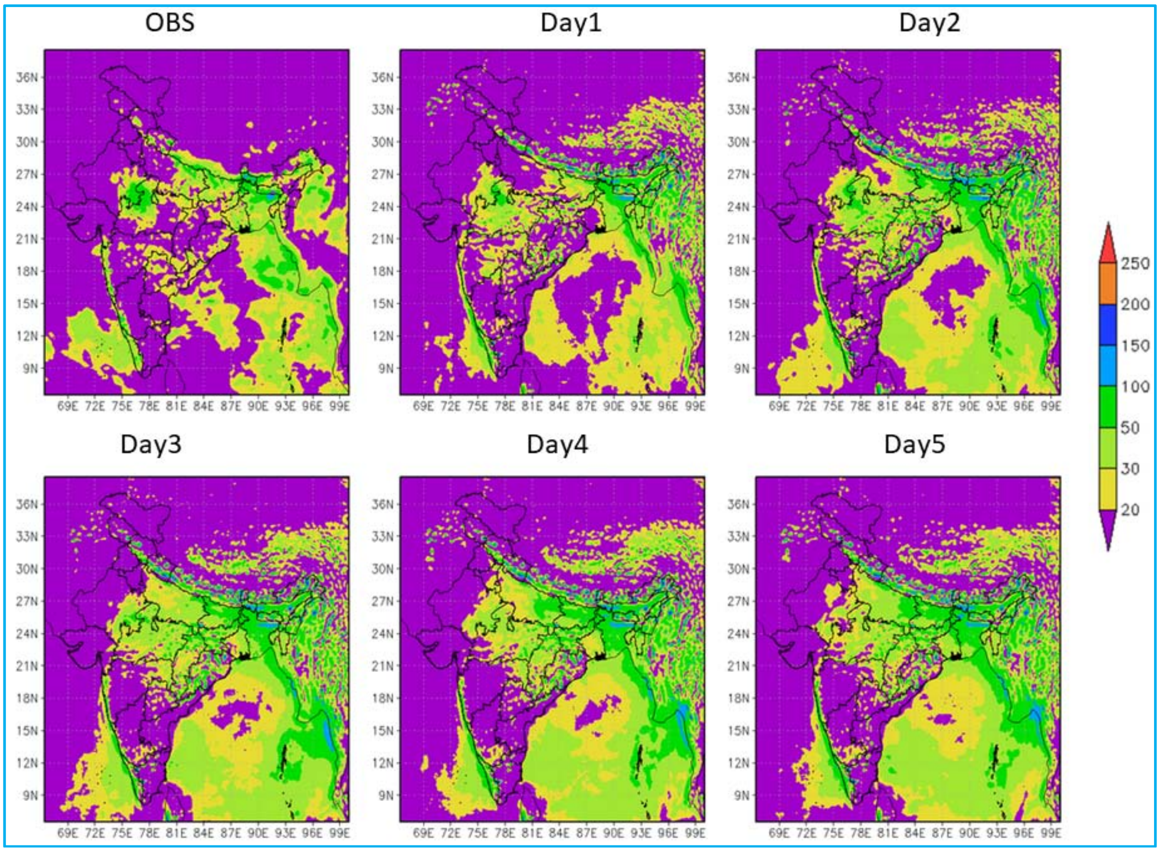

Fig. 2.13. Cumulative rainfall observed and GFS forecast for the month of August

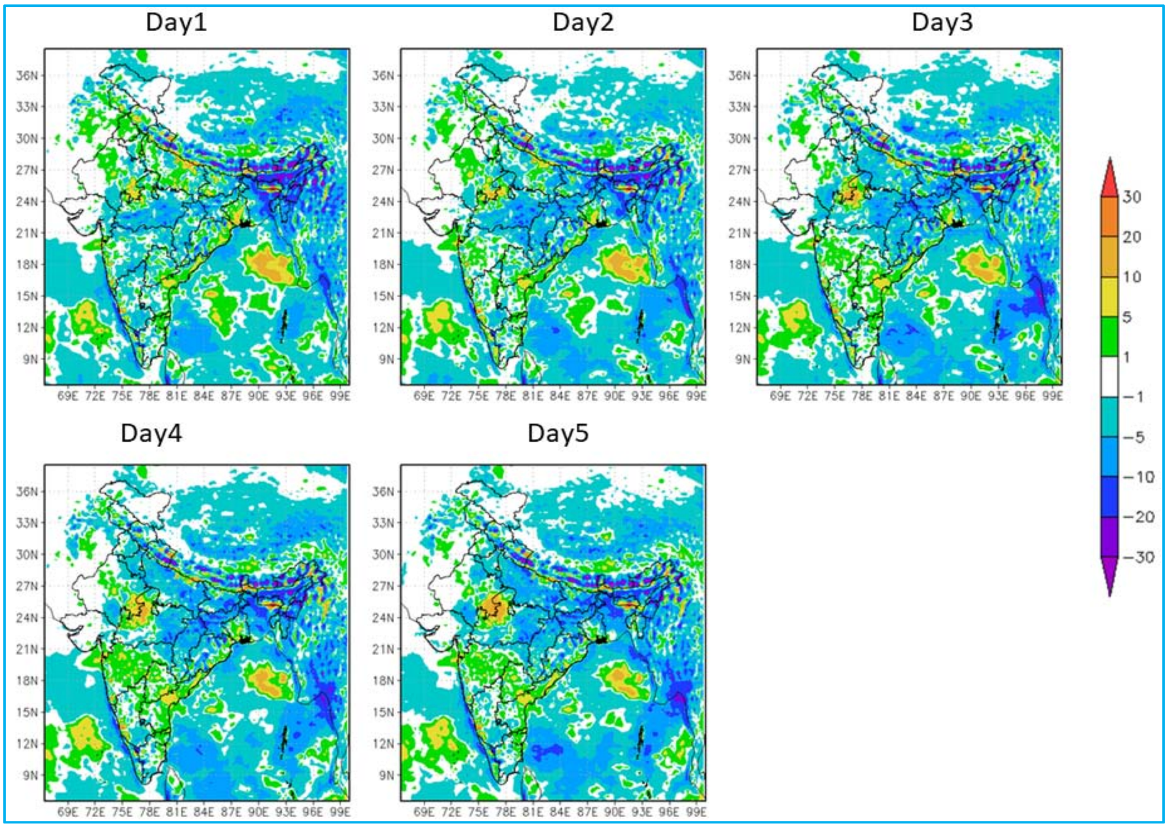

Fig. 2.14. Mean difference between observed rainfall and GFS forecast (observed-model) for the month of August

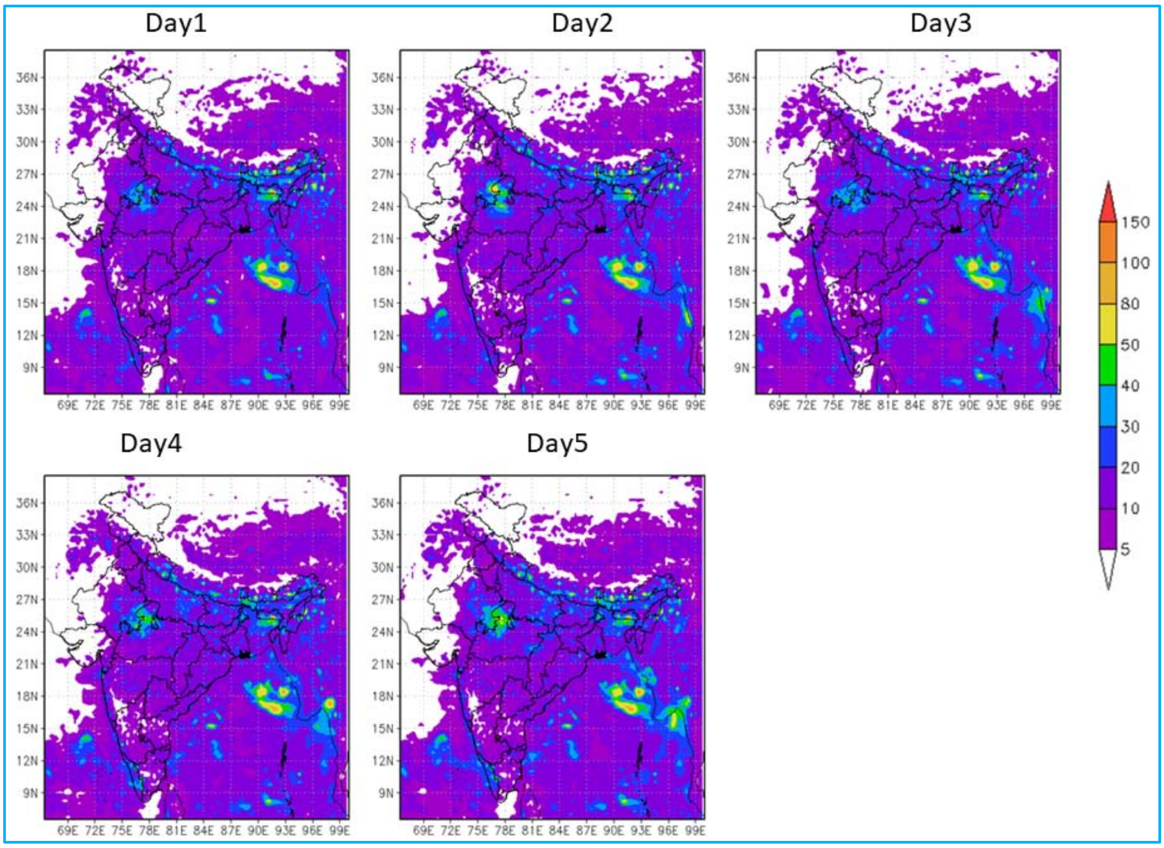

Fig. 2.15. RMS error in GFS forecasts with respect to observed rainfall August

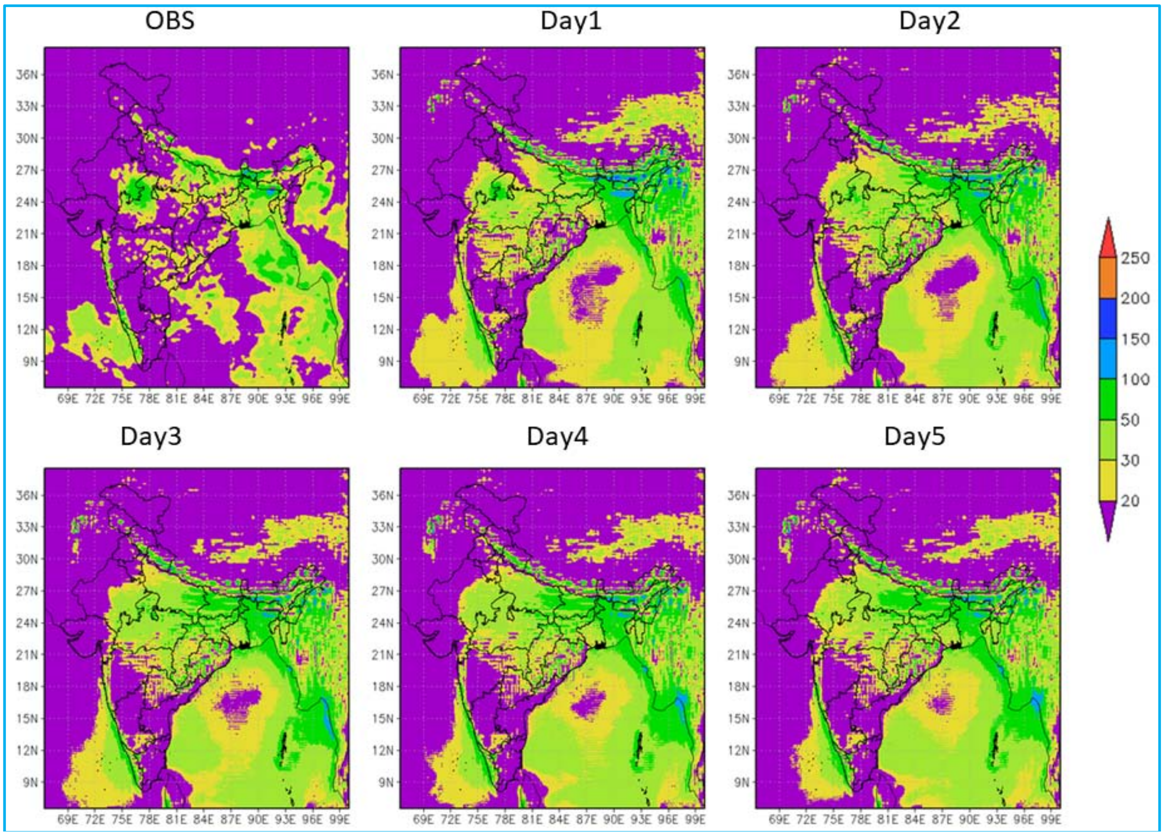

Fig. 2.16. Cumulative rainfall observed and GEFS forecast for the month of August

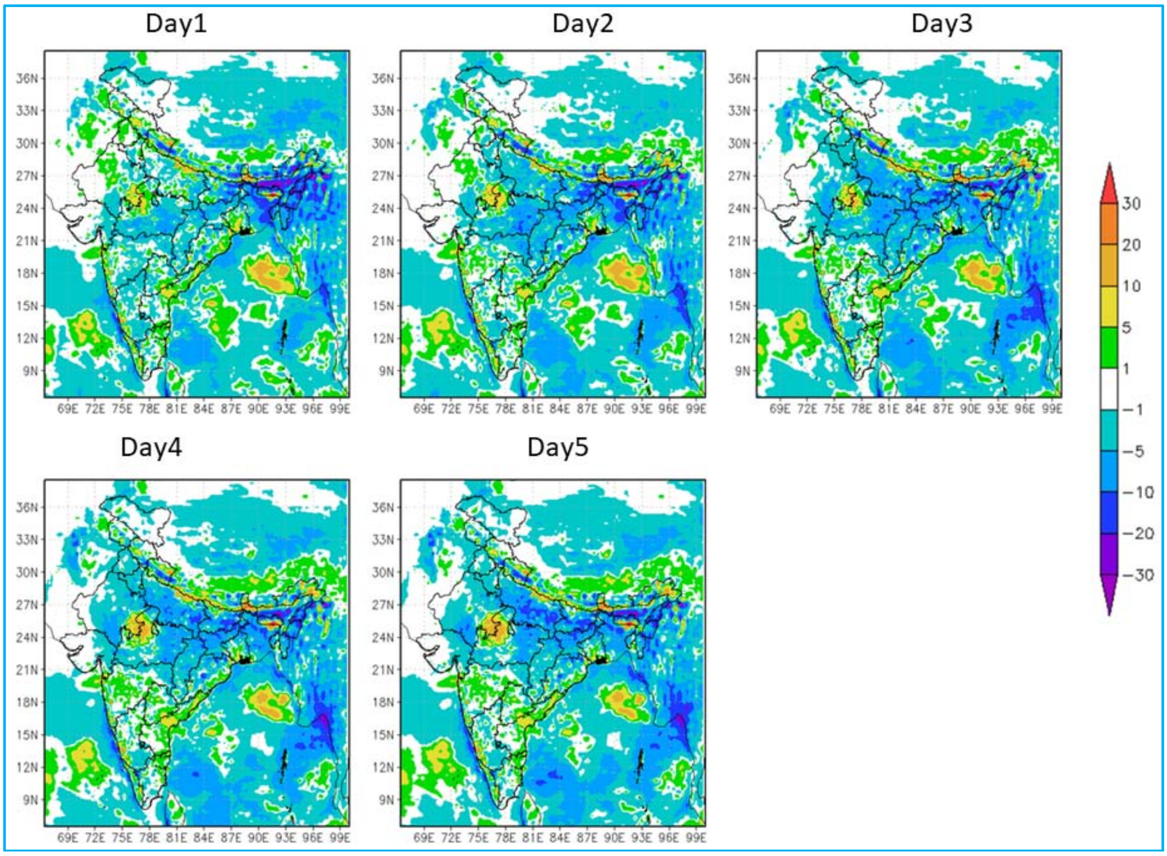

Fig. 2.17. Mean difference between observed rainfall and GEFS forecast (observed-model) for the month of August

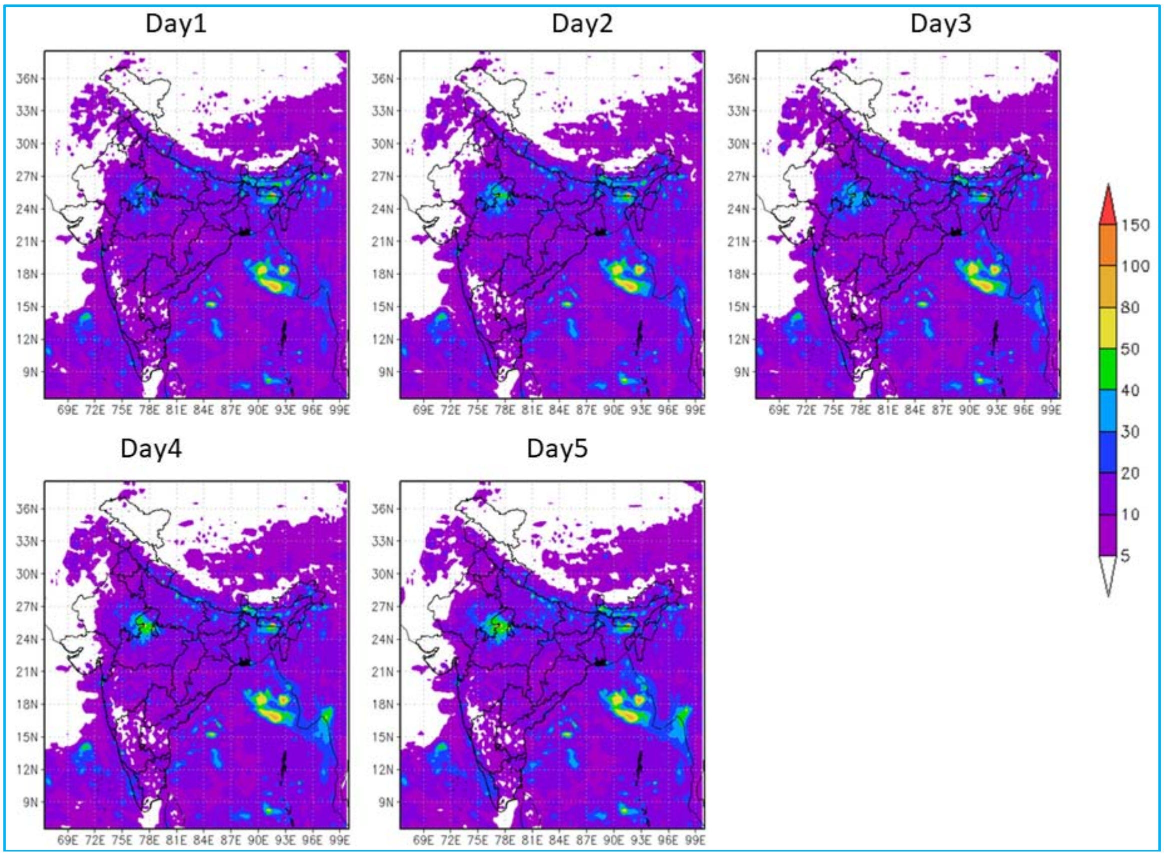

Fig. 2.18. RMS error in GEFS forecasts with respect to observed rainfall August

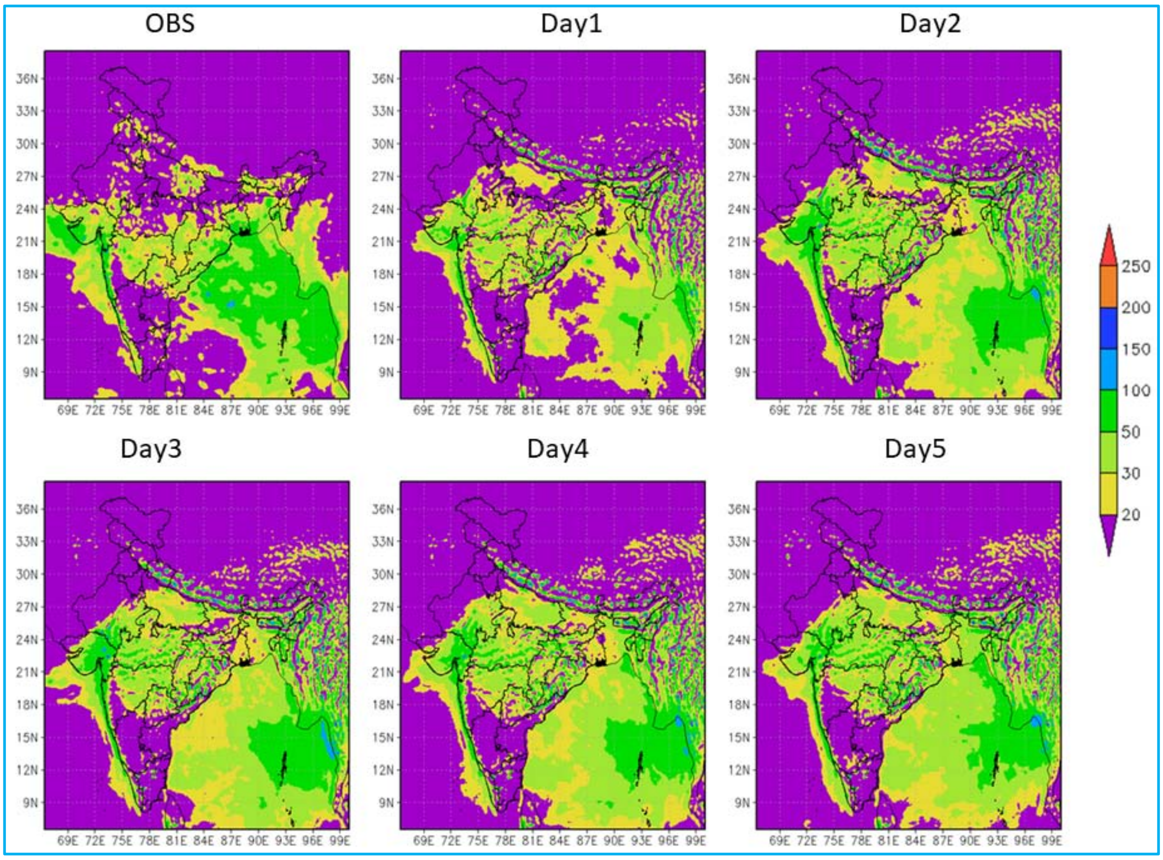

Fig. 2.19. Cumulative rainfall observed and GFS forecast for the month of September

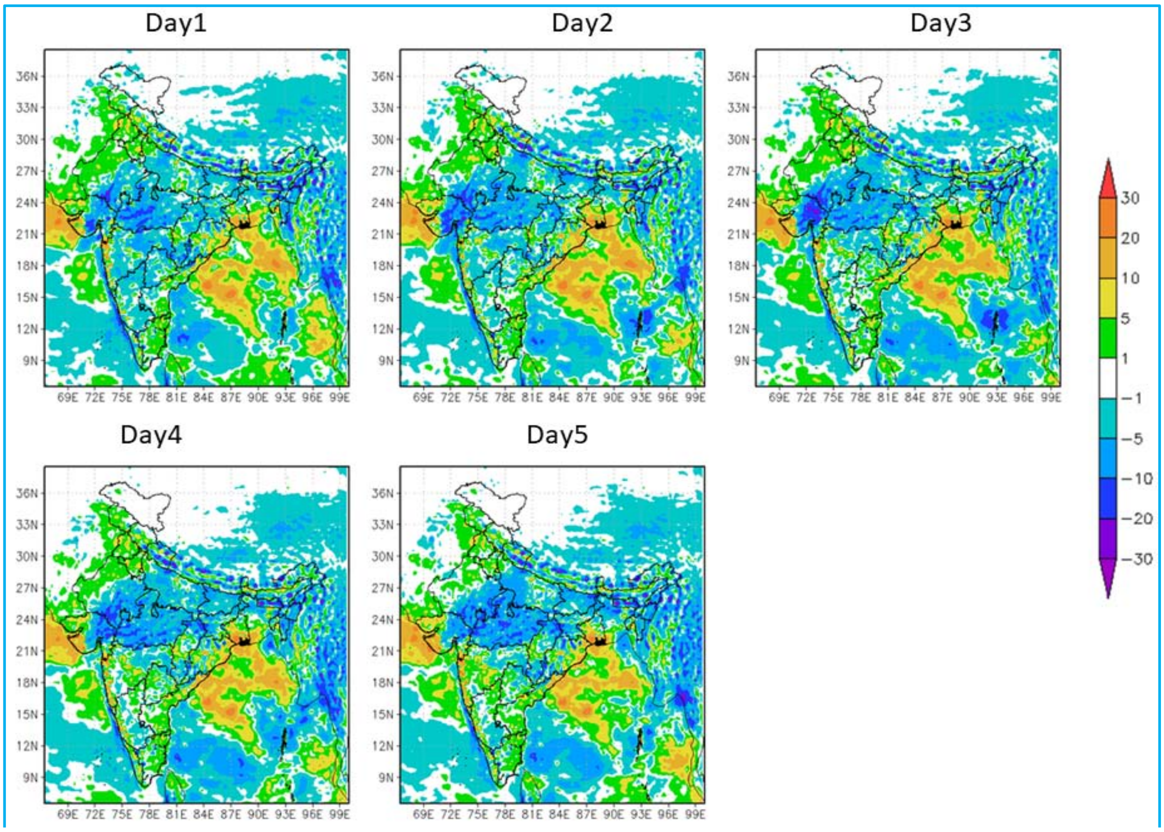

Fig. 2.20. Mean difference between observed rainfall and GFS forecast (observed-model) for the month of September

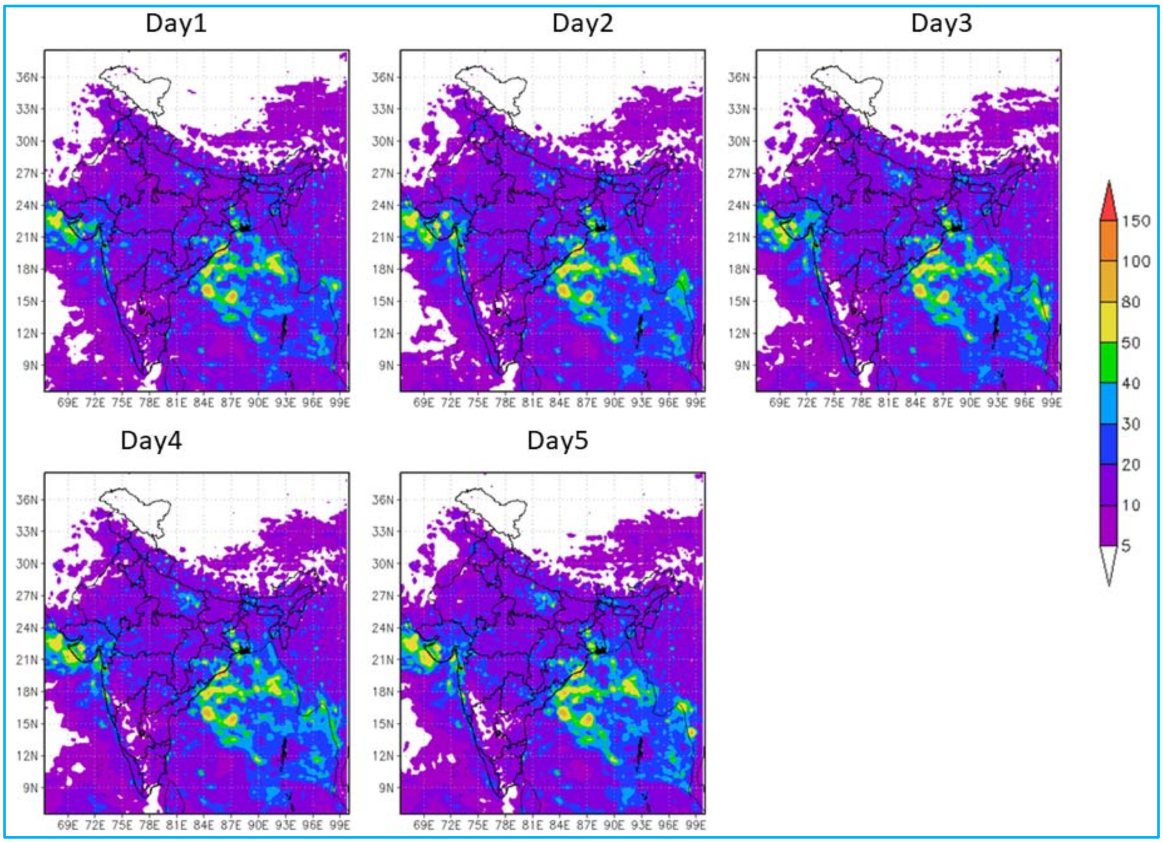

Fig. 2.21. RMS error in GFS forecasts with respect to observed rainfall September

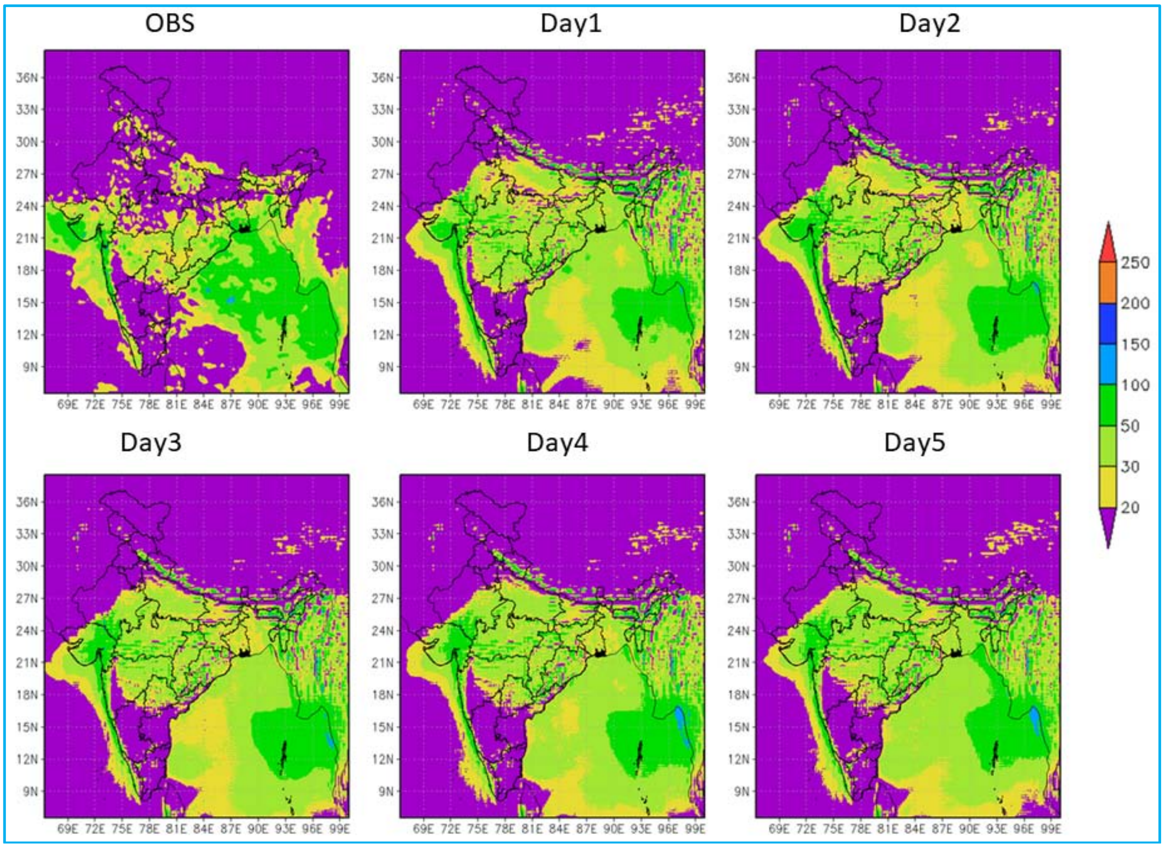

Fig. 2.22. Cumulative rainfall observed and GEFS forecast for the month of September

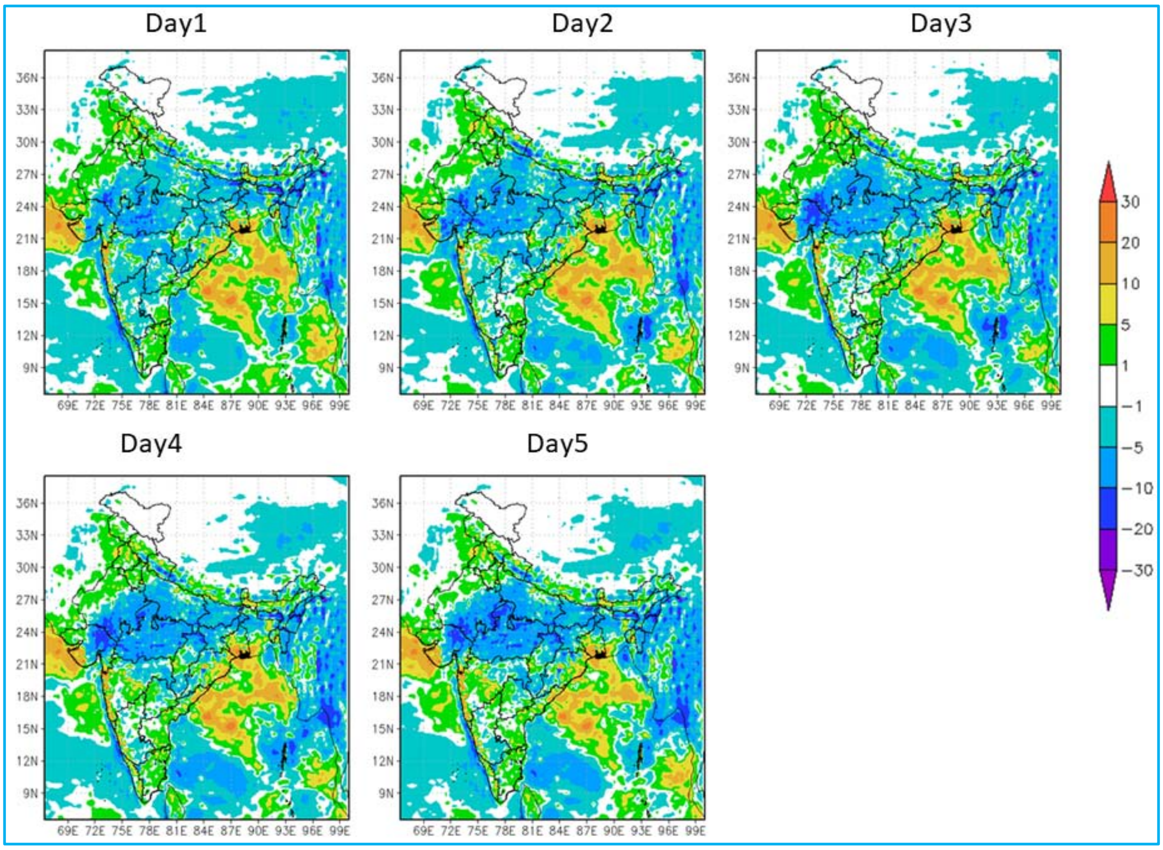

Fig. 2.23. Mean difference between observed rainfall and GEFS forecast (observed-model) for the month of September

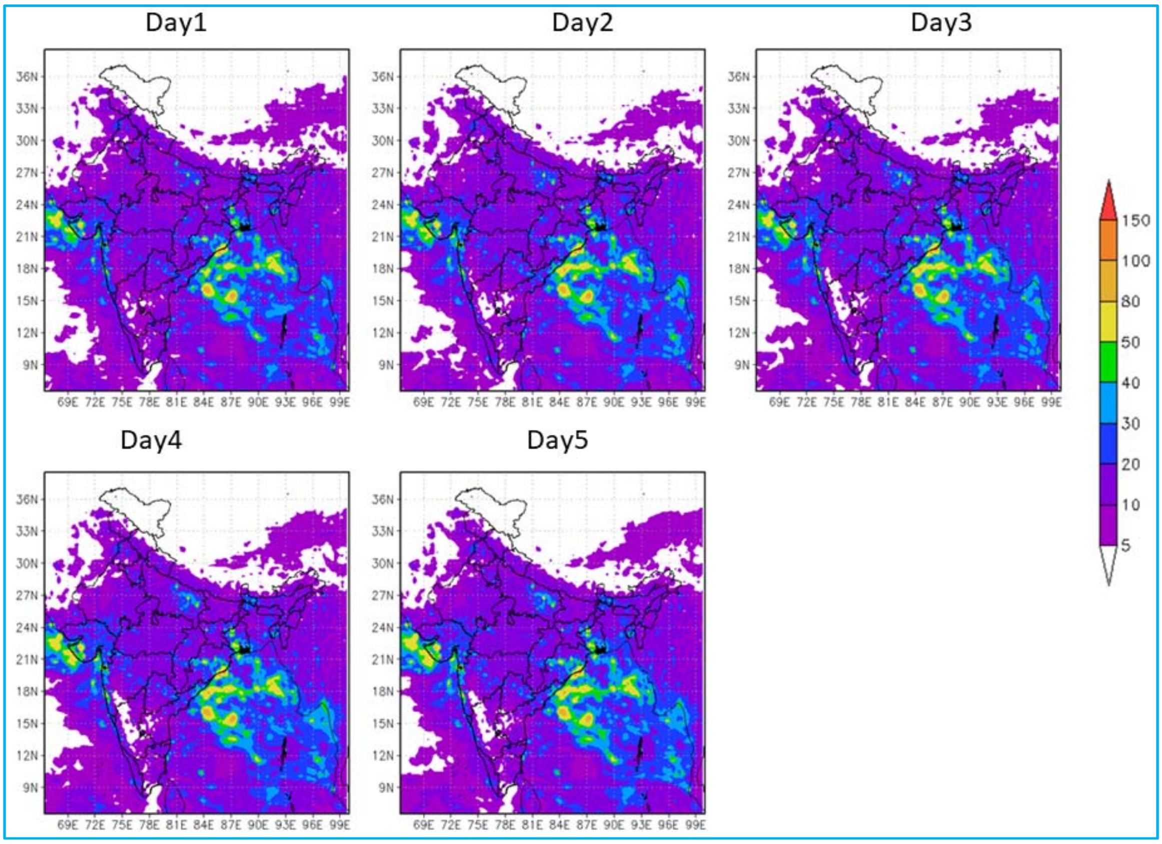

Fig. 2.24. RMS error in GEFS forecasts with respect to observed rainfall September

regions of Maharashtra and Goa very good amount of rainfall (even greater than 250 cm in some pockets) is observed. It can be seen that in day1 forecast rainfall over Himalayan foothill region, central and East India is not properly represented in IMD GFS forecast. Cumulative rainfall forecast of GEFS along with observation for July month is provided in Figure 2.8. It can be seen that in GEFS forecasts general characteristics of rainfall is represented in most of the regions. Mean difference between observation and model forecast for GFS and GEFS model is shown in Figure 2.9and Figure 2.10 respectively. In North East regions both the models were overestimated rainfall as seen in the month of June. In west coast model forecast show under estimation in both the models. RMSE plots are shown in Figure 2.11and Figure 2.12 respectively for GFS and GEFS. RMSE values are high over west coast and North and east Bay of Bengal in both the models. RMSE values over coastal Karnataka are more in GFS comparison to GEFS in day3 to day5 forecasts.

Cumulative rainfall observed in the August month and corresponding GFS model forecasts are shown in Figure 2.13. Major rainfall activity in August is seen over west coast, West Madhya Pradesh, East Rajasthan, East Uttar Pradesh, Bihar, Bengal and North East states. In west coast rainfall in the range of 50-100cm is reported in August. In GFS model forecasts rainfall over West Madhya Pradesh and East Rajasthan is over estimated to a large spatial extent except in day1 forecast. Mean difference between observations and GFS forecasts plots and RMSE is given in Figure 2.14 and 2.15 respectively. Cumulative rainfall observed in the August month and corresponding GEFS model forecasts are shown in Figure 2.16. As in case of GFS, spatial extension of rainfall activity over west Madhya Pradesh and East Rajasthan to nearby regions can be seen in the GEFS forecasts also. Mean difference in rain fall between observations and GEFS forecasts and RMSE in forecasts is shown in Figure 2.17 and 2.18 respectively. It can be seen that both the models over estimate rainfall over the North East region and sea region of west coast. The rainfall over land region of west coast and west Madhya Pradesh, East Rajasthan is under estimated in both the models. High RMS errors are seen over east central BOB, west Madhya Pradesh and East Rajasthan region, Himalayan Foothills and over Bangladesh. RMS errors over the west coast are relatively less compared to June and July. Along the border of Assam and Bangladesh cumulative rainfall amounts exceeding 200 cm is reported, which is not represented in both the model forecasts.

Cumulative rainfall observed in the September and corresponding GFS model forecasts are shown in Figure 2.19. Major rainfall activity in this month is reported over west coast especially over Gujarat and Konkan and Goa, Madhya Maharashtra, Marathwada, Chhattisgarh, Odisha, West Bengal, some parts of coastal Andhra-Pradesh, Telangana, East Uttar Pradesh, North East states, Punjab, Himachal Pradesh and Uttarakhand. It can be seen that model is able to predict the general characteristics of rainfall activity for the month. There is some over estimation of rainfall over central part of India, under estimation of rainfall over BOB in day1 forecast. Figure 2.20 shows the mean difference in observation and GFS model forecast for the month of September and RMSE plot is given in Figure 2.21. In forecasts over estimation can be seen over west Madhya Pradesh, East Rajasthan, some parts of Gujarat. As seen in the case of other months, rainfall is under estimated over land part of west coast, BOB, some parts of Saurashtra, Odisha and Bengal. Cumulative rainfall observed in the September and corresponding GEFS model forecasts is shown inFigure 2.22. Figure 2.23 shows mean difference in observation and GEFS model forecast for the month of September and RMSE plot is given in Figure 2.24.GEFS also shows similar characteristics as GFS. High RMS errors are seen over Gujarat region, BOB, West Bengal and Odisha in both the models.

2.5. Performance of Extreme Rainfall forecast

Extreme rainfall events over Indian region are investigated separately to find out ability of models to forecast these events. Extreme events are chosen using rainfall observations from IMD synoptic stations and applying criteria of more than 20 cm accumulated rainfall in 24 hours and highest rainfall in each subdivision in daily observations. Daily accumulated rainfall observations from previous day 3 UTC to current day 3UTC is compared with models forecasts up to lead time of day 5. In computing accumulated rainfall from model, maximum rainfall forecasted within 0.5 degree of station location is used for

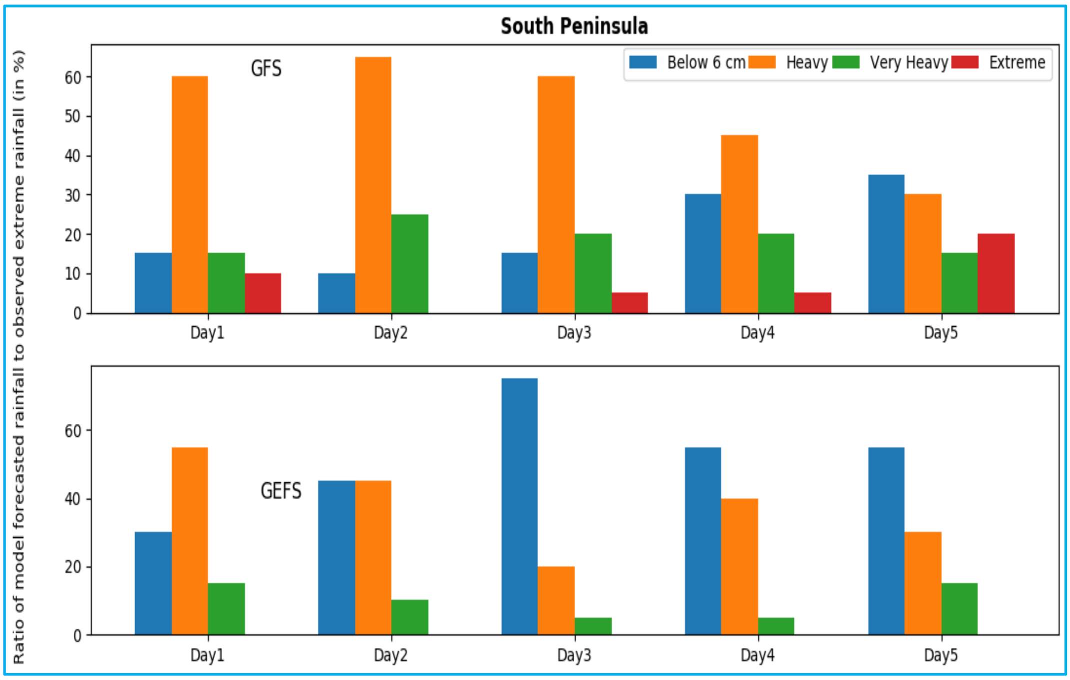

Fig. 2.25. Ratio model forecasted rainfall in different rainfall thresholds to extreme rainfall observations in South Peninsula

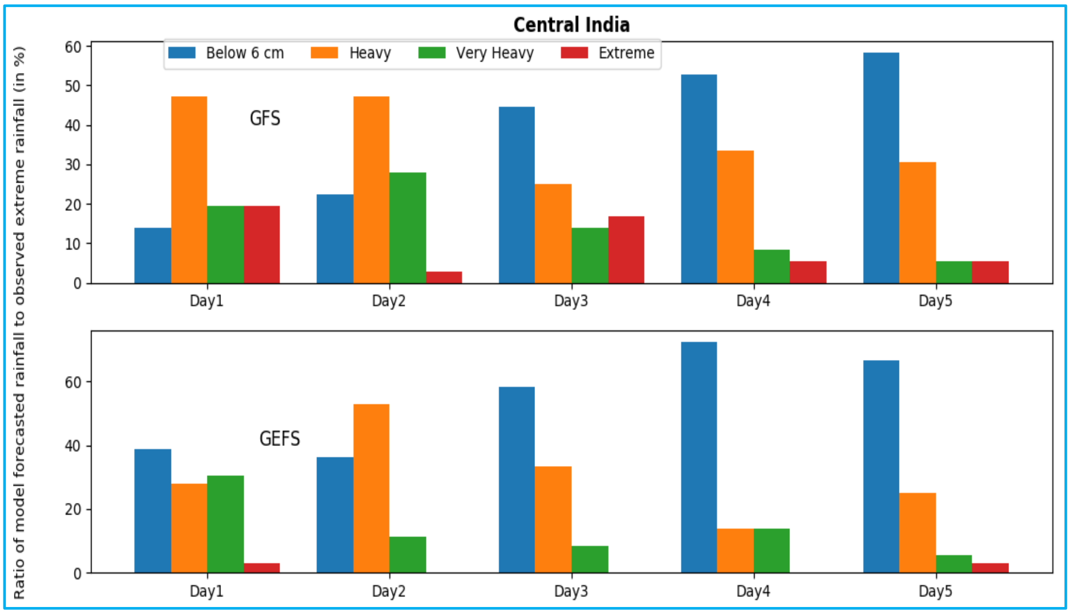

Fig. 2.26. Ratio model forecasted rainfall in different rainfall thresholds to extreme rainfall observations in Central India

comparing gridded model rainfall with the station observation. Extreme rainfall events are separated over four homogeneous regions as per IMD specification and forecast over each region is investigated. It is observed that model under estimates rainfall in most cases and rainfall amounts forecasted by models correspond to these extreme rainfall events is investigated.

In June month totally 23 extreme events are chosen as per defined criteria and almost half of them occurred in East and North East India region. In July month 44 extreme events are chosen and out of these 16 events occurred in Central India, 15 events in North West India and 10 events in South Peninsula. In July North East India region number of extreme events were less compared to other regions. In August 19 rainfall events were chosen and out of these 9 events were in East and North East region and 7 were in North West India. In August month number extreme cases were less in South Peninsula and Central India. In September 25 extreme events were chosen and out of these half of them occurred in Central India region.

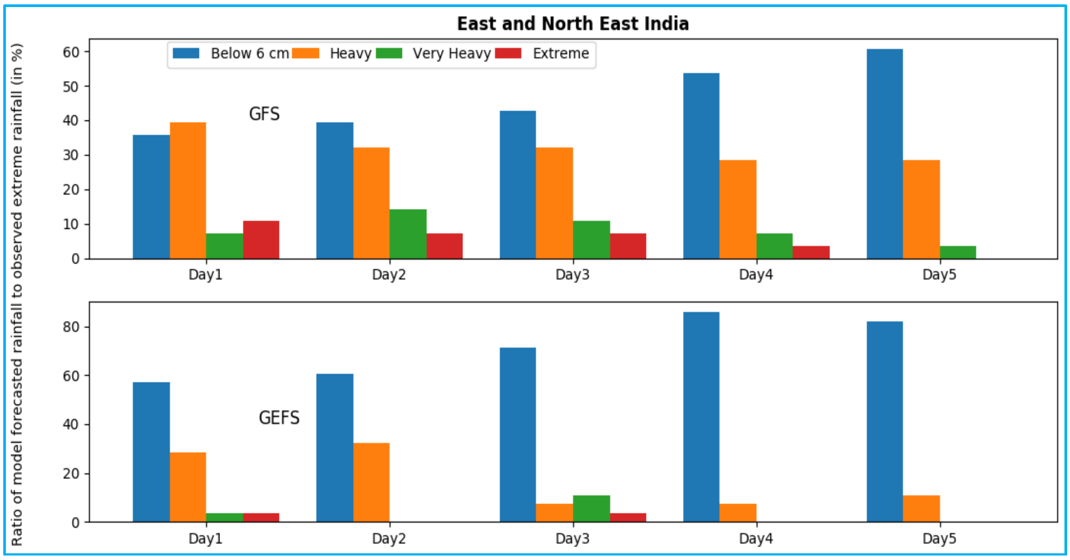

Fig. 2.27. Ratio model forecasted rainfall in different rainfall thresholds to extreme rainfall observations in East and North East India

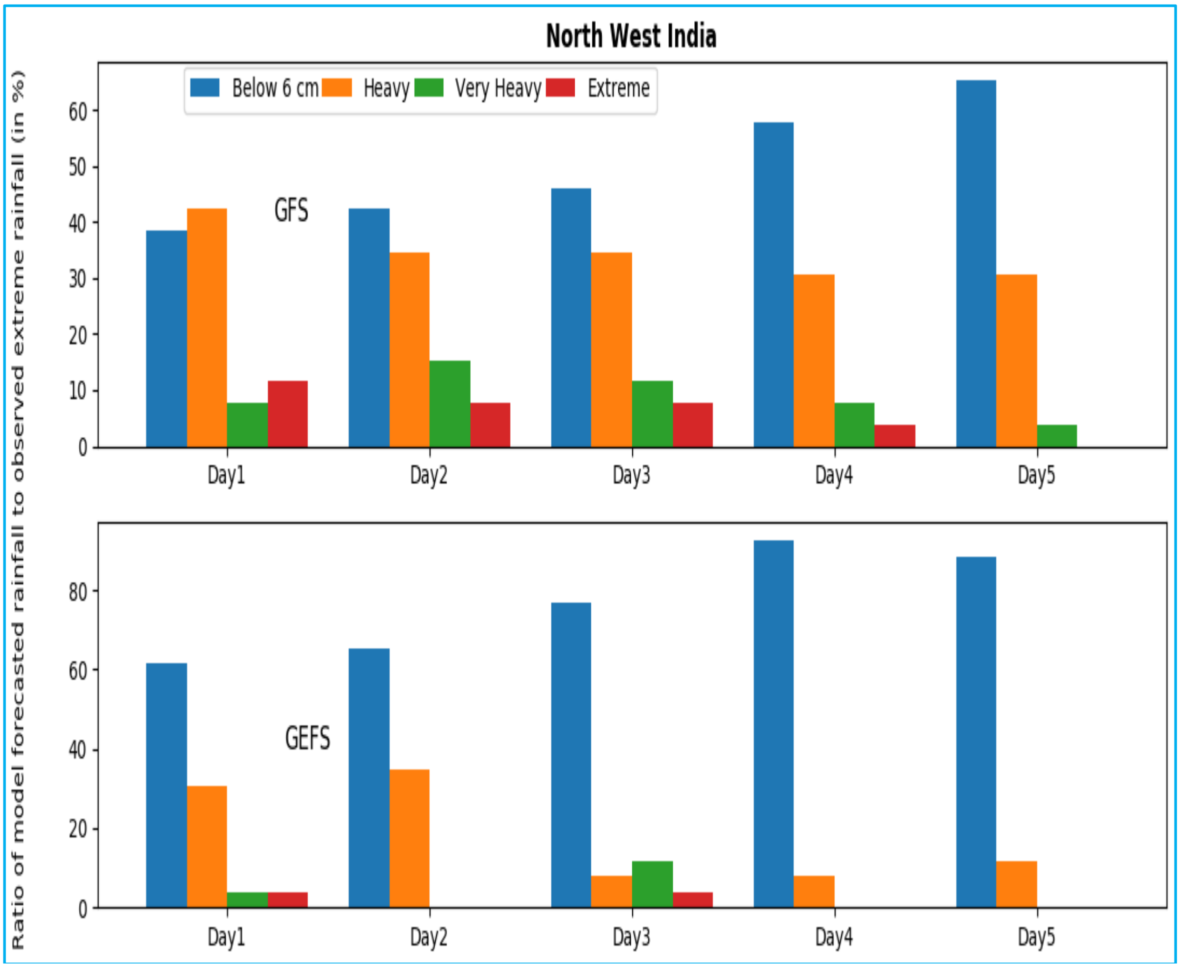

Fig. 2.28. Ratio model forecasted rainfall in different rainfall thresholds to extreme rainfall observations in North West India

Figure 2.25-2.28 shows the percentage of rainfall events models (GFS and GEFS) are able to capture in different rainfall threshold category (extreme, very heavy and heavy, below 6 cm) out of total observed extreme rainfall events in the homogeneous regions south peninsula, Central India, East and North East India and North West India respectively.

In south peninsula out of 20 extreme cases GFS model day1 forecast is able to predict 2 (10 %) in extreme rainfall category. In day 5 GFS forecasted20% of these events were in extreme rainfall category. GFS forecasted rainfall amount falls in very heavy or above category in 25 % of cases and falls in heavy rain and above category in 85 % of category. In GEFS forecasts none of these events fall into extreme rainfall category, 15 % cases rainfall falls above 11.5cm, and 70 % cases rainfall lies above 6.4cm.

In central India out of 36 extreme events GFS model predicted 7 events (~ 20 %) in extreme category, ~ 38 % in very heavy or above category and 85 % in heavy or above category their day1 forecast. There is a gradual fall in number of occurrences in each category with increase in forecast lead time, with 55% of the events fall in heavy rain or above category in day 3 forecast. GEFS model forecasted only one event in extreme category, ~ 33 % in very heavy or above category and ~ 60 % in heavy rain or above category in day 1 forecast. There are differences in number of rainfall events forecasted by GEFS in each category with different forecast lead times and number of events in each category is less in comparison to GFS.

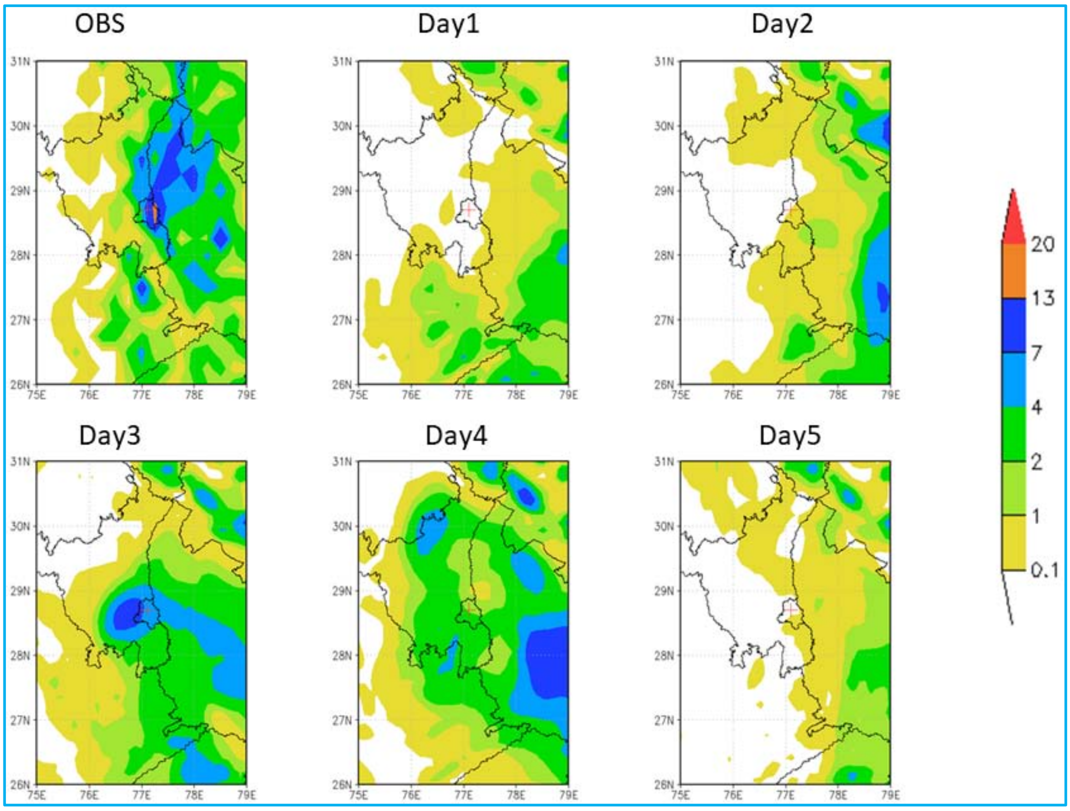

Fig. 2.29. Rainfall accumulated over 24 hours around Delhi valid on 03 UTC of August 21 in observations and GFS model forecasts. (Delhi is marked with cross)

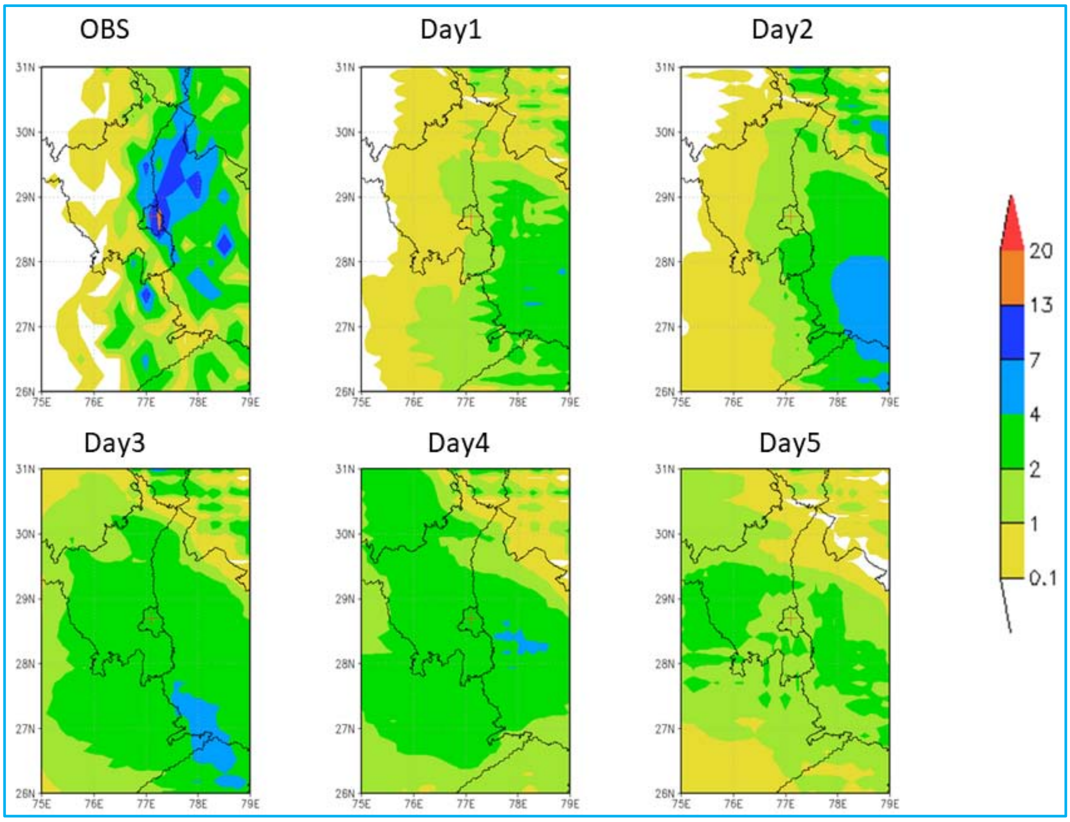

Fig. 2.30. Rainfall accumulated over 24 hours around Delhi valid on 03 UTC of August 21 in observations and GEFS model forecasts. (Delhi is marked with cross)

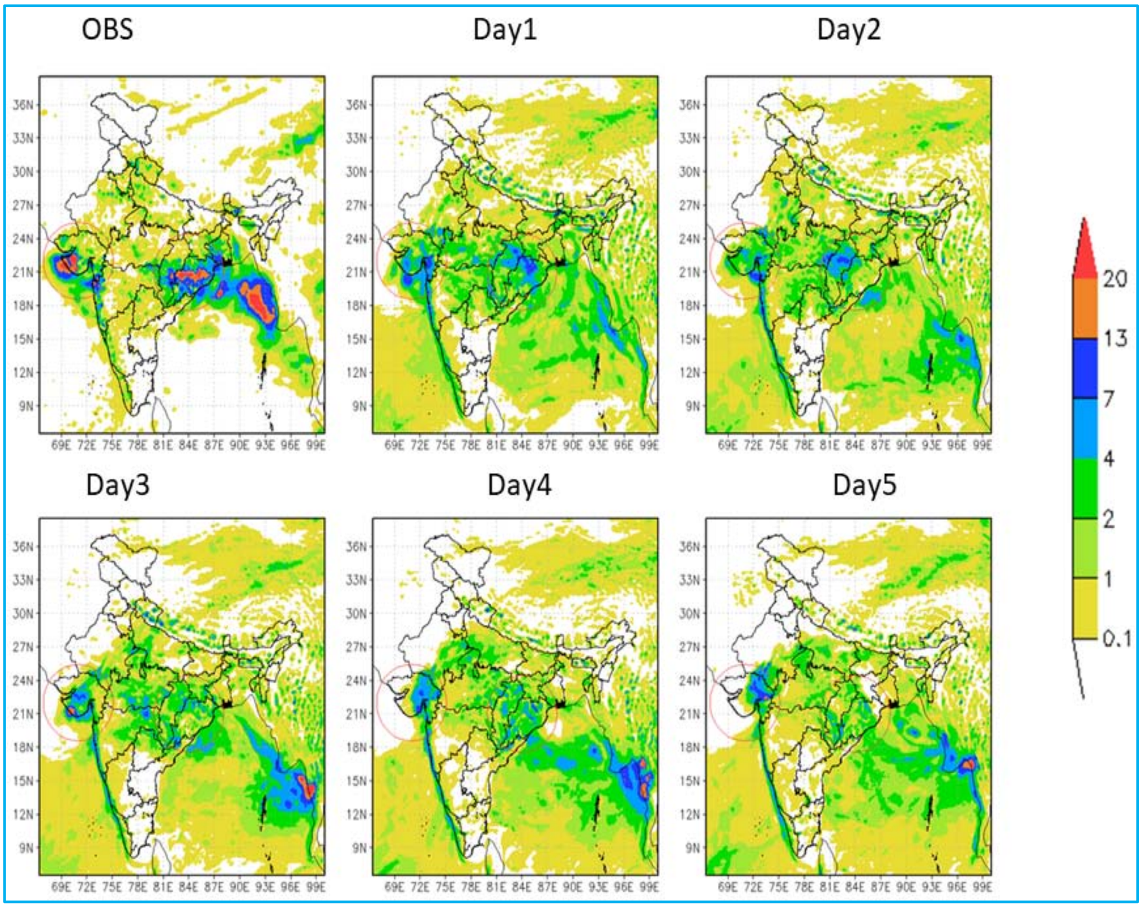

Fig. 2.31. Rainfall accumulated over 24 hours valid for 03 UTC of September 14 in observations and GFS model forecasts. (Region of interest is marked with circle)

In East and North East India out of 28 extreme events GFS model forecasted 4 events in extreme category in day3 forecast while 2 events in fall in extreme category in day1 forecast. In 25 % of cases Rainfall amount in GFS forecasts is in very heavy or above category and 82 % in heavy or above category. GEFS model not able to predict any of these events in extreme category while 10 % of events are predicted in very heavy category and 50 % of events in heavy or above category in day1 forecast. Again GEFS prediction skill comes down with increase in lead time and skill is less in comparison to GFS.

In North west India out of 26 cases, GFS predicted 3 (~ 10 %) cases in extreme category, while ~20 % in very heavy or above category and 60 % in heavy rain or above category in day 1 forecast. In day 2 forecast number of very heavy events are more than that predicted in day 1 forecast. In GEFS forecasts one event falls in extreme category in day1 and day 3 forecast while In 15 % of GEFS forecasts falls in very heavy or above category in day3 and 7 % falls in very heavy or above category in day1 forecast. GEFS forecasts are in heavy rain or above category in ~ 38 % of cases in day 1 forecast and number of cases decreases with increase in forecast lead time. Again it can be seen that forecast skill is less in this region in comparison to other regions in both the GFS and GEFS model.

Again two rainfall events, one very heavy rainfall over Delhi on August 21 and another extreme rainfall over Odisha and Gujarat region on September 14 is investigated separately. On August 21 Delhi received ~ 15 cm of rainfall in 24 hours. Figure 2.29 and 2.30 shows rainfall observations and model forecasts from GFS and GEFS models over Delhi respectively up to forecast lead time of 5 days. It can be seen that GFS model is able to forecast the event properly in day 3 forecast while missing in day1 and day2 forecast. In GEFS forecasts predicted rainfall amount is in the range of 2-4 cm. In September 14

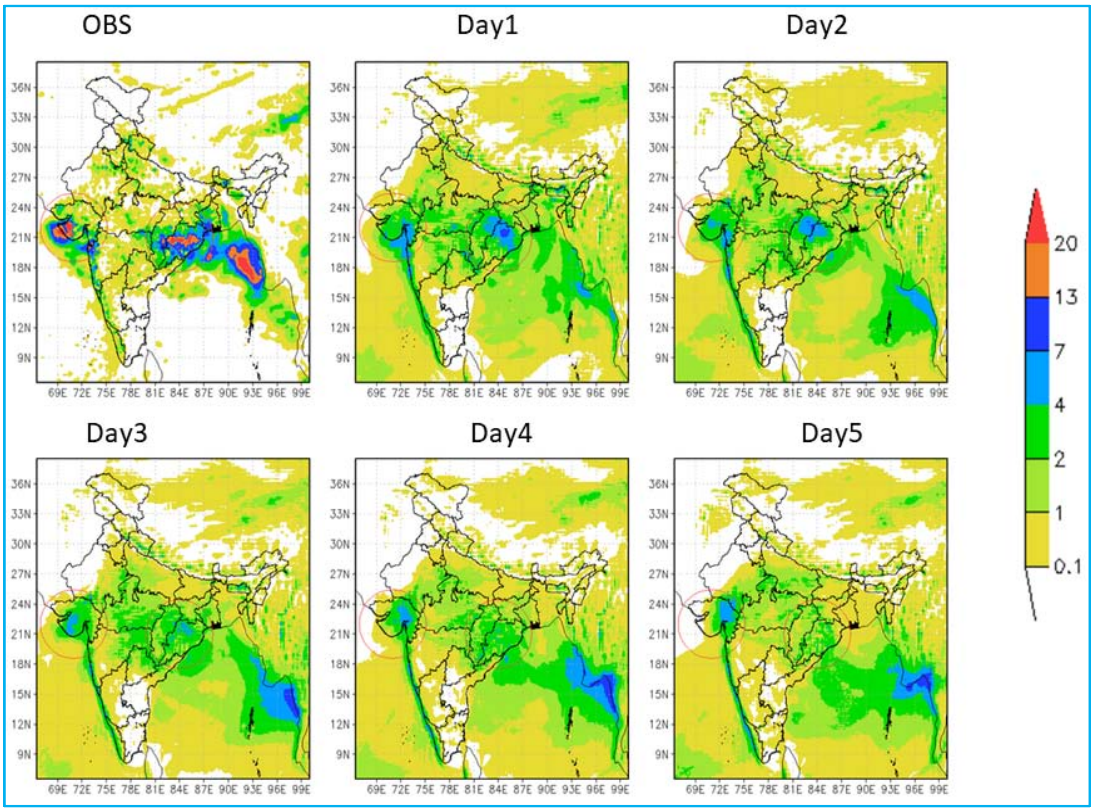

Fig. 2.32. Rainfall accumulated over 24 hours valid for 03 UTC of September 14 in observations and GEFS model forecasts. (Region of interest is marked with circle)

extremely heavy rainfall observed in Gujarat and Odisha. Figure 2.31 and 2.32 is similar plot for the extreme rainfall event on September 14. In both the models forecasted rainfall amount in these regions are in the range of 7-13 cm range and there are some differences in spatial distribution of rainfall also in comparison to observations.

2.6. Conclusions

Models are able to represent general characteristics of rain fall in all the months. There is an overall under estimation of rainfall over land region of west coast of India and over estimation of rainfall over North East region in both the models. In June and July GFS is not able to represent rainfall over central India region in day 1 forecasts which has come better at forecast of longer lead times and GEFS represented this rainfall in forecasts of all lead times. In August both the models over estimated rainfall over West Madhya Pradesh and East Rajasthan region. In the forecast of extreme rainfall events, there is under estimation in both the models while GFS forecasted these events better than GEFS. It is found that in the 3 homogeneous regions South peninsula, Central India and East North East India, GFS model forecasted 10% of the observed extreme rainfall events in extreme category, 25 % of observed extreme rainfall events in very heavy rain or above and 85 % observed extreme rainfall events in heavy rain or above category. In North West region out of observed extreme rainfall events, GFS forecasted 20 % of these events in very heavy rain or above category and 60 % in heavy rain or above category. In GEFS forecasts out of observed extreme rainfall events, number of extreme events predicted in each rainfall category is less compared to GFS. In comparison of model variables at different atmospheric levels GEFS model showed less error than GFS in temperature, wind and Geo-potential height forecast. Forecast errors of temperature, wind and Geo-potential height fields with respect to respective analysis were less over tropics compared to NHX and RSMC region.

Acknowledgements

Authors are thankful to NCMRWF and IITM team for the developments in operational GFS and GEFS forecast system.

References

Deshpande M., Johny C. J., Kanase R., Tirkey S., Sarkar S. Goswami, T., Roy K., Ganai M., Krishna R. P. M., Prasad V. S., Mukhopadhyay P., Durai V. R., Nanjundiah, R. S. and Rajeevan, M., (2020), "Implementation of Global Ensemble Forecast System (GEFS) at 12 km Resolution", ISSN 0252-1075, IITM Technical Report No.TR-06, ESSO/IITM/MM/ TR/02(2020)/200.

Durai V. R., Kotal, S.D. and Ray Bhowmik, S. K. (2011) Performance of Global Forecast System of IMD during summer monsoon 2010, Annual NWP performance report 2010, Meteorological Monograph No. NWP/Annual Report/01/2011.

Johny C.J. and Prasad V.S. Application of hind cast in identifying extreme events over India. *J. Earth. Syst. Sci*., 129, 163 (2020). https://doi.org/10.1007/s12040-020-01435-8.

Mitra A. K., Bohra A. K., Rajeevan M. and Krishnamurti T. N. (2009) Daily Indian precipitation analyses formed from a merge of rain-guage with TRMM TMPA satellite derived rainfall estimates; *J. Meteorol. Soc. Japan*, **87A**, 265–279.

Prasad V. S., Suryakanti Dutta, Sujata Pattanayak, C. J. Johny, John P. George, Sumit Kumar and S. Indira Rani (2021) Assimilation of satellite and other data for the forecasting of tropical cyclones over NIO, *MAUSAM*, Vol. **72**, No. 1.

White G, Yang, F. and Tallapragada, V. (2018 White, G., Yang, F. and Tallapragada, V. (2018) The Development and Success of NCEP's Global Forecast System; National Centers for Environmental Prediction: National Oceanic and Atmospheric Administration, USA.

CHAPTER 3

Operational Extended Range Forecast System of IMD

D. R. PATTANAIK, ASHISH ALONE and SATENDRA KUMAR
India Meteorological Department, New Delhi – 110 003

3.1. Introduction

Extended range forecast (ERF) covering the time scale from one week to about a month in the tropics are one of the most challenging tasks in atmospheric sciences. It fills the gap between medium-range weather forecasting and seasonal forecasting. The ERF time scale is certainly a difficult time range of weather forecasting, as the timescale is sufficiently long so that much of the memory of the atmospheric initial conditions is lost and on the other hand, monthly mean time average is not large enough for the atmospheric signal associated with the ocean anomalies to emerge over the atmospheric noise. Though the seasonal forecast of monsoon has its own relevance for the policy maker the forecast of monsoon in intermediate time scale are critical for the optimization of planting and harvesting. Thus, the forecasting of monsoon break in the extended range time scale, 2 to 4 weeks in advance is of great importance for agricultural planning (sowing, harvesting, etc.), which can enable tactical adjustments to the strategic decisions that are made based on the longer-lead seasonal forecasts and also will help in timely review of the prevailing monsoon conditions for providing outlooks to farmers. Several analyses have shown that sub-seasonal variability of monsoon has two preferred locations on a broader spatial scale, a strong continental convergence zone associated with convection over the land (continental) region (between 10°-25° N) and the other over the eastern equatorial Indian Ocean. The intra-seasonal variability can be defined as the see-saw pattern of the two convergence systems oscillating out of phase with one another. The oscillation is accompanied by a northward phase propagation of rainfall and other circulation feature anomalies. Hence, monsoon intra-seasonal oscillation (MISO) is associated with an explicit northward propagation of positive or negative precipitation (or convection) anomalies. Such oscillations bring a sequence of active monsoon and break monsoon situation, which is spells of dry and wet conditions, that often lasts for one to two week or more. Sub-seasonal variability of monsoon rainfall has dominant variance associated with 30-60 day periodicity, and has a common mode of variability with the seasonal mean, which is hypothesized to be strengthening (weakening) the seasonal mean in its active (break) phases and the large scale structure of active/break phases, 30-60 day mode and seasonal mean are often similar.

Forecasting of intra-seasonal oscillations and the synoptic variability is a great challenge and it is an integral part of India Meteorological Department's operational forecasting strategy. The forecast of Intra-seasonal oscillations provide forewarning and outlook in different time scales and hence it is important for several stakeholder applications. It is not only the agriculture sector which is benefited from the proper outlook of extended range forecast, a skilfulextended range forecast can also be very useful for reservoir operation in managing floods. Pattanaik and Das (2015) have recently demonstrated usefulness of extended range forecast in a pilot study over the Mahanadi River basin in Odisha in case of 2011 flood. Like the utility of ERF of Indian monsoon rainfall, cyclogenesis, northeast monsoon, the ERF of surface air temperature (including the heat wave and cold wave) for two to four weeks has a wide range of applications in agriculture, energy, health, insurance, power, financial sector etc. In May 2003 the heat wave claimed over 1,600 lives throughout the country with some 1,200 individuals died in the state of Andhra Pradesh alone. Like in 2003, during 2005 also India was under the grip of severe heat wave towards the third week of June due to stagnation of monsoon and recently in 2015 India witnessed large number of death due to severe heat wave over many parts of India. The prediction of heat waves and cold waves with significant accuracy can save lives and prevent damage to property from these dangerous weather events. The field of application of extended range forecast is vast and it can help several planning from the country level to state level to block-level scale. Advance planning of several activities e.g., crop sowing, application of pesticide and planning of irrigation, dam water management, health emergency warning associated with the heatwave and cold waves, vector-borne disease (Mandal *et al.* 2020) and several other applications can be based on extended range outlooks. A review article published by Pattanaik et al., (2019) have documented the evolution of operational ERF along with its applications in various sectors have been discussed.

3.2. Operational ERF system of IMD

The ERF of weather using numerical model requires the role of ocean and thereby a coupled model is most appropriate for the same. For the forecasting of monsoon on this time scale, models must simulate the statistics (amplitude, phase propagation and frequency spectra) of the Intra Seasonal Oscillation (ISO) correctly. Unlike the short-medium and seasonal forecast systems of IMD, which have long histories, the ERF system of IMD is very new. During the initial decade of 21st century there were three drought years *viz*., 2002, 2004 and 2009. The 2002 drought year was associated with long dry spell of July (with departure of -51%) with all India seasonal rainfall departure of -19%. None of the model could predict this long dry spell of July and ultimately the seasonal forecast of 2002 was also not correctly predicted. Similarly, the monsoon drought of 2004 was also associated with long dry spell of July. These two drought years in quick succession associated with long dry spells of monsoon was instrumental for IMD to think about the prediction of active-break cycle of monsoon in the real time. However, due to the non-availability of proper tools and also of very low predictive skill it was very challenging to start the monsoon intra-seasonal forecast operationally. However, considering the importance and demand of extended range forecast, IMD started to generate operationally in house the forecast products of precipitation and temperature based on available model products from different centres in India and abroad from 2008 onwards. Initially some empirical models were used and subsequently the available dynamical model outputs were also used for the same. The two groups of products as highlighted in Pattanaik *et al.*, (2019) used since 2008 are discussed in the review paper.

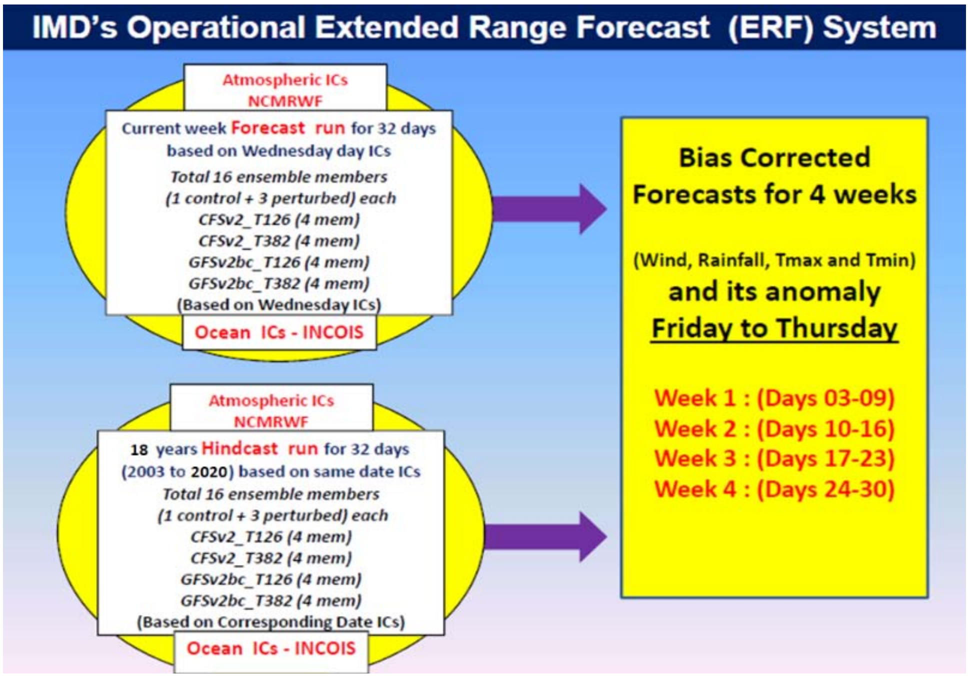

Fig. 3.1. IMD's Operational Extended Range Forecast (ERF) System

3.3. Current operational ERF system of IMD (since 2017)

At present the ERF system at IMD is running operationally once in a week on every (Wednesday) and the forecast is generated for 4 weeks starting from subsequent Friday to Thursday and so on. The current operational ERF modelling system is a suite of models at different resolutions based on the CFSv2 coupled model adopted from NCEP (Fig. 3.1). The operational suite is ported in ADITYA HPCS at IITM Pune for day-to-day operational run. As demonstrated in Fig. 3.1, the Multi-model ensemble (MME) out of the above 4 suite of models are run operationally for 32 days based on every Wednesday initial condition with 4 ensemble members (one control and 3 perturbed) each for CFSv2T382, CFSv2T126, GFSbcT382 and GFSbcT126. The oceanic component is the GFDL Modular Ocean Model V.4 (MOM4). The operational suite of models consists of (*i*) CFSv2 at T382 (≈ 38 km) (*ii*) CFSv2 at T126 ≺ 100 km) (*iii*) GFSbc (bias corrected SST from CFSv2) at T382 and (*iv*) GFSbc at T126 with 4 members each (Total 16 members). This is based on the Ensemble Prediction System (EPS) of IITM developed by Abhilash *et al.* (2014b) and Abhilash *et al.* (2015). For 2021 operational forecast the hindcast run is performed for 18 years (2003 to 2020) as shown in Fig. 3.1.The average ensemble forecast anomaly of all the 4 set of models runs of 4 members each (total 16 members) based on every Wednesday is calculated by subtracting corresponding 15- year model hindcast climatology on every Thursday, which is valid for 4 weeks for days 3-9 (week1; Friday to Thursday), days 10-16 (week2; Friday to Thursday), days 17-23 (week3; Friday to Thursday) and days 24-30 (week4; Friday to Thursday). This ERF system has the capability of predicting active-break cycle of monsoon which can be used for various applications.

The model was initially developed at IITM (Sahai *et al.*, 2013; Sahai *et al.*, 2015), which was run using the atmospheric and oceanic initial conditions available from NCEP once in every 5 days with forecast for 4 pentads. However, three major changes were carried out before it is implemented in IMD curing 2016 such as the hindcast and forecast runs are carried out with atmospheric and oceanic initial conditions available from NCMRWF and INCOIS respectively and not from NCEP. Secondly, the forecast day was fixed on Wednesday of every week and not at the interval of 5 days. Finally, the outputs are prepared for 4 weeks and not the pentads.

3.4. Verification of Extended Range Forecast

3.4.1. *Verification of ERF during monsoon 2021*

The 2021 monsoon rainfall over India during 1 June to 30 September 2021 has been 87.0 cm against long period average of 88.0 cm based on data of 1961-2010 [99% of its Long Period Average (LPA)] with the monthly rainfall over country as a whole was 110%, 93%, 76% and 135% of LPA during June, July, August and September respectively.

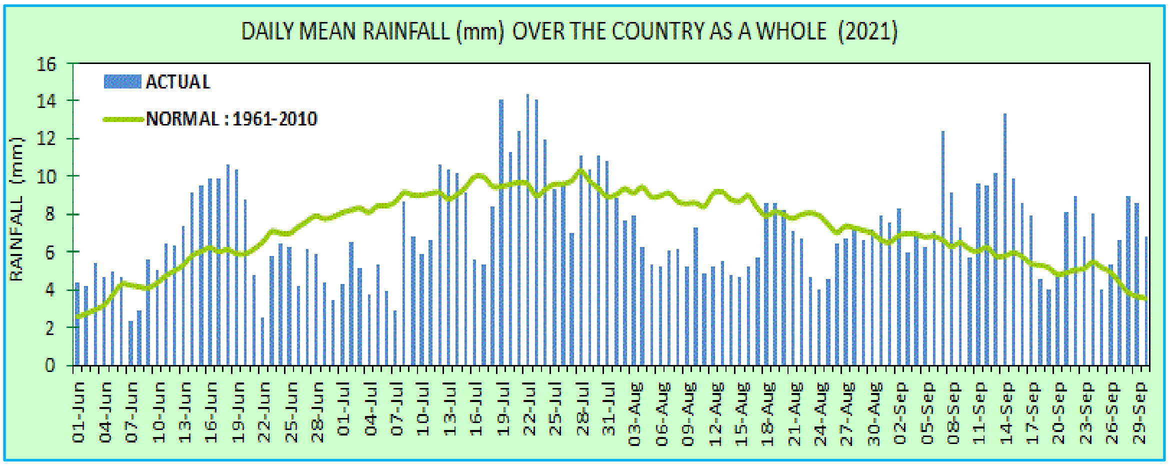

Fig. 3.2. Daily actual and normal rainfall over India during June to September, 2021

The daily monsoon rainfall over the country as a whole along with the normal rainfall is shown in Fig. 3.2. It may be mentioned here that the formation and movement of the cyclone TAUKTAE, over Arabian Sea (during 14-19 May) and severe Cyclonic storm “YAAS” over Bay of Bengal (during 23 to 28th May) helped to increase cross equatorial flow and the onset of monsoon. Subsequent features favored timely advance and monsoon covered entire country over many regions. However, monsoon cover entire country by 13thJuly against normal date of 8th July. In July, the country received slightly below normal rainfall (94% of LPA). The weak monsoon in July was mainly due to absence of any major monsoon disturbance over Bay of Bengal. Absence of such major systems in July also caused the weak monsoon trough. The monsoon trough lay to the north of the normal position or close to the foot hills of Himalayas on many days. It resulted in frequent and prolonged floods over northeastern India, Bihar and adjoining areas of east Uttar Pradesh. At the same time, major parts of central India received deficient rainfall. During August, many unfavorable features of monsoon appeared resulting in deficient rainfall for the country (76%). Negative Indian Ocean Dipole unfavorable for Indian monsoon prevailed during this month. Also, the absence of formation of monsoon depression and a smaller number of low pressure area (16-18 & 28-30 August) over Bay of Bengal caused this rainfall deficiency. Normally two monsoon depressions and two low pressure area forms in the month of August. Most of the days monsoon trough was located north of its normal position which cause subdued rainfall over Central Indian Region. Most of the days Madden Julian Oscillation (MJO) was in the phase 8, 1 and 2 which are unfavorable for monsoon rainfall activity. Also, there was less West Pacific Typhoon activity. Normally remnants of westward moving typhoons help to form Low Pressure Systems (LPS) over Bay of Bengal. In September, the country as whole received excess rainfall due to many favourable conditions for the monsoon. The negative Indian Ocean dipole weakened during the month of August and at the same time the cold anomaly in the equatorial Pacific strengthened. There was a monsoon depression and a cyclonic storm formed in the month of September. During most of the days MJO was in the phase 3, 4 and 5 which are favorable for monsoon rainfall activity and low pressure system. More West Pacific Typhoon activity and the remnants of these westward moving systems helped to form LPS over Bay of Bengal. All the LPSs followed west/northwestward track causing good rainfall activity, especially over central India and adjoining areas.

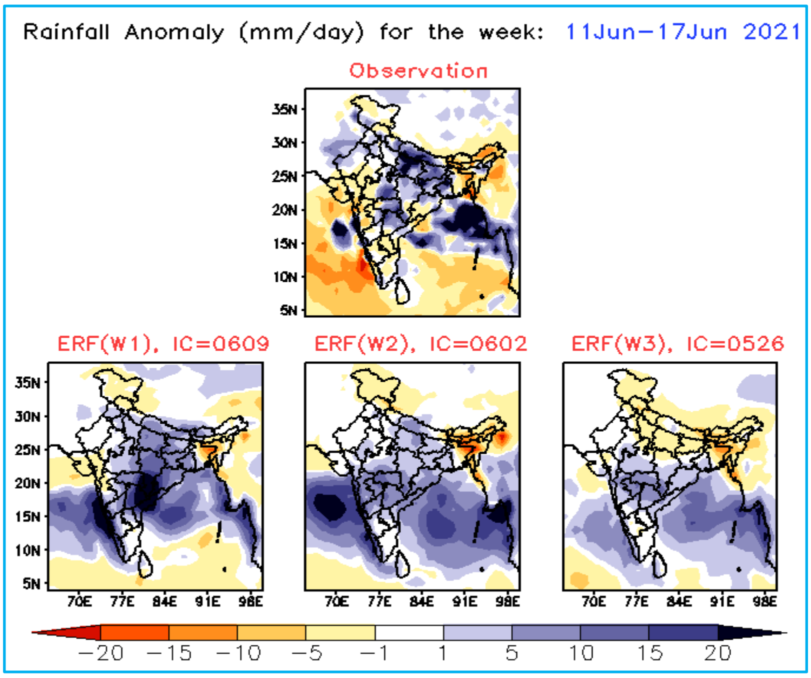

Fig. 3.3. Observed rainfall anomaly for the target week of 11-17 June 2021 with extended range forecast rainfall with three weeks lead time (ICs of 09 June, 2 June and 26 May, 2021)

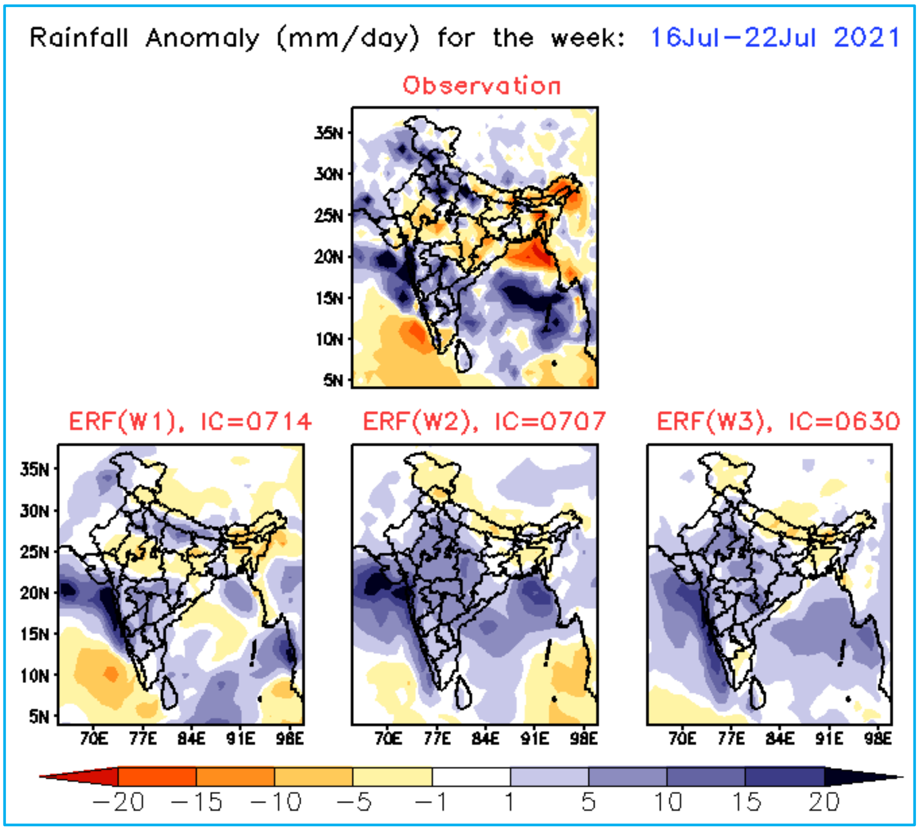

Fig. 3.4. Observed rainfall anomaly for the target week of 16-22 July 2021 with extended range forecast rainfall with three weeks lead time (ICs of 14 July, 07 July and 30 June, 2021)

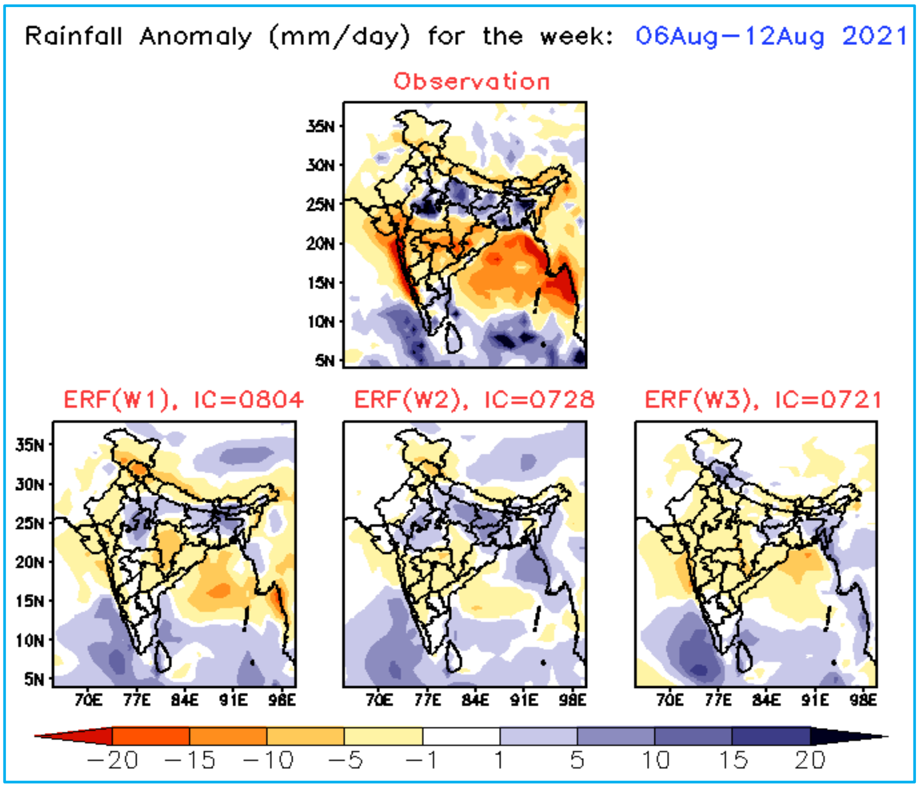

Fig. 3.5. Observed rainfall anomaly for the target week of 06-12 August, 2021 with extended range forecast rainfall with three weeks lead time (ICs of 04 Aug, 28 July and 21 July, 2021)

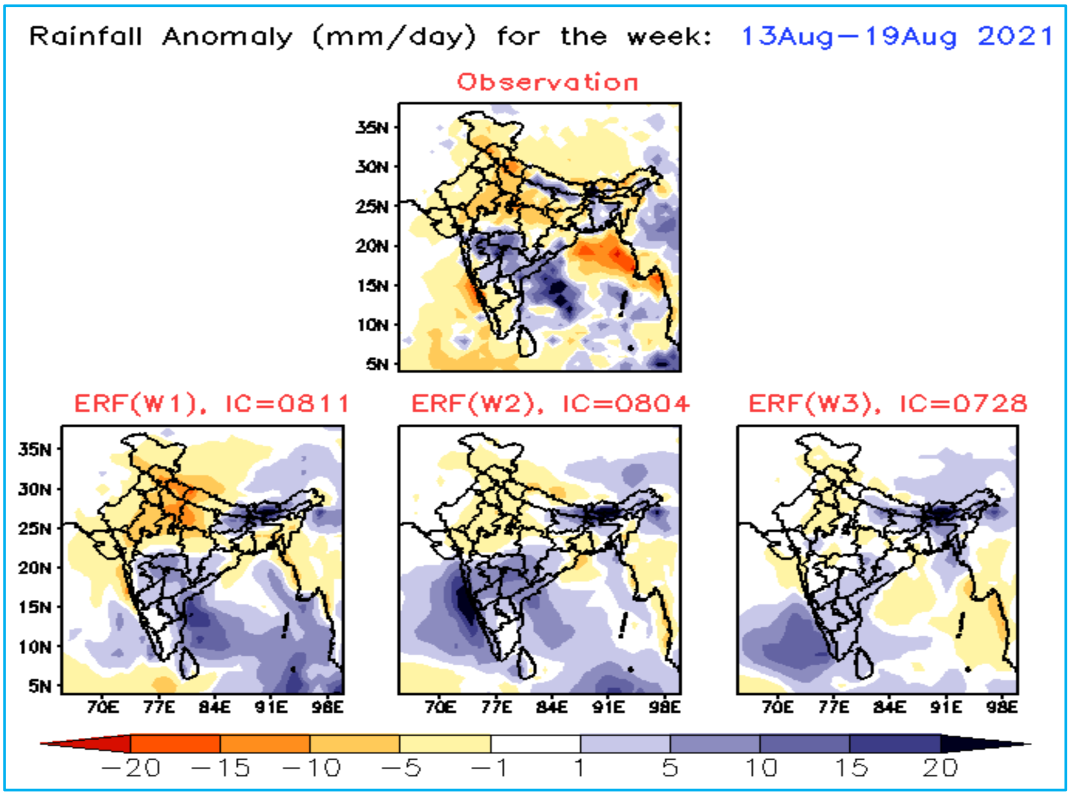

Fig. 3.6. Observed rainfall anomaly for the target week of 13-19 August, 2021 with extended range forecast rainfall with three weeks lead time (ICs of 11 Aug, 04 Aug and 28 July, 2021)

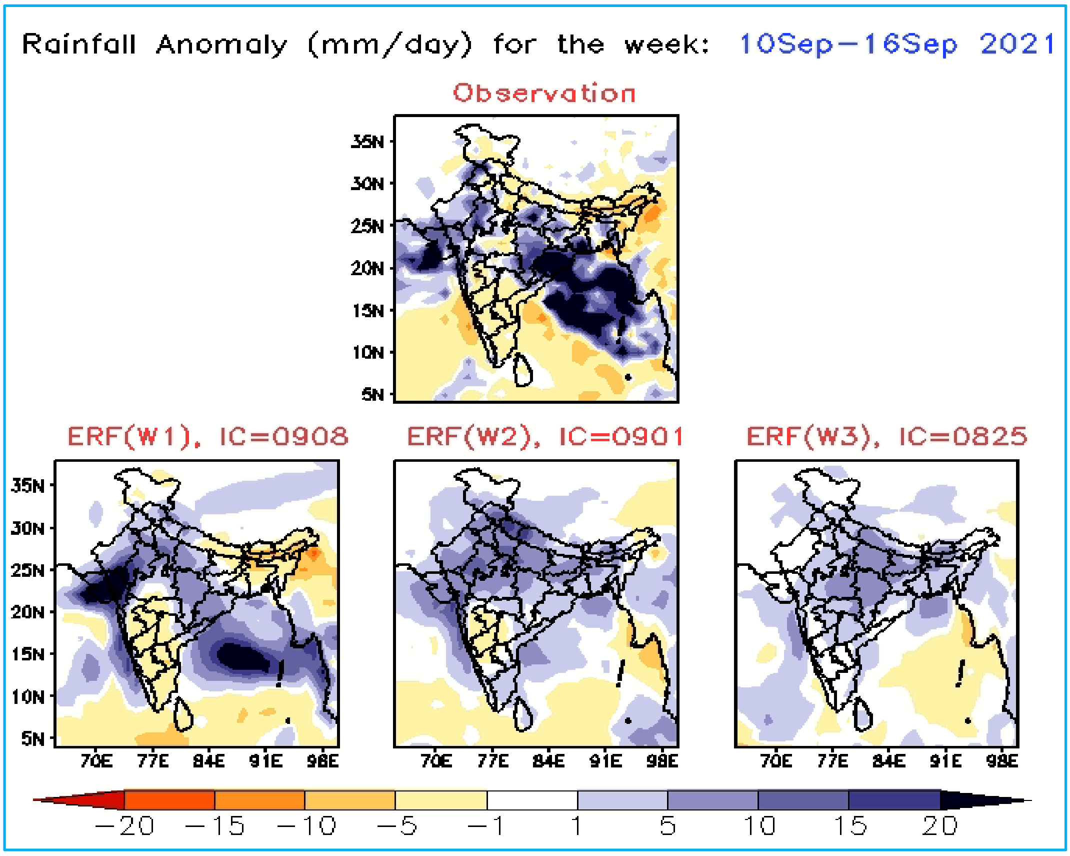

Fig. 3.7. Observed rainfall anomaly for the target week of 10-22 Sep 2021 with extended range forecast rainfall with three weeks lead time (ICs of 14 July, 07 July and 30 June, 2021)

The extended range forecast of rainfall during different phases of monsoon with forecast lead time of three weeks are shown in Fig. 3.3 to Fig. 3.7 for the target weeks of 11-17 June, 16-22 July, 2021, 06-12 August, 13-19 August and 24-30 September, 2021 respectively. Out of these five weeks, the target week from 11-17 June and 16-22 July are relatively active weeks of monsoon and the two weeks in August from 06 – 19 August are weaker monsoon phase and the last week of September from 24-30 September is the active monsoon period. The ERFs have captured the intra-seasonal variability very well.

Quantitatively, the ERF performance for the entire monsoon season of 2021 for 18 weeks period along with observed rainfall departure is shown in Fig. 3.8. As seen from Fig. 3.8 the operational ERF during 2021 monsoon season has captured the different phases of monsoon very well with significant correlation coefficients up to 4 weeks lead time.

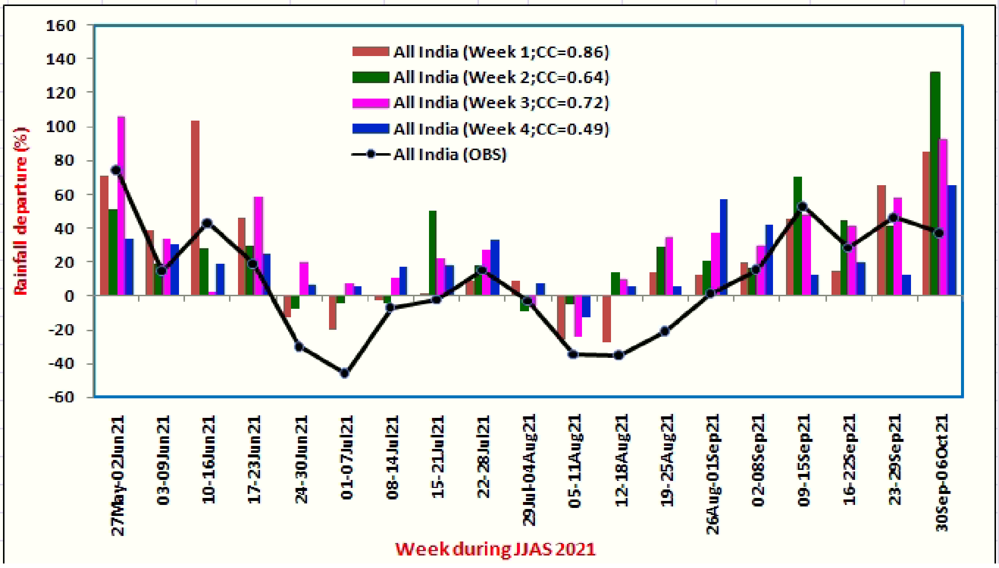

Fig. 3 .8. Weekly observed rainfall departure over India along with extended range forecast rainfall up to 4 weeks during the monsoon season from June to September 2021

3.4.2. *Met-subdivision and District level ERF for application in Agriculture*

As seen in the above analysis the ERF could capture the active and weak phases of monsoon along with its transition from active to break phase and vice versa. However, at very smaller spatial domains the model still has the problems. In view of that it is necessary to calculate the quantitative skill at smaller spatial domains. In order to see the quantitative verification of extended range forecast over the country as a whole (All India; ALI), four homogeneous regions of India and the rainfall over Monsoon Zone of India (MZI) as shown in Fig. 3.9 are considered for calculating the anomaly correlation coefficient (ACC). The four homogeneous regions of India are classified as Central India (CEI), Northeast India (NEI), Northwest India (NWI) and South Peninsular India (SPI) and the fifth zone is Monsoon Zone of India (MZI) covering mostly the central parts of India and little parts of northwest India as shown in Fig. 3.9.

The hindcast skill (Fig. 3.10) shows significant CC (95% level) for all India rainfall, MZI and CE India for week 3 forecasts. The CC, although positive it is slightly on the lower side for NW India, SP India and NE India. In week 4 only the CEI and MZI shows slightly higher CC, although not significant compared to other regions. The lowest skill over NE India in week 3 is basically due to the orographic rainfall over the region not predicted very well. Similarly, the lower skill over SP India compared to CE India and NW India is also associated with the west-coast rainfall not able to capture with sufficient lead time as it is also dominated by mountainous regions.

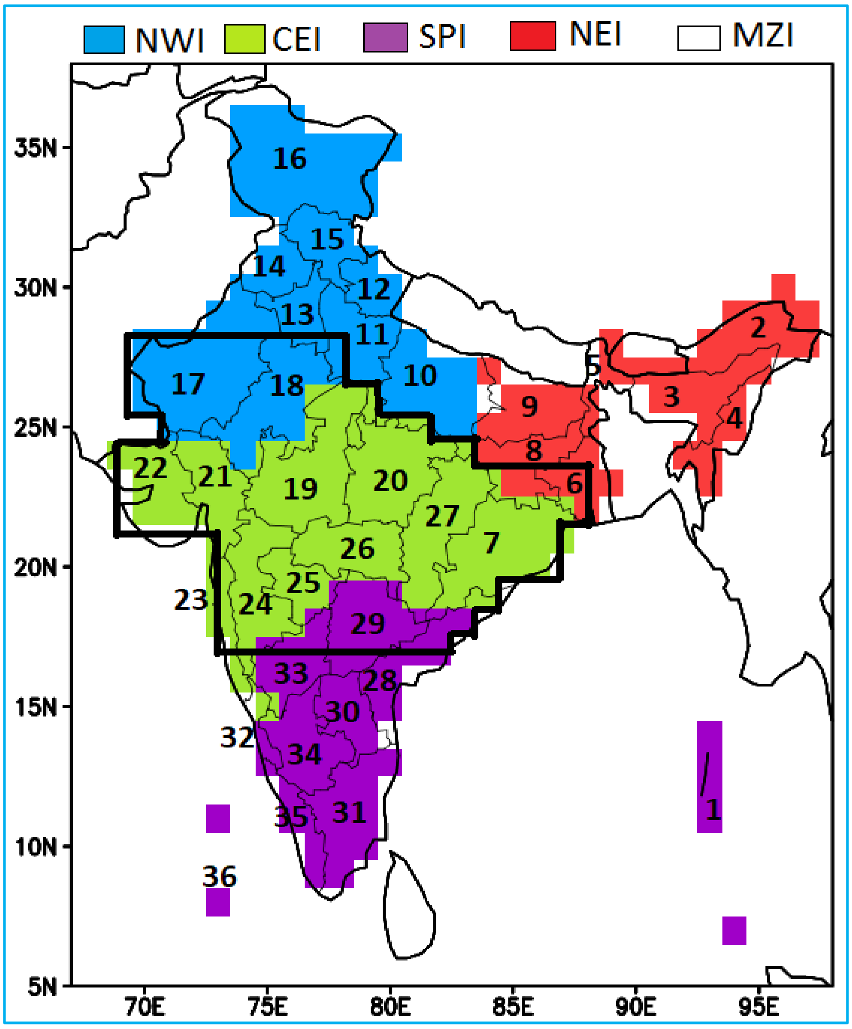

1 Andaman & Nicobar Islands
2 Arunachal Pradesh
3 Assam & Meghalaya
4 Nagaland Manipur Mizoram Tripura
5 Sub-Himalayan West Bengal & Sikkim
6 Gangetic West Bengal
7 Odisha
8 Jharkhand
9 Bihar
10 East Uttar Pradesh
11 West Uttar Pradesh
12 Uttarakhand
13 Haryana Chandigarh & Delhi
14 Punjab
15 Himachal Pradesh
16 Jammu & Kashmir
17 West Rajasthan
18 East Rajasthan
19 West Madhya Pradesh
20 East Madhya Pradesh
21 Gujarat Region
22 Saurashtra & Kutch
23 Konkan & Goa
24 Madhya Maharashtra
25 Marathwada
26 Vidarbha
27 Chhattisgarh
28 Coastal Andhra Pradesh
29 Telangana
30 Rayalaseema
31 Tamilnadu & Pondicherry
32 Coastal Karnataka
33 North Interior Karnataka
34 South Interior Karnataka
35 Kerala
36 Lakshadweep

Fig. 3.9. Homogeneous regions of India, NEI - Northeast India, NWI – Northwest India, CEI – Central India, SPI – South Peninsular India and MZI – Monsoon Zone of India

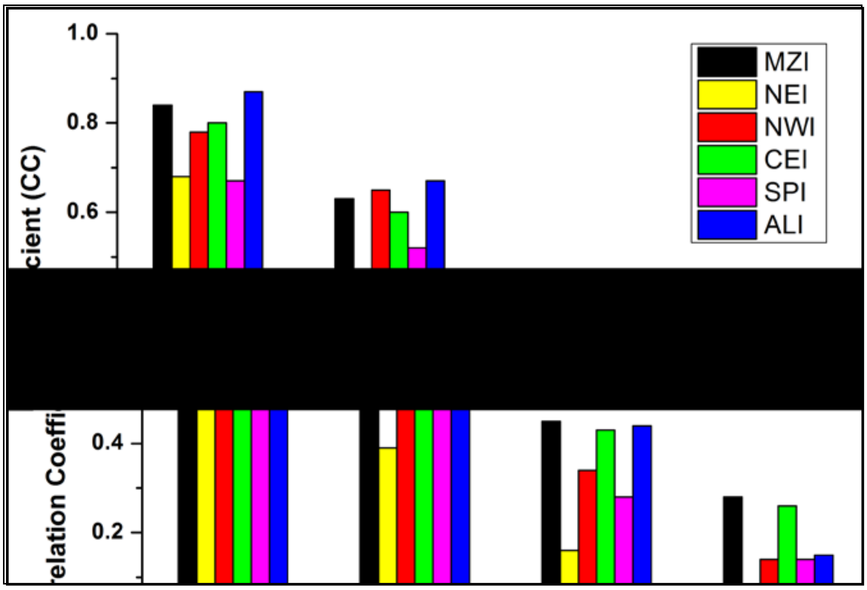

Fig. 3.10. The anomaly correlation coefficient for the hindcast period

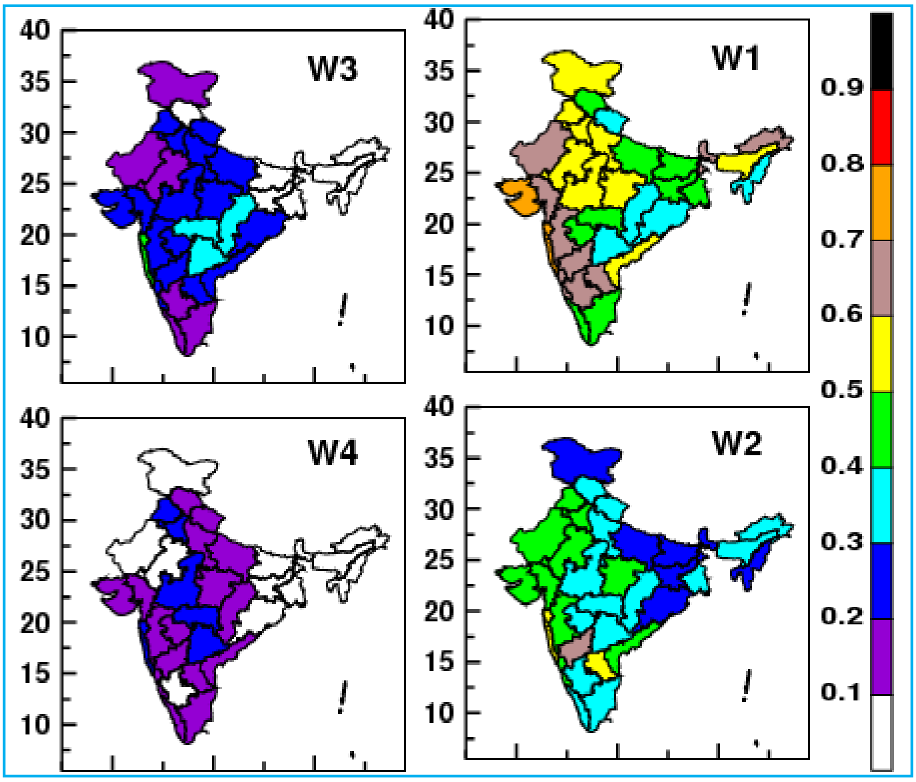

Fig. 3.11. Met-subdivision wise anomaly correlation co-efficient during the hindcast period

In order to see the forecast skill of extended range forecast for smaller spatial domains the 34 met-subdivisions of India is also considered for forecast verification as shown in Fig. 3.9. The met sub-division wise CC map is prepared for four weeks forecasts (Fig. 3.11) during the hindcast period from 2003 to 2020.As seen from Fig. 11 the week 1 forecast is mostly skilful over all the met-subdivisions of India. Week 2 forecast is also encouraging and skilful with many subdivisions with higher CCs, except some met subdivisions in north and northeast India, which have very poor skill. During week 3 and week 4 forecasts cases, parts of central India, northwest India and peninsula India are having higher skill and many met-subdivisions in eastern, northeast and northern India are with very lower skill. Thus, on met-subdivision level the forecast for at least two weeks can be used for various applications including the very important Agriculture sector.

In order to use the extended range forecast for Agromet applications the forecast for 36 met subdivisions of India is prepared for two weeks with categorising the subdivisions as below normal, normal or above normal category depending on the rainfall departure during the week. As per the classification a met-subdivision is considered to be above normal (AN) if rainfall departure≥ 20%; Normal (NN) if it is between +19% to -19% and Below Normal (BN) if it is≤ -20%. The sub-division wise observed rainfall departure over different met-subdivisions of India during the transition from active to weak phase of monsoon as sown in Fig. 3.8 is shown in Fig. 3.12a-b respectively. The two weeks forecast on met-subdivision level is widely used for application in Agriculture for farmers' advisory. Based on the forecast rainfall departure on met-subdivision level the two weeks forecast is prepared. The observed active to break transition of monsoon during 06-19 Aug, 2021 as shown in Fig. 3.12a and Fig. 3.12b is prepared for met-subdivision level forecast shown in Figs. 12a-b. As seen from Fig. 12a most of the meteorological subdivisions in central India and south peninsula changed into below normal category in week 1 forecast. The weak phase of monsoon in terms of below normal met-subdivisions over central and northern parts of India is also seen in week 2 forecast (Fig. 3.12b) over northwest India, however, monsoon is revised over south Peninsula India adjoining central India. Thus, the transition of monsoon from above normal to below normal is well captured in the extended range forecast, which is being used widely for Agromet advisory purpose.

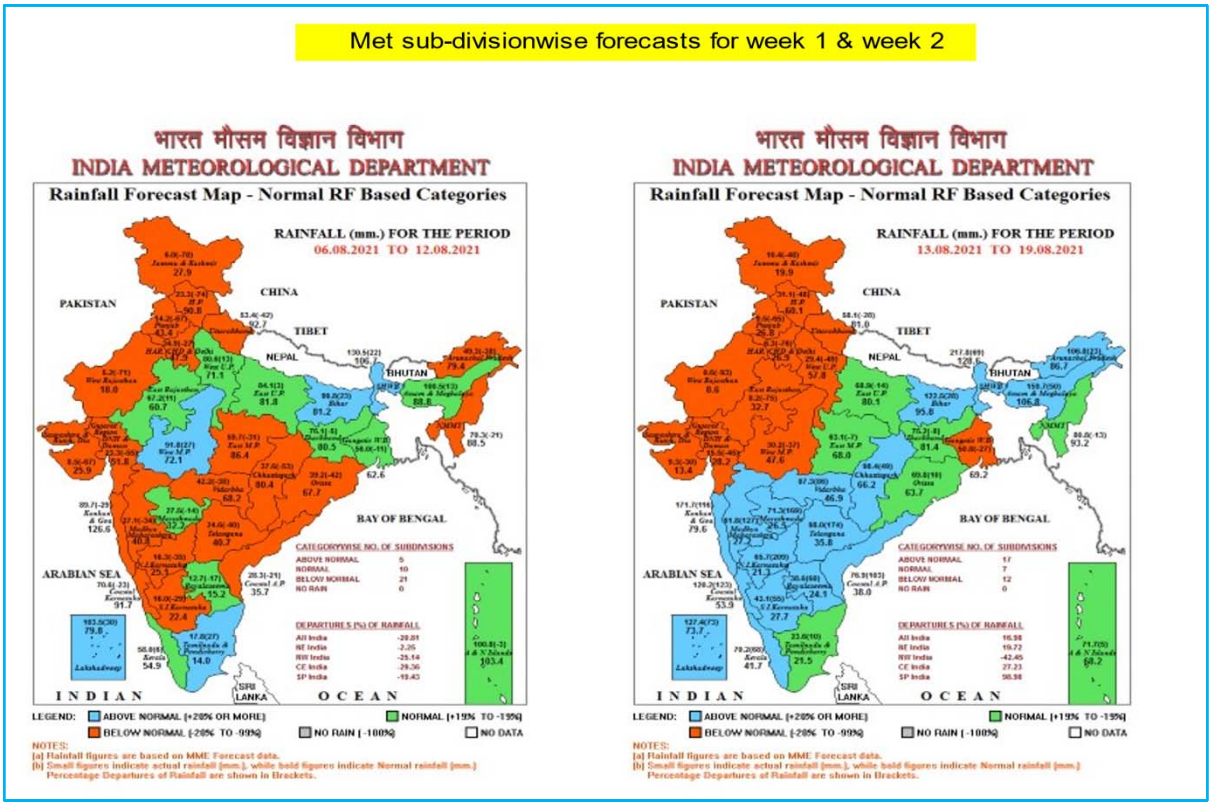

Fig. 3.12. Met-subdivision wise forecast for two weeks based on 04 August 2021 IC and forecast for (a) 06-12 August, 2021 and (b) 13-19 August 2021

3.4.3. *Verification of ERF of tropical cyclogenesis probability*

Pattanaik and Mohapatra (2021) in their review article have discussed the Evolution of IMD's operational extended range forecast system of tropical cyclogenesis over North Indian Ocean during 2010-2020. The ERF of cyclogenesis probability based on ECMWF and CFSv1 dynamical models had a modest beginning in 2010 with reasonable performance in case of severe cyclonic storm 'Jal' formed during the first week of November. The 2015 cyclone season with active Arabian Sea and inactive BoB was also very well captured in the real time ERF. IMD implemented CFSv2 coupled model for operational ERF in 2017 and based on it the Genesis Potential Parameter (GPP) is calculated for four weeks by using the dynamical variables like vorticity, divergence, vertical wind shear & mid-level relative humidity and was tested for the 'Ockhi' cyclone of 24-30 November, 2017. The GPP in case of 'Ockhi' cyclone was well predicted in the ERF, however, with a lead time of only one week.

The Improved GPP (IGPP) is used since 2019, which can be applied both over the Ocean and the land region. In the case of IGPP the vorticity and middle tropospheric humidity terms of GPP have been retained but the thermodynamic term is modified as the scaled and averaged equivalent potential temperature between 1000 and 500 hPa. The vertical shear between 850 and 200 hPa is scaled and averaged over an annular region between 100 and 200 km radii for each grid point. In case of Super cyclone "Amphan" it indicated the genesis of the system in "Week 1" and "Week 2" forecast and also its re-curvature northeastward like the observed track. The cyclone "Nisarga" over the Arabian Sea and its track towards western coast of India was well captured in week 1 forecast based on Initial Condition of 27

May, 2020. The IGPP also showed reasonable skill in ERF in predicting the genesis of three intense cyclones *viz*., 'Gati' during 21-24 November, 'Nivar' during 22-26 November and 'Burehi' during 30 November to 5 December and the two depressions of October, 2020. Considering the significant role of Madden Julian Oscillation (MJO) in BoB TC genesis, IMD is making use of the operational IGPP along with other parameters like current and forecast MJO, Tropical Cyclone Heat Potential etc and the value-added cyclogenesis probability outlook is being issued for two weeks on every Thursday (Pattanaik and Mohapatra 2021).

3.5. Districts level extended range forecast

The ERF at smaller spatial scales viz., at met-subdivision level and district level have been prepared for application in agriculture. As we have seen ERF is skillful and useful for two to three weeks.

Experimental ERF products are also being prepared for application in other sectors :-

- Agriculture and veterinary sector (The winter frost forecast and extreme low temperature will be used for crop advisory; high temperature for veterinary sector like poultry firm will be used)
- Water sector/Disaster management (The ERF forecast of active and break phases of monsoon, heavy rainfall, severe weather like cyclone etc will be generated for application in hydrological models and reservoirs operations).
- Health sector (indices like heat index, transmission windows for vector borne diseases, cold wave etc will be generated for services in health sector)
- Energy sector (The extreme high and low temperature forecasts products are being generated for potential use in power/energy sector)

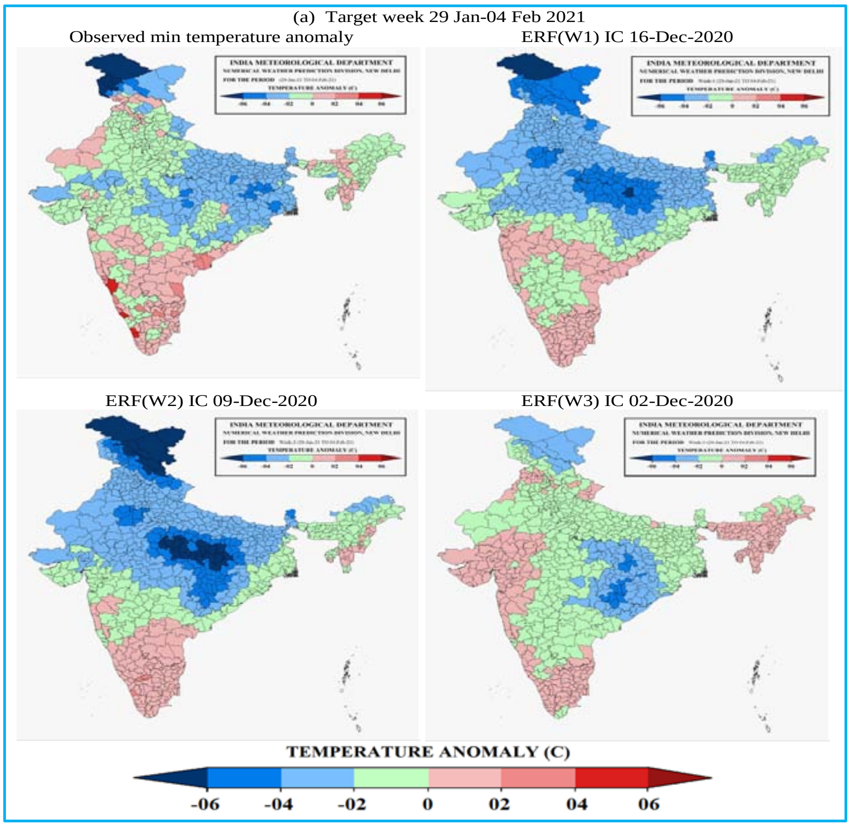

Fig. 3.13. Indicated the observed weekly minimum temperature anomaly and three weeks ERF minimum temperature anomaly for the same target week 29 Jan-04 Feb 2021

Fig. 3.13 indicated the observed weekly minimum temperature anomaly and three weeks ERF minimum temperature anomaly for the same target week 29 Jan-04 Feb 2021.

Like the district level forecast of maximum and minimum temperature the district level forecast of rainfall is also prepared on the experimental basis for various applications. Which is available in NWP's website.

Acknowledgement

The authors are thankful to the Director General of Meteorology, Dr. M. Mohapatra for providing all facility in IMD in carrying out this research work. Thanks are also due to the IITM's ERF Group, NCMRWF and INCOIS for collaborating with IMD in enhancing the extended range forecast activity of IMD in running the coupled model.

References

Pattanaik, D. R., Sahai, A. K., Mandal Raju, Phani Muralikrishna, R., Dey Avijit, Chattopadhyay Rajib, Joseph Susmitha, Tiwari Amar Deep, Mishra Vimal (2019) Evolution of operational extended range forecast system of IMD: Prospects of its applications in different sectors, *Mausam*, 70, 233-264.

Pattanaik, D. R., Sahai, A. K., Muralikrishna, R. P., Mandal Raju and DeyAvijit (2020) Active-Break Transitions of Monsoons Over India as Predicted by Coupled Model Ensembles. *Pure Appl. Geophys.*, https://doi.org/10.1007/s00024-020-02503-2.

Pattanaik, D. R., (2014) Meteorological subdivisional-level extended range forecast over India during southwest monsoon 2012. *Meteorology and Atmospheric Physics*, 124, 167–182.DOI 10.1007/s00703-014-0308-6.

Pattanaik, D. R., Das, Ashok Kumar (2015) Prospect of application of extended range forecast in water resource management: a case study over the Mahanadi River basin. *Natural Hazards*, 77, 575–595. DOI 10.1007/s11069-015-1610-4.

Sahai, A. K., Chattopadhyay, R., Joseph, .S, Mandal, R., Dey, A., Abhilash, S., Krishna, RPM, Borah, N., (2015) Real-time performance of a multi-model ensemble-based extended range forecast system in predicting the 2014 monsoon season based on NCEP-CFSv2. *Current Science*, 109, 1802-1813.

Sahai, A. K., Sharmila, S., Abhilash, S., Chattopadhyay, R., Borah, N., RPM Krishna, Joseph, S., Roxy, M., De, S., Pattnaik, S., Pillai, P.A. (2013) Simulation and extended range prediction of monsoon intra-seasonal oscillations in NCEP CFS/GFS version 2 framework. *Curr Sci*., 104, 1394-1408.

CHAPTER 4

High Resolution Rapid Refresh (HRRR) Modelling in IMD

AKHIL SRIVASTAVA, ANANDA K DAS, PRASHANT KUMAR and SAMBIT PANDA

ABSTRACT.IMD established the High-Resolution Rapid Refresh (defined hereafter as IMD-HRRR) modelling system in Aditya HPCS in January 2021 in collaboration with Space Applications Centre, Indian Space Research Organisation (SAC-ISRO). IMD-HRRR system domain extends for the entire Indian mainland by dividing it into three high-resolution domains, viz., Northwest (NW), East & Northeast (E&NE) and South Peninsular (SP) India domain. The IMD-HRRR system (based on WRF-ARW) is a real-time 2-km spatial resolution, an hourly updated, cloud-resolving, convection-allowing atmospheric model for three selected domains covering the entire Indian mainland. The IMD-HRRR modeling system is operationally run-in experimental mode by assimilating Radar data every hour (cyclic mode) and the forecasts for the next 12 hour is generated. This report presents a description of the operational IMD-HRRR model along with its performance in the month of August for duration (1st -10th August 2021). This report also provides IMD-HRRR model rainfall forecast products for the Chennai rainfall event of 30th December 2021.

4.1. Introduction

India Meteorological Department (IMD) is the operational arm of Ministry of Earth Sciences (MoES) with the mandate to provide weather related forecasts and severe weather warnings. In this regard, numerical weather prediction (NWP) model products and guidance are utilised to give forecasts for different temporal and spatial scales. There is a suite of numerical models which have been run by different institutions of MoES including IMD to achieve the above objectives. However, there has been a need to strengthen nowcasting service with the help of dynamical models. Thunderstorms occurring on a nowcast scale (upto 6/12 hours) are one of the most devastating and dangerous weather phenomena over the tropical region. However, at present, none of the NWP models run operationally in MoES institutions is dedicated for nowcast applications to forecast thunderstorms at very high resolution and with high temporal frequency.

The Doppler Weather Radars (DWRs) network is one of the most widely used observational systems for operational meteorology for forecasting in general, and is most crucial for nowcasting activities and for severe weather warning for the next few hours. DWRs have immense potential use in Meteorology, Hydrology and Cloud Microphysics applications due to its high spatial (~100 m) and temporal (~5-10 min) resolution. Polarimetric DWRs are especially important due to measurements of additional information related to the underlying microphysics and dynamics of the weather systems through polarimetric variables (e.g.. differential reflectivity, total differential phase, specific differential phase and cross-correlation coefficient). Doppler radar can be divided into several different categories according to the wavelength of the radar (e.g. L, S, C, X, K-band). L-band radars operate on a wavelength of 15-30 cm and a frequency of 1-2 GHz that are mostly used for clear air turbulence studies. S-band radars operate on a wavelength of 8-15 cm and a frequency of 2-4 GHz. Because of the wavelength and frequency, S band radars are not easily attenuated, which makes them useful for near- and far-range weather observation. C-band radars operate on a wavelength of 4-8 cm and a frequency of 4-8 GHz. The signal is more easily attenuated in C-band radar, so this type of radar is an optimal choice for short range weather observation. The frequency allows C band radars to create a smaller beam width using a smaller dish. X band radars operate on a wavelength of 2.5-4 cm and a frequency of 8-12 GHz. Because of the smaller wavelength, the X band radar is more sensitive and can detect smaller particles. These radars are used for studies on cloud development because they can detect the tiny water particles and also used to detect light precipitation such as snow. X-band radars also attenuate very easily and crucial for very short range weather observation. K-band radars operate on a wavelength of 0.75-1.2 cm or 1.7-2.5 cm, and a corresponding frequency of 27-40 GHz and 12-18 GHz. This band is split down the middle due to a strong absorption line in water vapour.

4.2. Radar Network Used for HRRR

To improve the nowcast to short-range forecasting of extreme weather hazards like thunderstorms, tremendous efforts and resources have been invested in the DWR network over the Indian region for detection and continuous monitoring of weather activities. A good number of DWR covers Indian landmass and they are maintained by IMD, Indian Air Force (IAF), and Indian Space Research Organisation (ISRO), and their utilization in the operational forecasting services are vital for nowcast. The details of 19 DWR stations (Location, Band) which are utilised for current IMD-HRRR modelling system is shown in Fig. 4.1. These DWR are extensively used over India for real time monitoring services, statistical nowcasting, particularly for Thunderstorms, lightening and related weather events which occur in a very short time period.

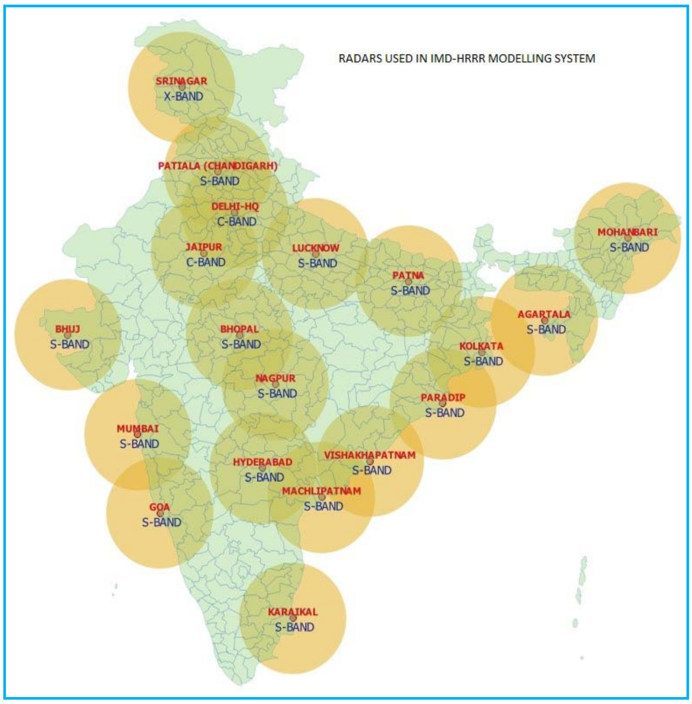

Fig. 4.1. DWR Network from IMD, IAF and ISRO over India

4.3. Methodology used for HRRR modelling system

To explore the potential of radar observations to improve short-range weather forecasts, various modelling studies were conducted earlier over different regions using three- or four-dimensional variational (3D-Var or 4D-Var) method, and most recently using hybrid data assimilation methods, a combination of variational and Ensemble Kalman Filter (EnKF). To explore the benefits of high temporal resolution in the very-short range weather prediction, initially 3-km convective-allowing High-Resolution Rapid Refresh (HRRR) system with Gridpoint Statistical Interpolation (GSI) data assimilation system was operationalized in NOAA/NCEP (Smith et al. 2008). The HRRR system used a specially configured version of the Advanced Research WRF (ARW) model and assimilated many novel and most conventional observations. The HRRR system was run using hourly cycling over a domain covering the entire conterminous United States using initial and boundary conditions from the hourly-cycled RAP (Rapid

Refresh Model). The HRRR provides unique convective-scale forecast guidance with high spatial and temporal resolution and demonstrated good skill and potential in providing nowcast guidance (Lee *et al.* 2019). In a study (Gowan *et al.* 2018) performance of HRRR model precipitation forecast was compared with coarse resolution NWP models over mountainous western US and it found better performance from HRRR due to better representation of topography. Similarly in a study (Cai & Dumais 2015) three weeks forecast from HRRR during 2010 summers over eastern United States was able to capture convective storm characteristics with regionally varying bias. In a separate study (Ikeda *et al.* 2013), HRRR winter season forecast for areal extent of precipitation and its timing was evaluated against observation across Eastern United States concluded that the larger synoptically forced systems were forecasted with better skills as compared to the small weather system. These studies showcasing the positive impact of the HRRR model gave a motivation for implementation of similar systems over the Indian region.

In order to strengthen the nowcasting activities and exploiting the importance of large DWR network over India, IMD established the High Resolution Rapid Refresh (defined hereafter as IMD-HRRR) modelling system in Aditya HPCS in January 2021 in collaboration with Space Applications Centre, Indian Space Research Organisation (SAC-ISRO). In the initial phase, the IMD-HRRR system was implemented over Northwest India. After successful implementation over this region, the IMD-HRRR system was further extended for the entire Indian mainland by dividing it into three high-resolution domains viz. Northwest (NW), East & Northeast (E&NE) and South Peninsular (SP) India domain (Fig. 4.2).

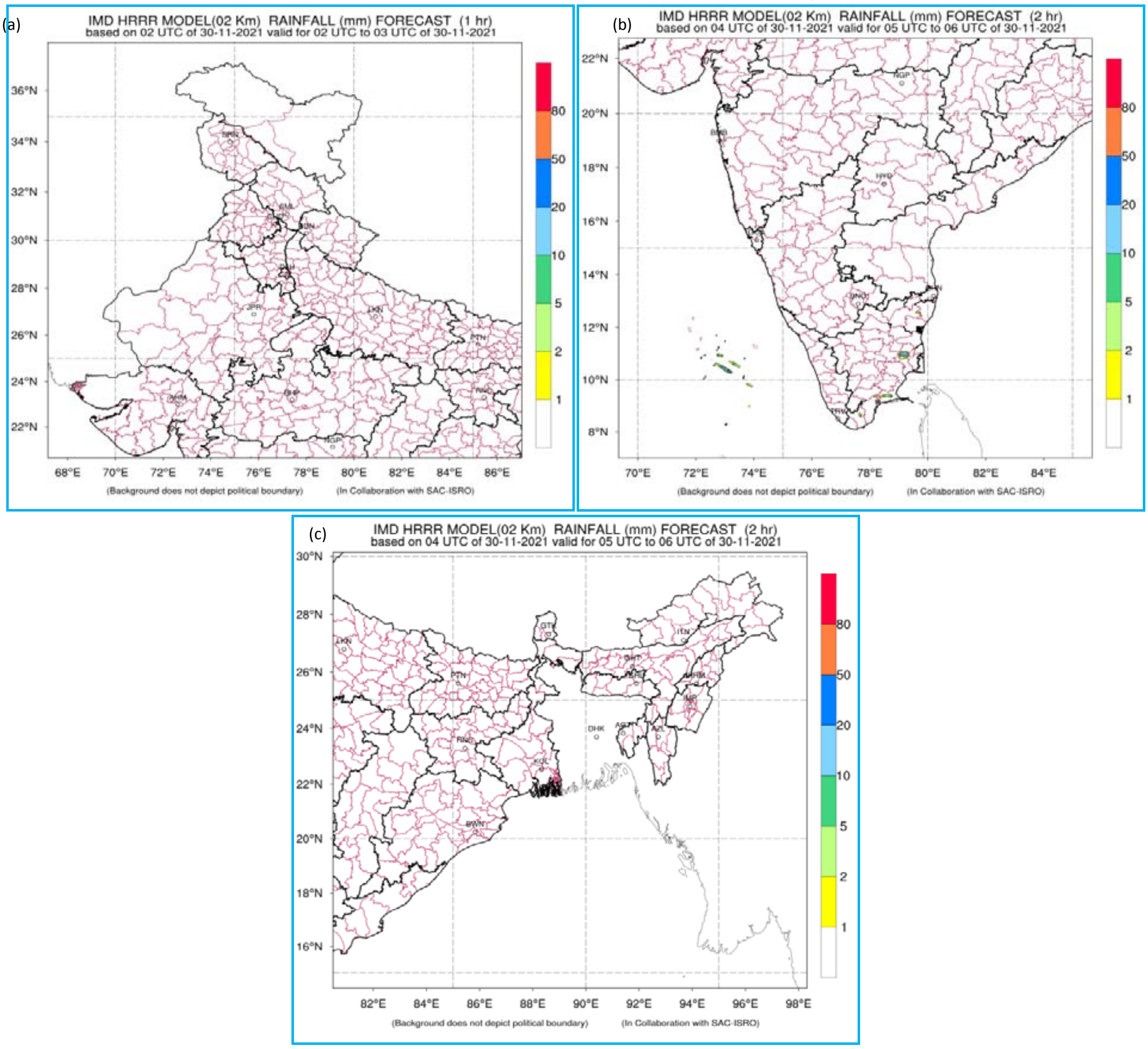

Figs. 4.2(a-c). The Three domains of HRRR (a) Northwest, (b) South Peninsular and (c) East & NorthEast

The IMD-HRRR system is a real-time 2-km spatial resolution, hourly updated, cloud-resolving, convection-allowing atmospheric model for three selected domains covering the entire Indian mainland. The IMD-HRRR modeling system used the WRF ARW core (ver 4.x) and it's 3D-Var data assimilation system. The global model (IMD-GFS; T1534L64) adopted from NCEP-GFS is operational in IMD since 2016. The details about the GFS T1534 can be found at https://www.emc.ncep.noaa.gov/emc/pages/numerical_forecast_systems/gfs.php), which is used to generate the initial and lateral boundary conditions of the regional model. Before incorporating the DWR data in the assimilation system, various pre-processing corrections like velocity de-aliasing, clutter management, beam blockage analysis etc. are implemented for all DWR stations (Details in Chapter 2). After these essential quality corrections, DWR data available in the time-window of + 30-minutes are assimilated in the IMD-HRRR system. Presently, 17 DWR stations (Figure 1) measured radial wind are assimilated into the IMD-HRRR modelling system. The IMD-HRRR modelling system is performed hourly and produces next 12 hour forecasts for nowcast applications. The experimental real time hourly rainfall and reflectivity forecast products are available on https://nwp.imd.gov.in/wrf_HRRR_nwp_sp.php.

The screen shot of the products available in IMD Website is given in Fig. 4.3.

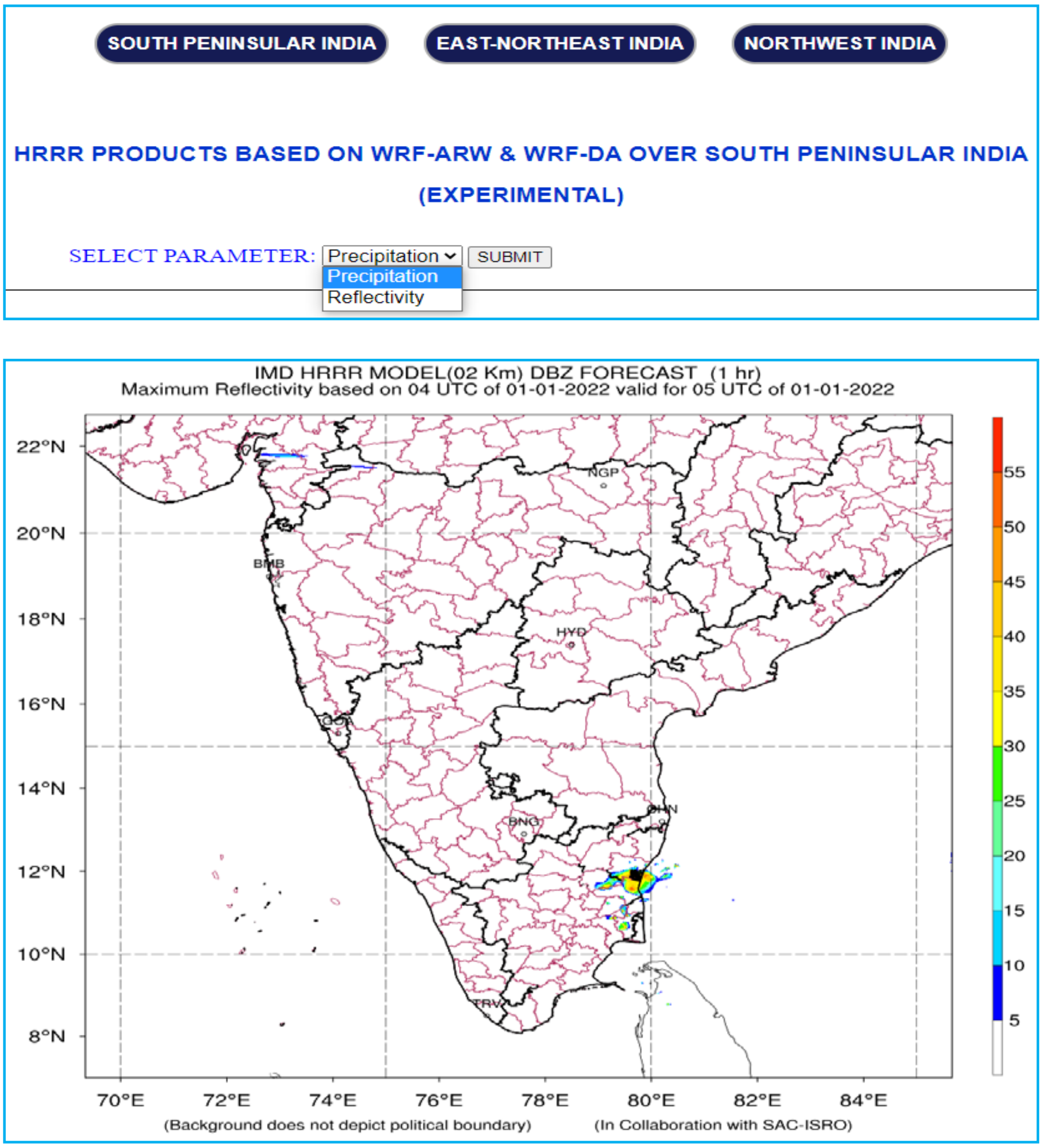

Fig. 4.3. Screen shot of the products available in IMD Website

Flowchart of HRRR system:-

Functional implementation of the HRRR model is shown via flowchart of the HRRR system in Fig. 4.4.

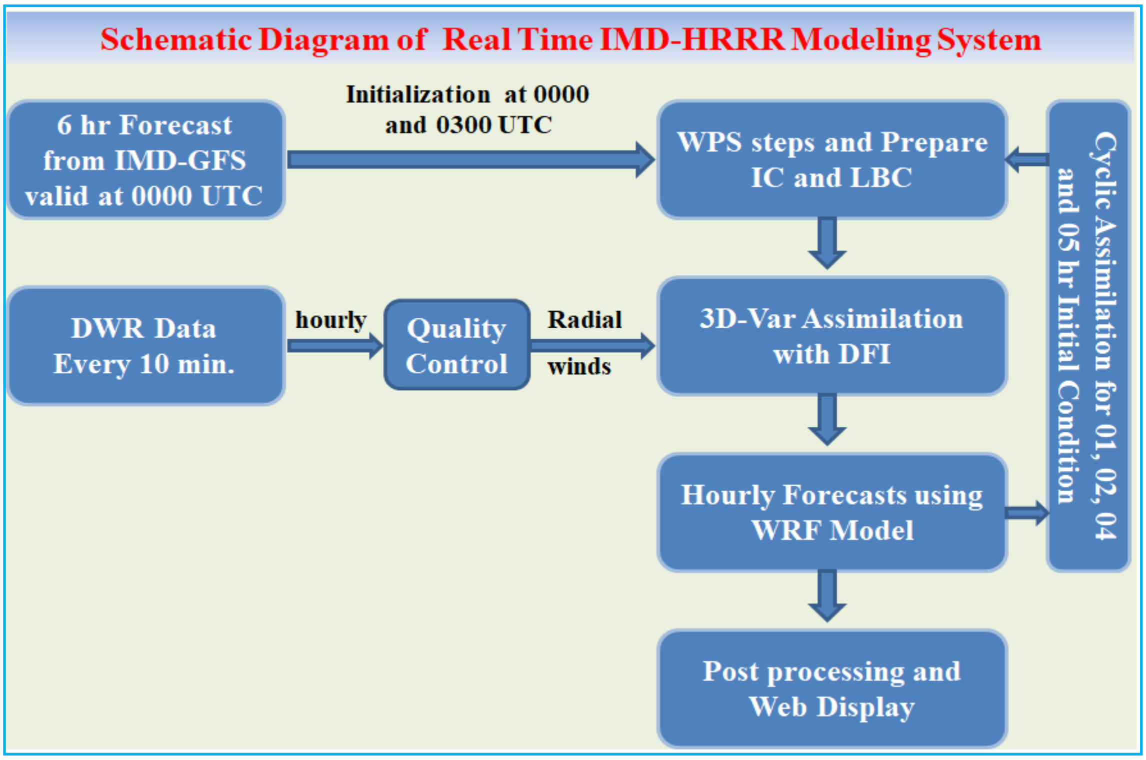

Fig. 4.4. Functional implementation of the HRRR model

The main functions of HRRR model can be divided into two parts:-

(a) Radar data quality control and pre-processing

(b) Hourly assimilation of high frequency Radar data into WRF model to generate forecast for nowcast applications.

The detailed description of DWR data processing and IMD-HRRR system are provided in section 4.4 and section 4.5 respectively. Results and discussions are given in section 4.6, details of IMD-HRRR forecast for Chennai event of 30th December 2021 in 4.7, and conclusion and future directions are presented in section 4.8.

4.4. Quality Control and Pre-processing of DWR Data

The weather radar functions on the basic idea of a reflection of energy. The radar sends out a signal, and the signal is then reflected back to the radar. The stronger that the reflected signal is, the larger the particle. Doppler radars apply Doppler effects and its measurement principle is shown in Fig. 4.5. The Radar data are obtained every 10-15 minutes through Global Telecommunication System (GTS) and these DWR observations are segregated based on different radar locations. However, the radar data suffer from various sources of noise (clutter) and errors. The most critical error in the radar reflectivity is the clutter (ground, sea, biological, anomalous propagation, etc.) and in velocity the most crucial source of errors are velocity foldings. Some other sources of errors include attenuation from heavy precipitation or wet radome, beam blockage, earth curvature effect, etc. Hence, the Radar Quality control procedures are of utmost importance, before utilizing the radar data into the WRF assimilation system. Propagation effect on the Radar beam and attenuation of radio waves are shown in Figs. 4.6 and 4.7. The description of various corrections implemented in the DWR for quality check and pre-processing is the first step before ingested data into the assimilation system. The following steps gives a brief account of the Radar Data observation, its quality control and pre-processing.

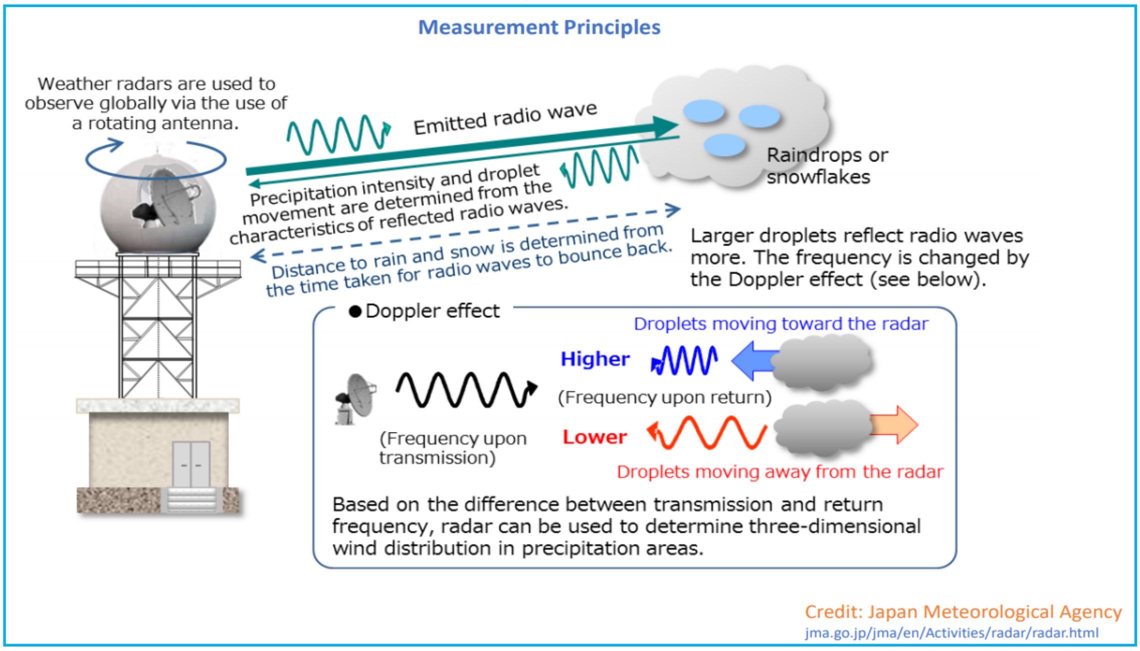

Fig. 4.5. Measurement Principles of Radar data

(i) Beam Blockage Analysis: - The beam blockage analysis is done using the wradlib beam-blockage library by identifying nearby hills etc. (Give references)

(ii) Clutter Mitigation:-The radar data is post-processed using Gabella filter algorithm (Gabella *et al.* 2002). It is used to identify non-meteorological echoes based on the fact that the non-meteorological echoes de-correlate rapidly in space and are spatially heterogeneous. The algorithm, in itself, is divided into two parts: the first part is a “spatial proximity” filter and the second is a test of compactness.

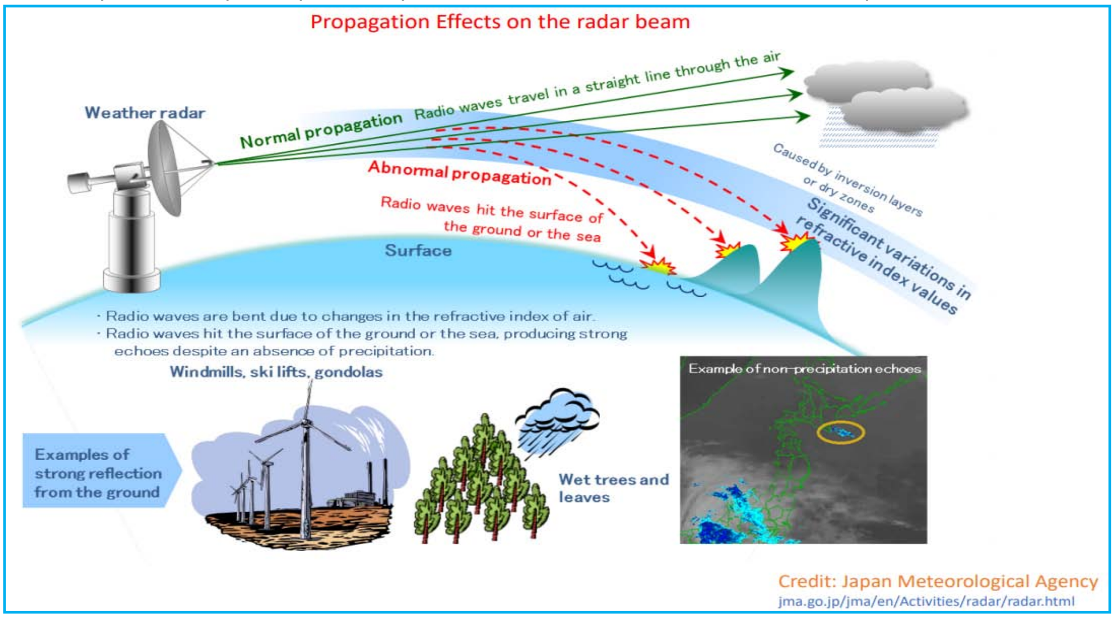

Fig 4.6. Error in Radar Data due to propagation effect on radar beam

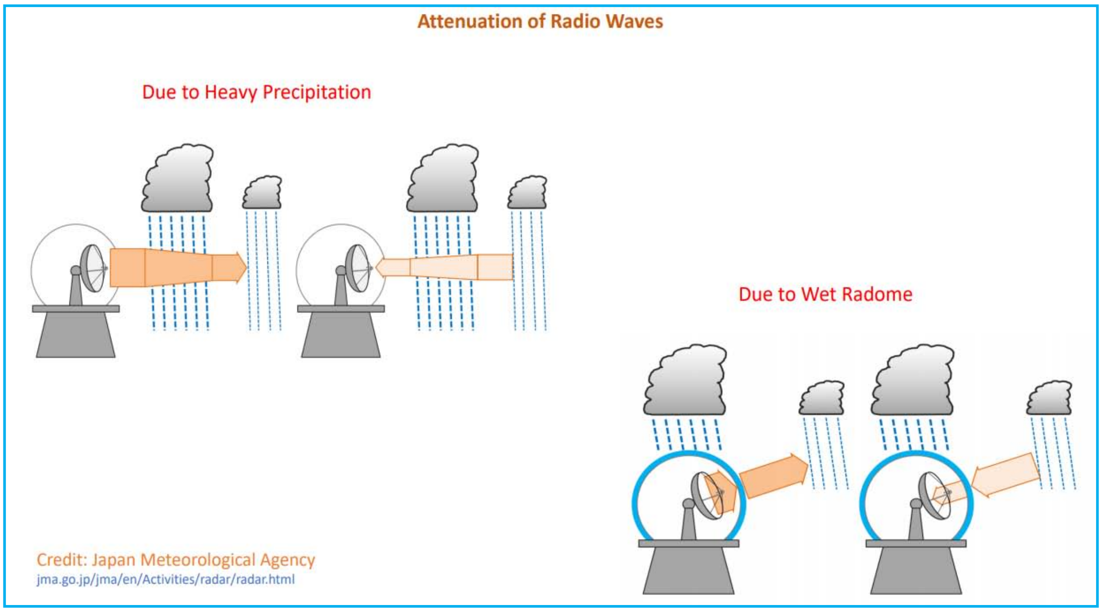

Fig.4.7. Error in Radar Data due to attenuation of Radio Waves

(iii) Fuzzy-logic based echo classification (Vulpiani *et al*. 2012): For each quality indicator Xj (i.e., X1= CMAP, X2 = V, X3 = TxZdr, X4 = TxRho, and X5 = TxPhi), the degree of membership in the non-meteorological target class is defined through a trapezoidal transformation function dj = d(Xj) [Vulpiani *et al.* (2012)]:

$$d(X_j) = \begin{cases} 0 & \text{if } X_j < X_{1,j} \text{ or } X_j > X_{4,j} \\ \dfrac{(X_j - X_{1,j})}{(X_{2,j} - X_{1,j})} & \text{if } X_{1,j} < X_j < X_{2,j} \\ \dfrac{(X_{4,j} - X_j)}{(X_{4,j} - X_{3,j})} & \text{if } X_{3,j} < X_j < X_{4,j} \\ 1 & \text{if } X_{2,j} < X_j < X_{3,j} \end{cases}$$

where $X_{i,j}$ is the i^{th} vertex of the trapezoid relative to the j^{th} quality indicator.

The parameterization used for defining dj is described in below Table 4.1.

Table 4.1.

Parameters used for the data quality evaluation

X_j	Weight	$X_{1,j}$	$X_{2,j}$	$X_{3,j}$	$X_{4,j}$
CMAP	0.5	10	30	70	∞
V	0.3	-0.2	-0.1	0.1	0.2
TxZdr	0.4	0.7	1.0	∞	∞
TxRho	0.1	1.1	0.15	∞	∞
TxPhi	0.4	15	20	∞	∞

(iv) Velocity De-aliasing: 2D multi-pass velocity de-aliasing technique is used which is based on spatial continuity of velocity fields [Zhang *et al.* 2006]. The velocity de-aliasing methodology is shown in flowchart at Fig. 4.8.

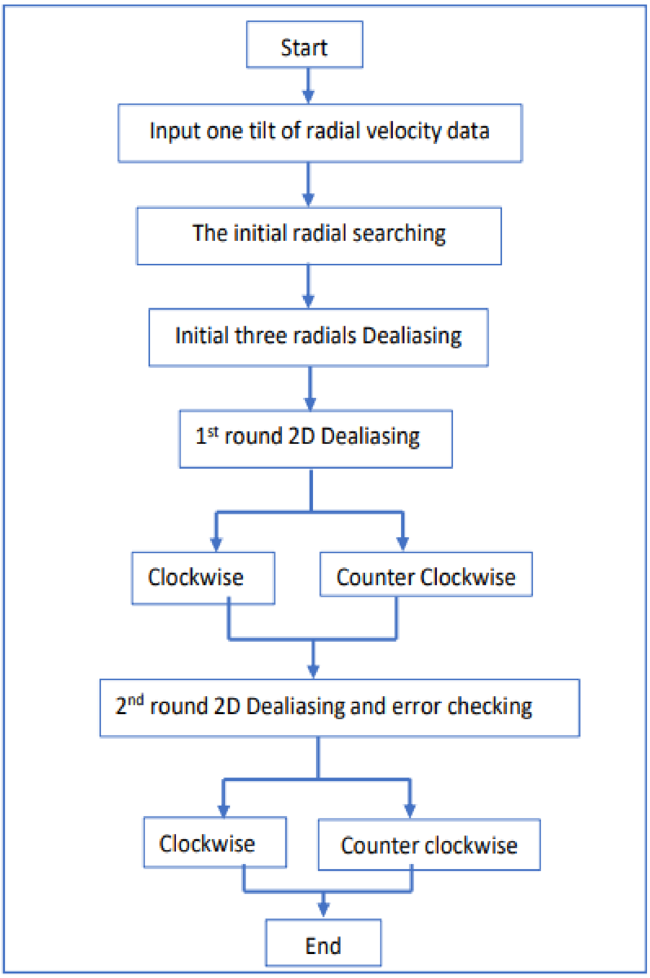

Fig.4.8. Flowchart for Velocity De-Aliasing

4.5. Methodology to implement IMD-HRRR System

The IMD-HRRR modelling system is implemented on the Aditya HPCS system to experimentally run on a real-time basis. The WRF model with a horizontal resolution of 2 km is run every hour to generate the forecast products for the next 12 hours after assimilating DWR measured radial winds available within ± 30 minutes time-window (DWR data available every 10-15 min frequency are utilized) using 3D-Var assimilation method available in the WRFDA software.

In IMD-HRRR implementation, WRF model is given cold start by utilising 6 hr forecast from IMD-GFS model as first guess. The quality controlled DWR winds are assimilated at this time step. After this cold start, the IMD-HRRR model is run on the cyclic mode by utilizing a 1 hr WRF forecast from the previous WRF run as the first guess followed by DWR assimilation that provided the initial condition for the subsequent cyclic runs. The model is integrated to produce a 12 hour forecast. For all simulations, lateral boundary conditions are opt from IMD-GFS global model (12 km resolution operationally runs at IMD). The block diagram of the implemented IMD-HRRR model is shown in Fig.4.9. Earlier, Sad *et al.* (2021) also suggested that the WRF maximum rainfall prediction skill is enhanced with DWR data assimilation experiment with DFI (Digital Filter Initialization) method and ensemble background error covariance statistics. Therefore to exploit the utility of DWR data, the IMD-HRRR model is implemented in IMD by assimilating DWR data with DFI method. However, at present the ensemble background error covariance statistics is not utilized, and may be a scope for further improvements with IMD-GFS ensembles. The details of model configuration and physics used in the IMD-HRRR system are presented in Table 4.2.

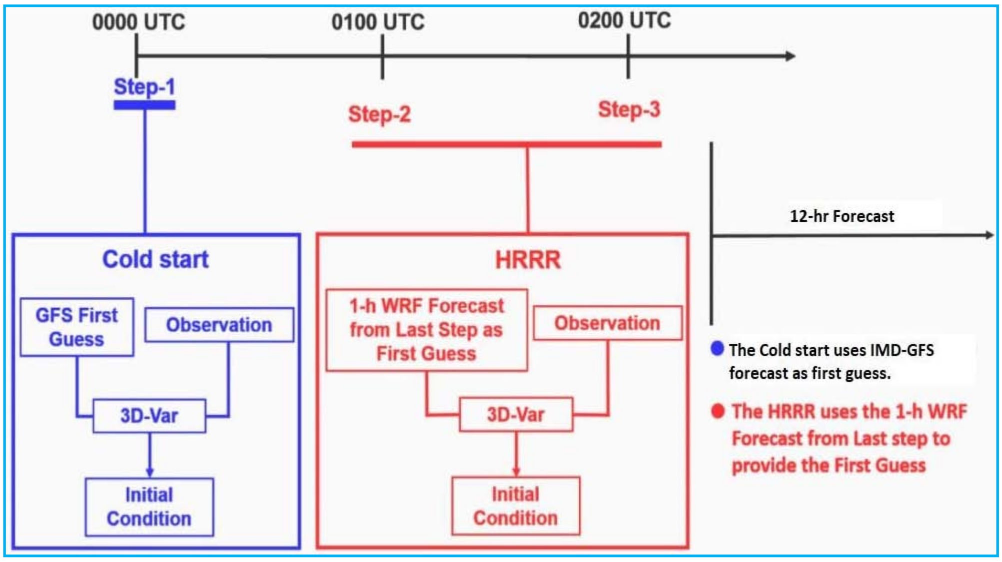

Fig. 4.9. Real time experimental setup of IMD-HRRR

Table4.2

Physics optics configured for IMD-HRRR model

IMD-HRRR model configuration (2 km Resolution)	
DOMAIN	Centre:- 29.6°N 77.1°E (968 X 968) NW DOMAIN Centre:- 22.5°N 89.4°E (921 X 881) NE DOMAIN Centre:- 15.0°N 77.5°E (881 X 881) SP DOMAIN
MAP PROJECTION	MERCATOR
GEO-PHYSICAL DATA RESOLUTION	SOURCE: USGS 30s
VERTICAL LEVELS IN ETA COORDINATES	36 levels in Normalized Pressure
TOP BOUNDARY	10 hPa
CLOUD MICROPHYSICS	Double-Moment 6-class (WDM6)
RADIATION LONGWAVE & SHORTWAVE	RRTMG Scheme
RADIATION SCHEME FREQUENCY	15 MINUTES
SURFACE LAYER OPTIONS	Monin-Obukhov (Janjic Eta) Similarity scheme
SURFACE LAYER PHYSICS	Noah Land-Surface Model
PLANETARY BOUNDARY LAYER	Mellor-Yamada-Janjic (Eta) TKE scheme
PBL SCHEME FREQUENCY	Every Time Step
CUMULUS PARAMETERIZATION	New SAS Scheme
CUMULUS PARAMETERIZATION FREQUENCY	EVERY 5 MINUTES

4.6. HRRR Forecast Validation

The HRRR forecast for the three domains (NW, SP and E&NE) is validated against the different synoptic observations (zonal winds, Meridional winds, Temperature, Pressure and Humidity) during 01st August to 10th August, 2021. The Root mean square deviation for zonal winds, Meridional winds, Temperature, Pressure and Humidity are shown in Fig. 4.10. The RMSD values for these meteorological parameters shows that the error spread is constant across the forecast hours with respect to synoptic observations. With respect to different domains, the least RMSD is seen for the South Peninsular domain for Humidity, Temperature and Pressure fields, whereas maximum deviation in error is seen for the North West Domain. However, for zonal winds the RMSD is maximum for south peninsular domain and minimum for East and NorthEast Domain. RMSD for pressure is about 1.5 hPa for East & SouthEast and South Peninsular domain, whereas it is less than 2 hPa for Northwest domain. The RMSD for Temperatures is 2-3 degree centigrades for East & SouthEast and South Peninsular domain, whereas it is about 4 degree centigrade's for Northwest domain. RMSD for meridional winds is comparable for all the three domains and is around 2m/sec. RMSD for Humidity is of the order of approx 6 g/kg for the northwest domain and is about 4 g/kg for other two domains.

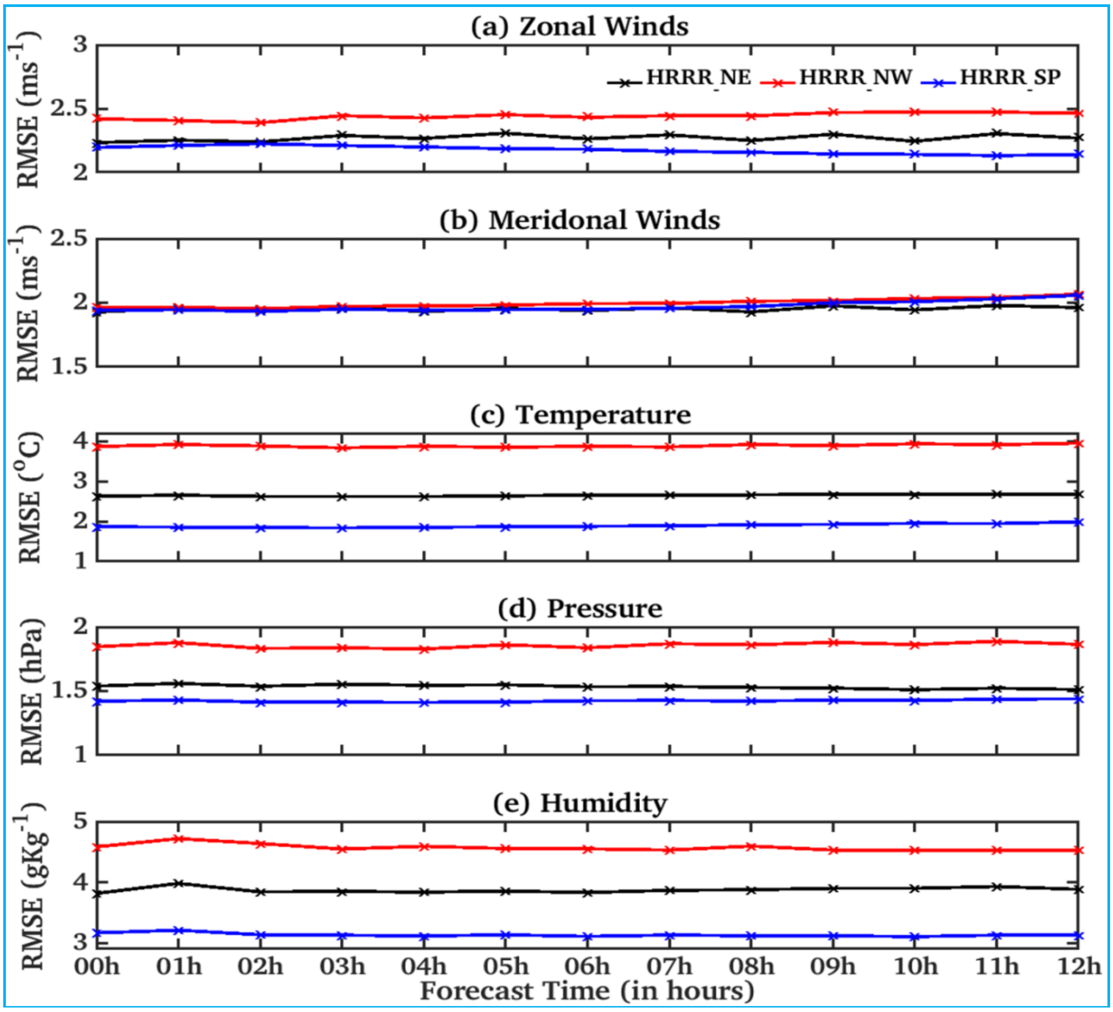

Fig. 4.10. Synoptic Validation

The HRRR forecast for East & NorthEast domain as well as for South peninsular domain is also validated against the Buoy observations as the domains cover some sea area as well. The RMSD displayed in Fig 4.11 shows that the Pressure and Winds (Zonal as well as Meridional) deviation are lesser for the South Peninsular domain as compared to the East & NorthEast domains. Whereas the error deviations for Temperatures are more for South Peninsular as compared to East and North East domain. RMSD for Pressure is close to 1 hPa for both the domains whereas temperature error is close to 1 for South Peninsular domain and is less than 1 for East & Northeast domain. The winds RMSD is approximately less than 4 m/s and near about 5 m/s for East & NorthEast domains for Meridional and zonal winds respectively.

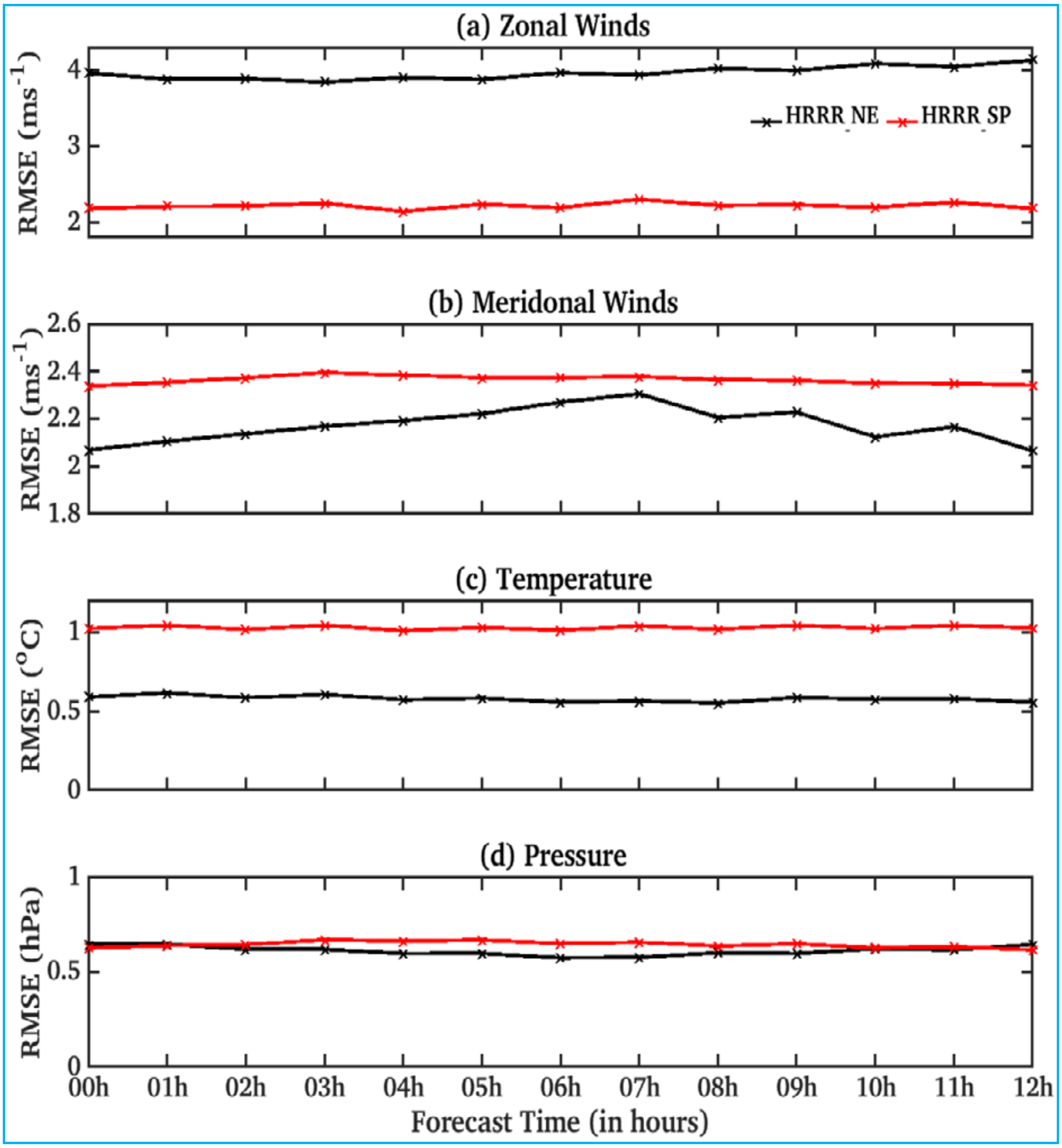

Fig. 4.11. Buoy Validation

The observed GPS Precipitable water is also used as reference for validation of HRRR forecast and statistics is shown in Fig. 4.12. The results shows that the more bias is seen for the South peninsular and Northwest Domain, where bias is approximately -0.5 mm and 0.5 mm respectively. The bias for East & NorthEast domain is very close to zero for the first 2 hours forecast and is less than 0.5 mm for other forecast hours. In terms of RMSD, minimum deviation in general is seen for Northwest domain and maximum deviation is seen for East & North East Domain for the first 5 forecast hours and then it becomes maximum for South Peninsular domain from 6th to 12th hour forecast. RMSD ranges between 3.2 mm to 3.6 mm for all three domains.

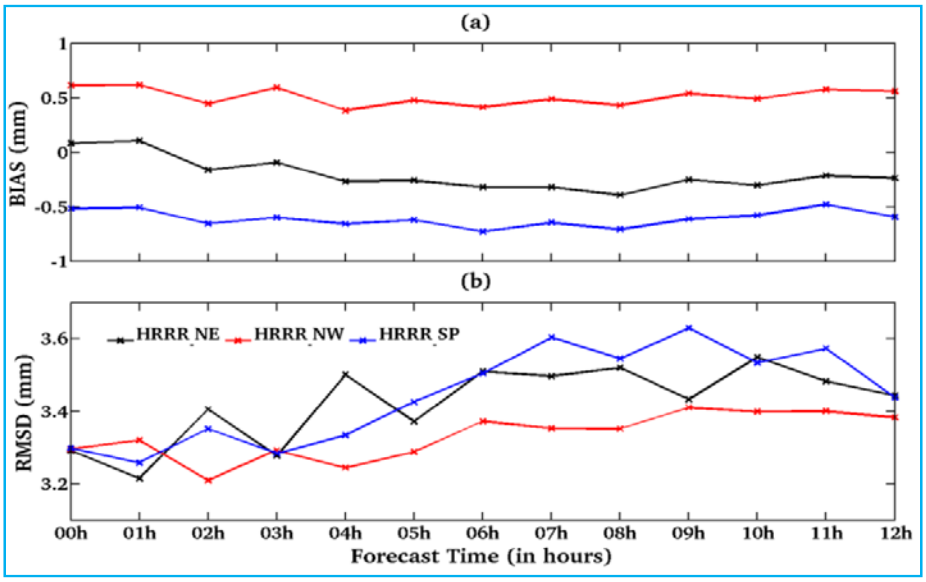

Fig. 4.12.GPSPW Buoy Validation

Scatter plots for GPSPW validation are also shown in Fig 4.13 for the three domains. Number of observations used for the E & NE domain is 5824, for the NW domain is 8826 and for the SP domain is 10331. The bias for the three domains SP, E & NE and NW are 0.06 mm, 0.02mm and -0.05mm respectively and corresponding RMSD is found out to be 0.34mm, 0.34mm and 0.33mm respectively for SP, E & NE and NW domains. Very strong correlation is also observed between the GPSPW observations and HRRR forecasts of the order of 0.99, 0.97 and 0.90 for E & NE, NW and SP domains respectively.

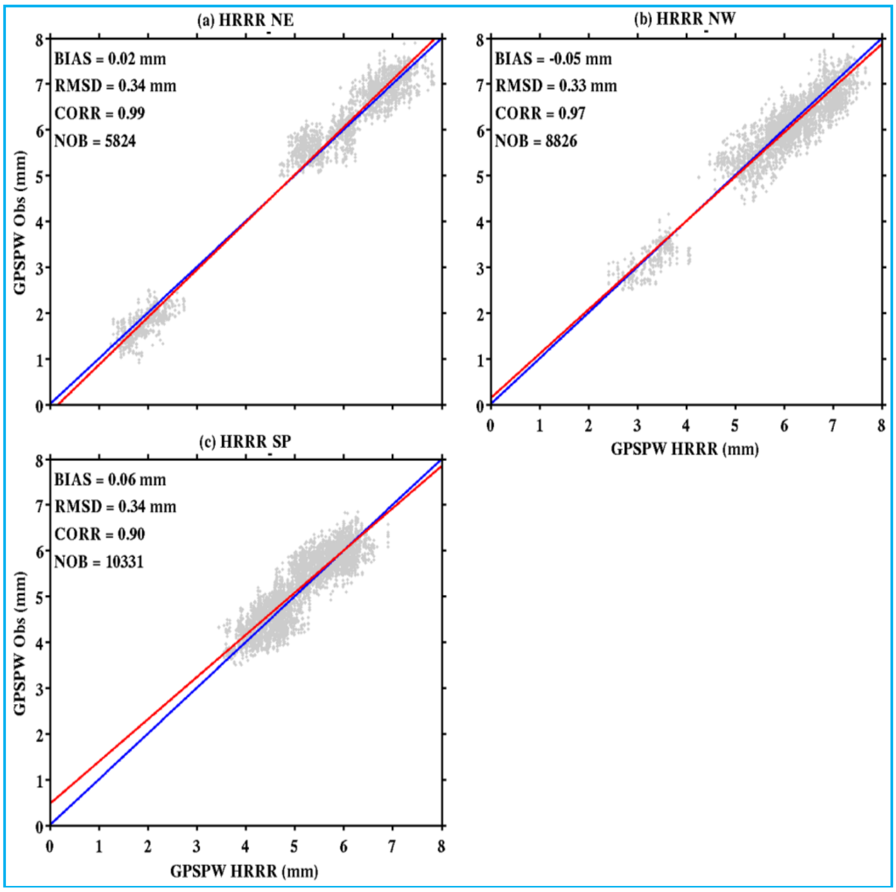

Fig. 4.13. GPSPW Scatter Plot

The HRRR forecast is also validated against the METAR observations for the three domains. The results are qualitatively similar to the synop validation where the SP domain is showing the minimum deviation and NW domain is showing the maximum deviation with respect to Humidity and Temperatures. For pressure fields maximum deviation is seen for SP domain whereas the RMSD for pressure is comparable between the E & NE and NW domains. The RMSD temperature value across the forecast hour is about 2 deg centigrade for SP domain and is close to 4 deg C for NW domain. The RMSD values for humidity are also 2 gm/kg for the SP domain and are close to 4 gm/kg for NW domain. The RMSD temperature and RMSD Humidity for E & NE domains are less than 3 deg centigrade and less than 3 g/kg respectively. The RMSD for zonal winds is comparable among the three domains and is of the order of 2 m/s where for meridional winds the RMSD is close to 1.5 m/s for SP domain whereas it is close to 2 m/s for SP as well as E & NE domains. The validation results with respect to METAR observations are shown in Fig. 4.14.

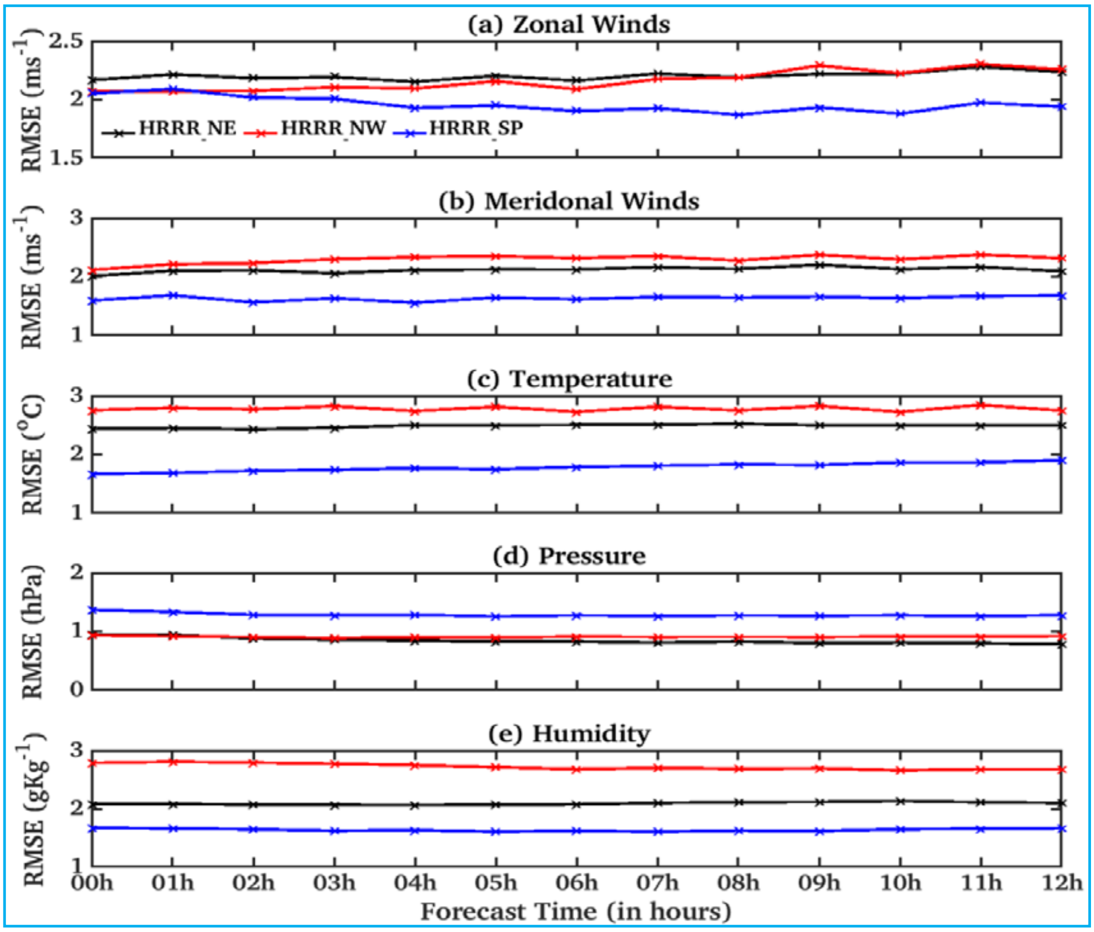

Fig. 4.14. METAR Validation

The Radar Data is the prime constituent for temporally high frequency of data assimilation used in HRRR. The HRRR forecast is also validated against the Radar observations and the results are shown in Fig 4.15 & Fig 4.16. Fig 4.15 shows the HRRR model predicted radial winds velocity against the Radar observed Radial winds velocity. The results show that the bias in radial winds is least for the E & NE domains and is close to 0.1 m/sec for the 12 hours forecast period. The maximum bias in radial winds is observed for the NW domain, where the bias is seen of the order of 0.6 m/sec for most of the forecast hours during 12 hours lead time. The SP domain also has a lesser bias in radial velocity of the order of 0.2 m/sec during the 12 hours forecast period. RMSD also shows the least deviation in errors for the E & NE domain with close to 5 m/sec during the forecast hours. Whereas for NW and SP domains the RMSD values with respect to radial velocity is close to 6 m/sec during the forecast hours.

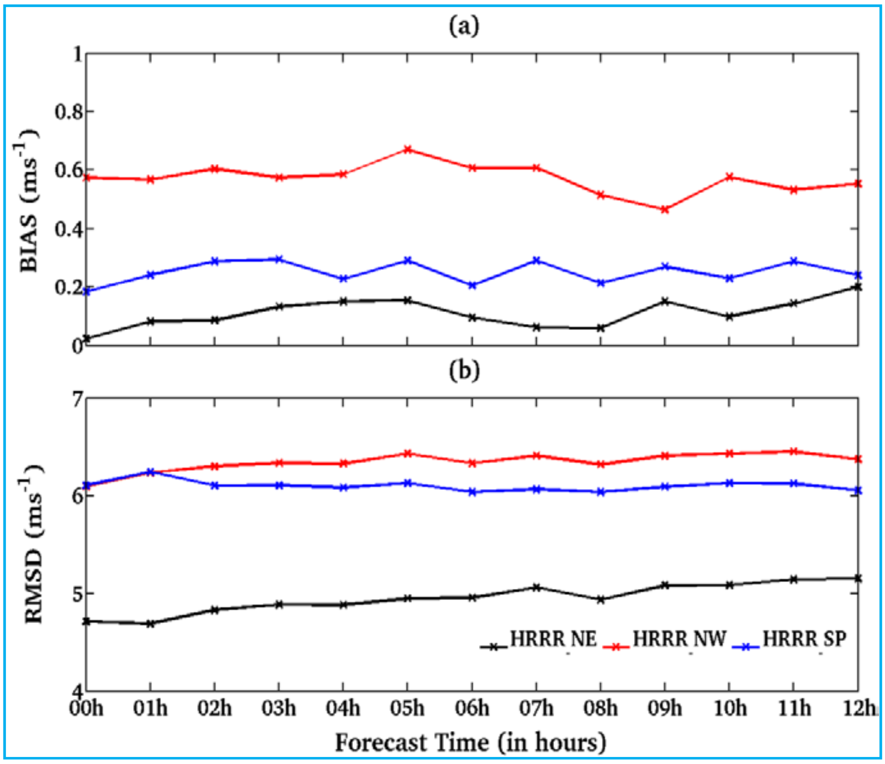

Fig. 4.15. Radar Observation Validation

The Fig. 4.16 shows the Radar Distribution of radial velocity. The X-axis shows the difference of DWR based radial velocity and HRRR forecasted Radial Velocity. The Y-axis shows the number of observations which are validated. It is seen with the help of the curve around 0, that the most of the Radar based radial winds observations are matching with the HRRR forecasted radial winds for all the three domains. For the E & NE domain the flattened curve shows the ratio of forecast having error is more as compared to other domains for more observations, more error in radial wind velocity as compared to other domains. The Bias for the three domains NW, E & NE and SP in terms of radial winds velocity is 0.6 m/s, 0.1 m/s and 0.2 m/s respectively. The corresponding RMSD is 6.3 m/s, 4.9 m/s and 6.1 m/s respectively for NW, E & NE and SP domains.

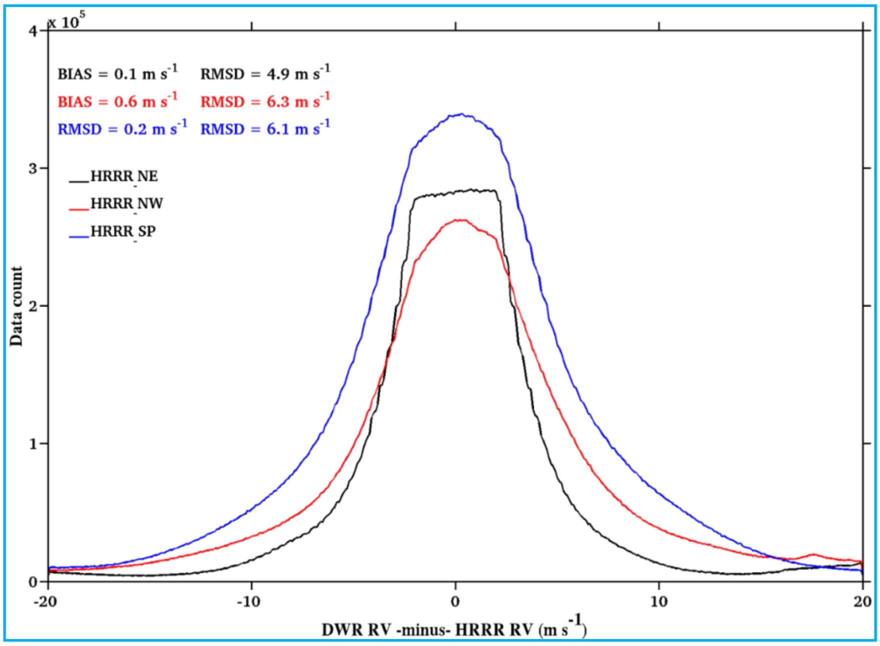

Fig. 4.16. Radar distribution

4.7. Conclusion and Future Prospects

The extremely heavy rainfall was reported in Chennai on 31st December 2021 (Rainfall occurred from 0830 IST of 30th December to 0830 IST of 31st December 2021). Fig 4.17 shows the district-wise rainfall recorded by IMD in Tamilnadu and Fig. 4.18 shows the significant amount of rainfall in different stations of Tamilnadu on 31st December 2021 respectively.

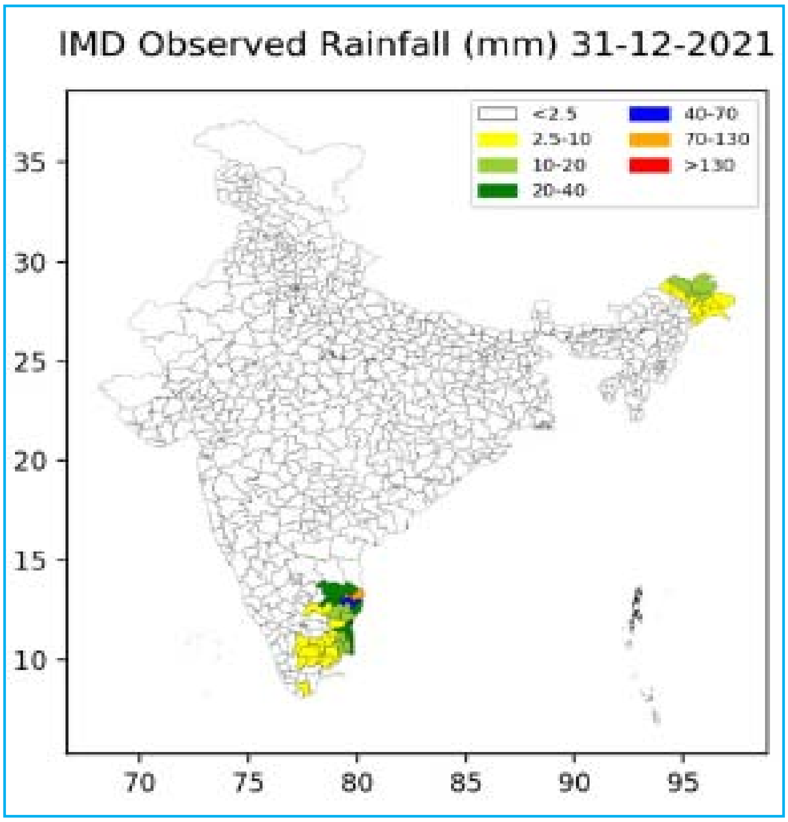

Fig. 4.17. Rainfall recorded District wise in Tamil Nadu on 31st December 2021

Significant Amount of 24 hr Rainfall recorded on 31 Dec 2021

Highest Rainfall is 24 Cm, DGP office Chennai

♦ **Significant amount of Rainfall** (7 cm or more): **Tamil Nadu**: **Chennai**: DGP office-24; MGR Nagar & Chennai (N)-20; Anna University-19; Anna University ARG, Perambur & Chennai AP-15; Sholinganallur-12; **Tiruvallur**: Ambathur & Poonamallee-20; Chembarabakkam-19; Koratur-12; Poondi & Red Hills-10; Cholavaram & Thamaraipakkam-9; **Mayiladuthurai**: Sirkali-11; Kollidam-10; Mayiladuthurai-7; **Kancheepuram**: Sriperumbudur-9; **Chengalpattu**: Kelambakkam-9; **Cuddalore**: Chidambaram AWS-7.

Fig. 4.18. Significant amount of Rainfall

The Tamilnadu rainfall event was well captured by IMD-HRRR model as shown below in Fig. 4.19 & 4.20 from the two operational forecasts based on initial conditions of 08 UTC of 30th December 2021 and 10 UTC of 30th December 2021.

IMD-HRRR Hourly Rainfall (mm) F/C based on IC 08 UTC 30 Dec 2021

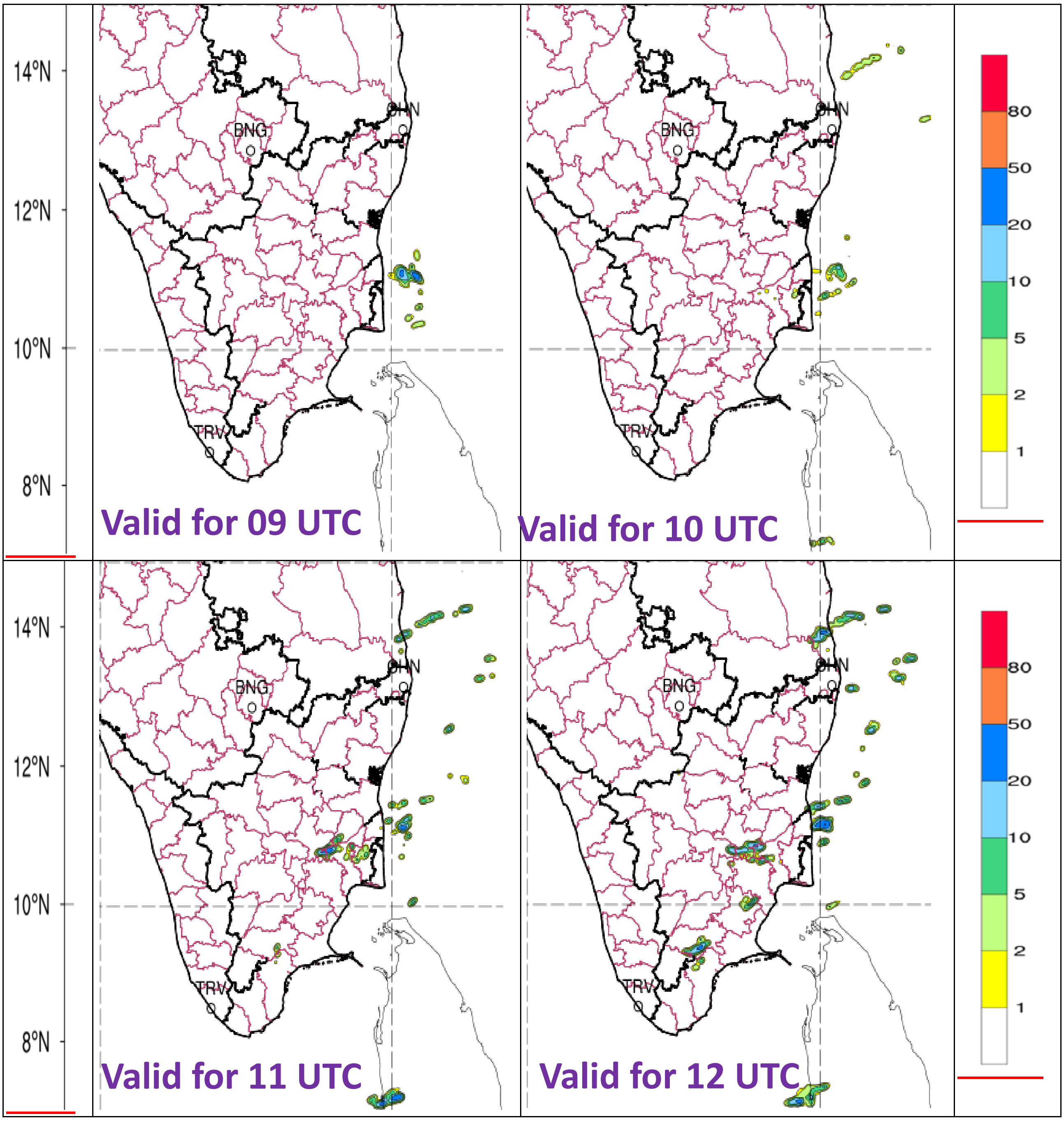

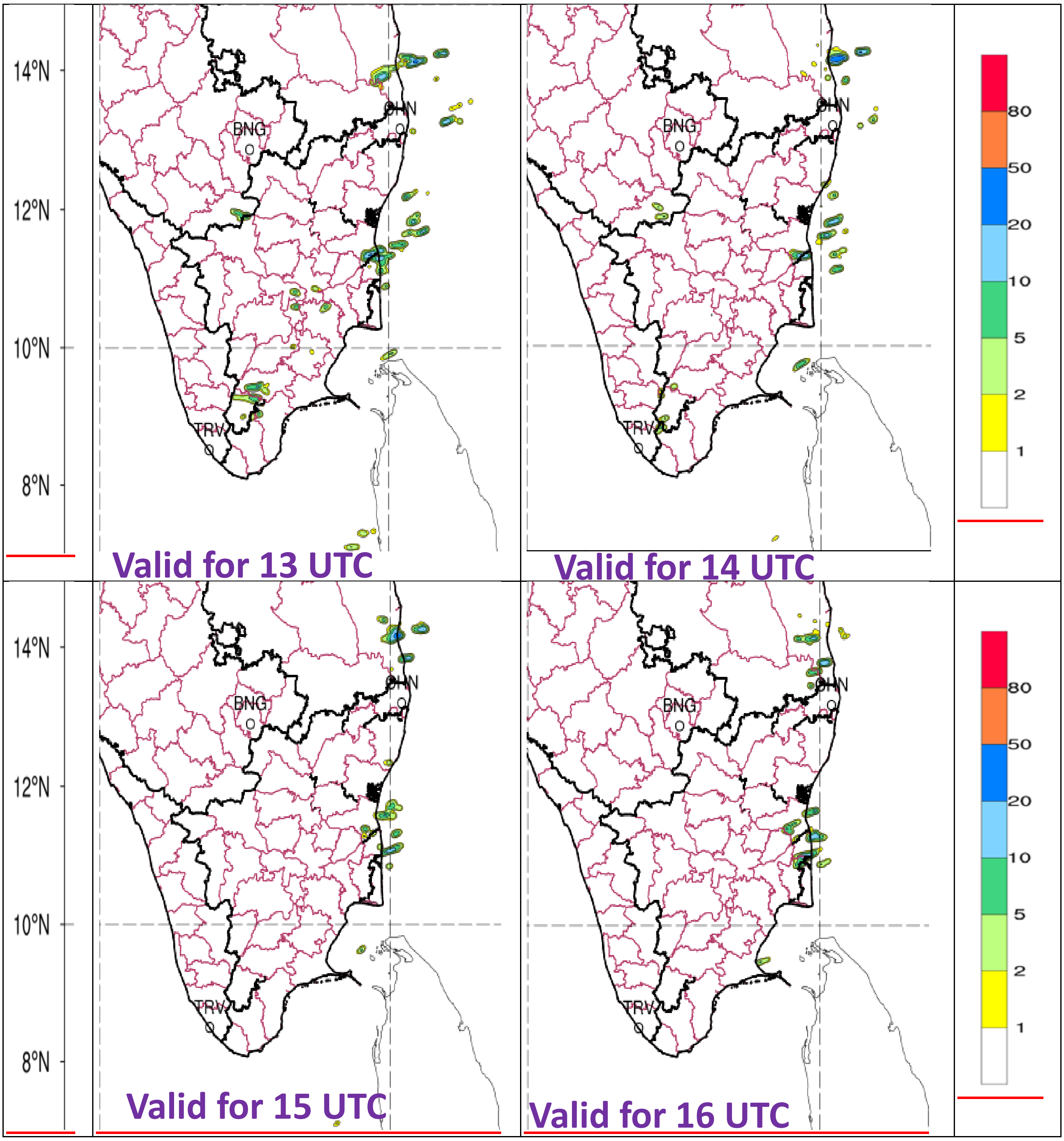
14°N
12°N
10°N
8°N
BNG
CHN
TRV
Valid for 13 UTC
Valid for 14 UTC
Valid for 15 UTC
Valid for 16 UTC
80
50
20
10
5
2
1

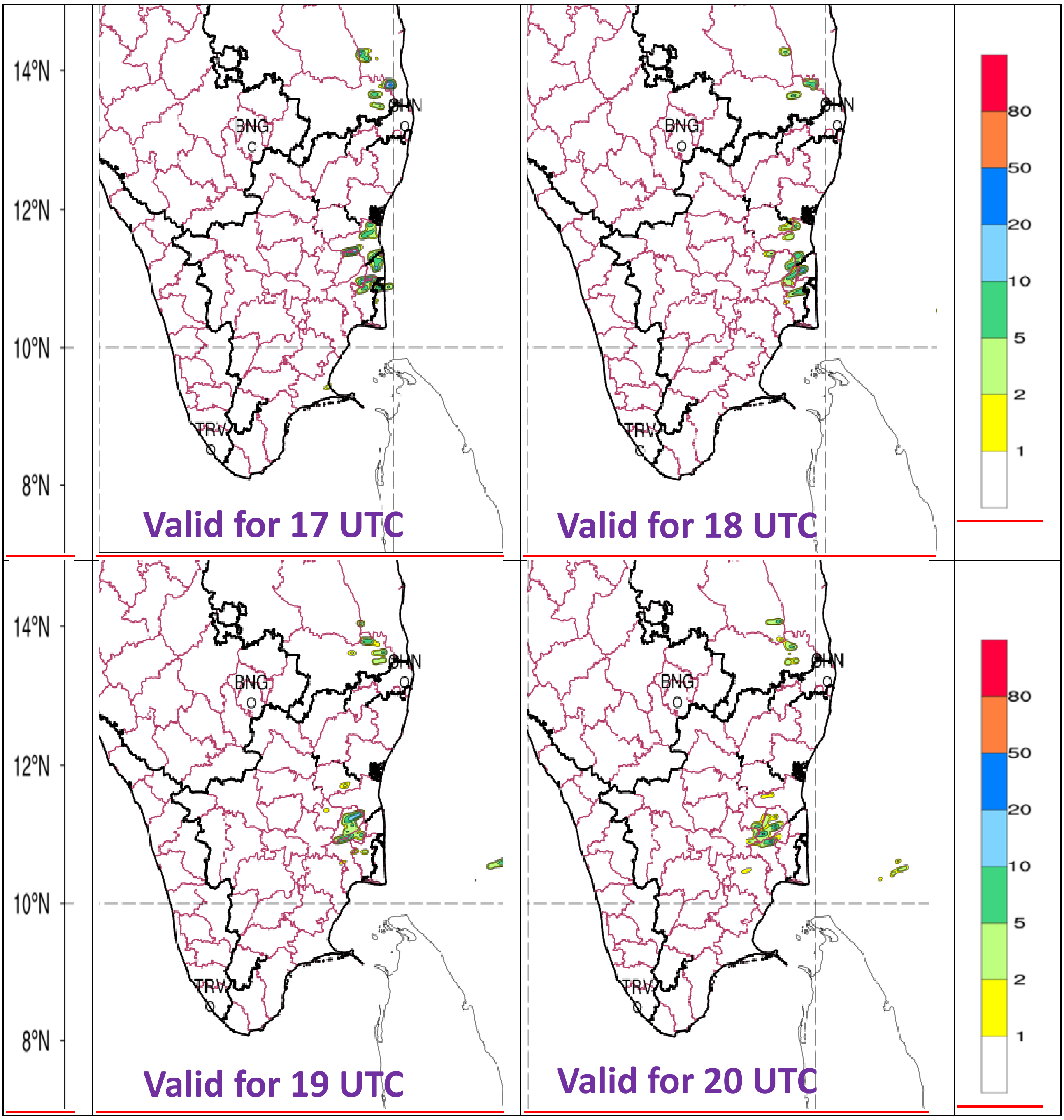

Fig. 4.19. IMD-HRRR model forecast based on IC 08 UTC of 30th December 2021

IMD-HRRR Hourly Rainfall (mm) F/C
based on IC 10 UTC 30 Dec 2021

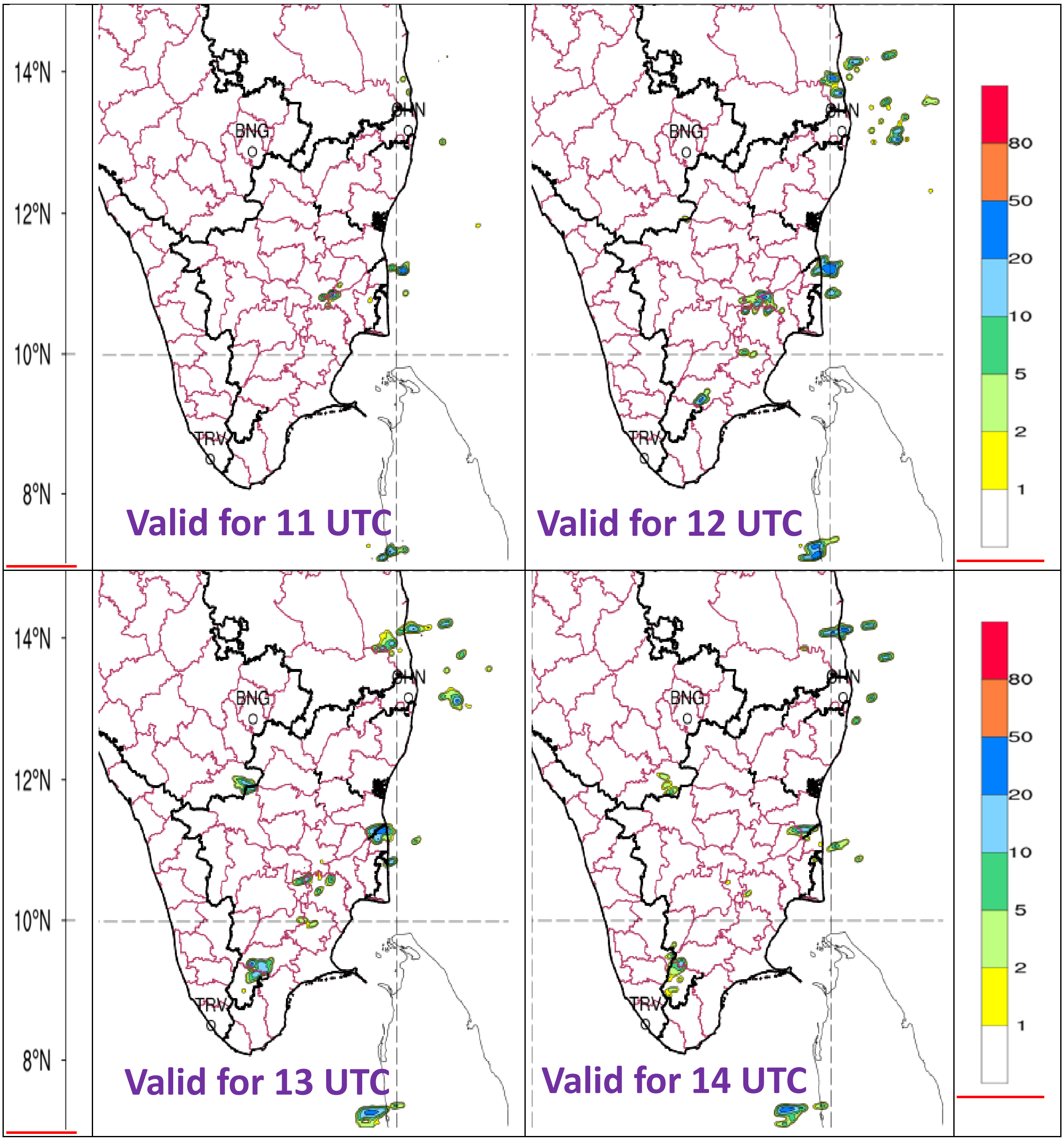

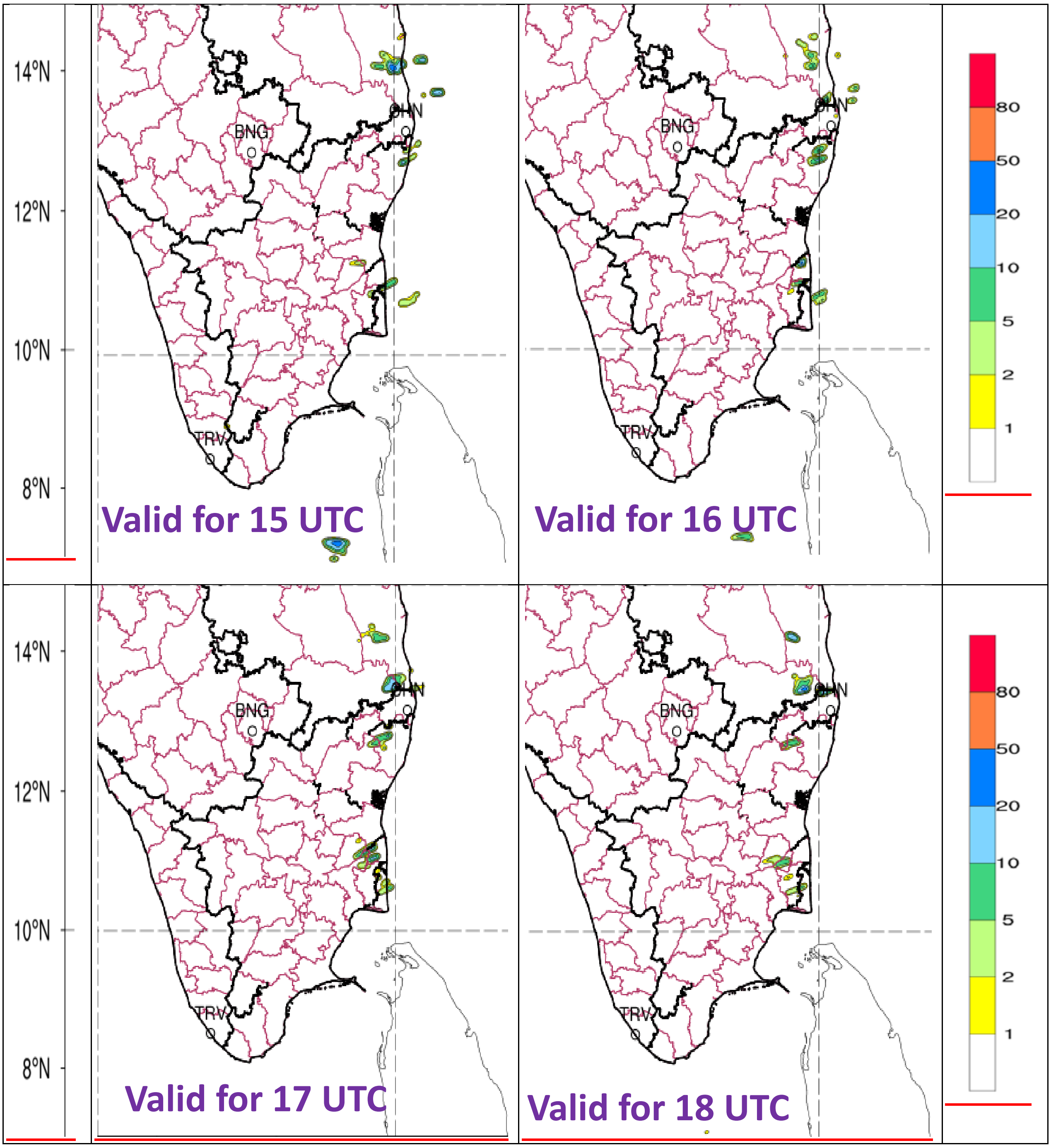
14°N
12°N
10°N
8°N
BNG
CHN
TRV
Valid for 15 UTC
Valid for 16 UTC
Valid for 17 UTC
Valid for 18 UTC
80
50
20
10
5
2
1

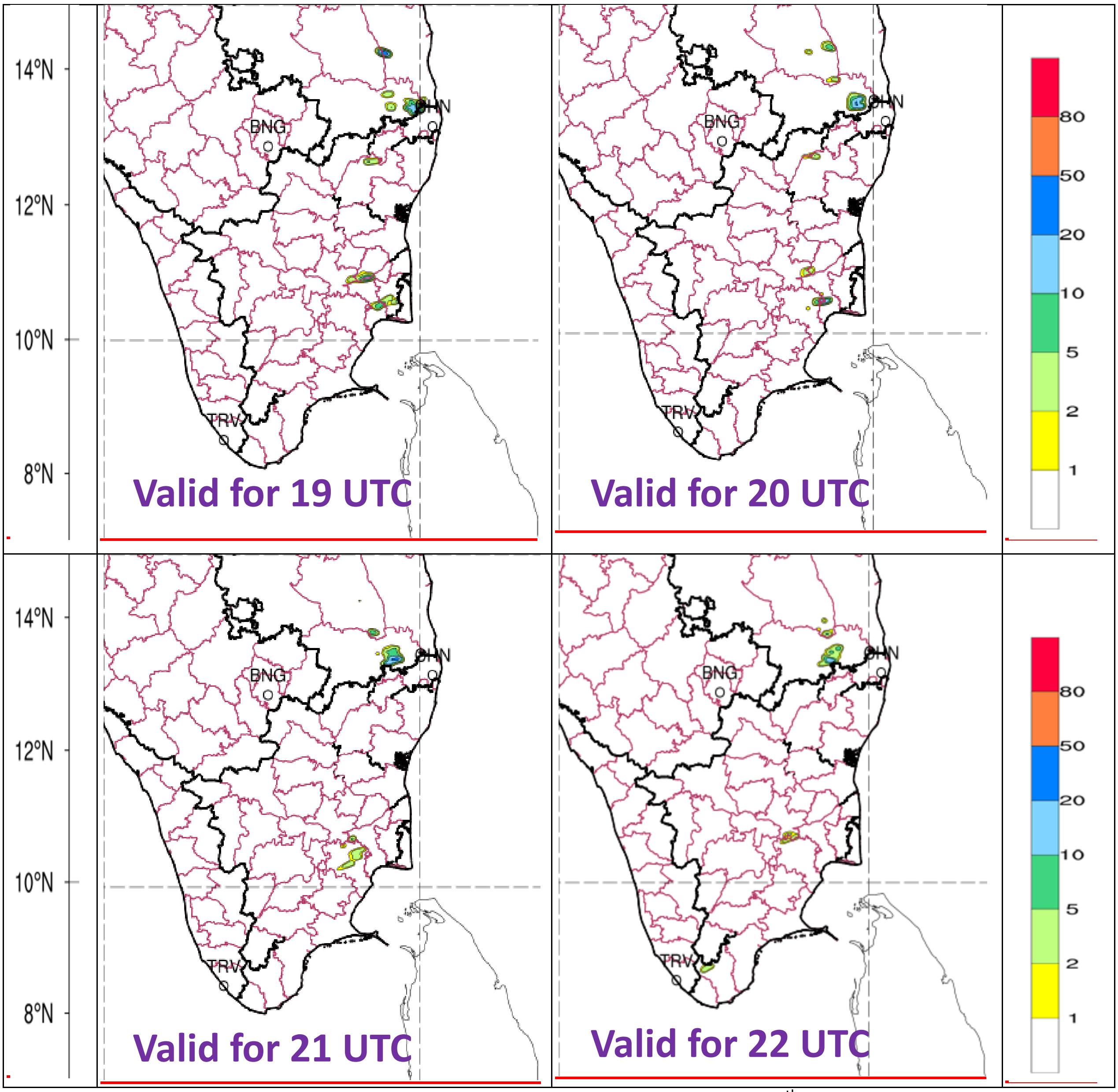

Fig. 4.20.IMD-HRRR model forecast based on IC 10 UTC of 30th December 2021

4.8. Conclusion and Future Prospects

The validation of the HRRR model forecast with respect to different observations is done to ascertain the skill of HRRR model forecasts. HRRR model forecast for the three domains (NW, E & NE and SP) shows good skill in the prediction of surface meteorological parameters (Temperature, Pressure, Humidity and winds). The validation shows that the predicted parameters are in good agreement with the observed values with small deviations. The Radial winds also show negligible mean bias and small RMSD values signifying good skill and potential in the HRRR model. The IMD-HRRR model was also able to capture the rainfall event in Tamilnadu on 30th December 2021.

The HRRR model is currently run at 2km horizontal resolution and in future the resolution may be further improved to 1 km horizontal resolution. Also efforts are due to assimilate and update the HRRR model more frequently with respect to the prepbufr as well as satellite observations. This further has potential to increase the skills of HRRR model forecasts. Some studies would be also required to understand the difference in performance of HRRR models for three different domains and to develop customized methods to improve HRRR model performance for respective domains.

Acknowledgements

The authors are thankful to Dr. M. Mohapatra, Director General, India Meteorological Department, for providing encouragement and facilities to carry out this work. We sincerely acknowledge Space Applications Centre, Indian Space research Organisation, Ahmedabad for providing technical support in pre-processing of radar data and implementation of High Resolution Rapid Refresh model at India Meteorological Department. Thanks are due to the office of Upper Air Instrument division for maintaining the radars and facilitating the data from different radars across India to be assimilated in numerical models.

References

Benjamin, S. G. and Coauthors, 2016, A North American hourly assimilation and model forecast cycle: The Rapid Refresh, *Mon. Wea. Rev*., **144**, 1669–1694.

Cai, H. and Dumais, R. E., Jr., 2015, Object-based evaluation of a numerical weather prediction model's performance through forecast storm characteristic analysis, *Weather and Forecasting*, **30**, 1451–68.

Gowan, T. M., Steenburgh, W. J. and Schwartz, C. S., 2018, Validation of mountain precipitation forecasts from the convection-permitting NCAR ensemble and operational forecast systems over the Western United States, *Weather and Forecasting*, **33**, 739–765.

Hari Prasad Sad, Prashant Kumar and Sambit Kumar Panda (2021) Doppler weather radar data assimilation at convective-allowing grid spacing for predicting an extreme weather event in Southern India, *International Journal of Remote Sensing*, 42:10, 3681-3707, DOI: 10.1080/01431161.2021.1880660.

Ikeda, K., Steiner, M., Pinto, J. and Alexander, C., 2013, Evaluation of cold-season precipitation forecasts generated by the hourly updating high resolution rapid refresh model, *Weather and Forecasting*, **28**, 921–939.

Lee, T. R., Buban, M., Turner, D. D., Meyers, T. P. and Baker, C. B. (2019) Evaluation of the High-Resolution Rapid Refresh (HRRR) Model Using Near-Surface Meteorological and Flux Observations from Northern Alabama, *Weather and Forecasting*, B(3), 635-663.

Marco Gabella and Riccardo Notarpietro. Ground clutter characterization and elimination in mountainous terrain. In Use of radar observations in hydrological and NWP models, 305–311. Katlenburg-Lindau, 2002. Copernicus. URL: https://porto.polito.it/1411995/.

Smith, T. L., S. G. Benjamin, J. M. Brown, S. Weygandt, T. Smirnova and B. Schwartz, 2008, Convection forecasts from the hourly updated, 3-km High Resolution Rapid Refresh (HRRR) model. 24th Conf. on Severe Local Storms, Savannah, GA, *Amer. Meteor. Soc*., 11.1.

Vulpiani, G., M. Montopoli, L. D. Passeri, A. G. Gioia, P. Giordano and F. S. Marzano, 2012, On the use of dual-polarized C-band radar for operational rainfall retrieval in mountainous areas. *J. Appl. Meteor. Climatol*., **51**, 405–425, https://doi.org/10.1175/ JAMC-D-10-05024.1.

Yue, H. and Gebremichael, M. (2020). Evaluation of high-resolution rapid refresh (HRRR) forecasts for extreme precipitation. *Environ. Res. Commun*., 2 065004.

CHAPTER 5

The Coupled HWRF Modelling System

ANANDA K. DAS, AKHIL SRIVASTAVA and ARUN SHARMA

Since 2011, time to time the HWRF modelling system is developed and customized atmospheric and ocean models with other associated pre-processing and post-processing components are implemented in IMD under the framework of MoU between MoES and NOAA. The HWRF version H217 has been ported on the MHIR HPCS with horizontal resolution of 18 km for parent domain and 6km & 2 km for intermediate and innermost nested domains following the center of cyclonic storm. The model is running with 61 vertical levels with parent domain, intermediate and innermost domain covering area of 80^{o}x80^{o}, 24^{o}x24^{o} and 7^{o}x7^{o} respectively. The special feature modified for tropical cyclone forecasting includes vortex initialization and correction, GSI based regional data assimilation, coupler for two-way coupling between atmosphere and ocean components and fine-tuned physical parameterization schemes. This model is customized specifically to forecast the track, intensity and structure of tropical cyclones. The HWRF modelling system uses the dynamics and infrastructure from the NMM WRF modelling system. It uses physics that are proven to be better for the tropics. Also, at this time, it is an Ocean coupled model system with a Moving two-way interactive nest, and advanced data assimilation. IMD is operationally running ocean coupled HWRF models during Tropical Cyclone events with two ocean models, viz., POM-TC and HYCOM. HYCOM initial conditions are provided through INCOIS whereas POM-TC is initialized based on climatology.

It is run 4 times a day in cyclic mode with GSI based (hybrid-EnVar) assimilation (80 members) with 6 hourly cycles in cycling mode. The operational configuration is given in the following table 5.1.

Table 5.1

HWRF atmospheric model operational configuration

Domain-Parent **Center :- Storm Center**	Size:- 80°X 80° Grid Spacing:- 18 Km Grid Points:-288 X 576
Intermediate Moving Nest **Center:- Storm Center**	Size:- 24° X 24° Grid Spacing:-06 Km Grid Points:-265 X 532
Inner Most Moving Nest **Center:- Storm Center**	Size:- 7° X 7°Grid Spacing:- 02 Km Grid Points:- 235 X 472
Map Projection	Rotated Latitude and Longitude
Vertical Levels	61 Hybrid Pressure Sigma Coordinates
Top Boundary	10 hPa
Cloud-Microphysics	Ferrier-Aligo Cloud Microphysics
Radiation	Rapid Radiative Transfer Model for GCM (RRTMG)
Surface Layer Physics	Modified Geophysical Fluid Dynamics Laboratory (GFDL)
Surface Flux Calculation	Monin-Obukhov
Land Surface	Noah Land Surface Model
Planetary Boundary Layer	Global Forecasting System (GFS) Eddy-Diffusivity Mass Flux
Cumulus Parametrization	Scale-Aware Arakawa-Schubert

The information about the ocean models while coupling with HWRF atmospheric model through NCEP coupler is given in table 5.2 below.

Table 5.2

Descriptions of ocean models coupled with HWRF in real-time run

Ocean Model	POM	HYCOM
Dynamics & Configurations	Hydrostatic, free-surface, primitive equations on C grid	
	1/12-degree	
	Rectangular Projection	Mercator Projection
	40 vertical sigma level	41 vertical Hybrid isopycnal-Z levels
Mixing Physics	Mellor-Yamada 2.5 closure	KPP (K-Profile Parameterization)
Initialization	Monthly GDEM3 Climatology + daily NCEP SST + Feature Model	6 hourly HYCOM analysis from INCOIS-RTOFS i.e., ITOPSI
Lateral Boundary	Adjusted T/S fields	6 hourly 2D and 3D INCOIS-RTOFS forecasts

The Unified Post-Processor (UPP) coverts raw model outputs from all three domains into standard GRIB1/2 format. Moreover, GFDL tracker generates track and intensity information in a standard ATCF (Automated Tropical Cyclone Forecasting System) format processing all GRIB files with a specified time interval (3 or 6 hours) as per requirement.

The modeling system was fully operational and predicted all cyclones during the year 2021. Whenever any low-pressure system intensified and became depression over both sub-basins of North Indian Ocean, the cyclic run of the modelling system had been initiated. The model utilized ocean initial state from the ITOPSI (INCOIS Tendral Ocean Prediction System – Indian Ocean Model) during each cycle to initialize the HYCOM ocean component. All available observed data including conventional and satellite observations were assimilated into the regional GSI system to improve further the initial condition after the vortex initialization of the atmospheric first guess state of the model forecast from previous cycle (except first cycle).

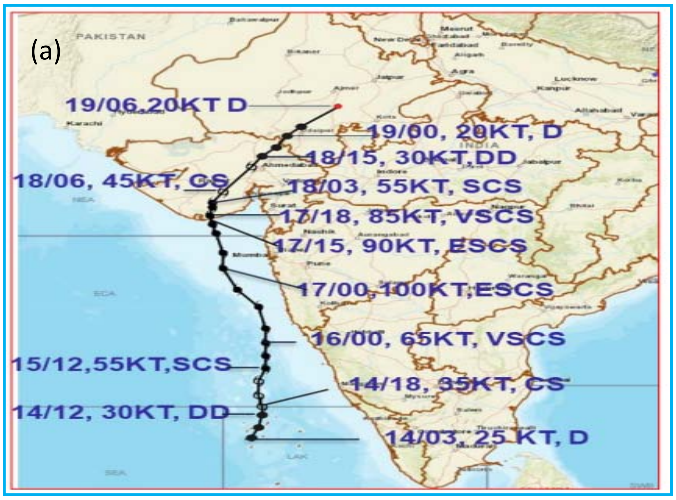

Fig. 5.1. Observed estimated best track of ESCS TAUKTAE during 14th-19th May, 2021

The hurricane WRF model was run operationally during the ESCS “TAUKTAE”. The best estimate of the track and intensity of the cyclone as provided by the Cyclone Warning Division of IMD which is also the Regional Specialized Meteorological Centre (RSMC) for South Asia (The link for the referred document may be found on the official site of RSMC, New Delhi) is shown in figure 5.1. The HWRF-HYCOM forecasts from 14 May 2021 00 UTC till 17th May 18 UTC were available on real-time basis. The HWRF model was cycled with 6-hour interval (00, 06, 12 and 18 UTC) and run to produce forecasts up 126 hours. The model is run with 3 nested domains for five days with ocean coupling as described above. A few forecast products for a few cycles from 00 UTC of 14th May to 18 UTC of 15th May 2021 during the cyclone "TAUKTAE" are furnished in the figure 5.2 to 5.4. The real-time forecasts for tracks along with intensities (Maximum sustained wind in knots and minimum central pressure in hPa) for all forecast hours generated in different forecast cycle are furnished in different panels of the figure 5.2 and 5.3.

The track and intensity of the forecasts from each cycle are verified against best estimated track and intensity values of the cyclone. The direct position error, cross track and along track errors are directly computed.

(a) 00 UTC of 14-05-2021

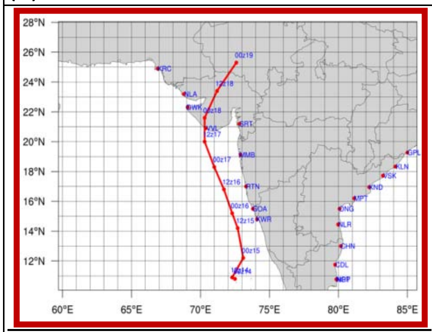

Dt/Hr.	Lat.	Lon.	MSLP	Vmax
00z14	10.8	72.50	999.0	31.
12z14	10.9	72.30	996.0	51.
00z15	12.2	73.10	983.0	59.
12z15	14.2	72.70	972.0	58.
00z16	15.2	72.30	963.0	73.
12z16	16.8	71.70	959.0	83.
00z17	18.3	71.00	944.0	96.
12z17	20.0	70.30	933.0	106
00z18	21.6	70.30	958.0	62.
12z18	23.4	71.20	981.0	51.
00z19	25.3	72.60	995.0	31.

(b) 06 UTC of 14-05-2021

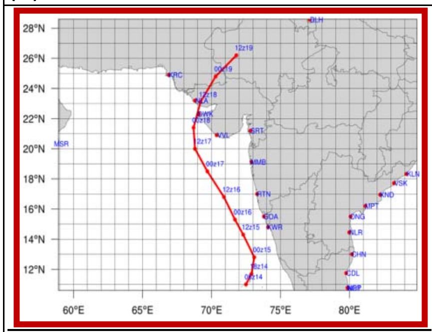

Dt/Hr.	Lat.	Lon.	MSLP	Vmax
06z14	11.0	72.5	999.	37.
18z14	11.7	72.9	992.	64.
00z15	12.8	73.1	982.	70.
12z15	14.3	72.3	970.	67.
00z16	15.3	71.7	961.	87.
12z16	16.8	70.9	954.	99.
00z17	18.5	69.7	941.	100
12z17	20.0	68.8	931.	112
00z18	21.4	68.7	934.	112
12z18	23.1	69.2	946.	93.
00z19	24.8	70.3	973.	49.
12z19	26.2	71.8	990.	32.

(c) 12 UTC of 14-05-2021

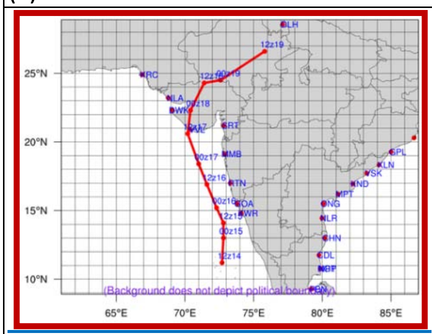

Dt/Hr.	Lat.	Lon.	MSLP	Vmax
12z14	11.2	72.7	996.	38.
00z15	13.0	72.8	985.	59.
12z15	14.1	72.8	975.	72.
00z16	15.2	72.3	969.	77.
12z16	16.9	71.6	951.	101
00z17	18.4	71.0	945.	93.
12z17	20.6	70.2	929.	114
00z18	22.3	70.4	962.	67.
12z18	24.3	71.4	986.	44.
00z19	24.5	72.6	998.	22.
12z19	26.6	75.8	1001	20.

(d) 18 UTC of 14-05-2021

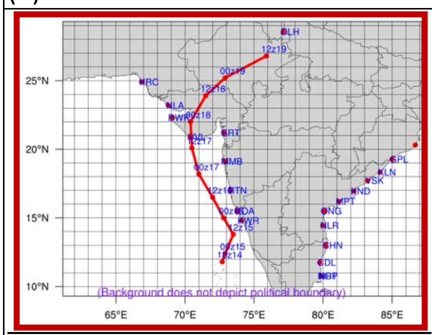

Dt/Hr.	Lat.	Lon.	MSLP	Vmax
18z14	11.8	72.7	996.	48.
00z15	12.4	72.9	988.	53.
12z15	13.8	73.5	983.	48.
00z16	15.0	72.8	974.	65.
12z16	16.5	72.0	966.	70.
00z17	18.2	71.0	944.	92.
12z17	20.1	70.5	934.	94.
00z18	22.0	70.4	958.	59.
12z18	23.9	71.5	983.	47.
00z19	25.2	72.9	998.	27.
12z19	26.8	75.9	1001	21.

(e) 00 UTC of 15-05-2021

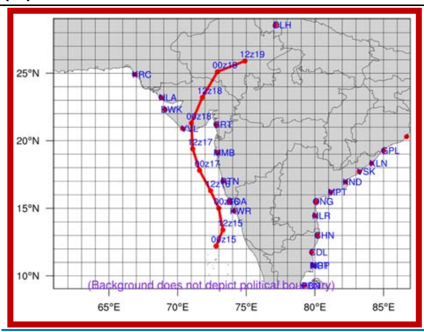

Dt/Hr.	Lat.	Lon.	MSLP	Vmax
00z15	12.2	72.80	990.0	46.
12z15	13.4	73.30	990.0	49.
00z16	15.0	73.00	988.0	59.
12z16	16.3	72.40	983.0	46.
00z17	17.8	71.60	972.0	61.
12z17	19.4	71.10	958.0	83.
00z18	21.3	71.00	956.0	70.
12z18	23.2	71.80	976.0	51.
00z19	25.1	72.90	995.0	32.
12z19	25.9	74.90	999.0	25.

(f) 06 UTC of 15-05-2021

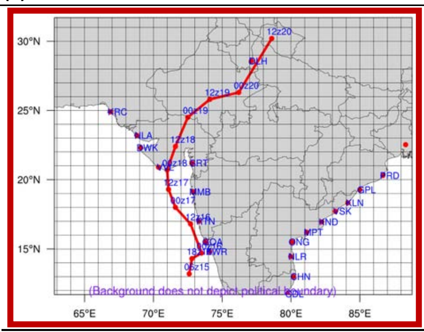

Dt/Hr.	Lat.	Lon.	MSLP	Vmax
06z15	13.2	72.6	990.	42.
18z15	14.3	72.8	990.	54.
00z16	14.7	73.5	985.	46.
12z16	16.8	72.7	984.	45.
00z17	18.0	71.6	975.	50.
12z17	19.3	71.1	968.	58.
00z18	20.7	71.0	958.	70.
12z18	22.4	71.6	972.	56.
00z19	24.5	72.5	992.	36.
12z19	25.8	74.1	1000	27.
00z20	26.3	76.2	1002	20.
12z20	30.2	78.6	1003	61.

(g)12 UTC of 15-05-2021

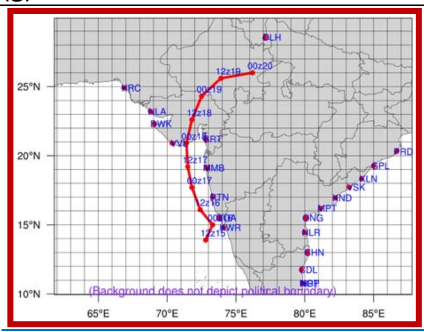

Dt/Hr.	Lat.	Lon.	MSLP	Vmax
12z15	13.9	72.8	983.	51.
00z16	15.0	73.3	988.	43.
12z16	16.1	72.4	983.	52.
00z17	17.7	71.8	975.	53.
12z17	19.2	71.5	964.	62.
00z18	20.9	71.4	957.	76.
12z18	22.6	71.8	968.	59.
00z19	24.3	72.5	989.	36.
12z19	25.6	73.9	997.	36.
00z20	26.0	76.2	1000	24.

(h)18 UTC of 15-05-2021

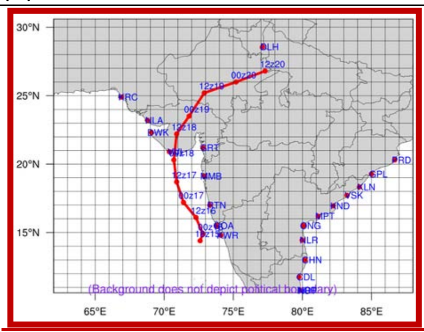

Dt/Hr.	Lat.	Lon.	MSLP	Vmax
18z15	14.4	72.6	983.	56.
00z16	14.9	72.8	977.	58.
12z16	16.1	72.3	971.	65.
00z17	17.2	71.4	952.	82.
12z17	18.7	70.9	937.	106
00z18	20.3	70.7	936.	105
12z18	22.2	70.9	957.	66.
00z19	23.5	71.8	980.	43.
12z19	25.2	72.9	992.	39.
00z20	26.0	75.2	998.	27.
12z20	26.8	77.3	1002	18.

Fig. 5.2. IMD-HWRF Track and intensity forecasts for cyclone Tauktae from 00 UTC 14 may to 18 UTC of 15 May, 2021

Whereas from the best estimated track the observed landfall point is detected and then landfall position error and landfall time errors are calculated accordingly for each forecasted track of the model with different initial conditions. The verification error statistics computed taking weighted averaging of all different errors are shown in Table 5.3.

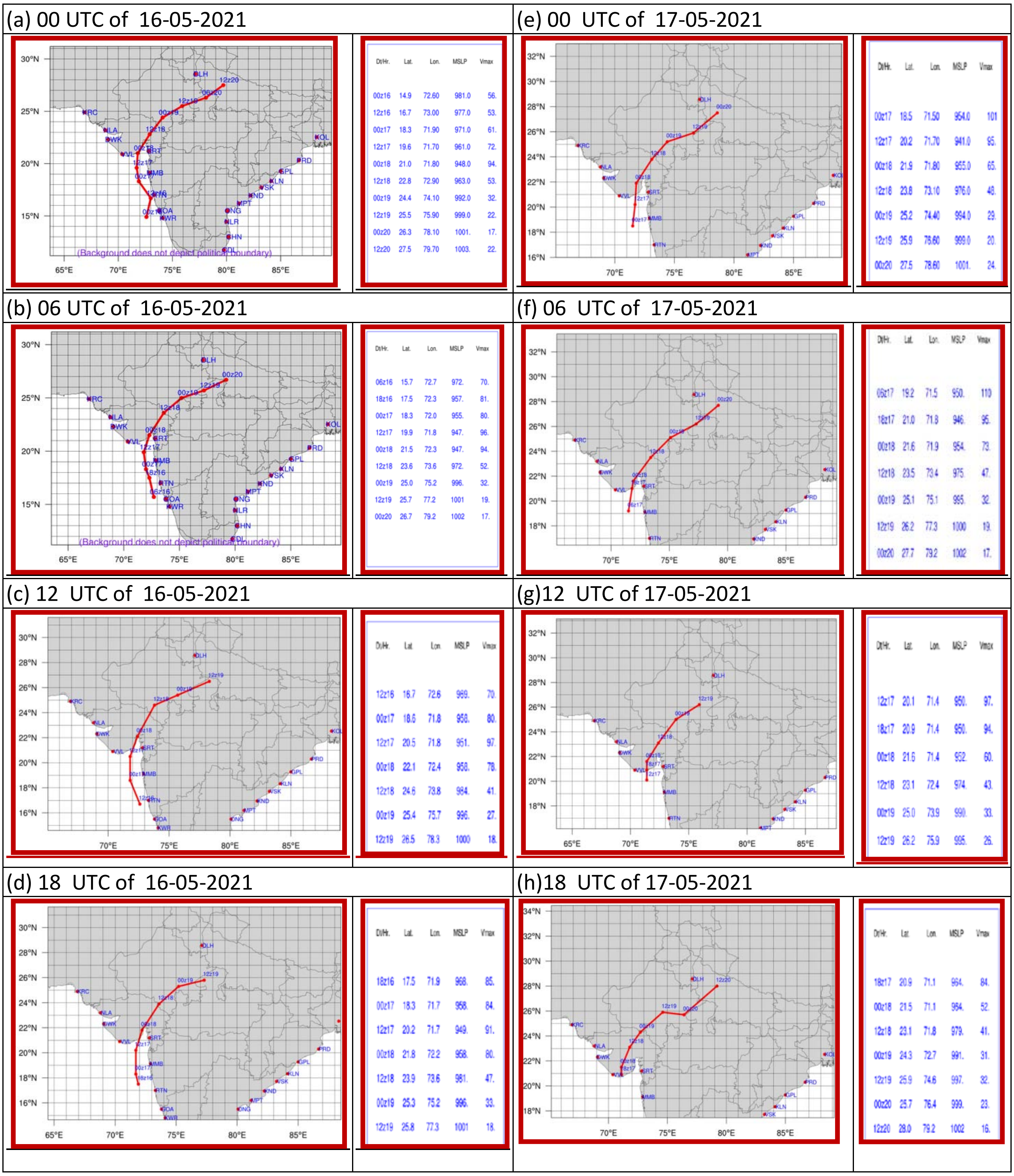

Fig. 5.2. IMD-HWRF Track and intensity forecasts for cyclone Tauktae

The initial Northwestward movement of the cyclonic system followed by Northeastward movement later on was captured during all the cycles of IMD-HWRF modeling system. Only during one of the initial cycles (06 UTC of 14th May 2021) the model predicted track was more towards the west of the observed track, however in the next cycle it corrected and the track was maintained similar to observed track.

Table 5.3

IMD-HWRF Track and intensity forecasts Error Statistics for cyclone Tauktae

ERROR STATISTICS FOR HWRF-HYCOM COUPLED MODEL FOR ESCS-TAUKTAE*										
Lead Time / **Errors**	12 Hr (15)	24 Hr (15)	36 Hr (15)	48 Hr (13)	60 Hr (11)	72 Hr (9)	84 Hr (7)	96 Hr (5)	108 Hr (3)	120 Hr (1)
Direct Position Errors (DPE) (km)	49	64	90	115	118	121	152	155	153	287
Along Track Errors (AT) (km)	42	44	49	64	74	82	93	128	122	78
Cross track Errors (CT) (km)	74	92	111	140	133	121	90	104	85	94
Landfall Point Errors (km)	59	99	88	49	24	88	90	N/A	N/A	N/A
Landfall Time Errors (hr)	+3	+3	+9	+6	+6	0	+3	N/A	N/A	N/A
Average Absolute Intensity Errors (AAE) (kts)	11.8	13.1	15.8	17.8	10.4	10.5	12.0	9.9	13.4	7.7
Root Mean Square Intensity Errors (RMSE) (kts)	14.3	16.7	20.2	21.5	13.5	13.1	15.2	10.8	19.2	10.4

(*Number of forecasts verified is given in the parentheses)

The IMD-HWRF forecasted track showed less than 100 km of average Direct Position Error during 36 hour forecast and less than about 150 km error for up to 108 hrs. Lead time. So IMD-HWRF modeling system consistently provided skilled track forecast for cyclone TAUKTAE. The Along the track and cross track errors are also shown in the Table. Average absolute intensity errors are in general between 10 knots to 20 knots during the forecast period. The landfall point error for cyclone TAUKTAE was less between 24 km to 99 km and landfall time error was in general up to +6 hours across the forecast lead time.

The Figure 5.3 shows the different IMD-HWRF coupled model forecast products for ESCS Tauktae cyclone. The figure 3(a) shows the core domain (innermost domain of IMD-HWRF modeling system) Mean Sea level Pressure (isobars) and 10 m winds. This domain is centered on the cyclone center and shows the symmetrical structure of ESCS Tauktae. The figure 3(b) shows the mid-tropospheric moisture (Relative Humidity) along with Geo-potential height and winds on the inner most domains centered on cyclone. Figure 3 (c) and 3(d) shows the vertical cross-section of winds and temperatures along East-West (E-W) and North-South (N-S) directions respectively. The system looks more symmetrical in N-S direction as compared to E-W direction with respect to wind speed. The Eastern side displays more wind speed as compared to western side and southern side has more as compared to northern side. Figure 3(e) and 3 (f) is showing the Meridional cross section and Zonal cross-section with respect to Total Winds, Meridional/Zonal winds, Temperature Anomaly, Relative Humidity and Relative vorticity.

Both the figures are showing the near symmetrical structure of cyclone with more winds towards the northern side in Meridional cross-section and towards Eastern side in Zonal cross-section. Dry air incursionis also captured in the zonal cross-section from the west side of the cyclone, however, no

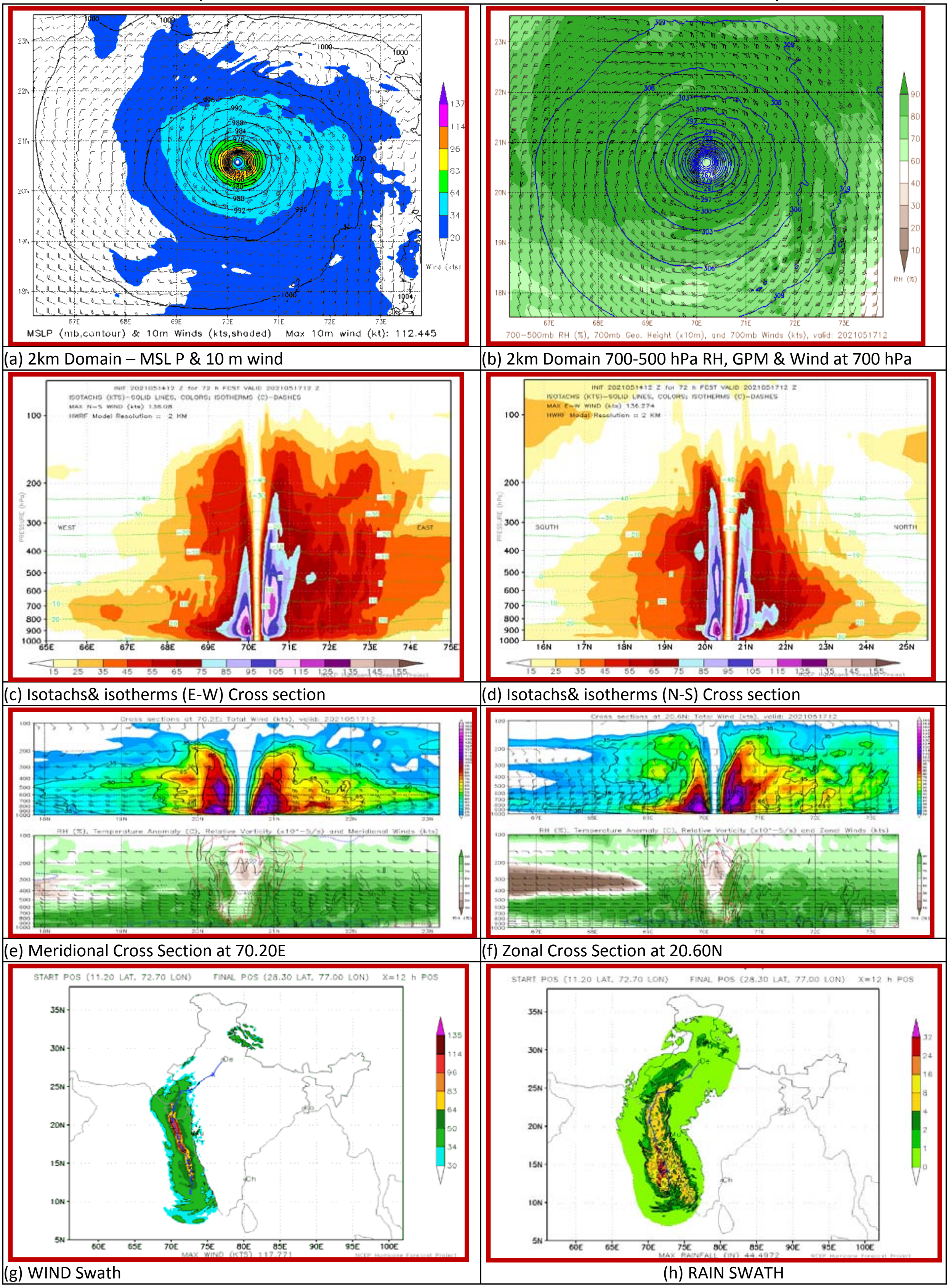

(a) 2km Domain – MSL P & 10 m wind
(b) 2km Domain 700-500 hPa RH, GPM & Wind at 700 hPa
(c) Isotachs& isotherms (E-W) Cross section
(d) Isotachs& isotherms (N-S) Cross section
(e) Meridional Cross Section at 70.20E
(f) Zonal Cross Section at 20.60N
(g) WIND Swath
(h) RAIN SWATH

Fig. 5.4. IMD-HWRF Model forecast products for Tropical Cyclone TAUKTAE

significant dry air incursion is seen in Meridional cross-section. Figure 3(g) and 3(h) are showing the Wind Swaths and Rain swaths respectively. Wind swath shows the wind during the next 5 days forecast along the cyclone track and rain swath shows the cumulative rain forecasted from IMD-HWRF modeling system along the predicted track of tropical cyclones. There are various other products as well which are generated based on the IMD-HWRF modeling system and are available on the NWP website.

Analysing the forecast results of HWRF modelling system for the ESCS TAUKTAE the following points can be summarized.

- IMD-HWRF model could provide useful guidance with regard to the track and intensity forecast of ESCS "TAUKTAE".
- Except the IC of 14th 06 UTC other ICs forecasts provided the forecast track similar to the observed track. The forecast with IC of 14th 06 UTC indicated more westerly track with landfall crossing is about 200 km west of actual position.
- The average forecast track error is found to be 64 km for 12 hour, 115 km for 48 hour, 121 km for 72 hour and 155 km for 96 hour.
- It is also found that the Cross Track (CT) error is found to be much higher than Along Track (AT) error during initial forecast hours (till 72 hours), whereas, beyond 72 hours the AT error is found to be in general higher than CT error.
- The landfall error is having no relationship with lead time and is found to be the lowest (24 km) with 60 hr lead is about 100 km with 24 hr lead. The landfall time is found to be slightly delayed and is varied from 3 hr to 9 hr with different lead time from 12 hr to 84 hr.

The coupled modelling system predicted all cyclonic storms over North Indian Ocean during 2021 on real-time basis 4 times daily with its cycling at 6-hour interval. The errors statistics as calculated for the cyclone Tauktae, the errors are also computed for all the cyclones against their best estimated tracks and intensities. The annual average statistics of all errors is summarized in table 5.4.

Table 5.4

IMD-HWRF Annual Track and intensity forecasts Error Statistics for all cyclones over North Indian Ocean during the year 2021

ERROR STATISTICS FOR HWRF-HYCOM COUPLED MODEL FOR ESCS-TAUKTAE*										
Lead Time / **Errors**	12 Hr (15)	24 Hr (15)	36 Hr (15)	48 Hr (13)	60 Hr (11)	72 Hr (9)	84 Hr (7)	96 Hr (5)	108 Hr (3)	120 Hr (1)
Direct Position Errors (DPE) (km)	49	64	90	115	118	121	152	155	153	287
Along Track Errors (AT) (km)	42	44	49	64	74	82	93	128	122	78
Cross track Errors (CT) (km)	74	92	111	140	133	121	90	104	85	94
Landfall PointErrors (km)	59	99	88	49	24	88	90	N/A	N/A	N/A
Landfall TimeErrors (hr)	+3	+3	+9	+6	+6	0	+3	N/A	N/A	N/A
Average Absolute Intensity Errors (AAE) (kts)	11.8	13.1	15.8	17.8	10.4	10.5	12.0	9.9	13.4	7.7
Root Mean SquareIntensity Errors(RMSE) (kts)	14.3	16.7	20.2	21.5	13.5	13.1	15.2	10.8	19.2	10.4

(*Number of forecasts verified is given in the parentheses)

CHAPTER 6

Dynamical and Statistical model for Tropical Cyclone forecast

S. D. KOTAL and S. K. BHATTACHARYA

6.1. Introduction

In recent years, human casualties due to tropical cyclones (TCs) over the densely populated coastal area surrounding the North Indian Ocean (NIO) have significantly decreased due to improved forecast accuracy. Super cyclone of Orissa (1999), the severest one during the recent time over the Bay of Bengal experienced wind speed of about 250 kmph. The massive destruction caused by the cyclone was the collapse of nearly 4 lakh houses, damage of about 19 lakh houses, took a toll of nearly 10000 human lives, and affected more than 25 lakh people. This devastating cyclone illustrates the need for accurate prediction of track and intensity. Despite skilled and well experienced, the forecasters were not well equipped with sophisticated NWP system and reliable tool that presently available. It is not possible to forecast track and probable landfall point and intensity five days ahead using synoptic method without reliable outputs from NWP models.

For all operationally designated tropical cyclones in the NIO, India Meteorological Department (IMD) has the responsibility to issue official forecast of TC centre (location) and intensity. Over the past decade, the performance of NWP models in forecasting TC tracks has improved significantly with sophisticated numerical techniques (new observing systems, advanced data assimilation algorithms, physical parameterizations, and advancements in computing power) and by the phenomenal increase in satellite observations.

India Meteorological Department (IMD) operationally runs two regional models, WRF and HWRF for short-range prediction and one Global model T1534L64 for medium range prediction (10 days). The Global Forecast System (GEFS) T1534L64 (12 Km) with 21 Members run at 00 UTC every day for real time forecast up to 8 days. Deterministic and Probabilistic Rainfall forecasts are generated from GEFS. The WRF-Var model is run at the horizontal resolution of 9 km and 3 km with 45 Eta levels in the vertical and the integration is carried up to 72 hours over three domains covering the area between lat. 23^{o} S to 46^{o} N long 40^{o} E to 120^{o} E. Initial and boundary conditions are obtained from the IMD Global Forecast System (IMD-GFS) at the resolution of 9 km. The boundary conditions are updated at every six hours interval. The HWRF model (resolution 18 km, 6 km and 2 km) is used for cyclone track prediction in case of cyclone situation in the north Indian Ocean. IMD also makes use of NWP products prepared by some other operational NWP Centres like, ECMWF (European Centre for Medium Range Weather Forecasting), GFS (NCEP), UKMO (UKMet), JMA (Japan Meteorological Agency). Ensemble prediction system (EPS) has been implemented at the NWP Division of the IMD HQ for operational forecasting of cyclones.

6.2. History of Track and intensity forecasts

In early days since 1998, IMD used to operate three regional models, Limited Area Model (LAM), MM5 model and Quasi-Lagrangian Model (QLM) for short-range prediction upto 72 h. The MM5 model was run at the horizontal resolution of 45 km with 23 sigma levels in the vertical for 72 h using initial and boundary conditions from the NCEP Global Forecast System (NCEP GFS) at the resolution of 1°x1° latitude/longitude. The LAM was run up to 72 h at the horizontal resolution of 0.75°x0.75° latitude/longitude with 16 sigma levels in the vertical using the initial and boundary conditions provided by the T-254 Global operational model run at NCMRWF (National Center for Medium Range Weather Forecast).

The Quasi-Lagrangian Model (QLM), a multilevel fine-mesh primitive equation model with a horizontal resolution of 40 km and 16 sigma levels in the vertical, was run for tropical cyclone track prediction up to 72 h. The integration domain size was 4440x4440 km^2centered on the initial position of the cyclone. For the day-to-day weather forecasting, IMD also used of NWP products prepared by some other operational NWP Centers like, NCMRWF (National Center for Medium Range Weather Forecast), ECMWF (European centre for medium range weather forecast), NCEP GFS. The QLM model for track prediction of tropical cyclone over the NIO discarded after 2012. The average track forecast errors of QLM during the period 1998-2012 was quite high, and the errors were 146 km, 233 km, 403 km at 24 h, 48 h, and 72 h respectively but no specific model was used for intensity forecasting.

IMD official (OFCL) track and intensity forecast over the NIO were subjectively generated largely based on persistence up to 24 h only till 2008, and track and intensity forecast errors were 155 km and 14.9 kt respectively at 24 h. The dynamical-statistical MME technique was developed and introduced for operational track forecasting in 2009 using sophisticated NWP models as mentioned in section 2 above. The dynamical-statistical model SCIP was developed and introduced for operational intensity forecasting in 2008 using NWP model output. Both the MME and SCIP generate track and intensity forecast up to 72 h and OFCL track and intensity forecasts also extended to 72 h from 2009. Further, forecast hours of MME and SCIP were extended up to 120 h and so as the operational forecasts also. In addition to the track and intensity component, other components of CPS like genesis, rapid intensification, and decay after landfall are briefly described in the following section.

6.3. Operational NWP Models at IMD

- GFS T1534L64 (12 km)
- WRF (3DVAR -9 km, 3 km)
- HWRF (18 km, 6 km, 2 km)
- GEFS (T1534)

6.3.1. *NWP Model product from Other Centres*

- ECMWF
- JMA
- NCEP GFS
- UKMO

6.3.2. *Model configuration*

HWRF

- v3.7 with GFS T1534 initial and boundary condition
- Triple Nested (18 Km, 6 Km, 2 Km) - Vertical level 61
- Run time 00, 06, 12, 18 UTC

WRF

- V3.6 with RADAR data assimilation using 3DVAR
- Horizontal resolution 9 km & 3 km
- Vertical level 45

GFS

- T1534L64 (12 Km)
- Run time 00, 06, 12, 18 UTC

GEFS

- Run time 00 UTC

6.3.3. *Dynamical-Statistical techniques*

- GPP (Genesis Potential)
- SCIP (for cyclone intensity prediction)
- MME (for cyclone track)
- RI-Index (Rapid Intensification)
- Decay after landfall (Decay model)

6.4. Dynamical-Statistical Cyclone Forecast System (CPS)

In addition to the above NWP models, IMD also run operationally “NWP based Objective Cyclone Prediction System (CPS)”.The method comprises of five forecast components, namely(a) Cyclone Genesis Potential Parameter (GPP), (b) Multi-Model Ensemble (MME) technique for cyclone track prediction, (c) Cyclone intensity prediction, (d) Rapid intensification and (e) Predicting decaying intensity after the landfall. Genesis potential parameter (GPP) is used for predicting potential of cyclogenesis and forecast for potential cyclogenesis zone. The multi-model ensemble (MME) for predicting the track (at 12h interval up to 120h) of tropical cyclones for the Indian Seas is developed applying multiple linear regression technique using the member models IMD-GFS, GFS (NCEP), ECMWF, UKMO and JMA. The SCIP model is used for 12 hourly intensity predictions up to 120-h and a rapid intensification index (RII) is developed and implemented for the probability forecast of rapid intensification (RI). Decay model is used for prediction of intensity after landfall. In this report performance of the individual models, MME forecasts, SCIP, GPP and Decay model for cyclones during 2020 are presented and discussed. The flow diagram of the five-step CPS is shown in Fig. 6.1.

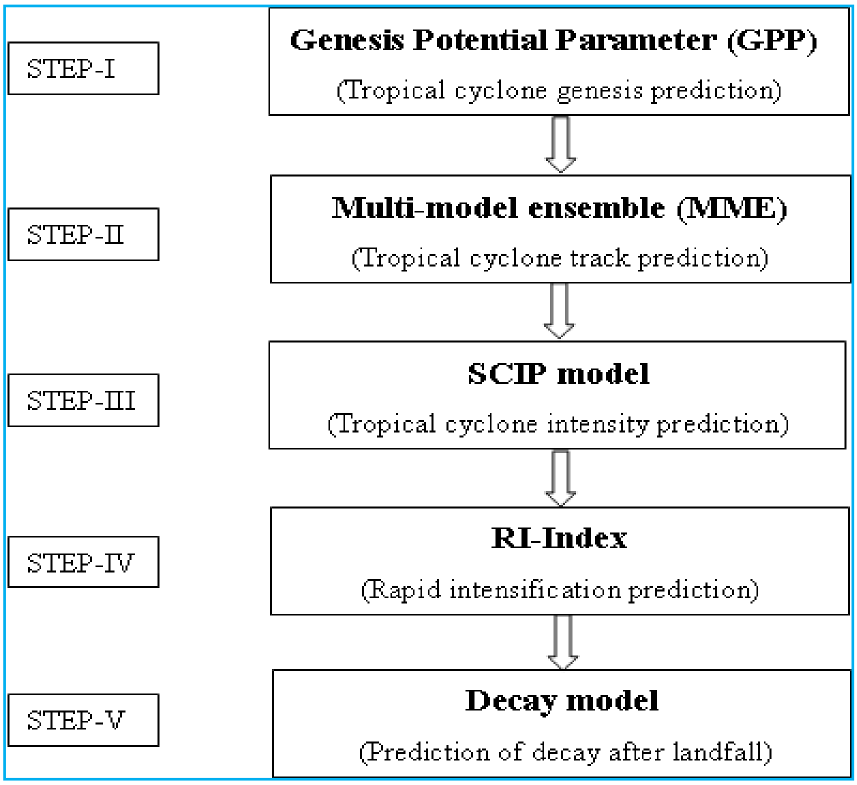

Fig. 6.1. Flow Diagram of Cyclone Prediction System (CPS)

A detailed description of CPS was provided by Kotal *et al.*, (2014, 2021). A brief description of CPS is presented in this section and performance of all five components of CPS is presented in the following section. The quantitative performance statistics on the probable forecast errors will provide the operational forecasters better guidance for better monitoring the TCs. The basic objectives of the CPS are:

- To improve the skill of dynamical model forecasts by statistical post processing.
- To generate a consensus single forecast among different forecasts from different NWP models.
- To develop a collective approach for improving various components of cyclone forecasting.

The five components of CPS for the operational forecasting of TCs over the NIO are briefly described below.

6.4.1. *Component-I: Genesis Potential Parameter (GPP)*

A genesis potential parameter (GPP) was developed for the NIO by Kotal *et al.* (2009). The GPP estimates the potential of a low pressure system for intensification into a tropical cyclone at the early stages of development. The parameter has been used operationally at IMD since 2008 for distinguishing non-developing and developing systems at the early stage of development. The spatial distribution of the parameter has also been used to identify the most favourable area of cyclogenesis over the Sea (Kotal and Bhattacharya, 2013).

6.4.2. *Component-II : Multi-model ensemble (MME) technique for track prediction*

The objective of this component was to generate a consensus track forecast, as there were variations of track forecasts among different NWP models. The MME track is generated from the model forecast positions by collective bias correction with respect to the observed position of TCs using multiple linear regression based minimization principle (Kotal and Roy Bhowmik, 2011). The MME technique has been used operationally at IMD since 2009 for real-time track prediction of TCs. The predictors selected for the ensemble technique are forecasts of latitude and longitude positions at 12 h interval up to 120 h of five global models (IMD-GFS, NCEP-GFS, ECMWF, UKMO and JMA).

6.4.3. *Component-III: Statistical Cyclone Intensity Prediction (SCIP) model*

The statistical cyclone intensity prediction (SCIP) model was developed by Kotal *et al.* (2008). The various parameters selected as predictors were determined from the forecast fields of NWP models for multiple regression analyses. Therefore, the SCIP model is principally a dynamical-statistical model. The dependent variable is intensity changes in knots (1 knot = 0.5144 ms^{-1}). The model estimates changes of intensity during 12 h, 24 h, 36 h, 48 h, 60 h, 72 h, 84 h, 96 h, 108 h and 120 h intervals. The SCIP model has been used operationally at IMD since 2008 for real-time forecasting of TC intensity.

6.4.4. *Component-IV: Rapid Intensification (RI) Index*

The rapid intensification index (RII) was formulated using threshold (index) values of eight large scale atmospheric variables for which statistically significant differences were found between the RI and non-RI cases (Kotal and Roy Bhowmik, 2013). The RI phase is defined as an increase of intensity by 30 kt (15.4 ms^{-1}) or more during 24 h. The RII technique estimates the probability of RI over the subsequent 24 h. The technique has been used at IMD since 2011 for real-time forecasting of RI.

6.4.5. *Component-V: Decay of Intensity after the landfall*

Considering the destructive potential and impact on human activities during landfall and after landfall, Roy Bhowmik *et al.* (2005) developed a Decay model for prediction of decaying intensity of TCs after landfall at 6 h interval up to 24 h. A correction method for updating forecasts after 6 h of landfall is also applied in the decay model using the decay rate of first 6 h. Roy Bhowmik *et al.* (2005) have explained the details of correction method. The decay model has been used at IMD for real-time forecasting since 2008.

6.5. Forecast skill of genesis potential parameter (GPP), average track and intensity forecast errors for cyclonic storms over the North Indian Ocean

6.5.1. *Forecast Skill of Genesis potential parameter (GPP)*

Since all low pressure systems do not intensify into cyclones, it is important to estimate the potential for intensification (into a cyclone) of a low pressure system at the early stages of development. Genesis potential parameter (GPP) used in real-time for distinguishing between developing and non-developing systems at their early stages (T-number 1.0, 1.5, 2.0) of development. The spatial distribution of GPP for two typical cyclone cases of Phailin [Fig. 6.2(a)] and Bulbul [Fig. 6.2(b)] show that the parameter was able to predict the most favourable zone of cyclogenesis for cyclone Phailin over the east Andaman Sea seven days ahead and for cyclone Bulbul over the north Andaman Sea five days ahead. In general, the GPP could able to predict the cyclogenesis zone four to five days ahead(Kotal and Bhattacharya, 2013).

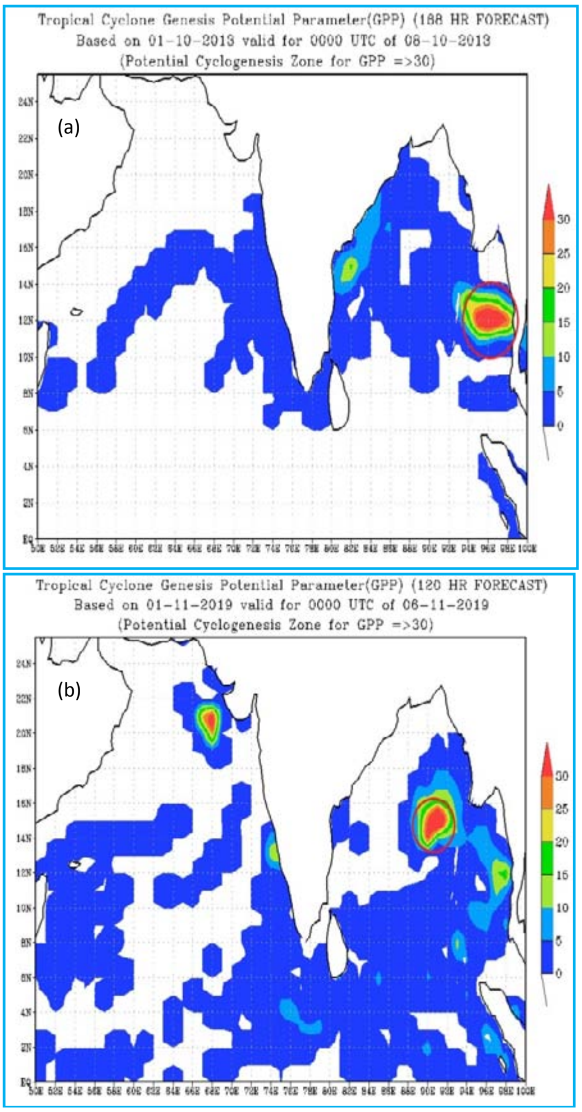

Figs. 6.2(a&b). Spatial distribution of GPP for (a) Phailin and (b) Bulbul

Prediction of cyclogenesis [Genesis Potential Parameter (GPP)] for 'DEPRESSION' over the Bay of Bengal during 2-3 April, 2021

Track of 'DEPRESSION' over the Bay of Bengal during (2-3) April 2021 is shown in Fig. 6.3. Grid point analysis and forecasts of GPP [Fig. 6.4(a-d)] clearly indicated weakening of the system over the Sea.

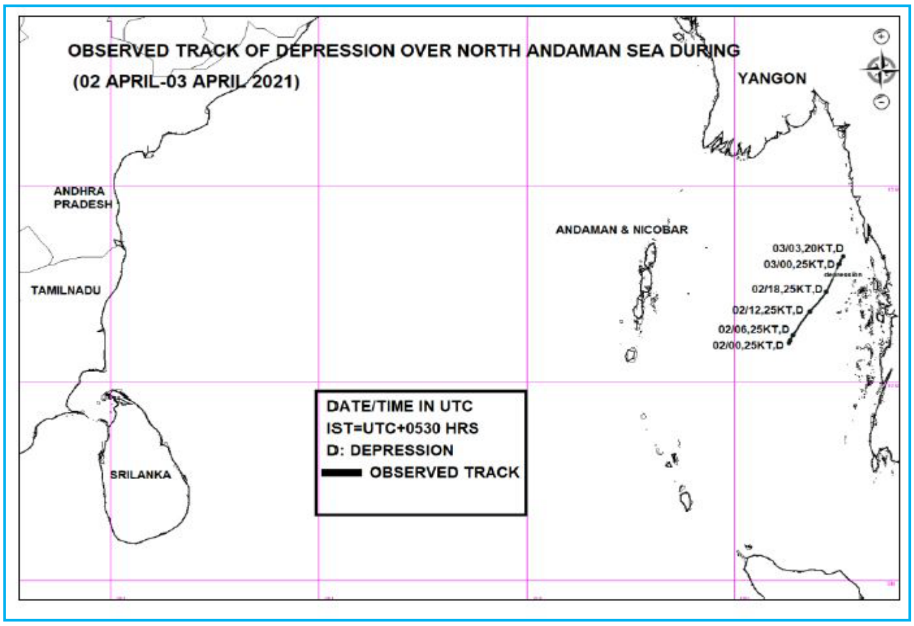

Fig. 6.3. Track of 'DEPRESSION' over the Bay of Bengal during (2-3) April 2021

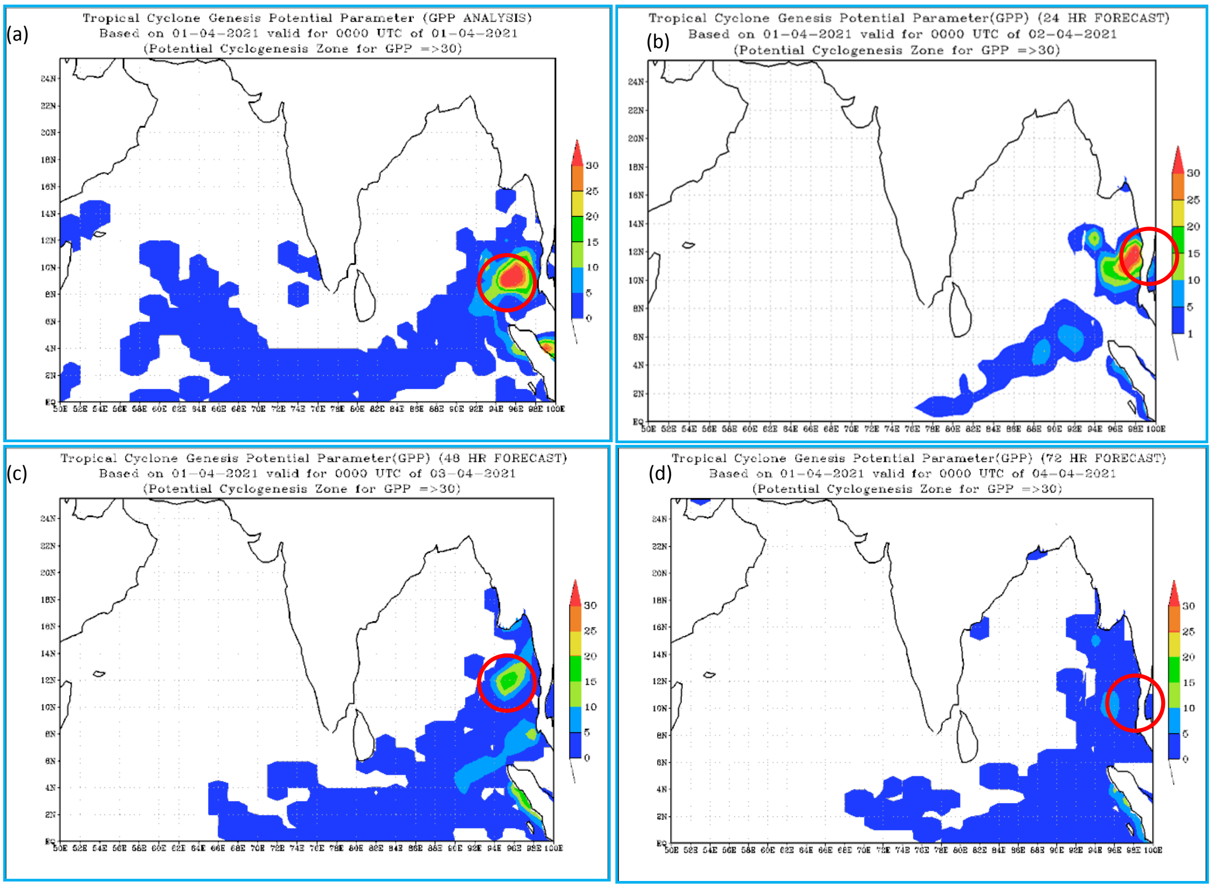

Figs. 6.4(a-d). Predicted zone of cyclogenesis

Area average analysis of GPP

Area average analysis and forecasts of GPP [Figs. 6.5(i-iv)] for the Depression also indicated weakening of the system over the Sea.

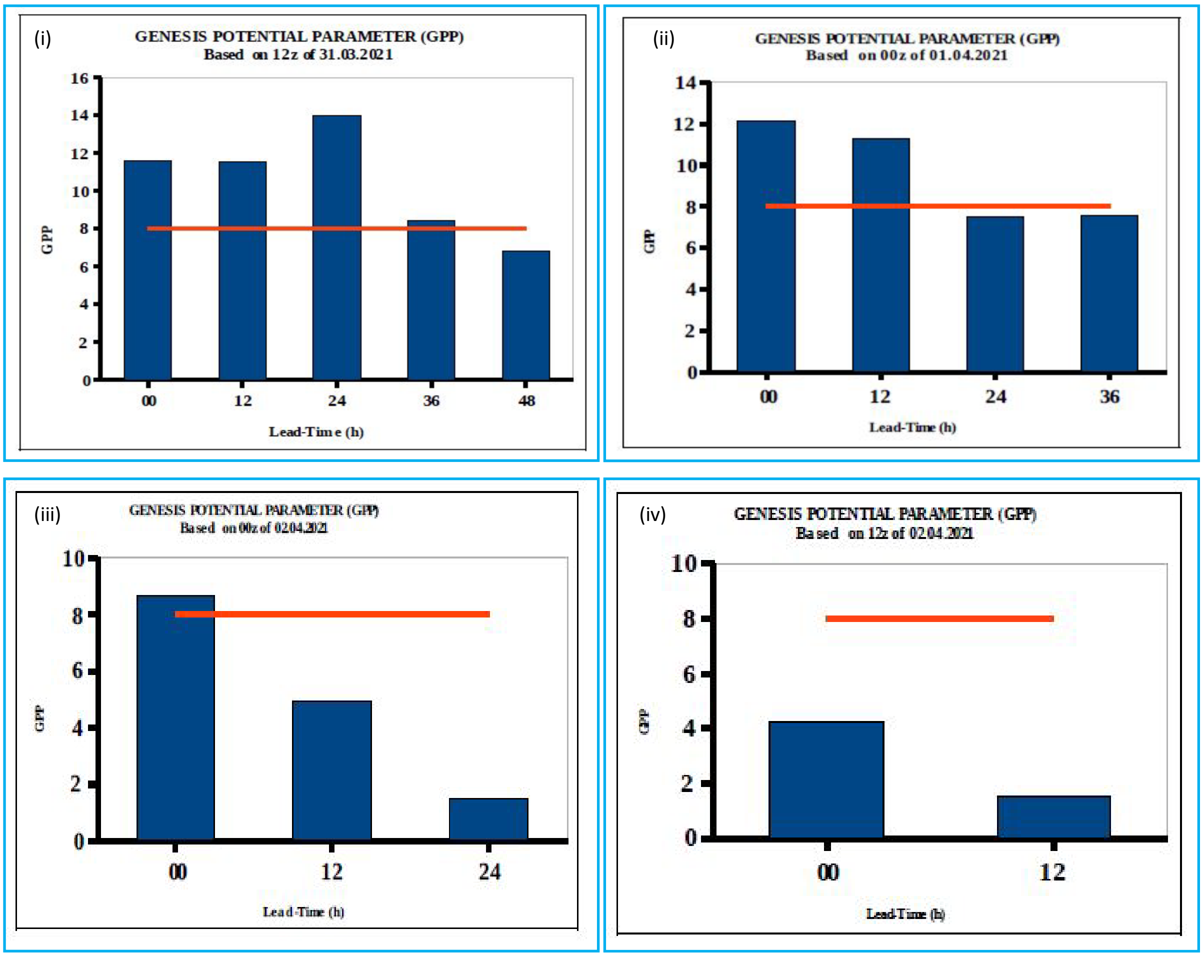

Figs. 6.5 (i-iv). Area average analysis and forecasts

Six metrics, such as the probability of detection (POD), the false alarm ratio (FAR), critical success index (CSI), equitable threat score (ETS), frequency bias (BIAS) and proportion correct (PC) for genesis forecasts by GPP during 2020 [Fig. 6.6(a)] and (2008-2020) [Fig. 6.6(b)] indicates skill score of GPP.

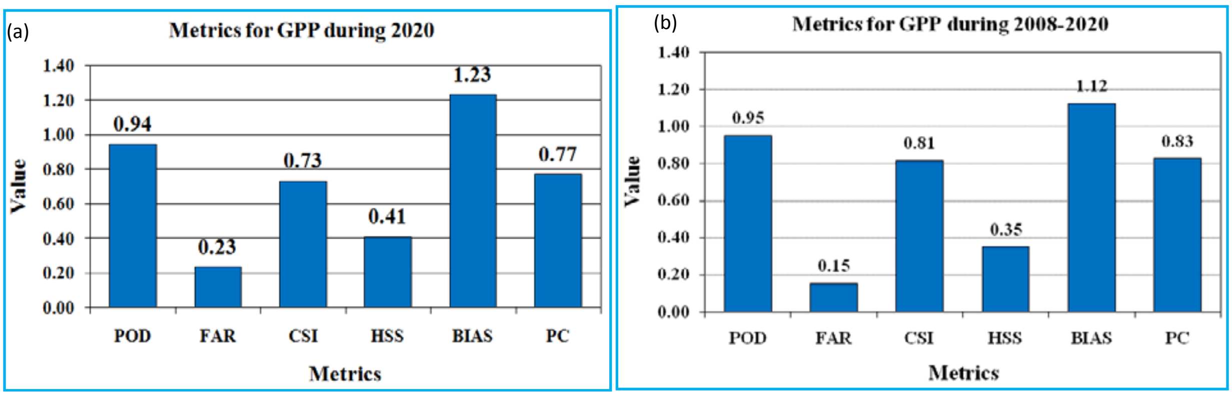

Figs. 6.6(a&b). POD, FAR, CSI, ETS, BIAS and PC for all genesis forecasts of GPP during (a) 2020 and (b) 2008-2020

6.5.2. *Mean track forecast error (km)*

The annual average track forecast errors (Direct position error (DPE)) of various models during the year 2020 are shown in Table 6.1. The 24 h track forecast errors is about 50 km for MME and less than 100 km for all models, 48 h track forecast errors is less than 75 km for MME, between 88-162 km for other models, 72h track forecast errors is less than 100 km for MME, between 92-233 km for all other models. The 96 h track forecast error is about 120 km for MME, and between 159-312 km for other models, and 120 h track forecast errors is less than 150 km for MME, less than 100 km for NCEP-GFS, and between 198-339 km other models. Consensus track forecast error of MME ranged from 49 km at 12h to 145 km at 120h. Mean MME track forecast errors (km) during 2010-2019 is shown in Fig. 6.7. Year wise mean MME track forecast error (km) during 2009-2020 is shown in Fig. 6.8 below.

Table6.1

Annual average track forecast errors (DPE) of various models for the year 2020 (Number of forecasts verified given in the parentheses)

Lead time →	12 hr	24 hr	36 hr	48 hr	60 hr	72 hr	84hr	96hr	108hr	120hr
MME	49(27)	51(27)	53(24)	71(18)	70(14)	84(11)	86(6)	119(4)	76(2)	145(1)
ECMWF	67(27)	75(27)	87(24)	104(18)	84(13)	92(10)	128(6)	202(4)	261(2)	339(1)
NCEP-GFS	58(27)	74(27)	87(24)	147(18)	160(14)	209(11)	194(6)	223(4)	171(2)	94(1)
IMD-GFS	79(27)	86(27)	123(24)	162(18)	178(14)	233(11)	228(5)	312(3)	221(2)	198(1)
UKMO	63(27)	71(27)	72(24)	88(18)	100(14)	121(11)	165(6)	159(4)	198(2)	215(1)
JMA	73(27)	98(27)	125(24)	126(18)	127(14)	150(11)	236(6)	-	-	-

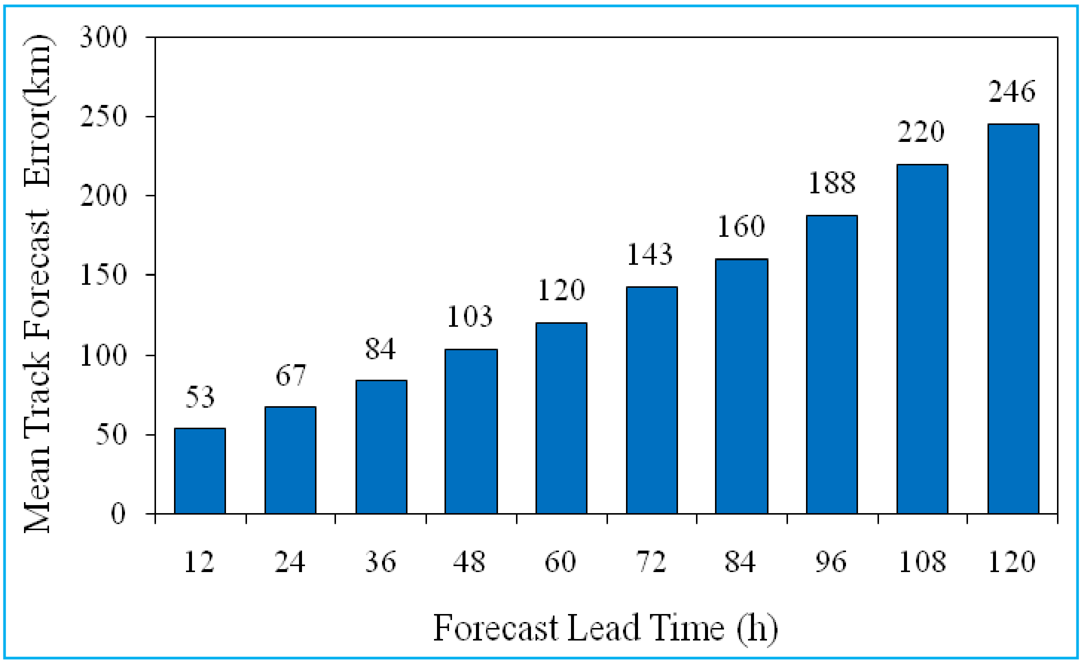

Fig. 6.7. Mean MME track forecast errors (km) during 2010-2019 (84 h to 120 h error from 2013-2019)

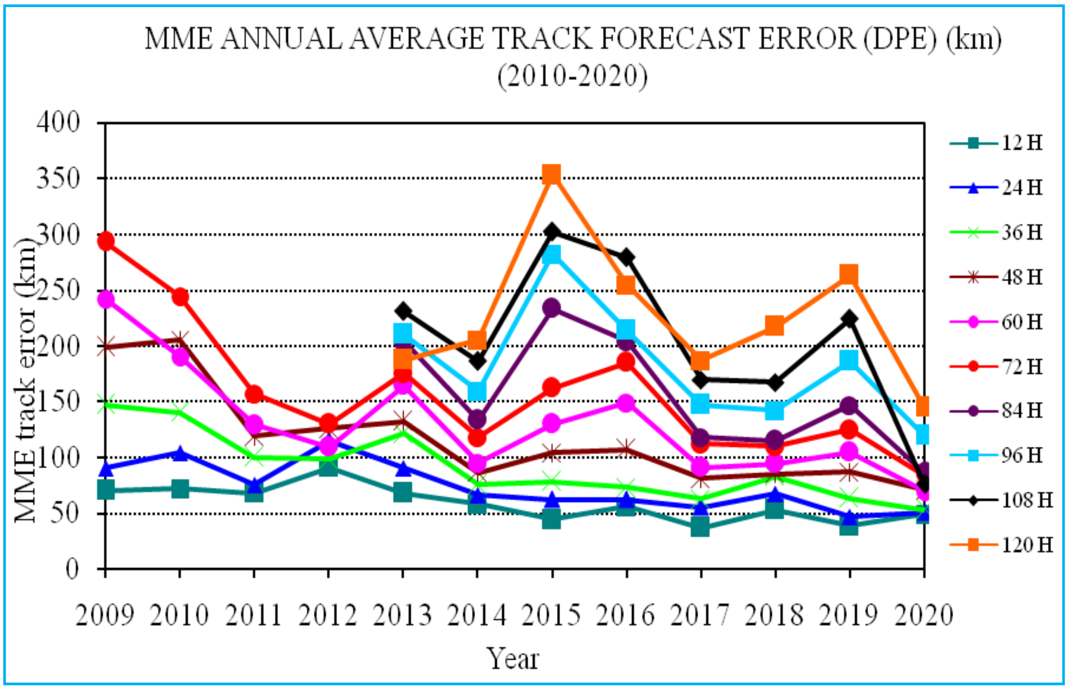

Fig. 6.8. Year wise MME track forecast error (km) during 2009-2020

Further trend analysis of track error shows that during the period 2010-2019, DPE of MME has reduced significantly by about 41% to 55% for forecast lead time 24 h to 72 h (Fig. 6.9).

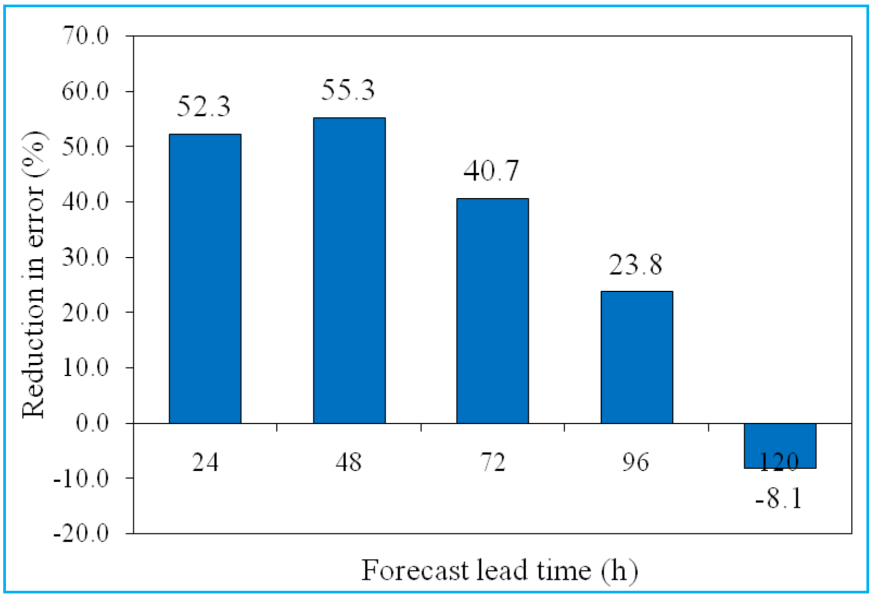

Fig. 6.9. MME track forecast error (DPE) reduction during 2010-2019

All forecast tracks of MME for each cyclone along with observed track for six typical individual land falling TCs (Phailin, Hudhud, Fani, Bulbul, Roanu, Mora) considering their wide diversity in nature in terms of intensity and track are shown in Fig. 6.10 to visualize the accuracy and consistency of MME track forecasts. In each case of the six TCs as shown in Fig. 6.10, colour tracks show all MME forecast tracks and black track shows observed track as per best-track data.

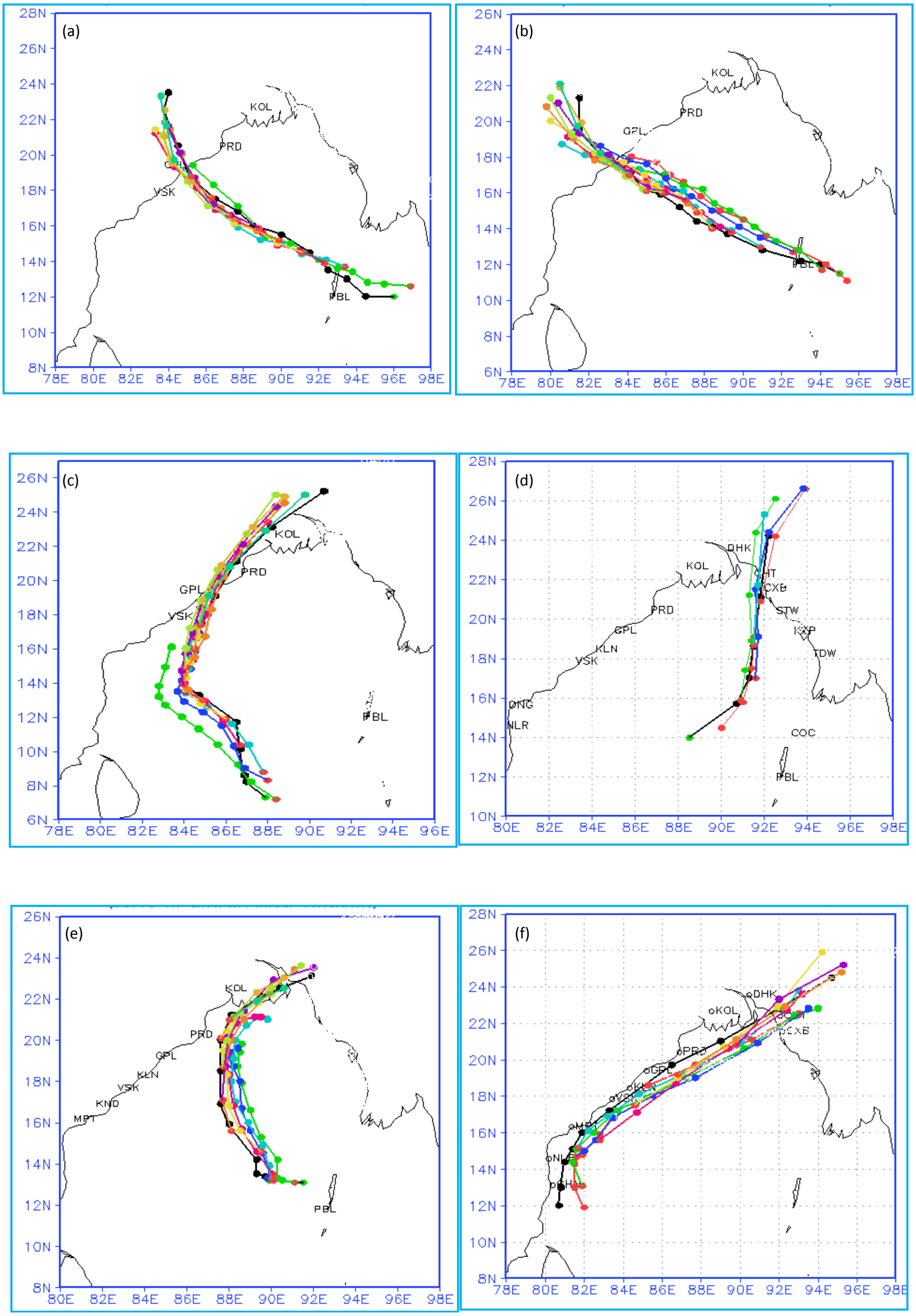

Figs. 6.10(a-f). Plots of all MME forecast tracks(colour tracks) along with observed track (black colour) in each panel for TCs (a) Phailin, (b) Hudhud, (c) Fani, (d) Mora, (e) Bulbul and (f) Roanu

Mean track forecast errors (km) (DPE) during 2010-2019 shows that IMD-MME outperformed all the forecasts (shown in the Fig. 6.11). It is also noted that among individual models, ECMWF performed better than all other models.

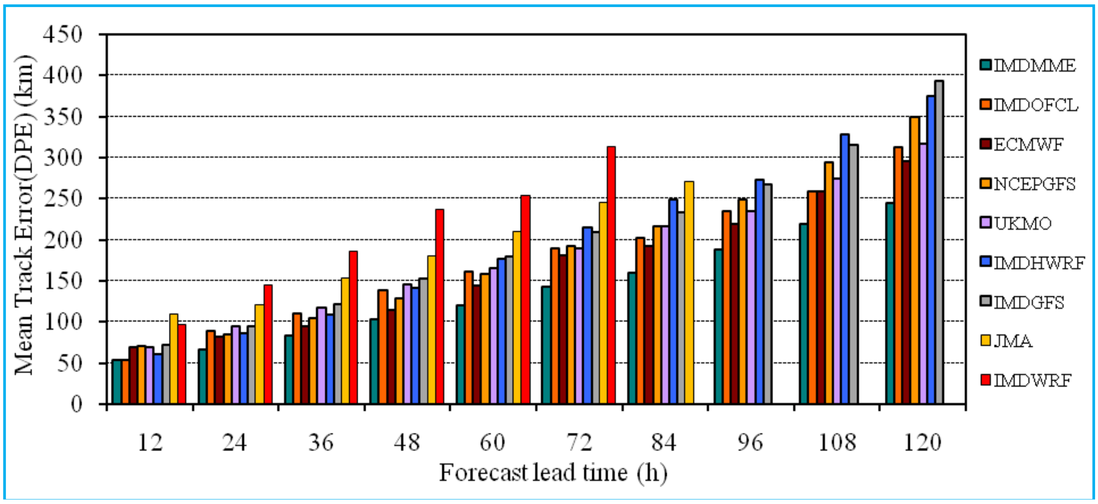

Fig. 6.11. Mean track forecast errors (km) (DPE) during 2010-2019 (84 h to 120 h error from 2013-2019)

6.5.3. *Mean Intensity forecast error (kt)*

The annual average intensity forecast errors of SCIP model for 2020 are shown in Table 6.2. The absolute average error (AAE) is 7.1 kts at 24h, 13.7 kts at 48h, 9.4 kts at 72h, 23.0 kts at 96 h and 19.0 kts at 108 h for all the cyclonic storms over the North Indian Seas during the year 2020. Year wise and mean intensity forecast error (kt) by SCIP model during 2008-2020 for 12h to 120h forecasts are presented in Fig. 6.12.

Table6.2.

The annual average intensity forecast errors (kt) AAE and RMSE (root mean square error) of SCIP for all the systems during 2020 (Number of forecast verified given in the parentheses)

Lead time →	12H	24H	36H	48H	60H	72H	84H	96H	108H
IMD-SCIP (AAE)	4.5 (25)	7.1 (21)	10.9 (16)	13.7 (13)	14.1 (9)	9.4 (5)	9.3 (3)	23.0 (2)	19.0 (1)
IMD-SCIP (RMSE)	5.9	10.2	14.7	17.1	18.1	9.9	9.7	23.0	19.0

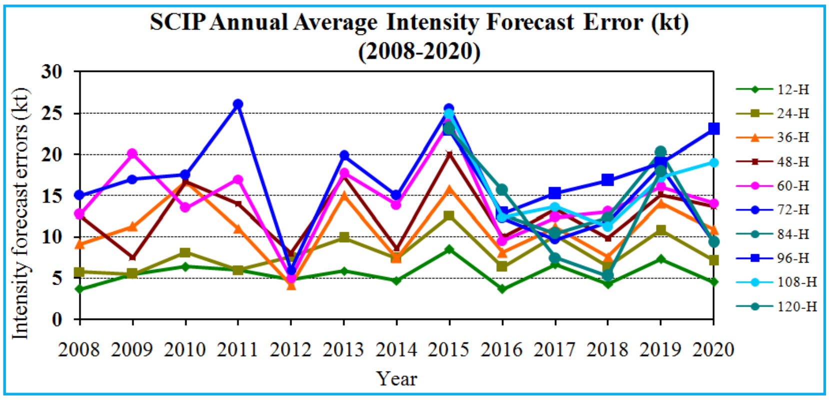

Fig. 6.12. Year wise intensity forecast error (kt) by SCIP model during 2008-2020 for 12 h to 120 h forecasts

The above analysis illustrates that CPS provided more robust guidance than most other forms of guidance in TC forecasting over recent years in the NIO.

6.5.4. ***Probability Forecast of Rapid Intensification (RI)***

The rapid intensification index (RII) is being used at IMD since 2011 for real-time forecasting of RI. The skill of the RII has been assessed for the period 2011-2019 by computing the Brier score (BS). The Brier score is defined as:

$$BS = \frac{1}{N}\sum (F - O)^2 \qquad (3)$$

where *F* is the probability of forecast, *O* the actual event observed (*O* = 0 if it did not happen and 1 if it happened) and N is the total number of forecasts. For example, when RI event is observed, a forecast probability of 75% would yield a BS= 0.0625 [i.e., $(0.75\text{-}1.0)^2$]. The BS = 0 considered as the best score and 1 the worst score. For 284 forecast events during the period 2011-2019, the BS is found to be 0.079. For 24 RI cases and 260 Non-RI cases the BS were 0.494 and 0.041 respectively. The overall score (0.079) for all 284 RI and non-RI cases shown RII achieved a good score for RI forecasting during the period.

6.5.5. ***Decay after landfall***

The average forecast errors (kt) at 6 h interval valid up to 24 h during the period 2010-2019 are shown in Fig. 6.13. The decay and updated decay after 6 h of landfall of extremely severely cyclonic storm HUDHUD is shown in Fig. 6.14. The mean error statistics show that the model forecasts for decaying intensity after landfall were reasonably good.

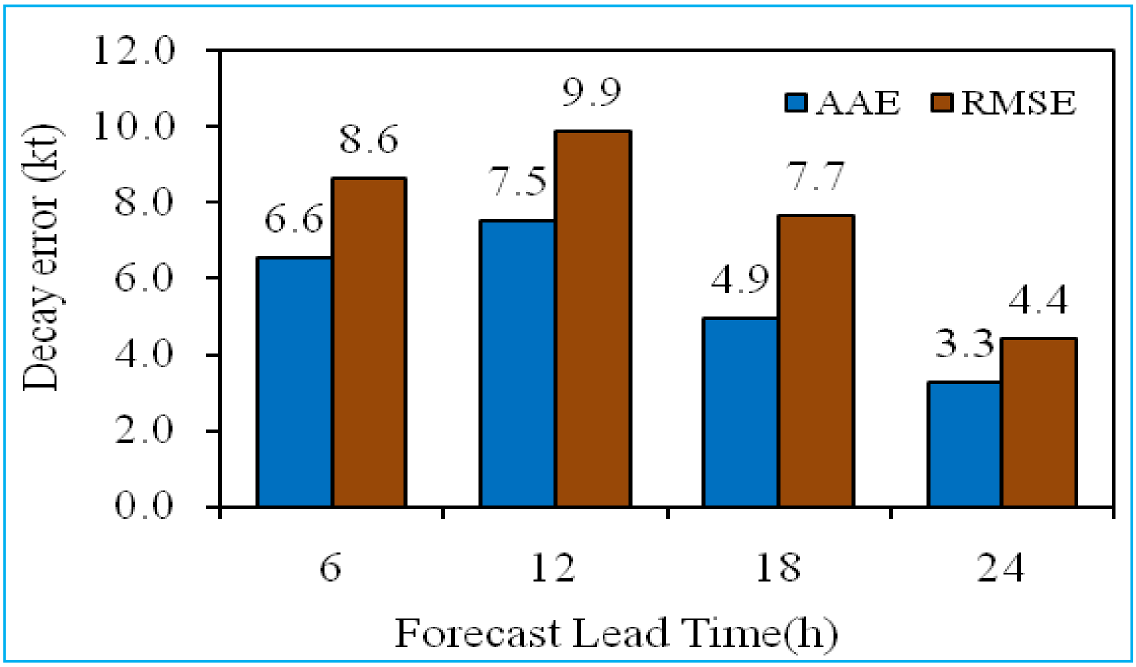

Fig. 6.13. Average absolute error (AAE) and root mean square error (RMSE) of decay (kt) after landfall during 2010-2019

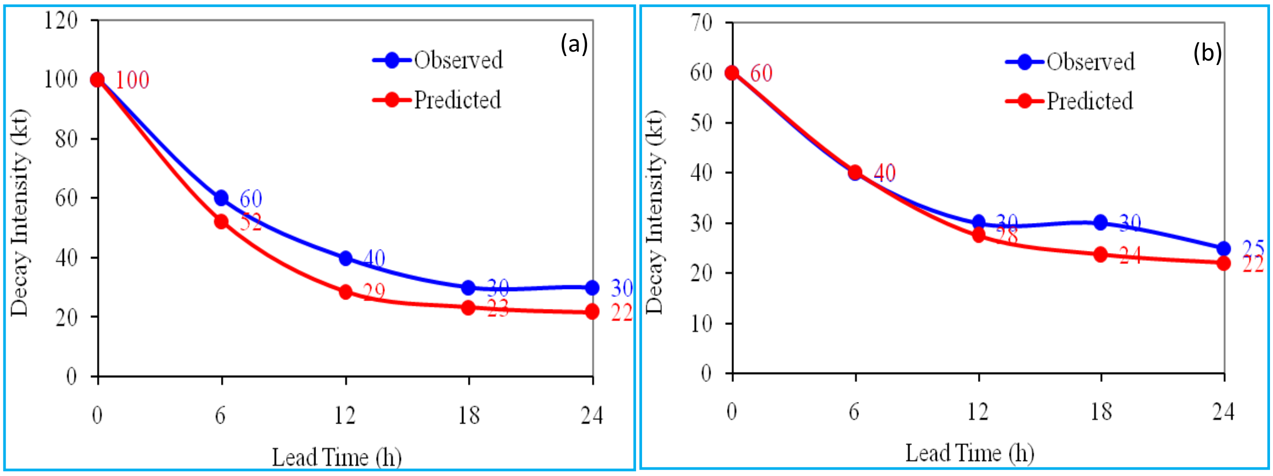

Figs. 6.14(a&b). Decay forecasts by Decay model *vs* Observed decay for TCs (a) Phailin at the time of landfall and (b) Phailin updated after 6h of landfall

7. Mean track and intensity forecast error of 2021

The annual average track forecast errors [Direct position error (DPE)] of various models during the year 2021 are shown in Table 6.3. The 24h track forecast error is about 50 km for MME and between 70 km to 80 km for all models, 48h track forecast error is 85 km for MME, between 100 -122 km for other models, 72h track forecast errors is 135 km for MME, between 145-231 km for all other models. The 96h track forecast error is about 258 km for MME, and between 145-424 km for other models, and 120h track forecast errors is 435 km for MME, and between 182-688 km other models.

Table 6.3

Annual average track forecast errors (DPE) of various models for the year 2021 (Number of forecast verified given in the parentheses)

Lead time →	12 hr	24 hr	36 hr	48 hr	60 hr	72 hr	84hr	96hr	108hr	120hr
MME	37(28)	52(28)	62(26)	85(23)	102(17)	136(13)	164(7)	258(5)	258(2)	435(1)
ECMWF	48(28)	76(28)	79(26)	100(23)	100(17)	110(13)	109(7)	146(5)	96(2)	182(1)
NCEP-GFS	72(27)	73(25)	109(24)	122(22)	148(16)	207(12)	297(7)	424(5)	413(2)	688(1)
IMD-GFS	64(28)	79(27)	97(23)	116(21)	154(16)	180(12)	191(7)	260(5)	294(2)	335(1)
UKMO	53(28)	70(28)	76(26)	99(23)	123(17)	144(12)	208(7)	304(5)	270(2)	443(1)
JMA	59(28)	72(27)	89(24)	118(20)	184(15)	231(12)	348(7)	-	-	-

The annual average intensity forecast errors of SCIP model for 2021 are shown in Table 6.4. The absolute average error (AAE) is 4.1 kts at 24h, 9.8 kts at 48h, 11.2 kts at 72h, 16.8 kts at 96 h and 22.0 kts at 108 h for all the cyclonic storms over the North Indian Seas during the year 2021.

Table 6.4

The annual average intensity forecast errors (kt) AAE and RMSE (root mean square error) of SCIP for all the systems during 2021(Number of forecast verified given in the parentheses)

Lead time →	12H	24H	36H	48H	60H	72H	84H	96H	108H
IMD-SCIP (AAE)	4.6 (28)	4.1 (26)	7.3 (24)	9.8 (21)	9.3 (14)	11.2 (10)	14.4 (7)	16.8 (5)	22.0 (2)
IMD-SCIP (RMSE)	5.6	5.2	8.8	13.8	13.8	15.8	21.4	23.2	28.4

6.6. Summary

The necessity of dynamical-statistical model for tropical cyclone forecast is mainly attributed to limitation of NWP models, variation of forecasts among models, and requirements for different forecast services. There is also need to generate more skillful, consensus, and requirement based products. In this report, the evolution and efficacy of forecast of dynamical-statistical cyclone prediction system (CPS) and forecast of NWP models used for real-time forecasting of TCs over the North Indian Ocean are presented for the past decade 2010-2019. The result shows that the dynamical-statistical technique can add skill to dynamical forecast. The performance analyses of NWP models and each component of CPS have brought out the probable forecast errors. Results show that the GPP was skillful for cyclogenesis prediction. Track forecasts by MME outperformed all individual models. The overall score for RI and non-RI cases show RII achieved a good score for RI forecasting during the period but RI is found to be most challenging. Intensity forecasts by SCIP model and decay model was found to be reasonably good. The performance of CPS demonstrates the efficacy of the system for improvement of cyclone forecast over the NIO in the past decade (2010-2019).

Acknowledgments

The authors are grateful to the Director General of Meteorology, India Meteorological Department for his encouragement, constant support and providing all facilities to carry out this work. Authors acknowledge the use of best-track data and track forecast data of tropical cyclones from the Regional Specialized Meteorological Centre (RSMC) in New Delhi. We thankfully acknowledge the use of model outputs of ECMWF, NCEP, UKMO and JMA in this report. Support rendered by the officers and staff of the NWP division is duly acknowledged.

References

Heming, J., 1994, Verification of Tropical Cyclone Forecast Tracks at the UK Met Office. NWP Gazette, **1**, 2-8.

Kotal, S. D. and Bhattacharya S. K., 2013, Tropical Cyclone Genesis Potential Parameter (GPP) and it's application over the North Indian Sea, *Mausam*, **64**, 149-170.

Kotal, S. D. and Bhattacharya S. K., 2020, Improvement of wind field forecast for tropical cyclones over the North Indian Ocean, *Tropical Cyclone Research and Review*, **9**, 53-66.

Kotal, S. D. and Roy Bhowmik S. K., 2011, A Multimodel Ensemble (MME) Technique for Cyclone Track Prediction over the North Indian Sea, *Geofizika*, **28**(2), 275-291.

Kotal, S. D. and Roy Bhowmik S. K., 2013, Large-Scale Characteristics of Rapidly Intensifying Tropical Cyclones over the Bay of Bengal and a Rapid Intensification (RI) Index, *Mausam*, **64**, 13-24.

Kotal, S.D., Kundu, P. K. and Roy Bhowmik S.K., 2009, Analysis of Cyclogenesis parameter for developing and non-developing low pressure systems over the Indian Sea, *Natural hazards*, **50**, 389-402.

Kotal, S.D., Roy Bhowmik, S.K., Kundu, P.K. and Das, A.K., 2008, A Statistical Cyclone Intensity Prediction (SCIP) Model for Bay of Bengal, *Journal of Earth System Science*, **117**, 157-168.

Kotal, S.D. and Bhattacharya S.K., 2021, Evolution of Tropical Cyclone Forecasts of Dynamical-statistical Cyclone Prediction System (CPS) over the North Indian Ocean during the decade (2010-2019). *Mausam*, **72**(1), 87-106.

Kotal, S. D., Bhattacharya S. K. and Roy Bhowmik S. K., 2014, Development of NWP based objective Cyclone Prediction System (CPS) for North Indian Ocean Tropical Cyclones – Evaluation of performance, *Tropical Cyclone Research and Review*, **3**(3), 162-177.

Roy Bhowmik S. K. and Kotal S. D., 2010, A dynamical statistical model for prediction of a tropical cyclone, *Marine Geodesy*, **33**, 412-425.

Roy Bhowmik S. K., Kotal, S. D. and Kalsi S. R., 2005, An empirical model for predicting decaying rate of tropical cyclone wind speed after landfall over Indian region, *Journal of Applied Meteorology*, **44**, 179-185.

Roy Bhowmik, S. K., 2003, An evaluation of cyclone genesis parameter over the Bay of Bengal using model analysis, *Mausam*, **54**, 351-358.

CHAPTER 7

Distribution of Observed Lightning Density over India and Development of NWP based Lightning Prediction Modelling System Using E-WRF Model

TRISANU BANIK, D. R. PATTANAIK, ANANDA K. DAS, S. D. PAWAR and S. S. KUNDU

7.1. Introduction

Lightning strikes are the worst killer in India among all the natural disasters as per the data of the National crime records bureau of India (ncrb.gov.in). Lightning strokes' major impact is human deaths and many people who survived after lightning strikes showed symptoms of “memory loss, dizziness, weakness, numbness, and other life-altering elements”. Lightning strikes can cause cardiac arrest and severe burns. Lightning strikes impact trees by vaporizing water present in the tree into steam and may blow the tree apart (nationalgeographic.com). The population density also plays a vital role in such a situation. The states like Uttar Pradesh, Bihar, Andhra Pradesh, Assam, Odisha, Maharashtra belong to high population density and high LSD. Therefore, in terms of human life threats and property damages, those states are highly vulnerable.Thepresent study aims to analyze lightning stroke density for the five consecutive years i.e., 2017, 2018, 2019, 2020 and 2021 respectively across the Indian subcontinent. The observance of lightning events, the installation of lightning sensors, data preparation and analysis were doneusing earth networks and Indian Institute of Tropical Meteorology's (IITM) ground-based sensors.

The 5 years’ climatology patterns show the Eastern Part of India is more lightning-prone than other parts of India. Major parameters like lightning strokes density (LSD) and total lightning events recorded in each state and union territories of India from 2017 to 2021 were reported in this study. The analyses with the existing lightning sensors distribution show the state Odisha evidence most lightning stroke events among all states and UT’s of India. After the state, Odisha, the states West Bengal, Jharkhand, Karnataka & Chhattisgarh are the next four highest lightning stroke event associated states.

Further, an extensive analysis of the Thunderstorm/Lightning events that happened during 25 June 2020 over the Uttar Pradesh and Bihar, that killed more than 100 People in a single event has been presented here. This observation of lightning is conducted to show the necessity of establishing an accurate lightning nowcast/forecast system for India. Therefore, understanding lightning physics, its occurrence time, duration, spatial distribution and forecast of lightning and disseminating the information to each doorstep is highly required. IMD is working for the last many years and collaborates with different scientific institutes like the North Eastern Space Applications centre, Indian Institute of Tropical Meteorology and generating lightning-related information, running lightning forecasts and disseminating the same with the various concerned departments.

7.2. Lightning Data used in the present study

Lightning sensors installation increased from 2017 to 2019 over India and thus accuracy in reporting of the forecast for lightning events also got improved effectively. Newly 10 and 8 Lightning sensors were installed in states like Karnataka, West Bengal in 2018 respectively, while 6 and 2 more lightning sensors were installed in Odisha, Assam and one each in Nagaland and Mizoram respectively in 2019. The increase in installation of lightning sensors in the West Bengal region improved in reporting lightning events in West Bengal, Odisha, Jharkhand states mainly in 2018 and as a result, we observed an increase in the number of lightning strokes in the Eastern region of India in 2018. Similarly, lightning events were more accurately reported in North-Eastern states and Odisha in 2019. During 2019, 2020 and 2021 we have utilized the IITM ground-based sensors data due to the unavailability of the Earth Networks datasets.

7. 3. Annual climatology of lightning stroke density

7.3.1. *Five Years Lightning Climatology*

The phenomena of lightning can be analyzed using various parameters and one of them is Lightning Strokes Density (LSD). In Fig. 7.1, five consecutive years (2017-2021) accumulated LSD has been produced. The LSD climatology based on five years of ground-based lightning data has been represented through lightning stroke count per 9 square kilometer area in Fig. 7.1. The fig. 7.1 reflects the high LSD over North East India, over the states Odisha, West Bengal, Lower Assam, Meghalaya Bihar, Jharkhand, Chattishgarh etc. The peninsular India eastern and western coast of India is also receiving a large number of lightning events each year. Some lightning hotspot areas are visible in the plot over the western and eastern peninsular India over the states like Andhra Pradesh, Telangana, Maharashtra, Karnataka, Kerala, and Tamilnadu apart from the big hotspot over East India. The expansion of ground-based lightning sensors over the Northern part of India needs more improvement. One of the lightning hotspots (evident from TRMM–LIS data) over the extreme north-western part of India including surrounding countries is not well captured by the ground-based networks due to the sparsity of lightning sensors over Kashmir and the surrounding region. But the increment of several ground-based lightning sensors over the years improves the network's lightning detection efficiency significantly. But more uniform detection capability is required for further improvement of the ground-based lightning networks.

This is very important to note that, even a single lightning incident can be deadly to anyone out there during a storm. Therefore, regardless of some states have low LSD, it does not intend those states to be free from lightning calamities. One incident on 25 June 2020 proved that. A thunderstorm with a high amount of CG lightning killed more than 100 people in Uttar Pradesh and Bihar. Therefore, providing lightning forecasts and spreading awareness about the deadly lightning outcome may help people to know about it and save their lives and properties.

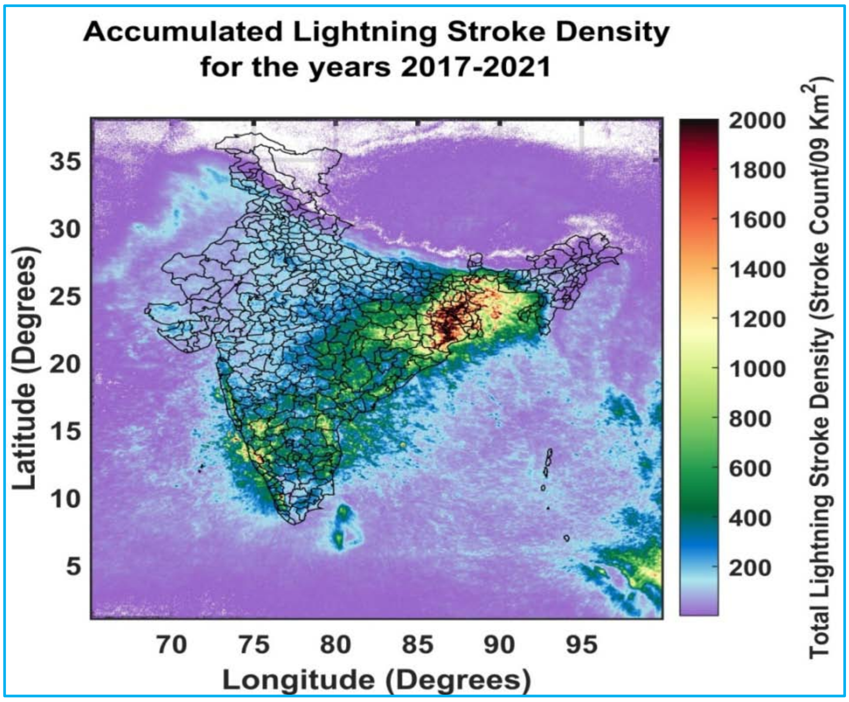

Fig. 7.1. Five years (2017-2021) of Lightning Stroke Density (LSD) Climatology for India using the Ground-based lightning data (Earth Networks data (2017, 2018) & IITM data (2019, 2020, 2021)

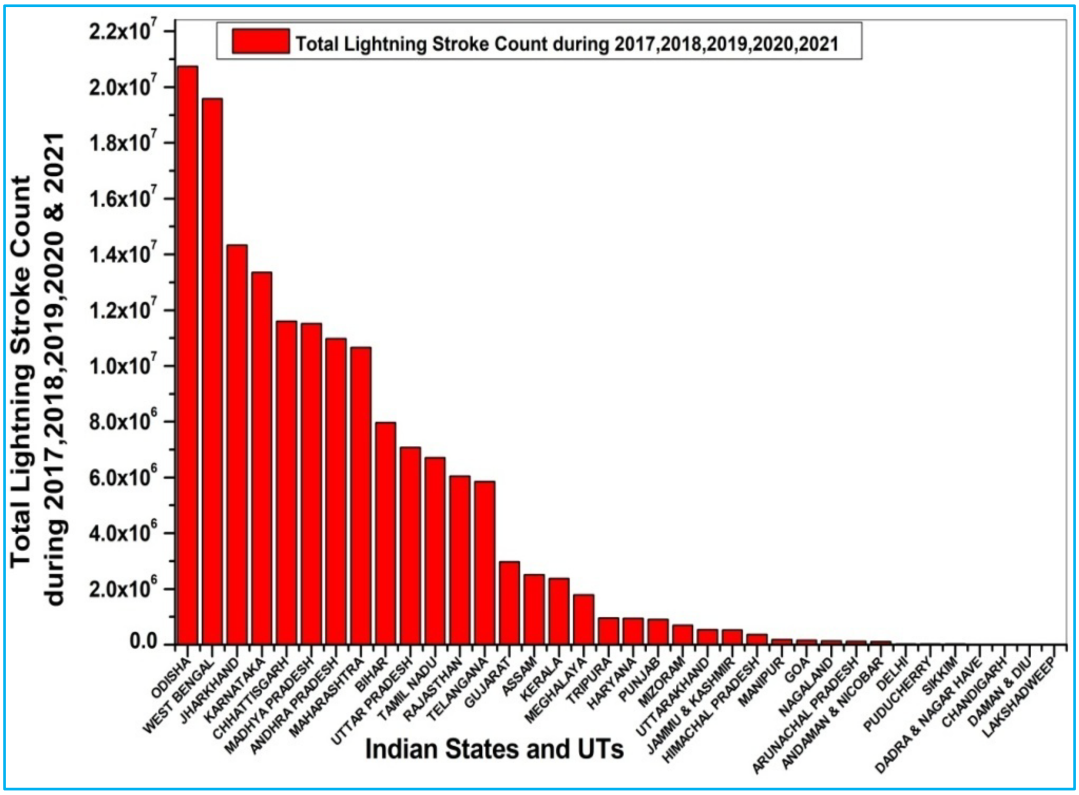

Fig. 7.2. Indian State & Union Territory wise Total Lightning Stroke Counts combining the analyses years 2017 to 2021 using Earth Networks (2017, 2018) and IITM datasets (2019, 2020, 2021)

We have further calculated the state-wide lightning stroke count for all five years in a cumulative manner and represented in Figure 7.2. The total numbers of lightning counts for all the five years (as shown in Fig 7.2) showed that Odisha, West Bengal and Jharkhand states were recorded the highest numbers of lightning strokes counts while among union territories Andaman and Nicobar Islands, Puducherry and Delhi were recorded the highest number of lightning strokes. Across the North-eastern states of India Assam, Meghalaya and Mizoram were recorded the highest number of lightning strokes. Deaths and significant impact due to lightning strikes were observed mainly in the Uttar Pradesh and Bihar region of India although these states were not among the maximum lightning counts in the country as we observed data year-wise. Significant causes of death impacts and severity to cattle and human beings due to lightning strikes can be reduced using more lightning sensors and providing information to people at least 30 minutes to 1 hour prior to lightning strikes in the region. Building of Lightning safety structures that can be used before lightning strikes or making present structures safe from lightning in India's rural region is an essential requirement for safety due to lightning. Installation of lightning sensors in West Bengal, Odisha, and North Eastern states increased the reporting of lightning events across these regions in the year 2018 and 2019 respectively. The increased installation of lightning sensors will help accurately determine lightning and provide early warning to people in the region of severe lightning events and reduce the impacts due to lightning strikes in India.

7.4. Case study of lightning strike in Bihar on 25th June, 2020

7.4.1. *Districts affected by the lightning strikes*

Last year big lightning events killed more than 100 people over the UP and Bihar on 25 June, 2020. The detailed scientific report we are presenting here;

Districts affected by lightning strike in Bihar and Uttar Pradesh on 25th June, 2020

The major districts where deaths due to lightning stroke occurred on 25th June 2020 in Bihar were Gopalganj (13), Madhubani (8), Nawada (8), Siwan (6), Bhagalpur (6), East Champaran (5), Darbhanga (5), Banka (5), Aurangabad (3), Khagaria (3), West Champaran (2), Buxar (2), Kaimur (2), Kishanganj (2), Jehanabad (2), Jamui (2), Purnia (2), Supaul (2), Sitpular (1), Sheohar (1), Madhepura (1), Saran (1), Sitamarhi (1). Lightning sensors installed by IITM, Pune at Gaya (Bihar), Ranchi (Jharkhand) and Gorakhpur (Uttar Pradesh) to provide lightning information for all locations of Bihar inan advance period of 30 minutes.

(a)

(b)

Figs. 7.3. (a&b). District Map of (a) Bihar and (b) Uttar Pradesh

Major districts where deaths due to lightning stroke occurred in Uttar Pradesh on 25th June 2020 were Deoria (9), Parayagraj (6), Ambedkar Nagar (3), Barabanki (2), Balrampur (1), Kushinagar (1), Unnao (1), Fatehpur (1) as shown in Fig. 7.3(a-b). The thunderstorm/lightning-associated clouds during 25thJune 2020 were different from monsoon clouds and this needs high surface heating and moisture for their formation. Surface heating due to the summer season and moisture through the onset of monsoon from south to north leads to the formation of thunderstorms and lightning clouds in the regions of Uttar Pradesh (UP), Bihar and Peninsular India. As monsoon sets completely in the entire region the formation of thunderstorms and lightning clouds will be reduced accordingly. Due to the prolonged western disturbances, a huge amount of lightning incidents were evidenced over Up and Bihar during the May & June months of 2020. Moisture abundancy due to the rapid progress of monsoon currents from the Bay of Bengal branch is also present in the region of Uttar Pradesh and Bihar. Thus, the combination of western disturbance instability and moisture abundancy leads to the creation of thunderstorms and lightning clouds in the Uttar Pradesh and Bihar region mainly. The region in terai belt at the foothills of Himalayas, then surface heating and moisture present in the region along with its geographic location as the Himalayas provides orographic lift to thunderstorm and lightning clouds due to their steep gradient. The lifting mechanism of the Himalayas was cause for night lightning strikes but major deaths events occurred day time when people were out in open.

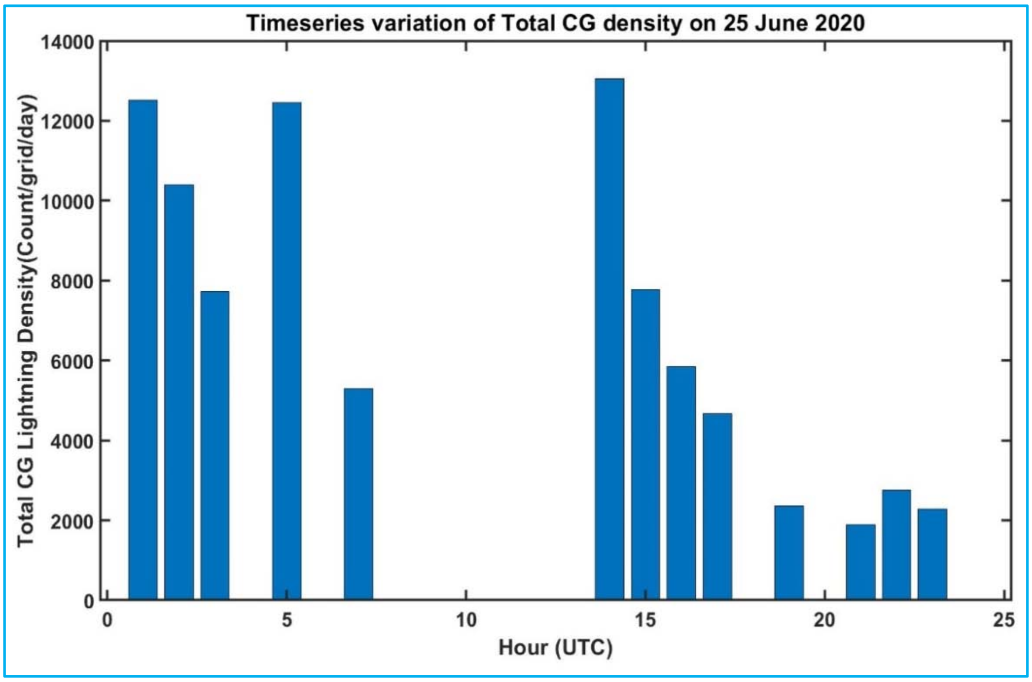

Fig. 7.4. Time series Variation of Total CG Lightning Density over Uttar Pradesh & Bihar on 25th June 2020

This is clear from Fig 7.4 there was a gap of lightning activity between8 UTC (01:30 PM) to 13 UTC (06:30 PM). But a large surge of lightning flash density in noticed during the 14 UTC (7:30 PM). As a consequence of this more than 100 people were killed at UP and Bihar.

IC Lightning stroke on 25th June 2020

The state-wise distribution of IC lightning density is also calculated and tabulated below. The intra and inter-cloud lightning strokes density on 25th June 2020 across India vary in numbers with the maximum density in Uttar Pradesh, Bihar, Jharkhand, West Bengal and peninsular India. Details are shown in Table 7.1.

Table 7.1

IC Lightning Stroke Density (LSD) in India on 25th June 2020

S.No.	IC Lightning Stroke Density(count/grid/day)	States
1.	0-100	Rajasthan, Punjab, Uttarakhand, Gujarat, Haryana, Assam, Kerala, Jammu and Kashmir
2.	100-300	Jharkhand, West Bengal, Meghalaya, Madhya Pradesh, Chhattisgarh, Odisha
3.	300-500	Uttar Pradesh, Bihar, Maharashtra, Karnataka, Andhra Pradesh and Tamilnadu

7.4.2. *Distribution of CG & IC LSD over India during 25 June 2020*

We have plotted the distribution of CG and IC LSD all over India on 25 June 2020 (Fig. 7.5). The plots clearly show that over UP and Bihar the abundance of lightning was significantly higher than in any other part of India.

We have further plotted (Fig 7.6) the LSD over UP and Bihar only so that the district-wise distribution of lightning can be represented properly. This Fig 7.6 explains the high LSD over different districts of UP and Bihar. One of the most affected districts Gopalganj suffers an LSD of more than 1000000 Lightning strokes Count/ 3 km^2/Day.

The CG LSD is divided into two categories i.e., positive CG and Negative CG LSD. Cloud to ground lightning strokes that will transfer negative charge from clouds to ground is called negative CG lightning stroke while those transfer positive charges from cloud to ground are called positive CG lightning strokes. The details regarding positive and negative LSD over whole India on 25th June, 2020 are represented in Fig. 7.7. Negative CG LSD in the range of 100-500 counts/grid/day dominant in the region of eastern Uttar Pradesh, Bihar, Jharkhand, West Bengal, Meghalaya, Madhya Pradesh, Chhattisgarh, Odisha, Maharashtra, Karnataka, Andhra Pradesh and Tamilnadu.

Positive CG LSD in the range of 10-60 counts/grid/day dominant in the region of eastern Uttar Pradesh, Bihar, Jharkhand, West Bengal, Meghalaya, Madhya Pradesh, Chhattisgarh, Odisha, Karnataka, Andhra Pradesh and Tamilnadu. Maharashtra has a positive lightning stroke density in the range of 60-100 counts/grid/day on 25th June, 2020.

(a)

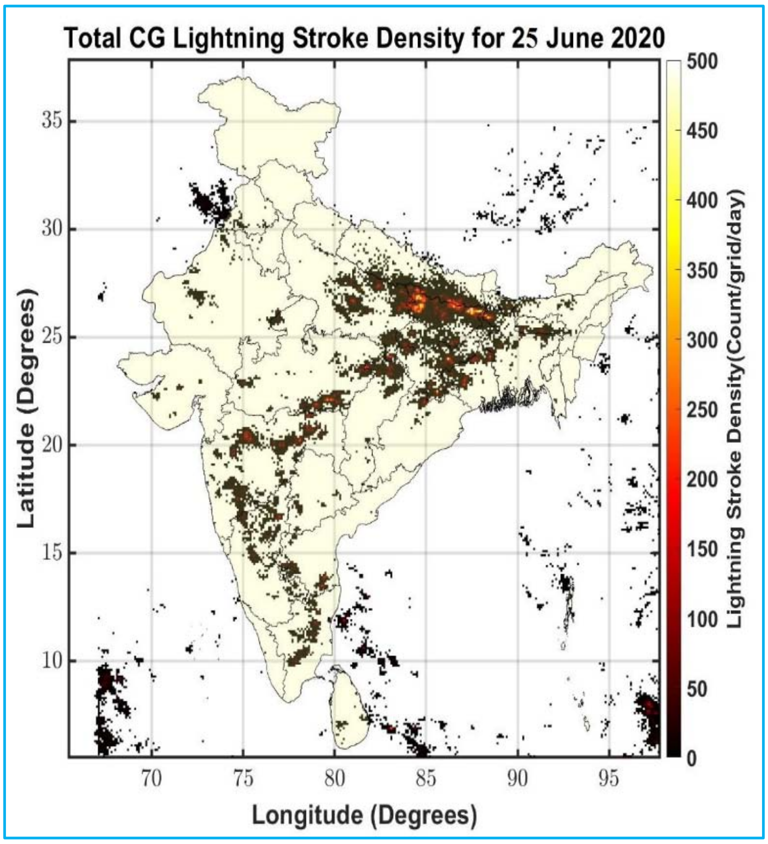

(b)

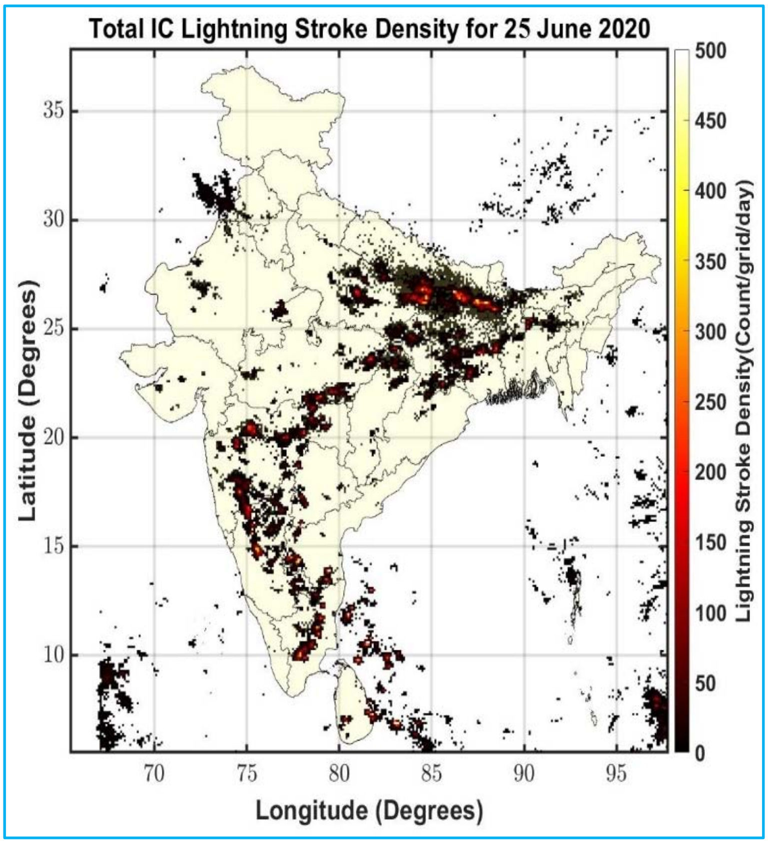

Figs. 7.5 (a&b). Total CG and IC LSD over India on 25 June, 2020 using Earth Networks datasets

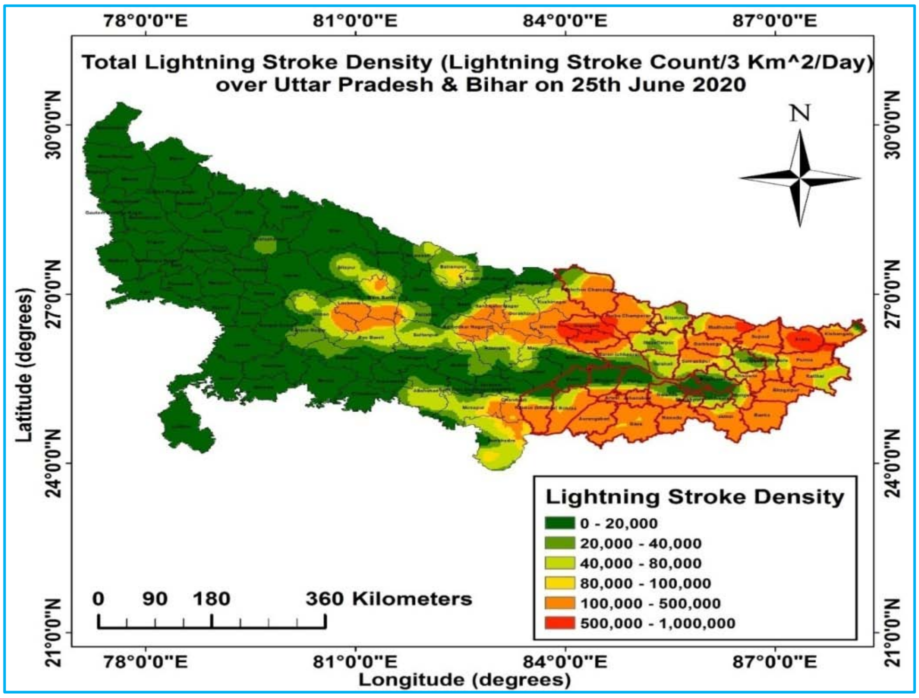

Fig. 7.6. District wise distribution of Lightning Stroke Density over UP and Bihar on 25 June, 2020 using Earth Networks datasets

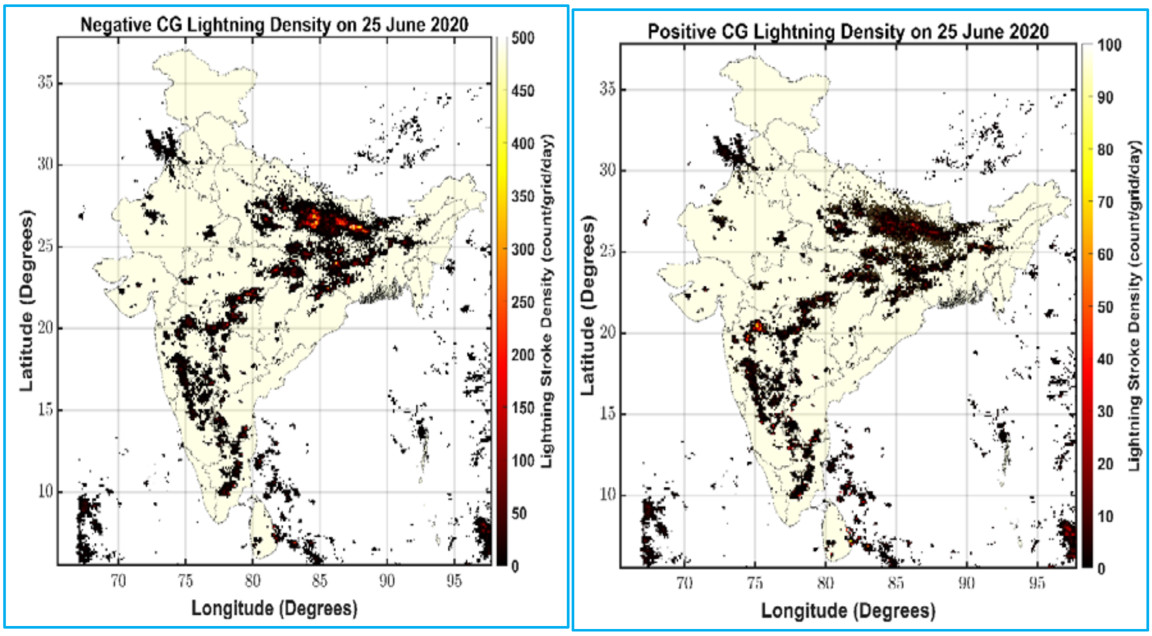

Fig. 7.7. Total CG and IC LSD over India on 25 June, 2020 using Earth Networks datasets

There were certain areas in Uttar Pradesh & Bihar, where positive CG lightning exceeds negative CG lightning which was represented by positive CG by negative CG LSD ratio in Fig 7.8. Positive CG by Negative CG LSD ratio greater than 4 in the region of eastern Uttar Pradesh, Bihar, Jharkhand, West Bengal, Meghalaya, Madhya Pradesh, Chhattisgarh, Odisha, Maharashtra, Karnataka, Andhra Pradesh and Tamilnadu and minor regions of Punjab, Telangana, Rajasthan, Gujarat and Assam. Average Negative and positive peak current distribution and magnitudes are represented by Fig 7.9. Average Negative CG peak current exceeds $0.5X10^4$to $1X10^4$ampere frequently in the region of eastern Uttar Pradesh, Bihar mainly. Negative CG peak current exceeds 10^4 Amp frequently in the regions of Jharkhand, West Bengal, Meghalaya, Madhya Pradesh, Chhattisgarh, Odisha, Maharashtra, Karnataka, Andhra Pradesh and Tamilnadu minor regions of Punjab, Telangana, Rajasthan, Gujarat and Assam. Average Positive CG peak current exceeds $4X10^4$ ampere very frequently in the region of eastern Uttar Pradesh, Bihar, Jharkhand, West Bengal, Meghalaya, Maharashtra, Karnataka and minor regions of Andhra Pradesh, Tamilnadu, Madhya Pradesh, Chhattisgarh, Odisha, Punjab, Telengana, Gujarat & Assam.

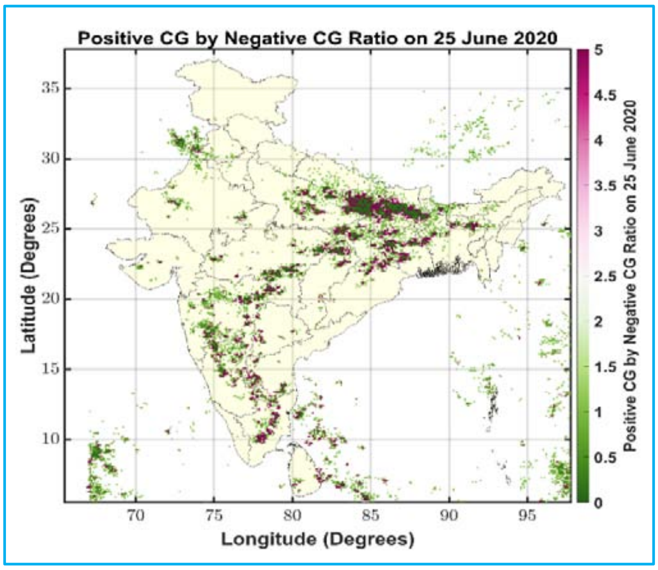

Fig. 7.8. Positive CG by Negative CG LSD ratio on25 June, 2020 using Earth Networks datasets

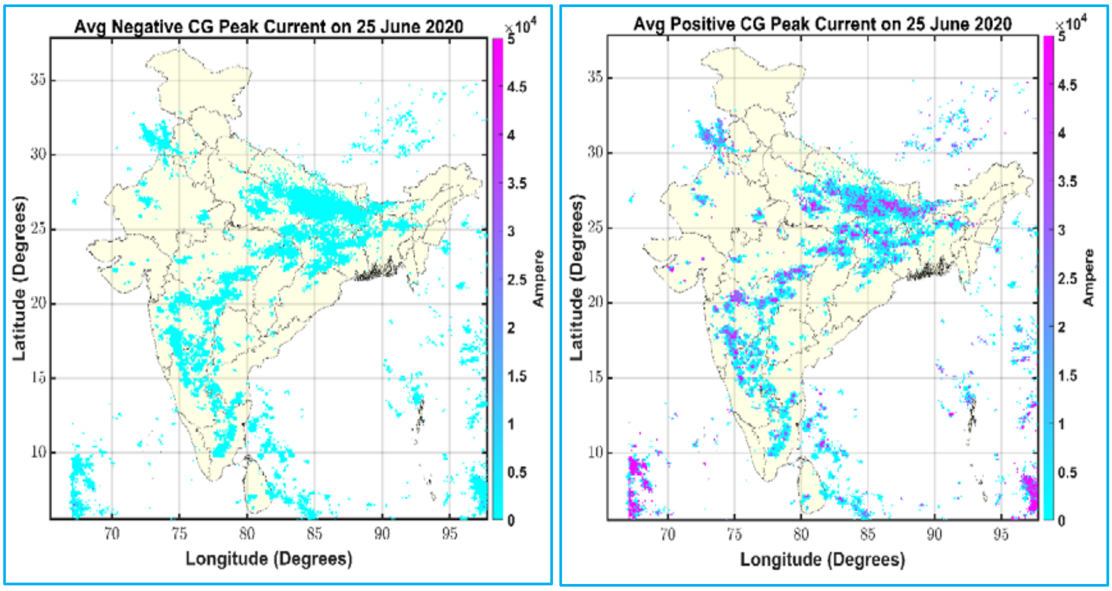

Fig. 7.9. Average Negative and Positive CG peak current (Ampere) over India on 25 June, 2020 using Earth Networks datasets

A significant amount of CG activity is evidence over Bihar and UP. Specifically, district like Gopalgang suffers a high amount of CG lightning activity during the morning as well as evening time. Such calamities of lightning and thunderstorm consumes more than 100 lives on 25 June, 2020.

7.4.3. *Need to Have NWP based Lightning Prediction system*

Considering the huge occurrence of lightning events and the death and property damages associated with such events. We from IMD are on the way to implementing a numerical weather prediction model Electric-WRF (EWRF) all over India. The model will provide lightning density all over the country well in advance. The model is based on an electrification physics mechanism that directly calculates the electric field inside the cloud and mixed-phase region and based on that it further generates lightning events. Such a modelling system will be fulfilling the need for lightning nowcast in a more accurate manner.

In this modeling system of EWRF, we are assimilating the ground-based lightning data as well. The details of the report along with a few case studies are represented in the next part. This is the first time approach where the observation of lightning and Numerical Weather Prediction model-based products are displayed on the same platform. We have started this work on an experimental basis and will soon operationalize it over the PAN India.

7.5. Forecast of Lightning Activity over the India using NWP Model with Ground based lightning data assimilation

7.5.1. *Introduction*

As already explained in the previous sections the lightning report that lightning is one of the prime natural disasters in India. Fig 7.10 is the LSD utilizing the data of Lightning Imaging Sensor on-board satellite TRMM for March, April, May from 1998 to 2013. This is very clear from the image that India is one of the lightning-prone countries all over the globe. Each year more than two thousand people are killed by the lightning strike. Therefore, predicting lightning well in advance is highly essential for a country like India where a large number of people are working in agricultural fields.

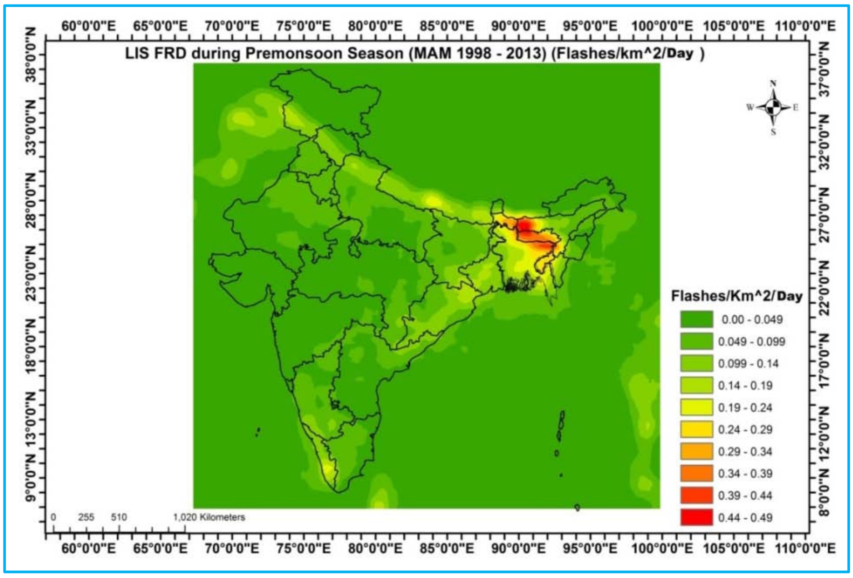

Fig. 7.10. The distribution of lightning density from LIS onboard TRMM satellite over India during pre-monsoon for the years 1998-2013

Considering such necessity Numerical Weather Prediction Division (NWP) of the India Meteorological Department (IMD), New Delhi, working on a specialized model to forecast lightning all over India well in advance. The forecast system will also implement a ground-based lightning data assimilation for the improvement of the model performance. This is the fast ever successful effort in India to implement such ground-based lightning data assimilation into the numerical weather prediction model. The model has already been tested over North East India from North Eastern Space Applications Centre (NESAC) for consecutive three years and the associated results are very much encouraging. Therefore, we from NWP division IMD in collaboration with are working to scale the whole model for PAN India. Few testing and optimization in terms of computational power have already been done and we successfully reached a stable configuration for the operational run purpose.

7.5.2. *Objectives*

Therefore, the primary objectives are listed below;

- Build up a Numerical Weather prediction model-based lightning forecast system over India.
- Utilize the ground-based lightning detection sensor's data into the model for assimilation.
- Testing the performance of the model with respect to the observed lightning data.

7.5.3. *Methodology*

Presently, all over the globe, two different approaches are available for lightning forecasts in cloud-scale (i.e., <5 km) models.

(i) Lightning can either explicitly predicted using an electrification physics mechanism.

(ii) Lightning can be diagnosed via combinations of kinematic and/or microphysical proxy variables known to be well correlated with the occurrence of lightning.

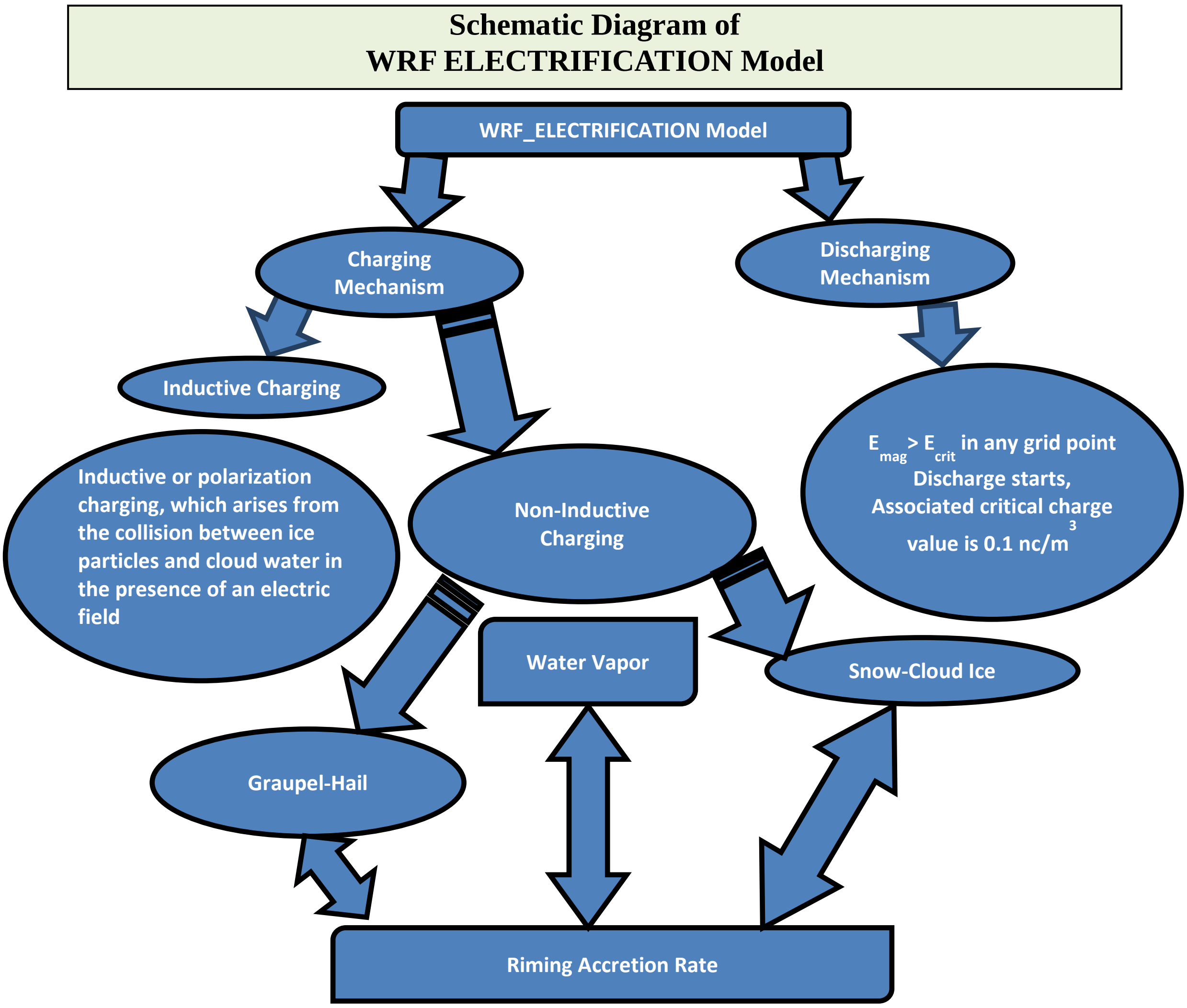

Fig. 7.11. Schematic Diagram of EWRF modelling system

Here we follow the first approach and go through the proper and explicit electrification physics mechanism through which the model generates the electric field over the different grid points of the domain.

The details of the methodology are depicted in Fig. 7.11 in a flow chart and also explain thereafter. This electrification mechanism has separate charging and discharging schemes based on different laboratory experiments. In the charging mechanism, Inductive and no-inductive processes have been introduced.

We have further arranged the continuous supply of IITM ground-based lightning location data to assimilate it into the model.

The charging process follows the below-mentioned formula for the generation of the electric field.

$$\frac{\partial \rho_{xy}}{\partial t} = \beta \delta q_{xy} \left(1 - E_{xy}\right) E_{xy}^{-1} \left(n_{xacy}\right),$$

Where, ρ_{xy} is the space charge (Cm^{-3}) separated during a collision between hydrometeor species x and y, δq_{xy} is the weighted average separated charge (C) per rebounding collision between hydrometeor species x and y, ß is an arbitrary factor limiting charging at low temperatures n_{xacy} is the number concentration collection rate integral, E_{xy} is the collection efficiency.

The assimilation equation that we implemented into the model through the nudging process is depicted below.

$$Q_v = AQ_{sat} + BQ_{sat} \tanh(CX)\left[1 - \tanh\left(DQ_g^{\alpha}\right)\right],$$

where X is the flash rate, Q_{sat} is the water vapour saturation mixing ratio (g/kg), and Q_g is the graupel mixing ratio (g/kg). Here ground-based lightning data assimilation modifies the water vapor content in the mixed-phase region of the cloud as a function of gridded flash rate.

Several discharge models with varying degrees of complexity have been developed in the last three decades. The most realistic, explicit branched ''fractal-like'' lightning parameterizations (e.g., Mansell *et al.* 2002) are currently impractical for even regional forecast applications due to thehigh computational cost. The discharge model implemented in this study is a ''bulk'' type adapted from Ziegler and MacGorman (1994) and MacGorman *et al.* (2001). First, the lightning discharge scheme identifies lightning initiation points atall grid cells at which E_{mag} exceeds a prescribed critical threshold E_{crit} [set in the following simulations to120 kVm^{-1}, consistent with the break-even field magnitude indicated by Gurevich *et al.* (1992) for middle levels of the troposphere].

A discharge is centered around each initiation point and involves all points within a cylinder of fixed radius R extending vertically through the entire depth of the simulation domain. The domain we used for the model run is given below with a 3 km resolution. We tested the model with different domain configurations and ultimately optimized it interms of computation run time along with the performance of the forecast. We have utilized the NCEP-GFS 50 km data for model initialization over NER of India. But for PAN India we have used IMD-GFS 12 km data for model initialization.

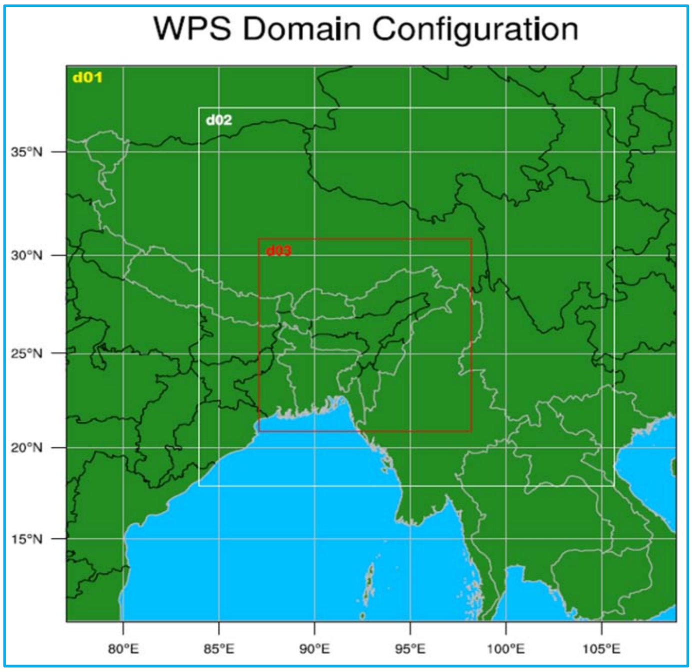

Fig. 7.12. The domain we prepared for North-East India is represented

This modeling system we implemented over North East India first and now scaling the same over PAN India. The domain we prepared for North-East India is represented in Fig. 7.12. A few of the case studies over North East India are given below followed by a few results over PAN India. The associated domain over PAN India is also presented in Fig. 7.13. Each day three forecasts have been generated based on the severity of the lightning occurrence utilizing the ground-based lightning data assimilation. The 1st Forecast is from 00 UTC to 09 UTC, 2nd forecast is from 06 UTC to 14 UTC and 3rd forecast is from 08 UTC to 18 UTC. All the forecast has been uploaded to the NERDRR website and also sent to all the concerned state-wise district disaster management authority.

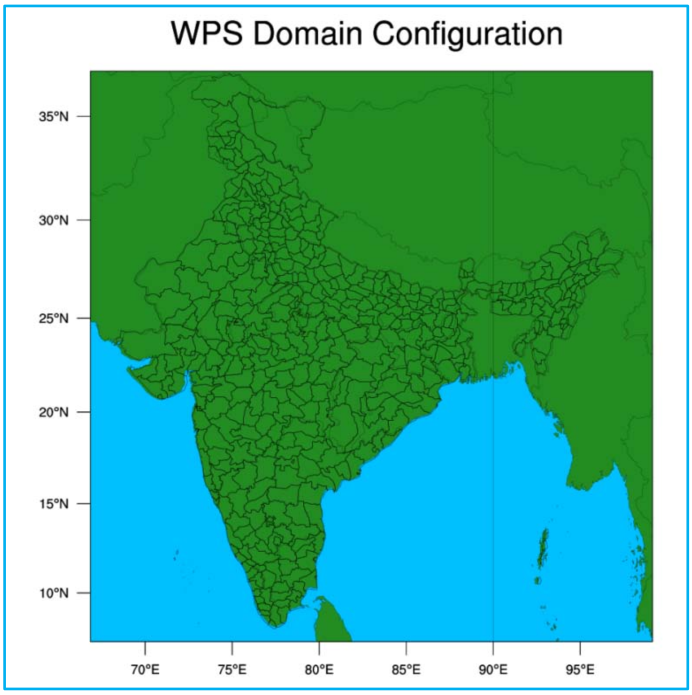

Fig. 7.13. Domain Structure over PAN India

For the simple understanding, of the general public as well as various officials we have classified the various lightning density count into Moderate, High and Severe section and represents the same with only three colour green, yellow and red respectively.

7.5.4. *Results of a few case studies*

One of the case studies for the 17th May 2019 has been depicted in Fig. 7.14. where the simulated Lightning flash origin density (FOD) is represented on the left side and the ENTLN detected lightning location has been plotted on the right side of figure 7 with a lead time of 1 hour, 2 hours and 3 hours of lead times after ground-based lightning data assimilation. The simulated FOD for 02 to 03 UTC, 03 UTC to 04 UTC and 04 UTC to 05 UTC has been plotted in addition to its observation counterparts from ENTLN lightning sensors.

Another case study we performed was during 20 June 2019 and we captured a lightning event very well during 7 to 8 UTC of 20 June 2019. A vigorous lightning event that strikes the North Eastern Space Applications Centre, Shillong on 20 June 2019 is presented in Fig. 7.14. The associated simulated and observed plots are shown in the right-side panel of Fig 7.14.

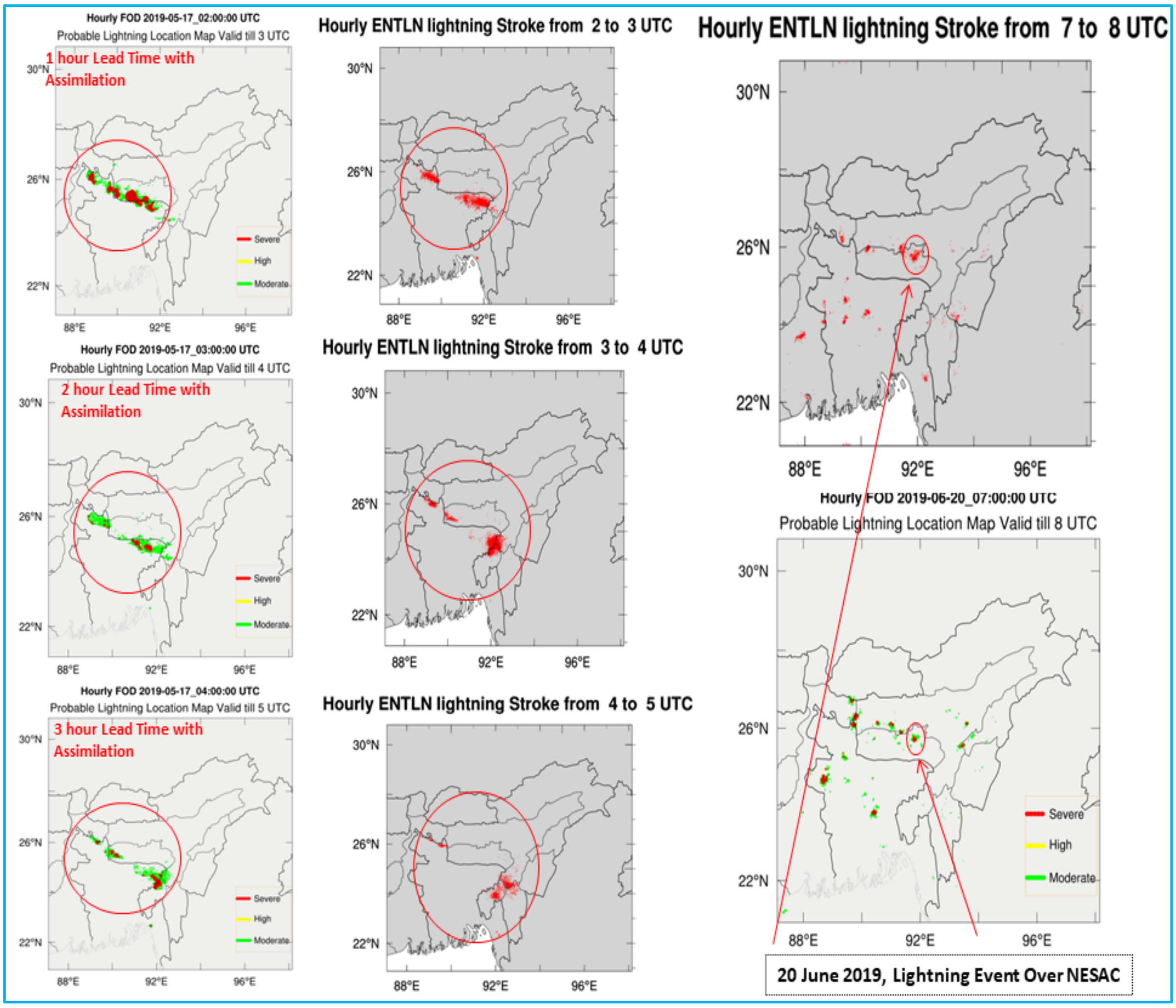

Fig. 7.14. Forecasted lightning flash origin density for 17 May 2019 for the 2, 3, 4 UTC with ground-based lightning data assimilation (left), the right side represents the observed lightning location. The right panel presented a lightning incident over North Eastern Space Applications Centre on 20 June 2019, which was well captured by the model simulation (top) and the associated observed ENTLN lightning (bottom)

A squall line formed during 8th April 2019 has been well captured by the model simulation. The simulated plots and observed locations of lightning activity are plotted in Fig. 7.15. The simulated FOD has been generated for 7 to 8 UTC and 8 to 9 UTC and the same hours lightning plots have been generated and plotted on the left side of figure 8. A spatial shift in between simulated and observed lightning locations has been visible in both plots. The possible reason could be the lightning data assimilation time interval, we have implemented 20 minutes interval for the nudging of lightning location data into the model. The interval of 20 minutes for such a big squall line could not be enough and we should reduce the insertion of the data interval to 10 minutes to improve the forecast capability.

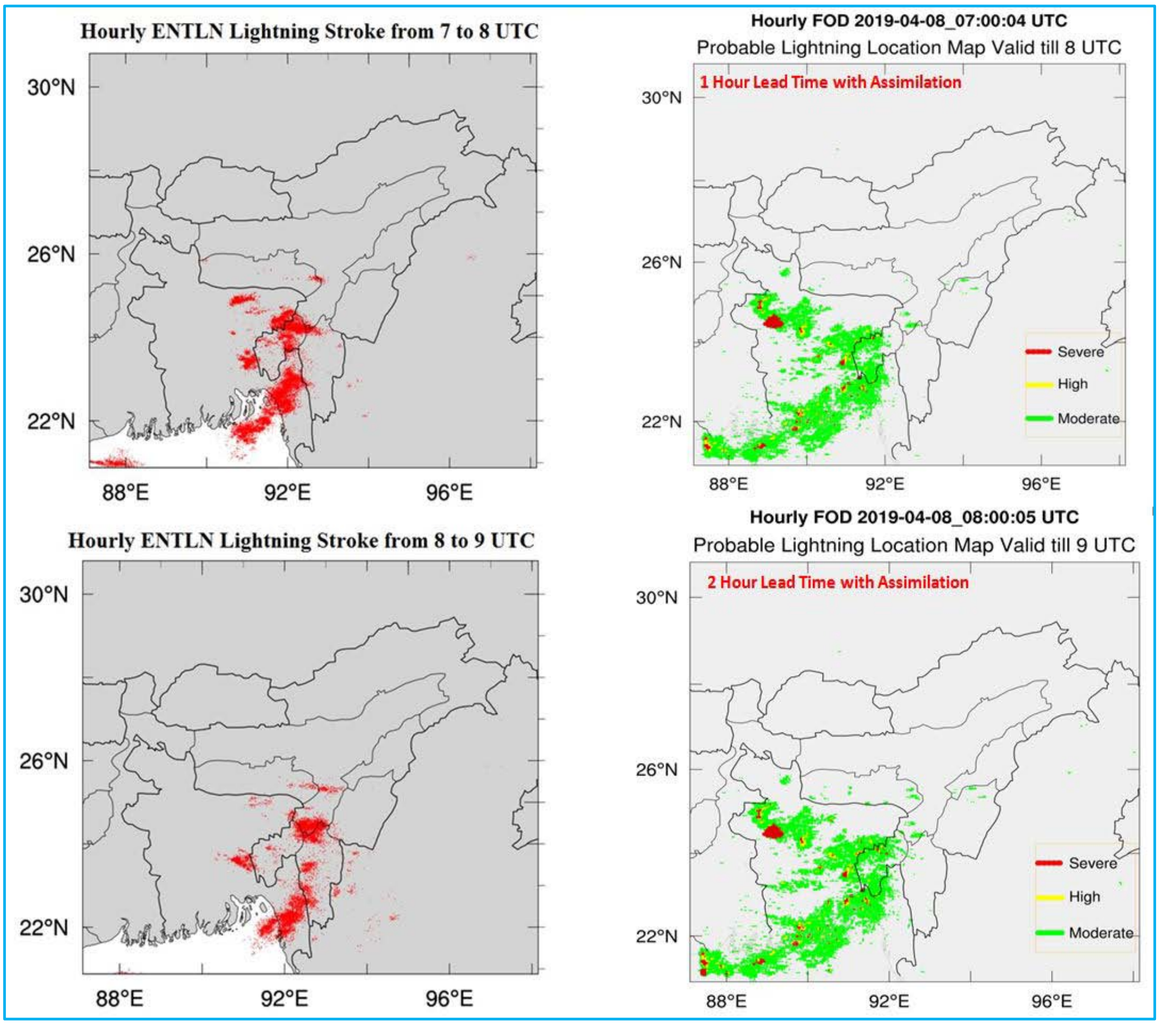

Fig. 7.15. Forecasted lightning flash origin density for 8th April, 2019 for the 7, 8 UTC with ground-based lightning data assimilation (right), Left side represents the observed lightning location detected by Earth Networks lightning sensors

Presently, we are working on the EWRF model to operationalize it over the whole of India. We have tested several combinations to optimize its performance and forecast output. A few of the case studies are given below for references. This is ongoing work and needs more time to complete the validation analyses.

We have run the model in the control condition and also with ground-based lightning data assimilation. We have utilized IITM, Pune established ground-based lightning data and successfully implemented its assimilation into the EWRF model.

The left panel shows the EWRF simulated Flash Origin Density (similar to Flash Density) in the control run scenario, IITM observed lightning is represented by the red dots in the middle panel and the right panel shows the EWRF simulated lightning density after ground-based lightning data assimilation. The model starts at 00 UTC 15 September, 2021 and it took 1 hour to spin up and start producing a forecast. Therefore for the first hour, we don't get any lightning density information. Then 01 UTC onwards model starts generating the forecast.

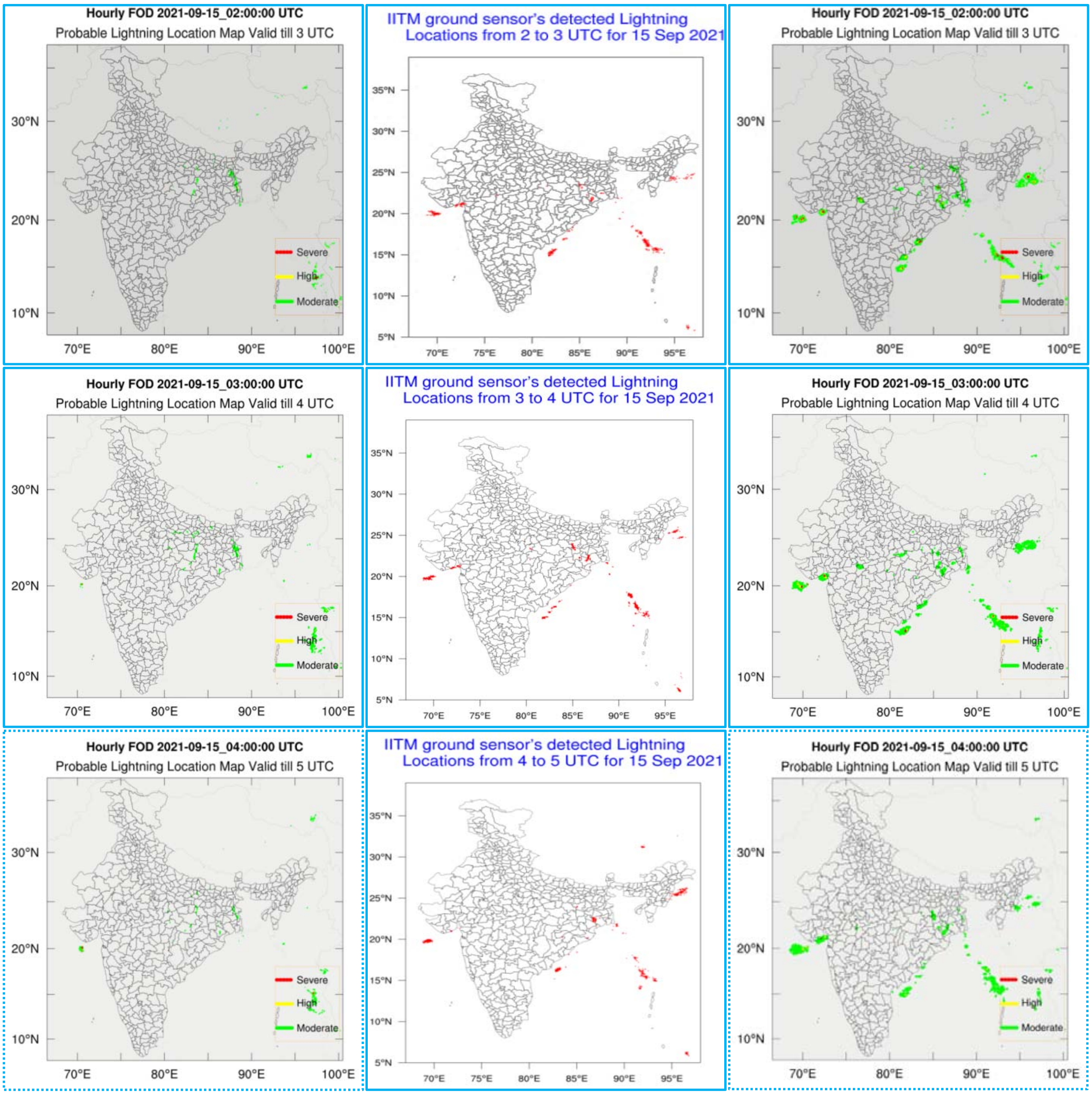

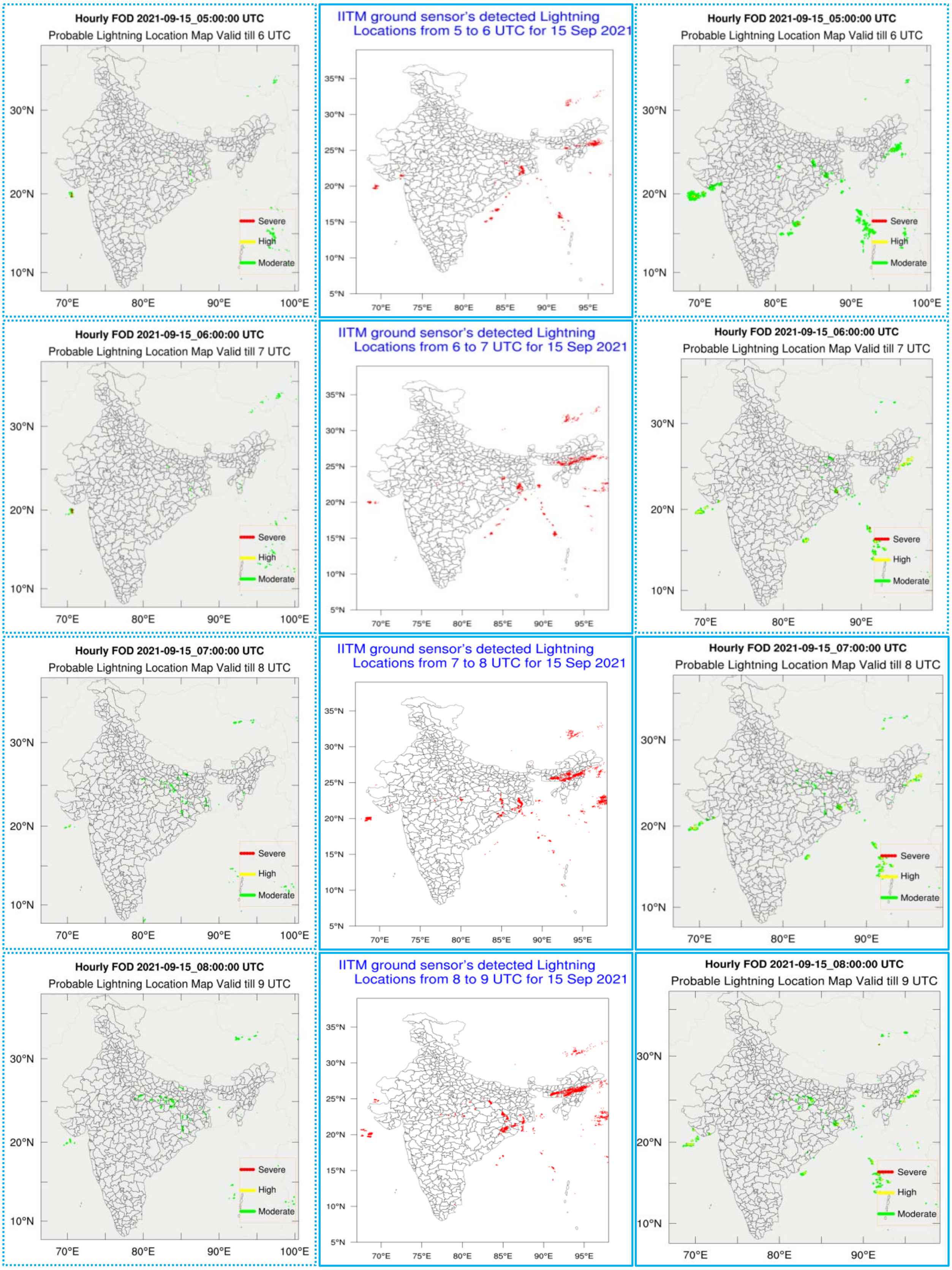
Hourly FOD 2021-09-15_05:00:00 UTC
Probable Lightning Location Map Valid till 6 UTC
Severe
High
Moderate
IITM ground sensor's detected Lightning Locations from 5 to 6 UTC for 15 Sep 2021
Hourly FOD 2021-09-15_05:00:00 UTC
Probable Lightning Location Map Valid till 6 UTC
Severe
High
Moderate
Hourly FOD 2021-09-15_06:00:00 UTC
Probable Lightning Location Map Valid till 7 UTC
Severe
High
Moderate
IITM ground sensor's detected Lightning Locations from 6 to 7 UTC for 15 Sep 2021
Hourly FOD 2021-09-15_06:00:00 UTC
Probable Lightning Location Map Valid till 7 UTC
Severe
High
Moderate
Hourly FOD 2021-09-15_07:00:00 UTC
Probable Lightning Location Map Valid till 8 UTC
Severe
High
Moderate
IITM ground sensor's detected Lightning Locations from 7 to 8 UTC for 15 Sep 2021
Hourly FOD 2021-09-15_07:00:00 UTC
Probable Lightning Location Map Valid till 8 UTC
Severe
High
Moderate
Hourly FOD 2021-09-15_08:00:00 UTC
Probable Lightning Location Map Valid till 9 UTC
Severe
High
Moderate
IITM ground sensor's detected Lightning Locations from 8 to 9 UTC for 15 Sep 2021
Hourly FOD 2021-09-15_08:00:00 UTC
Probable Lightning Location Map Valid till 9 UTC
Severe
High
Moderate

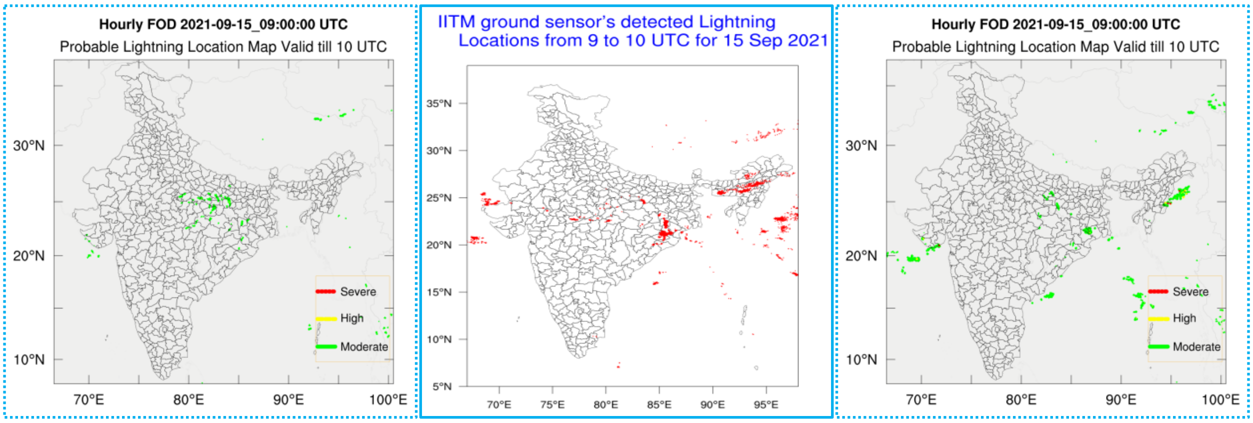

Fig. 7.16. Observed Lightning (middle panel, red dots), simulated Flash Origin Density in the control condition (left panel), simulated Flash origin density with ground-based lightning data assimilation (right panel) for 02 to 09 UTC of 15 Sep, 2021

We noticed the assimilation improved the simulated lightning density drastically and were able to identify the region of lightning events very well. A case study during 15 September 2021 is plotted above in Fig. 7.16. The simulation started at 00 UTC and ended on 09 UTC 15 Sep 2021. The assimilation was performed for initial two hours with a gap of 15 minutes. The observed lightning data assimilation improved the simulated Flash Origin Density and provide a good estimate of future lightning events upto the next 8 hours.

Later on, we further run the simulation 2nd time on the same day from 08 UTC to 18 UTC with initial 2 hours of lightning data assimilation. We noticed assimilation improve the simulated Flash Origin Density drastically; therefore in the 2nd part of the simulation, we plotted the observed lightning along with simulated Flash Origin Density with lightning data assimilation for 15 Sep 2021 in Fig. 7.17.

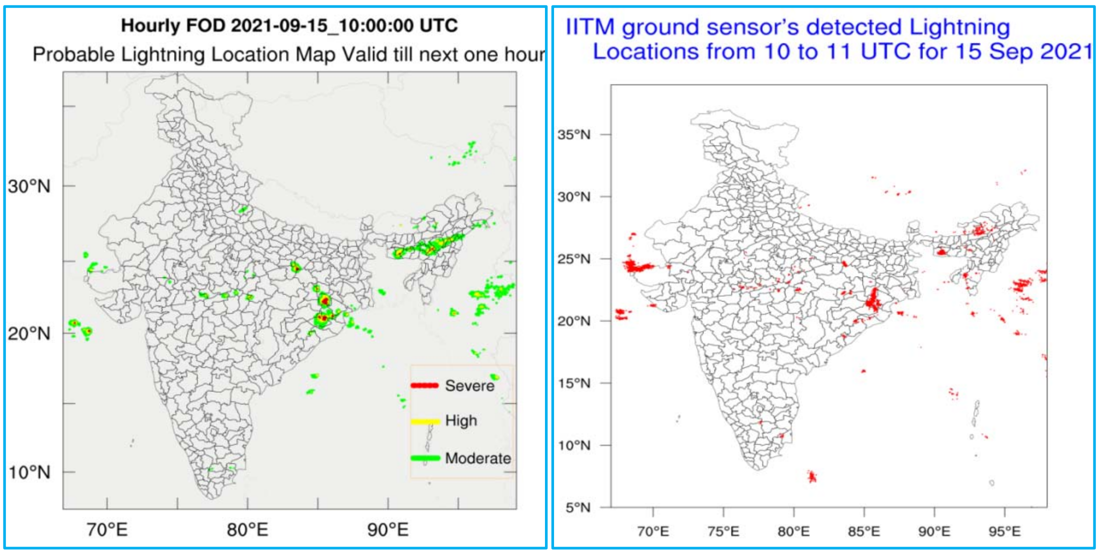

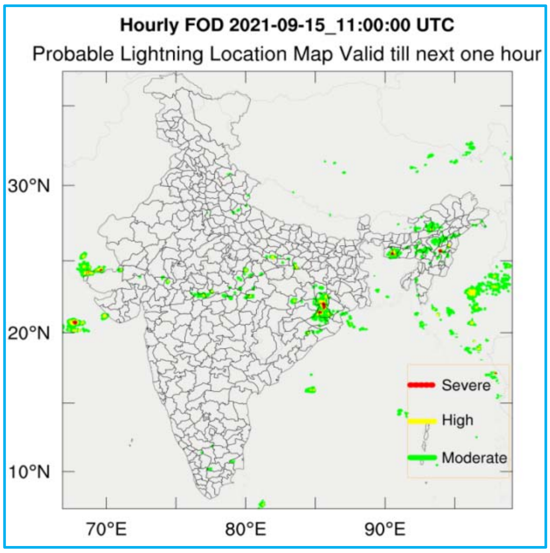
Hourly FOD 2021-09-15_11:00:00 UTC
Probable Lightning Location Map Valid till next one hour
30°N
20°N
10°N
70°E
80°E
90°E
Severe
High
Moderate

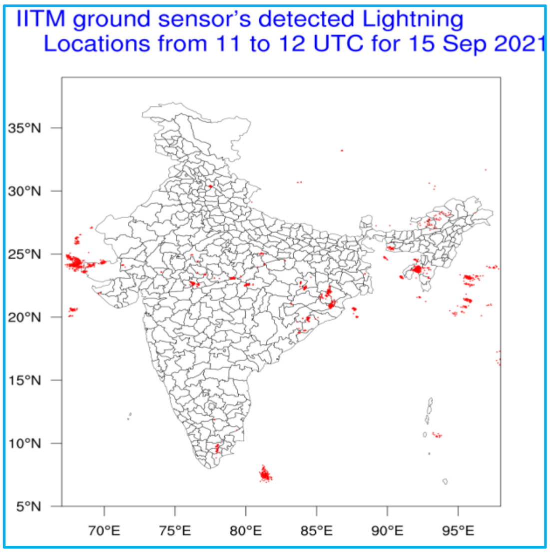
IITM ground sensor's detected Lightning Locations from 11 to 12 UTC for 15 Sep 2021
35°N
30°N
25°N
20°N
15°N
10°N
5°N
70°E
75°E
80°E
85°E
90°E
95°E

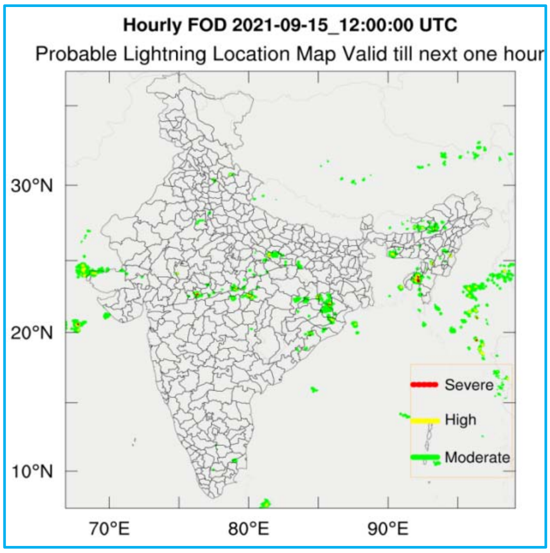
Hourly FOD 2021-09-15_12:00:00 UTC
Probable Lightning Location Map Valid till next one hour
30°N
20°N
10°N
70°E
80°E
90°E
Severe
High
Moderate

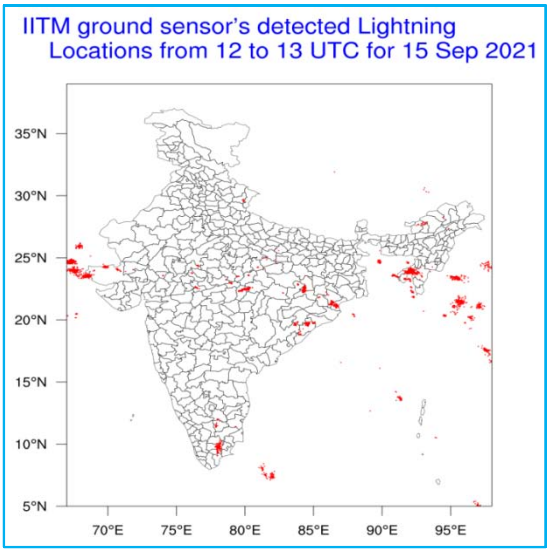
IITM ground sensor's detected Lightning Locations from 12 to 13 UTC for 15 Sep 2021
35°N
30°N
25°N
20°N
15°N
10°N
5°N
70°E
75°E
80°E
85°E
90°E
95°E

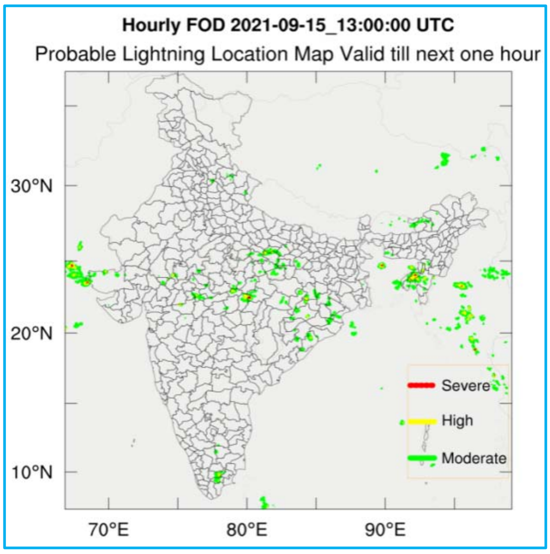
Hourly FOD 2021-09-15_13:00:00 UTC
Probable Lightning Location Map Valid till next one hour
30°N
20°N
10°N
70°E
80°E
90°E
Severe
High
Moderate

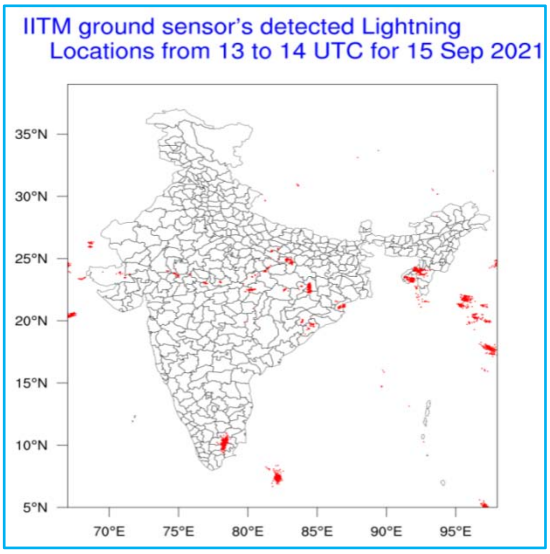
IITM ground sensor's detected Lightning Locations from 13 to 14 UTC for 15 Sep 2021
35°N
30°N
25°N
20°N
15°N
10°N
5°N
70°E
75°E
80°E
85°E
90°E
95°E

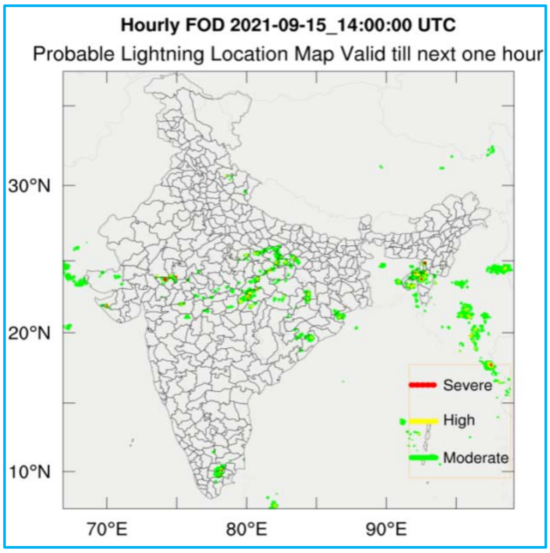
Hourly FOD 2021-09-15_14:00:00 UTC
Probable Lightning Location Map Valid till next one hour
30°N
20°N
10°N
70°E
80°E
90°E
Severe
High
Moderate

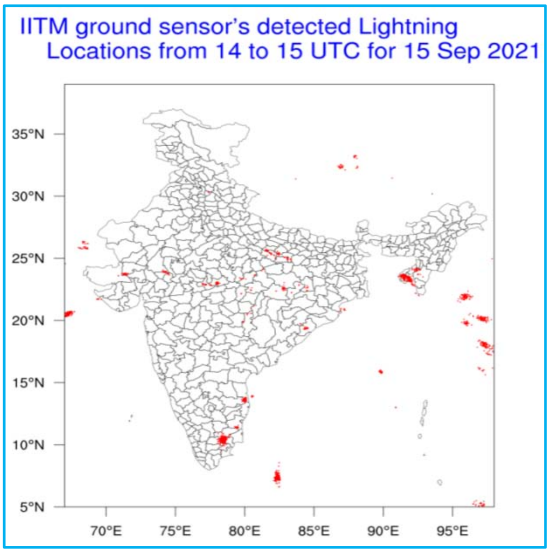
IITM ground sensor's detected Lightning Locations from 14 to 15 UTC for 15 Sep 2021
35°N
30°N
25°N
20°N
15°N
10°N
5°N
70°E
75°E
80°E
85°E
90°E
95°E

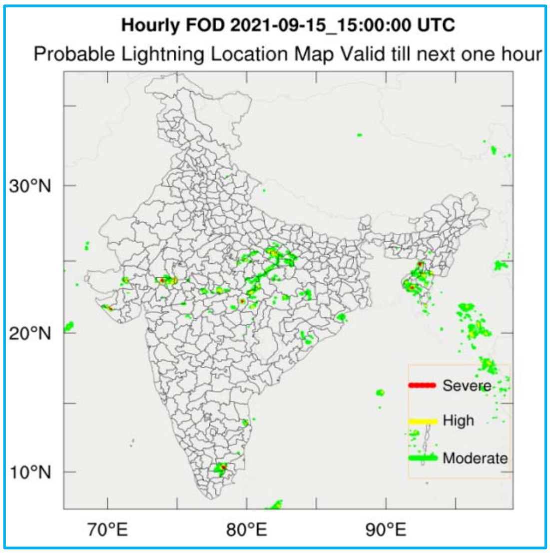
Hourly FOD 2021-09-15_15:00:00 UTC
Probable Lightning Location Map Valid till next one hour
30°N
20°N
10°N
70°E
80°E
90°E
Severe
High
Moderate

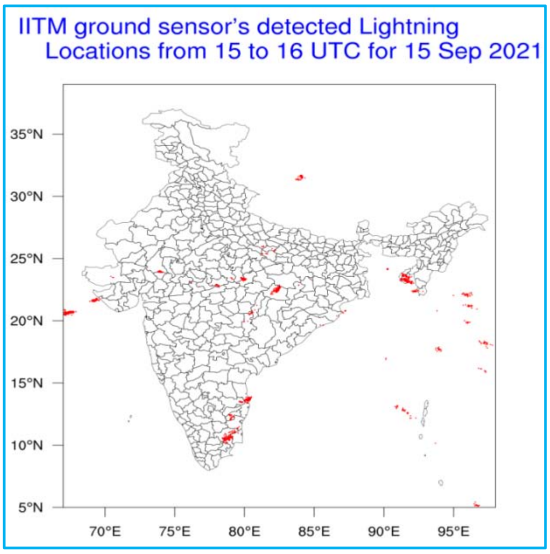
IITM ground sensor's detected Lightning Locations from 15 to 16 UTC for 15 Sep 2021
35°N
30°N
25°N
20°N
15°N
10°N
5°N
70°E
75°E
80°E
85°E
90°E
95°E

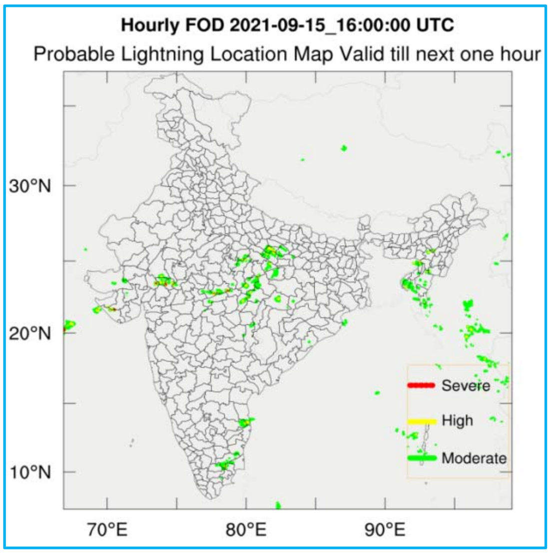
Hourly FOD 2021-09-15_16:00:00 UTC
Probable Lightning Location Map Valid till next one hour
30°N
20°N
10°N
70°E
80°E
90°E
Severe
High
Moderate

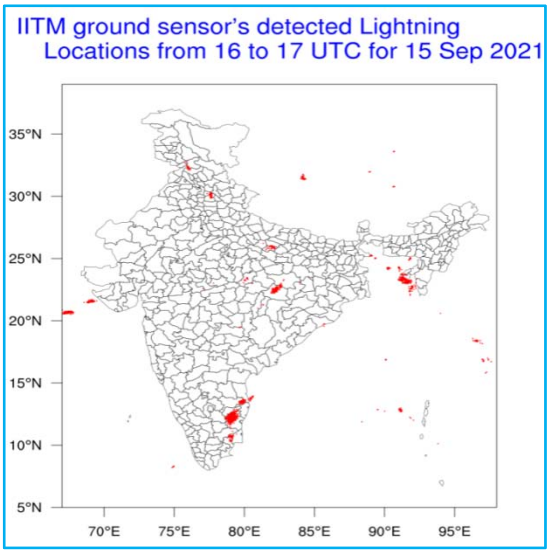
IITM ground sensor's detected Lightning Locations from 16 to 17 UTC for 15 Sep 2021
35°N
30°N
25°N
20°N
15°N
10°N
5°N
70°E
75°E
80°E
85°E
90°E
95°E

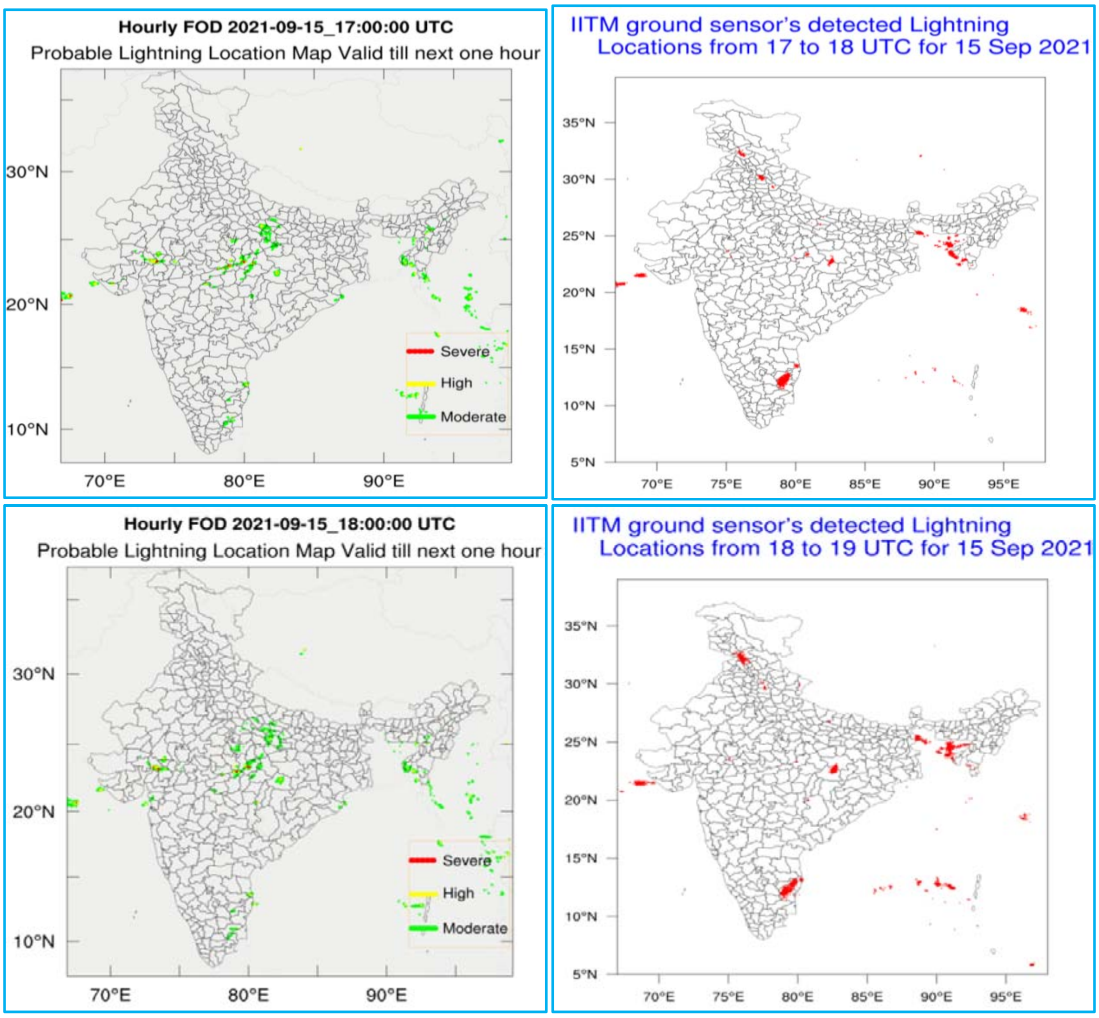

Fig. 7.17. Observed Lightning (right panel, red dots), simulated Flash Origin Density with ground-based lightning data assimilation (left panel) for 10 to 18 UTC of 15 Sep, 2021

Few other case studies over PAN India and the validation work over North-East India have already been done and we are going to test and validate the model for PAN India very shortly.

7.6. Main Summaries

The specialized electrical physics-based model EWRF has been implemented on a research basis and we are checking its performance before making it operationalize over India. As we have discussed the model has already been implemented over North-East India (for eight states) during the last three years making North Eastern Space Applications Centre a base institute. Now we are from IMD are working to implement the EWRF along with ground-based lightning data assimilation for PAN India. We have already showcased a few case studies and results are encouraging and getting good resembles of forecasted lightning density and observed lightning events. Statistical analyses for multiple case studies are going on and we will soon implement the same over India.

Acknowledgement

Authors are thankful to the North Eastern Space Applications centre for the overall help for getting the Earth Networks datasets along with the all-around support to initiate the work for North East India.

CHAPTER 8

Customized NWP Based Medium Range Weather Forecast Products for Sectoral Applications

M. T. BUSHAIR, D. R. PATTANAIK and PRADEEP MISHRA

8.1. Introduction

Numerical weather prediction (NWP) models are important tools for the understanding of meteorological phenomena, as well as for predicting weather in future. The predictability of these models is highly depended on initial conditions provided to the model (Lorenz, 1965). Errors that occur during the specification of initial conditions may cause large uncertainties in numerical prediction systems (Thompson, 1957). The uncertainties in the weather prediction may arrives also due to the differences in the representation of physical process in the models (Krishnamurti *et al.*, 2004; van Lier *et al.*, 2012). The knowledge of systematic errors arrives due to these uncertainties is of paramount importance in the realization of improvements in the forecasting system, with a view to minimizing the errors, and helping meteorologists in the preparation of weather forecasts. The minimization of errors in the forecast can be achieved by considering errors of the multiple models. This can be done by taking ensemble average of individual forecasts. The straight average approach assigns an equal weight of 1.0 to all the models and the super ensemble methods assigns different weights to each model, based on its performance, geographically, vertically, and for each variable separately. The error of the ensemble mean is often 30% smaller than the typical error of individual models, which again is the value predicted by the indistinguishable interpretation (Palmer *et al.* (2006), Christiansen (2018, 2019).

The technique of combining forecasts made by numerical models has been well explored by various researchers (Krishnamurti *et al.* 2000b, Tebaldi *et al.*, 2004; Weigel *et al.*, 2010; Chandler *et al.*, 2013). Almost all of the articles that have been written on this subject agree that the combination of several different forecasts provides significant improvements. The questions that arise are those dealing with the method used to combine the forecasts. Recent research in climate modelling suggests that combination schemes with unweighted means provide better results than schemes with weighting based on the performance of each model (Christensen *et al.*, 2010; Déqué and Somot, 2010). And, according to Weigel *et al.*, (2010) and Knutti *et al.* (2010), the combination of models taking into account the concept of weighting must be treated with great care, principally when applied to climate change. Now in the area of weather forecasting, inter comparisons among forecasts from different types of numerical models have shown that the performance of each can vary in time as well as in space (Saulo *et al.*, 2001; Silva Dias *et al.*, 2006). Thus, a combination among the results of various types of models, considering the performance of each model, can produce forecasts of greater reliability (Johnson and Swinbank, 2009; Roy Bhowmik and Durai, 2010; Kotal and Roy Bhowmik, 2011). The concept of using the multi model ensemble (MME) for the improvement of the predictions was first discussed by Krishnamurti *et al.* (1999, 2000a, b) and has been widely used (Yun *et al.*, 2003; Chakraborty *et al.*, 2007; Lenartz *et al.*, 2010). Roy Bhowmik and Durai (2008, 2010), applying a linear regression technique to a set of forecasts, made by four numerical models, showed that combining the predictions of each model and their respective correlation coefficient produces significant improvements in predictions of precipitation over India. In studies, addressing the monsoons of India, Krishnamurti *et al.* (2009), Mitra *et al.* (2011) and Kumar *et al.* (2012) assert that when predictions are generated from a set of numerical models their quality is improved and their mean square errors reduced. At India Meteorological Department (IMD) is using outputs from various NWP models that are running operationally by IMD as well as other national and international centres. Based on these operational NWP models outputs, IMD is generating the Multi Model Ensemble (MME) forecast products for use by the different forecasting offices of IMD in giving appropriate weather warning to users. In the present report, the MME based forecast products prepared in the real-time at different spatial scales based on different NWP models outputs for applications in various sectors particularly for the year 2021 are presented. The MME based forecasts at stations levels (1447 station), district level (732 districts), coastal regions (16 regions) and met-subdivision level (36 met subdivisions) spreading all over India is presented.

8.2. NWP model Data Used

In this study forecasts from five global NWP models data are used for preparing the MME forecast.

8.2.1. *NWP models operational at IMD*

8.2.1.1. *Global Forecasting system (GFS)*

The main operational model at IMD for the medium range forecast (up to 10 days) is a very high-resolution deterministic Global Forecast System (GFS) with spectral resolution of T1534 (~12.5 km) with 64 hybrid vertical levels (top layer around 0.27 hPa) which was implemented in June 2018. The global atmospheric model in GFS is a global spectral model (GSM) version 14.1.0, adopted from National Centres for Environmental Prediction (NCEP) (http://www.emc.ncep.noaa.gov/GFS/doc.php). Model uses two-time level semi-implicit semi-Lagrangian dynamics and a time step of 450 seconds is used in dynamics computations. The semi-Lagrangian advection calculations and physics are treated on a linear, reduced Gaussian grid in the horizontal domain. Model uses Gaussian grid of 3072 x 1536 grid points horizontally and vertically 64 hybrid sigma pressure levels and a time step of 225 seconds is used in physics computations. The initial conditions for IMD-GFS model are generated from hybrid four-dimensional ensemble-variational data assimilation system (4DEnsVar) by the NCMRWF through the global data assimilation system (GDAS) cycle. The assimilation system runs four times a day which has more Indian observations in it. The GFS T1534 model is run daily for 10 days and the output is stored every 3 hr interval (Johny and Prasad, 2020).

8.2.1.2. *Global Ensemble Forecast System (GEFS)*

GEFS is an operational weather model at IMD to address underlying uncertainties in the input data such limited coverage, instruments or observing systems biases, and the limitations of the model itself. GEFS quantifies these uncertainties by generating multiple forecasts, which in turn produce a range of potential outcomes based on differences or perturbations applied to the data after it has been incorporated into the model. Each forecast compensates for a different set of uncertainties. Global Ensemble Forecast System (GEFS) at IMD is adopted from NCEP and it runs in ~12 km (T1534) resolution. The total number of 21 Ensembles (20 perturbed forecasts + 1 control forecast) constitutes the ensemble system. These 20 ensembles analysis are generated by Ensemble Kalman Filter (EnKF) method from the forecast perturbation of the previous cycles four times a day (00, 06, 12 and 18 UTC) at all 64 model vertical levels. These analysis perturbations are added to the reconfigured analysis obtained from the hybrid four-dimensional Ensemble variational data assimilation system (GDASHybrid4DEnsVar) as part of the suite. The 243 hour forecast of GEFS is routinely generated based on 00UTC and 12UTC initial conditions which include a control forecast starting from GDAS assimilation and 20 (20 perturbations) ensemble members with each perturbed initial conditions (Deshpande *et al.*, 2020).

8.2.2. *NWP models forecasts data used from other operational centres*

8.2.2.1. *NCEP Global Forecasting system (NCEP-GFS)*

GFS is an operational weather model at NCEP/NOAA, USA. On March 22nd, 2021, NCEP implemented GFS version 16. In addition to the numerous model and data assimilation changes NCEP is merging the operational standalone global deterministic WAVEWATCH III based wave model Multi_1 into the GFS system with this upgradation. NCEP-GFS model has a spectral resolution of ~12.5 km with127 vertical pressure levels (top layer around 80 km) and it generates forecast four times in day up to 384 hours. IMD receives NCEP-GFS model data through ftp in real time.

8.2.2.2. *NCRWF Unified Model (NCUM)*

The NCUM assimilation-forecast system is adapted from the Unified Model (UM) system of 'UM Partnership' (George *et al.* 2016; Rajagopal *et al.* 2012). This seamless prediction system allows using the same dynamical core and parameterization schemes across a broad range of spatial and temporal scales. Hybrid 4D-VAR data assimilation method (Clayton *et al.* 2013) is used in the NCUM global NWP system, in which flow-dependent background errors are from NCUM Ensemble Prediction System (NCUM-EPS). The forecast model in the NCUM system used in this study is UM Version 10.8. This model uses Even Newer Dynamics for General atmospheric modelling of the environment (ENDGame), which employs semi-implicit Lagrangian discretization of the governing equations (Wood *et al.* 2014). The NCUM global model's horizontal resolution is N1024 (~12 km) and has 70 levels in the vertical, reaching up to an altitude of 80 km. Surface analysis system (SURF) adapted from the “UM Partnership” does the surface analysis preparations. This system prepares surface analysis of snow, soil moisture, SST, and Sea Ice analysis (Donlon *et al.* 2012). The assimilation system runs four times a day and forecast runs two times a day for 10 days (Sumit *et al.*, 2020). IMD receives NCUM model data through ftp in real time.

8.2.2.3. *Japan Meteorological Agency (JMA) model*

The operational medium range weather forecasting model operational at Japan Meteorological Agency (JMA) is Global Spectral Model (GSM). 4D-Var data assimilation method is used in the JMA/GSM model. This model has a horizontal resolution roughly equivalent to 0.1875° × 0.1875° (20 km) in latitude and longitude and 120 stretched sigma pressure hybrid levels reaching up to 0.01 hPa. JMA generates forecasts from GSM model four times a day (JMA, 2019). IMD receives JMA model data at 25 km resolution through ftp in real time.

8.3. Methodology used for preparing customized NWP based products

IMD generates location based as well as area averaged forecast from five models also its MME in real time for decision support. The NWP model forecasts available with IMD is of different spatial resolution (Table 8.1). Forecast of different weather parameters (rainfall, maximum temperature, minimum temperature, wind speed, wind direction, relative humidity and cloud cover) and its MME is generating for Indian cities, districts, meteorological subdivisions and coastal regions. Weather parameters are estimated from model output data using the geographic information system (GIS) packages like gdal, rasterio, geopandas, etc available with Python. The model data are first converted to raster format (GeoTiff) to estimate the values over required location/domain. MME forecast of each weather parameter is calculated by giving same weight to all model forecast. MME forecast along with individual forecast is disseminating to the forecasters thorough NWP website and Information System and Services Division (ISSD) system.

Table 8.1
The NWP model forecasts and its spatial resolution available with IMD

	Model	Agency	Resolution
1	GFS	IMD	12 km
2	GEFS	IMD	12 km
3	GFS	NCEP	25 km
4	UM	NCMRWF	12 km
5	GSM	JMA	25 km

8.3.1. *Generation of MME forecast for Indian cities*

Seven days forecast of rainfall, maximum temperature, minimum temperature, wind speed, wind direction, relative humidity (at 3 UTC and 12 UTC) and total cloud cover (entire atmosphere) from each model is generated by selecting the nearest grid point corresponds to the each city's latitude/longitude. Then MME forecast of for each weather parameter is generated by giving equal weight to the forecast from all the 5 NWP models mentioned in Table 8.1. Currently, forecast of 1447 cities including coastal stations, tourist spots, nowcast stations, hydro project locations are generating. Figure 8.1 shows the locations of the cities where forecast is generating. These forecasts are hosted in NWP division website (www.nwp.imd.gov.in, Screenshot shown in Figure 8.2 and 8.3) and also handing over to ISSD as csv files for the dissemination to the RMCs (Regional Meteorological Centres) and MCs (Metrological Centres).

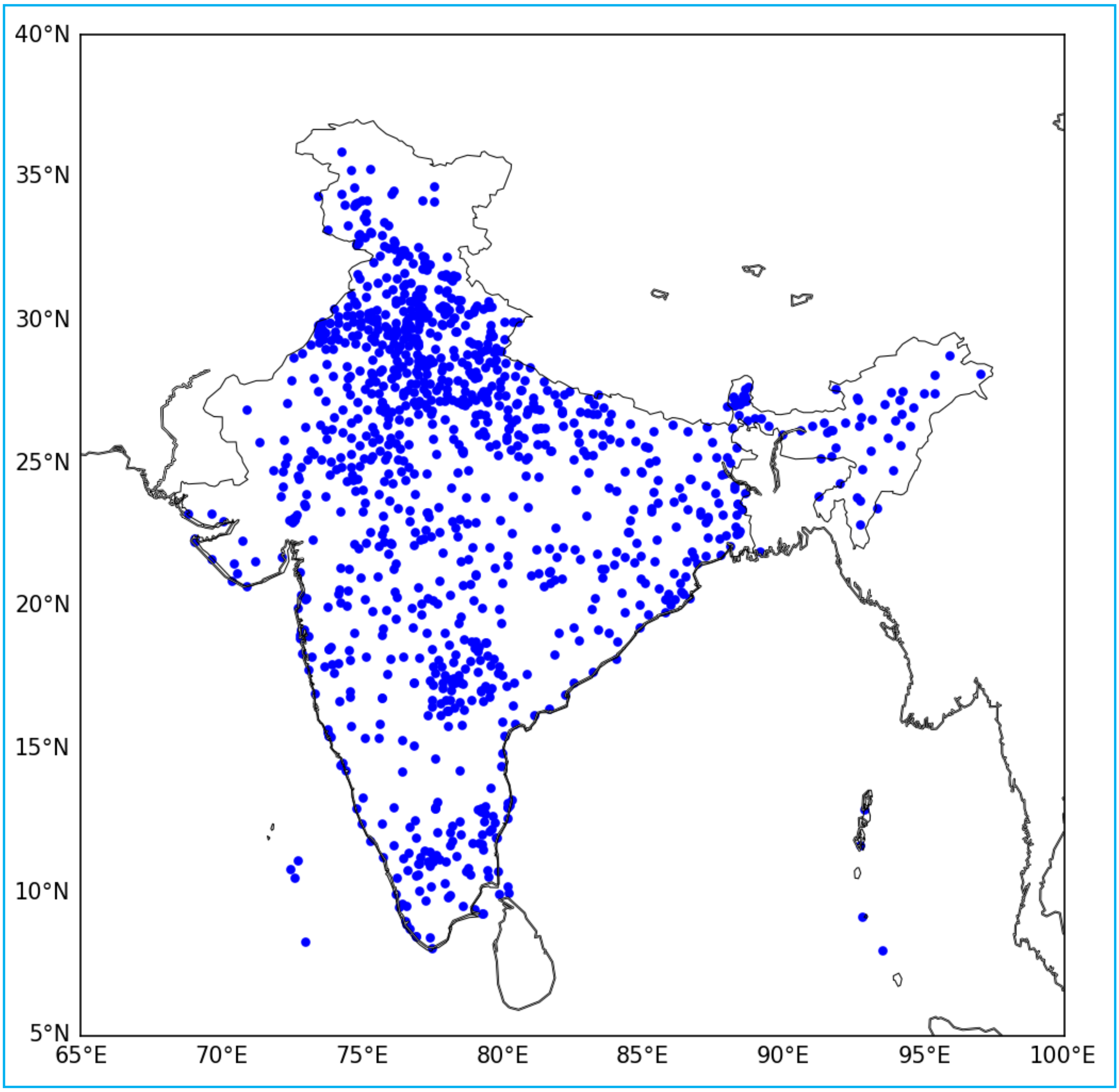

Fig. 8.1. Locations of cities where forecast is issued (1447 cities)

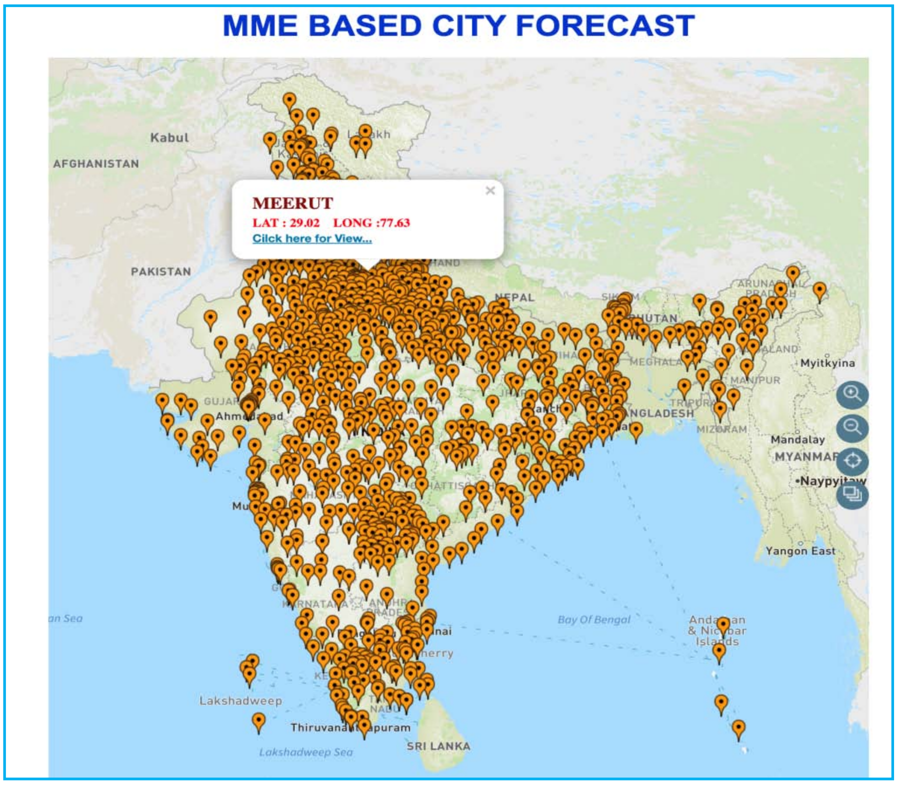

Fig. 8.2. Screenshot of city weather forecasting page from NWP division's website

https://nwp.imd.gov.in/models/input/JAIPUR.php - Google Chrome

https://nwp.imd.gov.in/models/input/JAIPUR.php

MME BASED CITY FORECAST FOR :JAIPUR

MAXIMUM TEMPERATURE (DEG. C)BASED ON 20220102

MODEL	DAY1	DAY2	DAY3	DAY4	DAY5	DAY6	DAY7
GFS	22.7	23.3	15.5	17.6	22.1	20.1	21.4
GEFS	22.0	22.5	16.1	17.9	20.1	21.7	22.2
NCEP	21.6	22.9	21.6	21.9	23.9	23.3	23.1
NCUM	18.7	20.2	20.0	19.0	17.3	17.2	17.8
JMA	21.9	23.2	21.4	18.7	18.2	17.1	18.6
MME	21.4	22.4	18.9	19.0	20.3	19.9	20.6

MINIMUM TEMPERATURE (DEG. C) BASED ON 20220102

MODEL	DAY1	DAY2	DAY3	DAY4	DAY5	DAY6	DAY7
GFS	15.0	16.5	15.0	12.3	13.1	15.9	15.2
GEFS	14.9	15.9	14.1	13.3	13.5	14.7	15.4
NCEP	10.9	12.5	15.8	13.5	14.0	14.7	14.6
NCUM	8.1	9.0	12.2	11.3	13.0	12.6	13.3
JMA	8.9	9.9	15.8	13.2	14.2	14.7	13.4
MME	11.6	12.8	14.6	12.7	13.6	14.5	14.4

RAINFALL (mm) BASED ON 20220102

MODEL	DAY1	DAY2	DAY3	DAY4	DAY5	DAY6	DAY7
GFS	0.0	0.0	2.94	6.31	0.0	11.25	10.12
GEFS	0.0	0.0	4.5	8.6	1.9	6.1	9.3
NCEP	0.0	0.0	0.0	0.88	0.75	3.0	5.62
NCUM	0.0	0.0	0.06	7.97	2.91	11.09	2.03
JMA	0.0	0.0	0.06	4.19	0.12	3.25	8.5
MME	0.0	0.0	1.5	5.6	1.1	6.9	7.1

RELATIVE HUMIDITY (%) BASED ON 20220102

MODEL	DAY1	DAY2	DAY3	DAY4	DAY5	DAY6	DAY7
GFS	36.7	28.6	38.3	32.1	61.8	67.0	83.1
GEFS	69.7	89.6	67.1	89.1	72.2	76.4	50.0
NCEP	32.8	27.1	36.7	34.4	65.0	77.1	87.6
NCUM	73.5	88.6	64.2	86.6	62.0	83.6	54.5
JMA	42.9	38.0	44.6	38.5	45.3	45.3	69.3
MME	61.7	79.1	58.4	94.0	76.6	76.5	55.6

WIND DIRECTION (360 Of Compass) BASED ON 20220102

MODEL	DAY1	DAY2	DAY3	DAY4	DAY5	DAY6	DAY7
GFS	54.8	83.7	77.6	89.7	69.8	128.5	112.6
GEFS	59.7	98.0	88.8	105.5	85.1	91.1	74.7
NCEP	68.4	88.1	35.9	71.8	62.2	141.3	328.6
NCUM	45.0	45.0	45.0	45.0	45.0	45.0	45.0
JMA	19.5	18.3	73.2	100.8	78.2	110.9	97.8
MME	48.3	68.2	64.4	76.9	64.1	109.0	66.8

WIND SPEED (m/sec) BASED ON 20220102

MODEL	DAY1	DAY2	DAY3	DAY4	DAY5	DAY6	DAY7
GFS	1.0	0.8	2.7	3.8	4.1	6.0	1.6
GEFS	1.5	1.2	3.3	2.3	3.1	3.5	1.8
NCEP	1.0	1.7	2.3	4.4	3.3	3.5	0.2
NCUM	1.7	1.8	3.0	4.4	7.1	3.6	4.4
JMA	1.0	0.9	2.2	1.8	2.6	3.6	0.9
MME	1.2	1.1	2.5	3.1	3.9	3.4	1.5

CLOUD COVER (%) BASED ON 20220102

MODEL	DAY1	DAY2	DAY3	DAY4	DAY5	DAY6	DAY7
GFS	1.0	0.0	100.0	2.0	0.0	100.0	4.0
GEFS	0.0	4.0	100.0	90.0	48.0	47.0	68.0
NCEP	100.0	42.7	100.0	97.5	50.2	24.3	91.5
NCUM	0.0	0.0	0.0	13.38	13.56	84.12	80.38
JMA	33.98	50.63	96.44	56.1	60.94	99.95	56.4
MME	33.7	24.3	99.1	61.4	39.8	67.8	55.0

Fig. 8.3. Screenshot of city weather forecasting page from NWP division's website showing digital values of forecast

8.3.2. *Generation of MME forecast for Indian districts*

Five days of the area-averaged forecast of rainfall, maximum temperature, minimum temperature, wind speed, wind direction, relative humidity (at 3 UTC and 12 UTC), and cloud cover from each model is generated for Indian districts, followed by MME-mean forecasts have been generated. The political boundary of districts represented using ESRI shape files. Mean of all grid points within the district boundary polygon is computed and is available as the weather parameter of that region. Currently, forecast over 732 districts are generating in real time. Over these spatial domains, forecast of rainfall distribution also calculated by estimating the percentage of grids reporting a rainfall amount greater than 2.5 mm/day. The rainfall distribution is categorized as dry, isolated, scattered, fairly widespread and widespread if the percentage is 0, 0-25, 25-50, 50-75 and >75 respectively. Figure 8.4 shows the 24 hour MME rainfall intensity forecast for Indian districts for a typical day. These forecasts are disseminating to the operational forecasters at RMCs and MCs as a decision support while issuing forecast. These forecasts (as digital values) and figures are also available at NWP division's website.

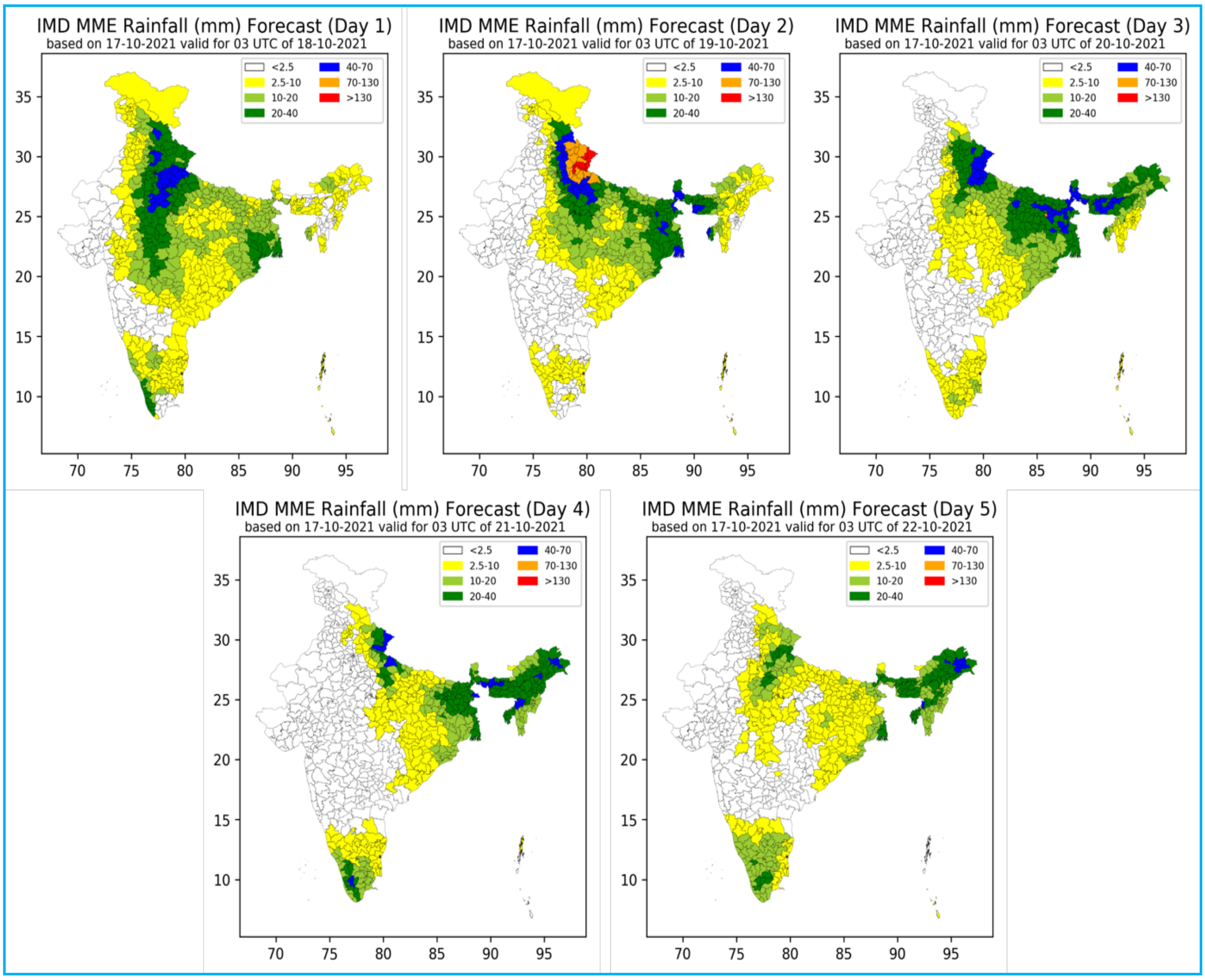

Fig. 8.4. MME rainfall forecast based on 17-10-2021for next five days over Indian districts

8.3.3. *Generation of MME forecast for meteorological sub-division*

Similar to the forecasts generating for Indian districts, five days of the area-averaged forecast of rainfall, maximum temperature, minimum temperature, wind speed, wind direction, relative humidity, and cloud cover are also generating for 36 meteorological sub divisions in India. Then MME forecast of each weather parameter is also generating by giving equal weight to all model forecast. Additionally, the forecast of heavy, very heavy and extremely heavy rainfall are also generated separately for each sub divisions by taking the distribution of the grid points over from all models showing respective thresholds. Figure 8.5 shows the 24 hour MME rainfall intensity forecast for meteorological sub-divisions for a typical day. These forecasts (as digital values) and figures are available at NWP division webpage (www.nwp.imd.gov.in). The screenshot of the meteorological sub-divisional weather forecasting web page, which contains digital values of rainfall intensity and distribution are shown in Figure 8.6 and 8.7 respectively.

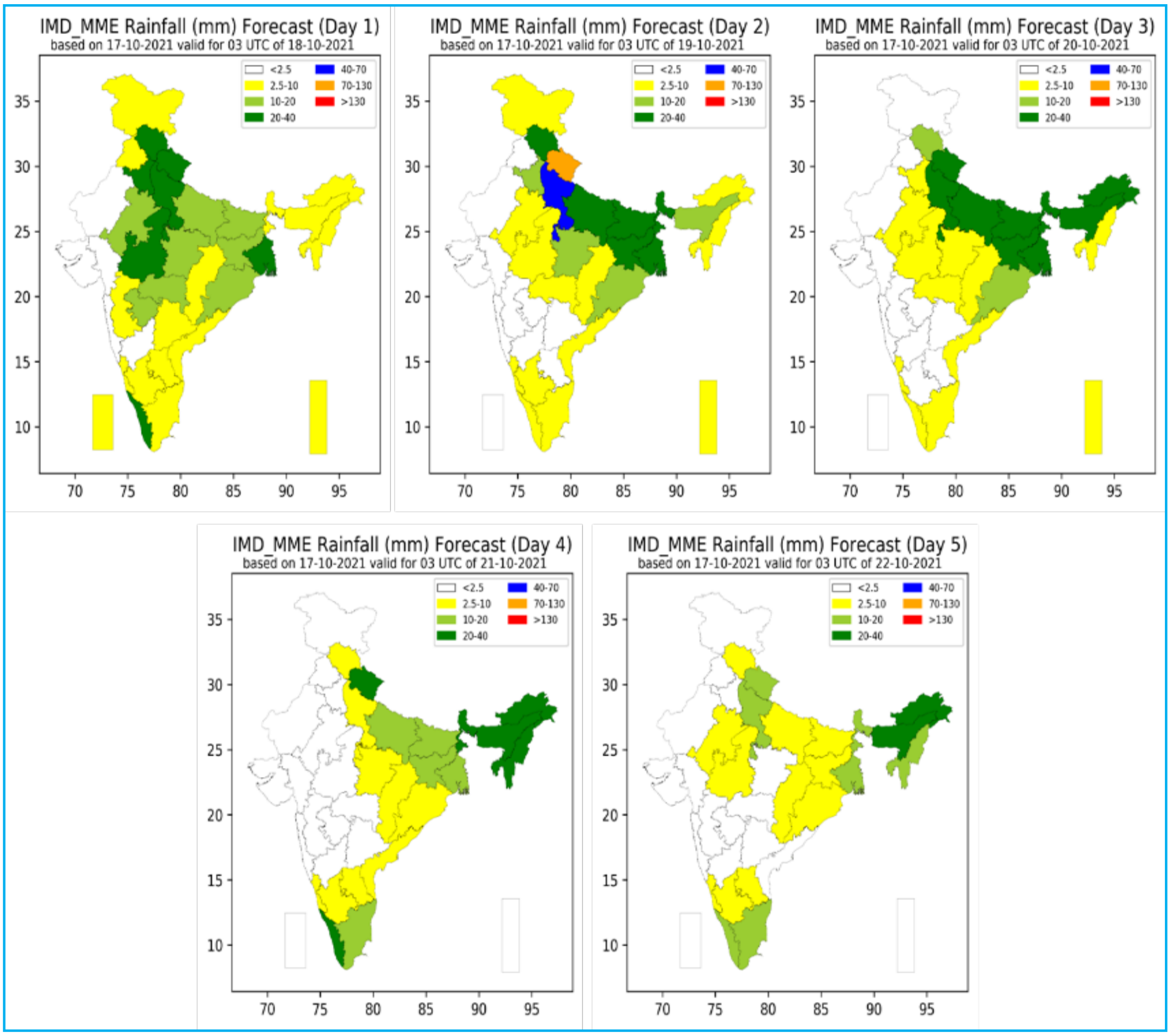

Fig. 8.5. MME rainfall forecast based on 17-10-2021for next five days over meteorological sub-divisions

DAY-01 DAY-02 DAY-03 DAY-04 DAY-05

Please check the Date of Rainfall Intensity Forecast as different Models has different updation time

DAY-01

S.NO.	SUB-DIVISION	DAY-01:GFS - FCST BASED ON :02012022 :VALID FOR:03012022	DAY-01:JMA - FCST BASED ON :02012022 :VALID FOR:03012022	DAY-01:NCUM - FCST BASED ON 02012022 :VALID FOR:03012022	DAY-01:NCEP - FCST BASED ON 02012022 :VALID FOR:03012022	DAY-01:GEFS - FCST BASED ON 02012022 :VALID FOR:03012022
		GFS	JMA	NCUM	NCEP_GFS	GEFS
01	A & N ISLAND	4	5	3	3	2
02	ARUNACHAL PRADESH	0	0	0	1	0
03	ASSAM & MEGHALAYA	0	0	0	0	0
04	N M M T	0	0	0	0	0
05	SHWB & SIKKIM	0	0	0	0	0
06	GANGETIC WEST BENGAL	0	0	0	0	0
07	ORISSA	0	0	0	0	0
08	JHARKHAND	0	0	0	0	0
09	BIHAR	0	0	0	0	0
10	EAST UTTAR PRADESH	0	0	0	0	0
11	WEST UTTAR PRADESH	0	0	0	0	0
12	UTTARAKHAND	0	0	0	0	0
13	HAR.CHD & DELHI	0	0	0	0	0
14	PUNJAB	0	0	0	0	0
15	HIMACHAL PRADESH	3	4	3	8	2
16	JAMMU & KASHMIR	8	6	3	3	2
17	WEST RAJASTHAN	0	0	0	0	0
18	EAST RAJASTHAN	0	0	0	0	0
19	WEST MADHYA PRADESH	0	1	1	0	0
20	EAST MADHYA PRADESH	0	0	2	0	0
21	GUJARAT REGION	0	0	0	0	0
22	SAURASHTRA & KUTCH	0	0	0	0	0
23	KONKAN&GOA	0	0	0	0	0
24	MADHYA MAHARASHTRA	0	0	2	0	0
25	MARATHWADA	0	0	1	0	0
26	VIDARBHA	0	0	0	0	0
27	CHHATTISGARH	0	0	0	0	0
28	COASTAL ANDHRA PRADESH	1	0	2	2	0
29	TELANGANA	0	0	2	0	0
30	RAYALASEEMA	2	0	2	0	0
31	TAMILNADU & PONDICHERY	30	3	10	17	14
32	COASTAL KARNATAKA	0	0	0	0	2
33	N.I.KARNATAKA	0	0	1	0	0
34	S.I.KARNATAKA	0	0	0	0	0
35	KERALA	6	0	5	4	0
36	LAKSHADWEEP	0	0	1	3	0

Fig. 8.6. Screenshot of meteorological sub-division wise rainfall (intensity) forecasting page from NWP division's website

DAY-01 | DAY-02 | DAY-03 | DAY-04 | DAY-05

Please check the Date of Rainfall Distribution Forecast as different Models has different updation time

DAY-01

S.NO.	SUB-DIVISION	DAY-01:GFS - FCST BASED ON:02012022 :VALID FOR:03012022	DAY-01:JMA - FCST BASED ON:02012022 :VALID FOR:03012022	DAY-01:NCUM - FCST BASED ON02012022 :VALID FOR:03012022	DAY-01:NCEP - FCST BASED ON02012022 :VALID FOR:03012022	DAY-01:GEFS - FCST BASED ON02012022 :VALID FOR:03012022
		GFS	JMA	NCUM	NCEP_GFS	GEFS
01	A & N ISLAND	SCT	ISOL	SCT	SCT	ISOL
02	ARUNACHAL PRADESH	DRY	DRY	DRY	ISOL	DRY
03	ASSAM & MEGHALAYA	DRY	DRY	DRY	DRY	DRY
04	N M M T	DRY	DRY	DRY	DRY	DRY
05	SHWB & SIKKIM	DRY	DRY	DRY	DRY	DRY
06	GANGETIC WEST BENGAL	DRY	DRY	DRY	DRY	DRY
07	ORISSA	DRY	DRY	DRY	DRY	DRY
08	JHARKHAND	DRY	DRY	DRY	DRY	DRY
09	BIHAR	DRY	DRY	DRY	DRY	DRY
10	EAST UTTAR PRADESH	DRY	DRY	DRY	DRY	DRY
11	WEST UTTAR PRADESH	DRY	DRY	DRY	DRY	DRY
12	UTTARAKHAND	DRY	DRY	DRY	DRY	DRY
13	HAR.CHD & DELHI	DRY	DRY	DRY	DRY	DRY
14	PUNJAB	DRY	DRY	DRY	DRY	DRY
15	HIMACHAL PRADESH	ISOL	ISOL	ISOL	ISOL	ISOL
16	JAMMU & KASHMIR	ISOL	ISOL	ISOL	ISOL	ISOL
17	WEST RAJASTHAN	DRY	DRY	DRY	DRY	DRY
18	EAST RAJASTHAN	DRY	DRY	DRY	DRY	DRY
19	WEST MADHYA PRADESH	DRY	ISOL	ISOL	DRY	DRY
20	EAST MADHYA PRADESH	DRY	DRY	ISOL	DRY	DRY
21	GUJARAT REGION	DRY	DRY	DRY	DRY	DRY
22	SAURASHTRA & KUTCH	DRY	DRY	DRY	DRY	DRY
23	KONKAN&GOA	DRY	DRY	DRY	DRY	DRY
24	MADHYA MAHARASHTRA	DRY	DRY	ISOL	DRY	DRY
25	MARATHWADA	DRY	DRY	ISOL	DRY	DRY
26	VIDARBHA	DRY	DRY	DRY	DRY	DRY
27	CHHATTISGARH	DRY	DRY	DRY	DRY	DRY
28	COASTAL ANDHRA PRADESH	ISOL	DRY	ISOL	ISOL	DRY
29	TELANGANA	DRY	DRY	ISOL	DRY	DRY
30	RAYALASEEMA	ISOL	DRY	ISOL	DRY	DRY
31	TAMILNADU & PONDICHERY	SCT	ISOL	ISOL	FWS	SCT
32	COASTAL KARNATAKA	DRY	DRY	DRY	DRY	ISOL
33	N.I.KARNATAKA	DRY	DRY	ISOL	DRY	DRY
34	S.I.KARNATAKA	DRY	DRY	DRY	DRY	DRY
35	KERALA	ISOL	DRY	ISOL	ISOL	DRY
36	LAKSHADWEEP	DRY	DRY	ISOL	SCT	DRY

Fig. 8.7. Screenshot of meteorological sub-division wise rainfall forecasting (distribution) page from NWP division's website

8.3.4. *Generation of MME forecast for coastal regions*

Similar to the forecasts generating for Indian districts and meteorological sub-divisions, five days of the area-averaged forecast of rainfall, maximum temperature, minimum temperature, wind speed, wind direction, relative humidity, and cloud cover are generating for 16 coastal regions in India. Over coastal regions visibility, significant wave height, and wind gust also generating along with other weather parameters. Visibility and significant wave height is not available as a direct product from the model forecast in listed Table 8.1. Thus, these two parameters are estimated using the approximation listed in Table 8.2 which is available in standard operation procedure of IMD (https://mausam.imd.gov.in/imd_latest/contents/pdf/cyclone_sop.pdf,https://mausam.imd.gov.in/imd_latest/contents/pdf/forecasting_sop.pdf,). The maximum value of rainfall predicted by all models over this region also tabled to understand the variability in the predicted rainfall. Additionally, the forecast of heavy, very heavy and extremely heavy rainfall are also generated separately by taking the distribution of the grid points from all models showing respective thresholds. Similarly, the maximum and minimum wind speed forecasted by all models and its mean are also tabled to get the variability in the wind forecast. All these forecasts are provided for generating GIS based image to host in IMD's webpage (https://mausam.imd.gov.in/imd_latest/contents/coastal_forecast.php). The screenshots of these pages from IMD's webpage are shown in Figure. 8.8 to Figure 8.10.

Table 8.2

Conditions used for estimating wave height and visibility

Wave Height Estimation		
Wind speed (knots)	Estimated significant wave height (m)	Descriptive term
0	0	Calm (Glassy)
1-3	0-0.1	Calm (Rippled)
4-10	0.1-0.5	Smooth
11-16	0.5-1.25	Slight
17-21	1.25-2.5	Moderate
22-27	2.5-4.0	Rough
28-33	4.0-6.0	Very rough
34-40	6.0-9.0	High
41-63	9.0-14.0	Very high
64 and above	Over 14	Phenomenal
Visibility Estimation		
Rainfall distribution	Estimated visibility (NM)	
Fairly wide spread or wide spread with heavy rainfall	< 2 Nautical Miles (NM)	
Wide spread	2-3	
Fairly wide spread	3-4	
Scattered	4-6	
Isolated	6-8	
Fair	8-10	

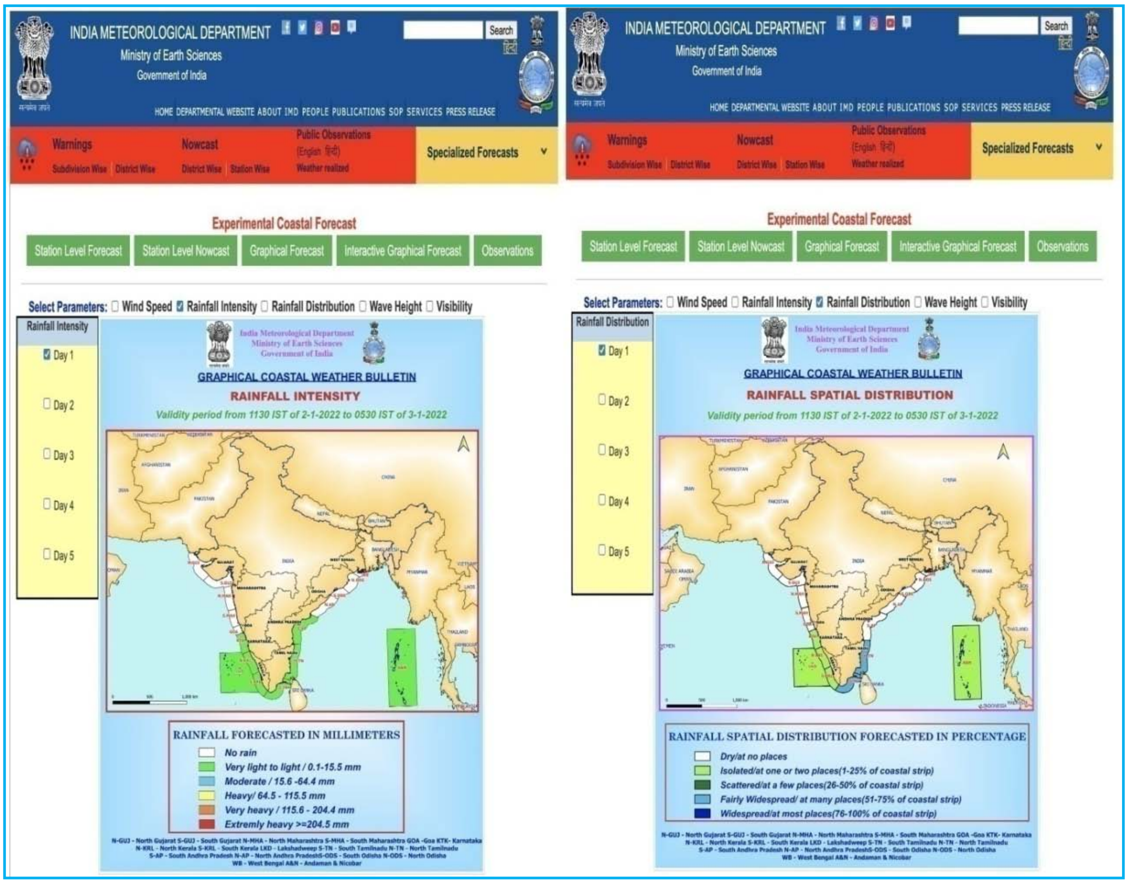

Fig. 8.8. Screenshot of coastal weather forecasting page from IMD's website

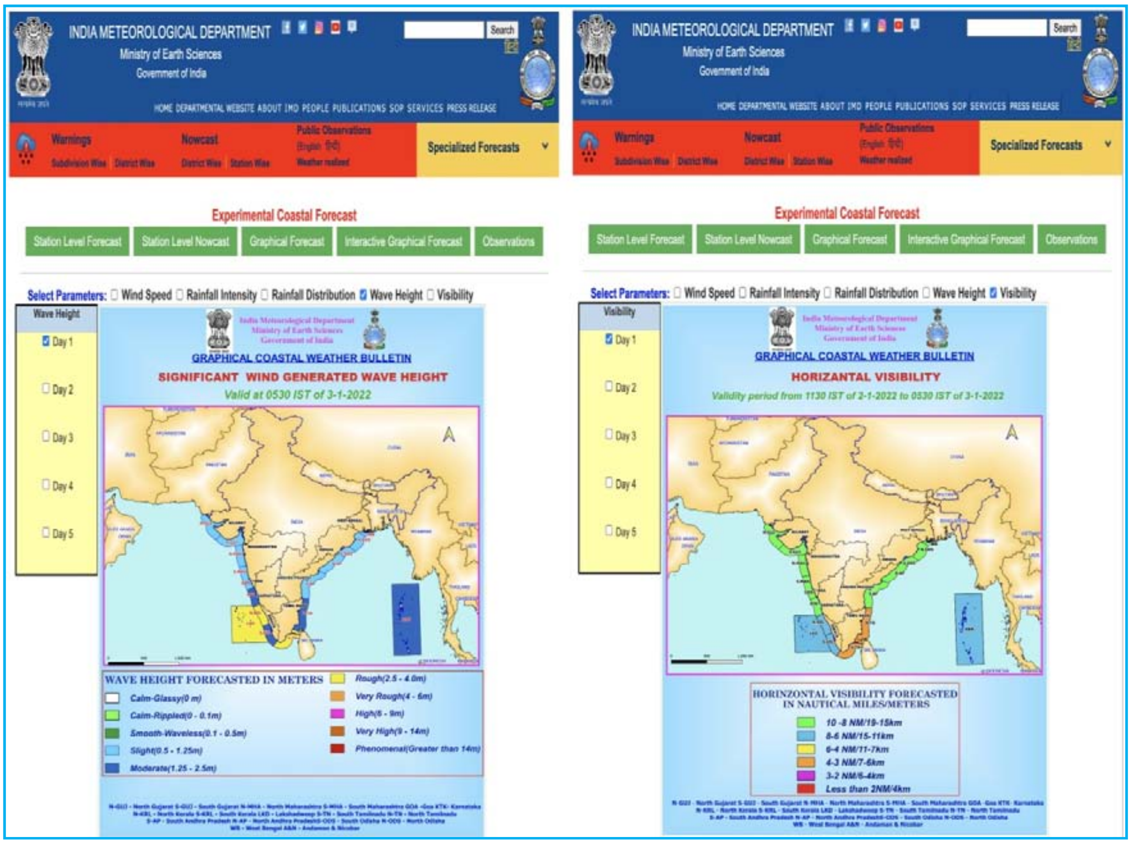

Fig. 8.9. Screenshot of coastal weather forecasting page from IMD's website

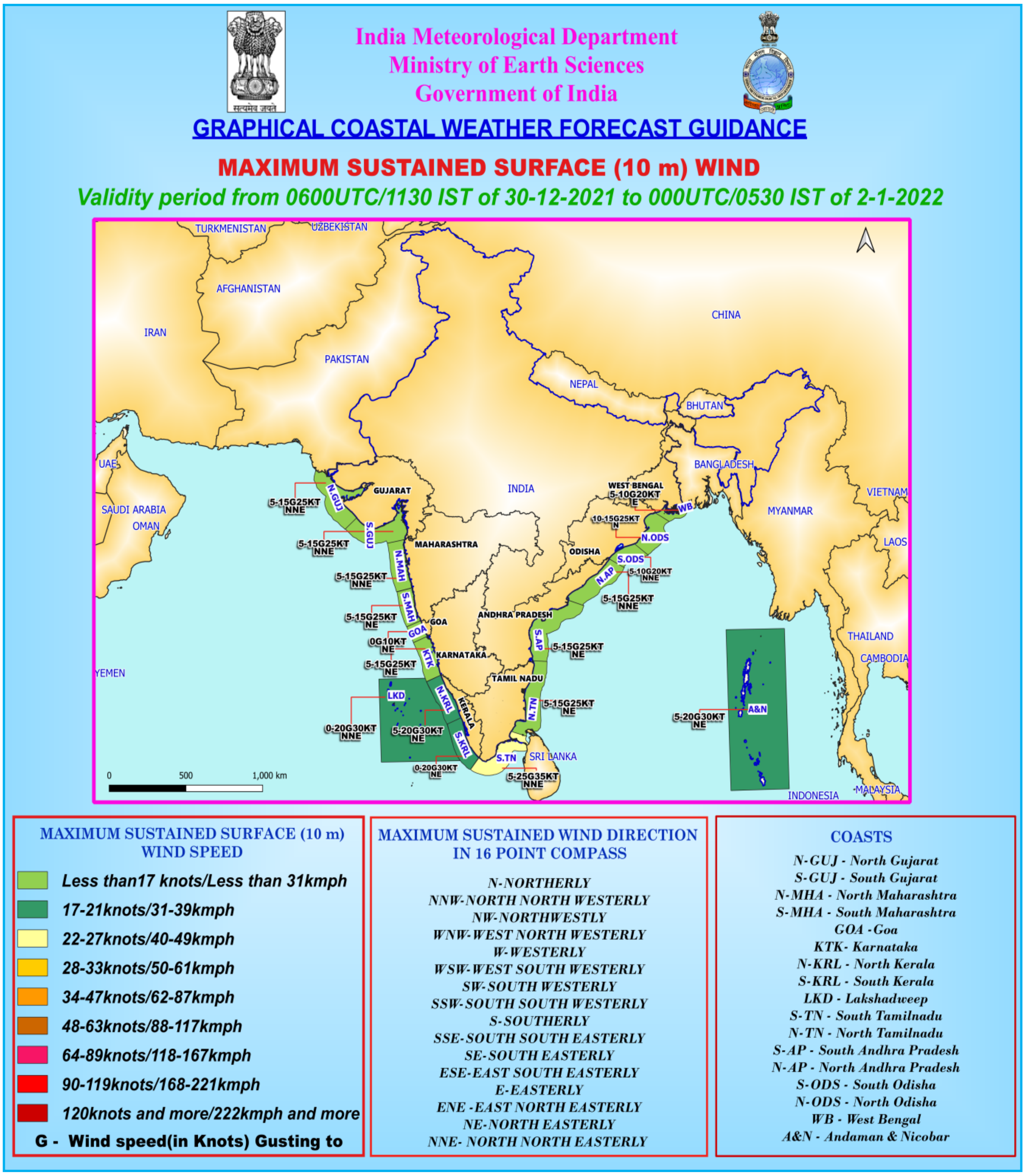

Fig. 8.10. Screenshot of coastal weather forecasting page from IMD's website

8.4. Verification of district level forecast rainfall against IMD observations

The district rainfall forecast from different NWP model and MME are compared against IMD 0.25° gridded data during July to October 2021. A case study is presented in this report to evaluate the performance of MME forecast qualitatively over Indian districts. The extremely heavy rainfall reported at Uttarakhand state on 19th October, 2021 is compared qualitatively with the MME forecast (Figure). The extremely heavy rainfall observed at Uttarakhand [Figure (a)], is well predicted in MME day 1, day 2 and day 3 forecast.

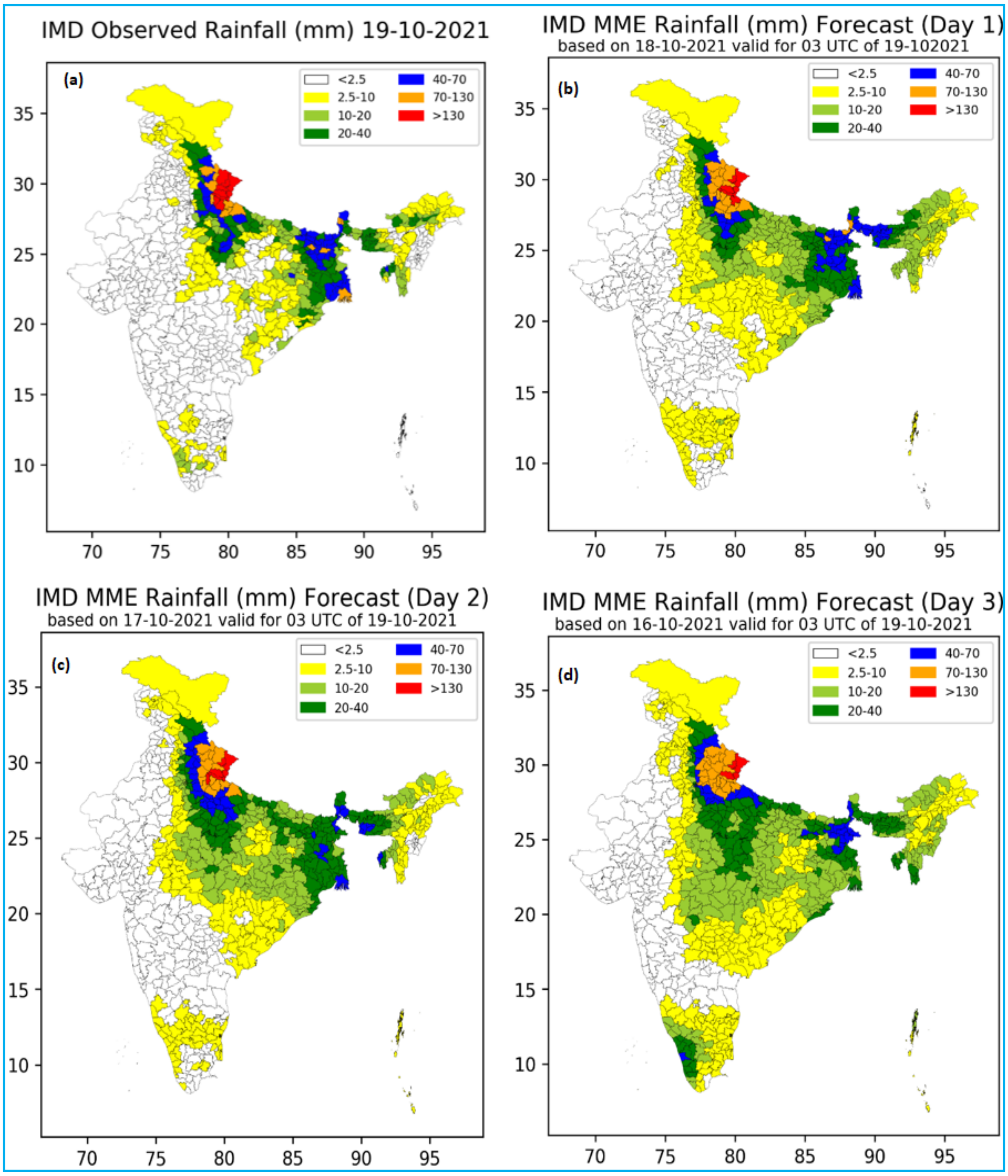

Figs. 8.11 (a-d). IMD observed rainfall and MME day 1, day 2, and day 3 rainfall forecast for 19th October 2021

The performance of each model forecast and MME forecast are validated up to day 5, and scatter plots between forecasts and observations are generated routinely at NWP division of IMD. Correlation coefficient, root mean square error and bias are routinely monitoring as part of this verification process. Figure 8.12 shows the scatter plot of MME rainfall forecast up to day 5 between IMD observed rainfall valid for 10 October 2021. Similar to Figure 8.12, scatter plot of GFS, GEFS, NCEP, NCUM and JMA forecast against IMD observation is regularly generating at NWP division (not shown in this report). At the end of the season, the rainfall forecast of whole season from NWP model and MME are validated against IMD observed rainfall, and different statistical scores are generated. The Scatter plots of rainfall forecast against observation is shown in Figure 8.13.

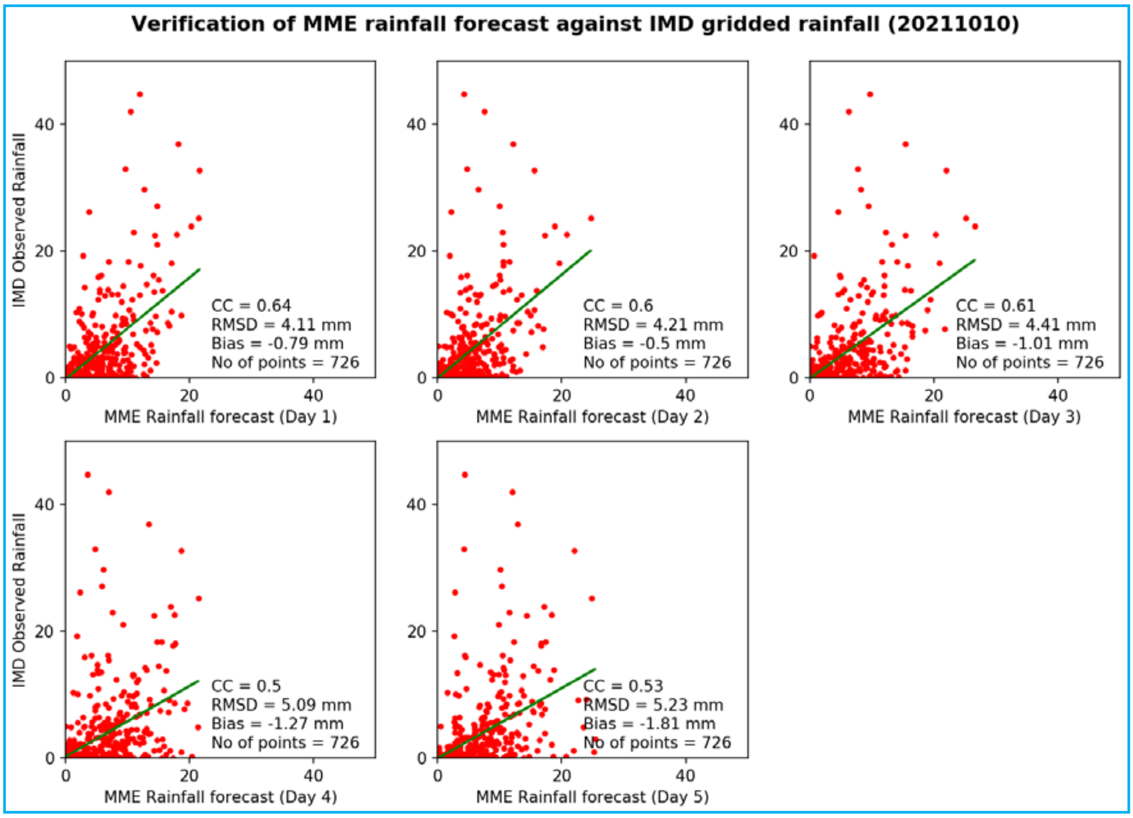

Fig. 8.12. Scatter plot of MME rainfall forecast up to day 5 against IMD observed rainfall valid for 10 October 2021

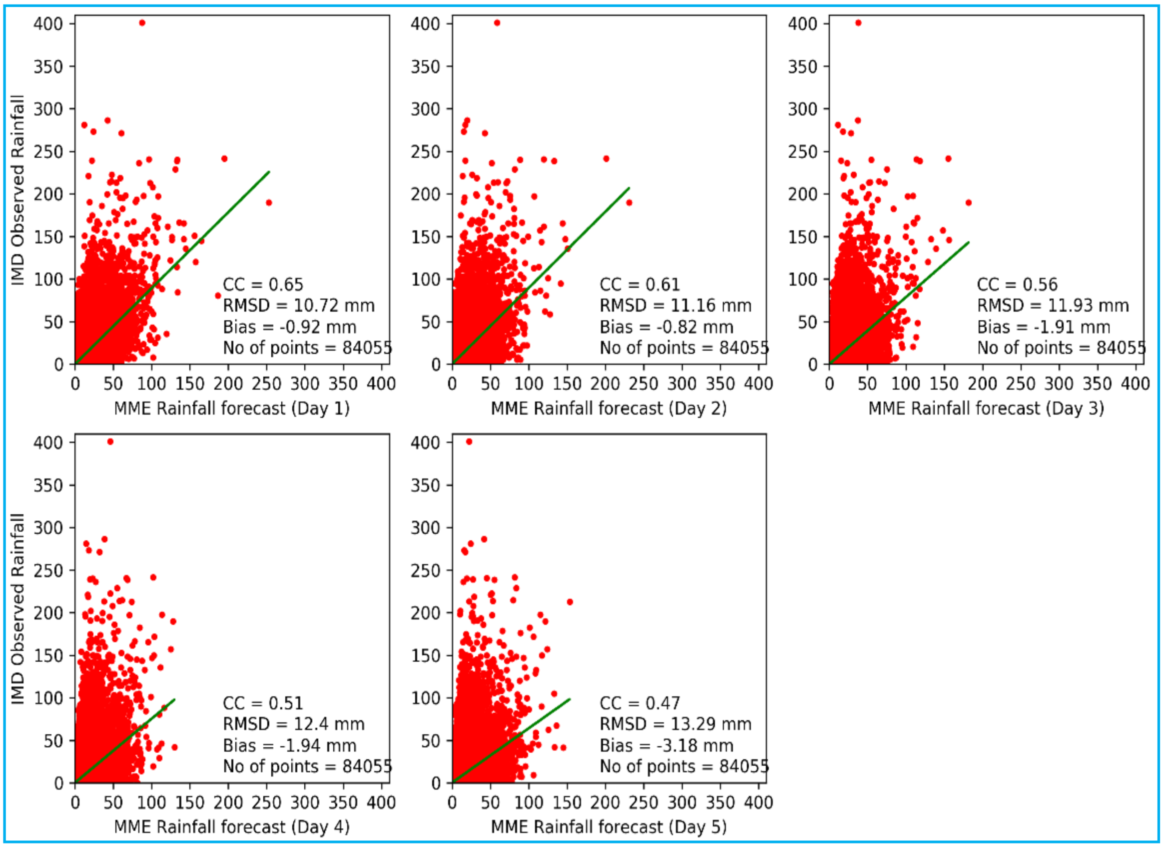

Fig. 8.13. Scatter plot of MME rainfall forecast up to day 5 against IMD observed rainfall valid for July-October 2021

Numerical Weather forecasts should also be evaluated for the forecast quality in terms of skill of the prediction. At NWP division, different skill scores like accuracy, bias score, critical success index (CSI), probability of detection (POD), false alarm ratio (FAR), probability of false detection (POFD), Heidke skill score (HSS), equitable threat score (ETS) and extreme dependency ratio are also generating routinely for each model forecast. This scores has been carried out using IMD gridded rainfall data. Figure 14 to 16 shows the different skill scores of MME day 1 rainfall forecast valid for 18 October 2021. Similarly skill score of all models listed in Table 8.1 are routinely generating and evaluating their performance.

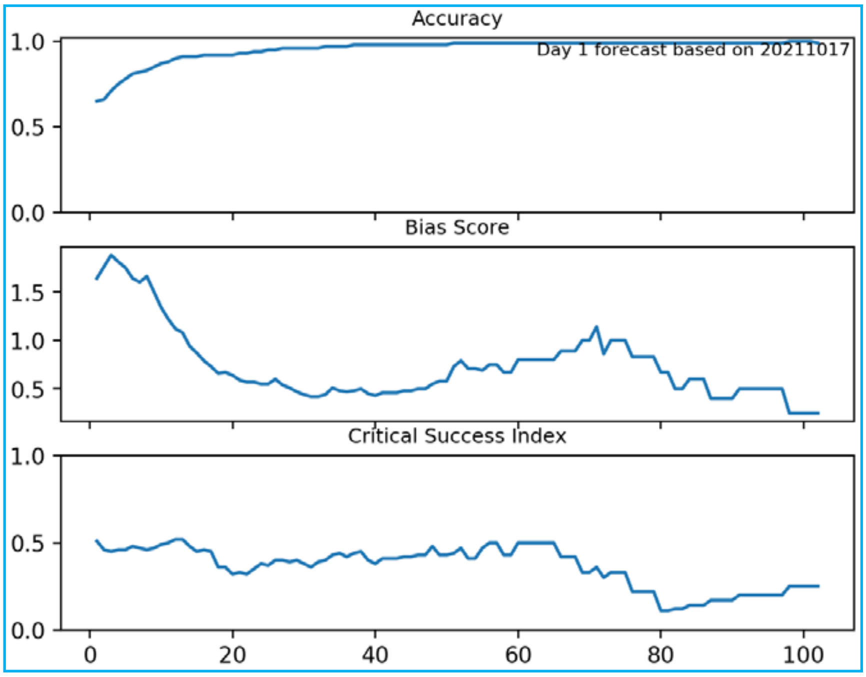

Fig. 8.14. Accuracy (top), Bias score (middle) and CSI (bottom) skill scores in Day 1 MME rainfall forecast valid for 18 October 2021

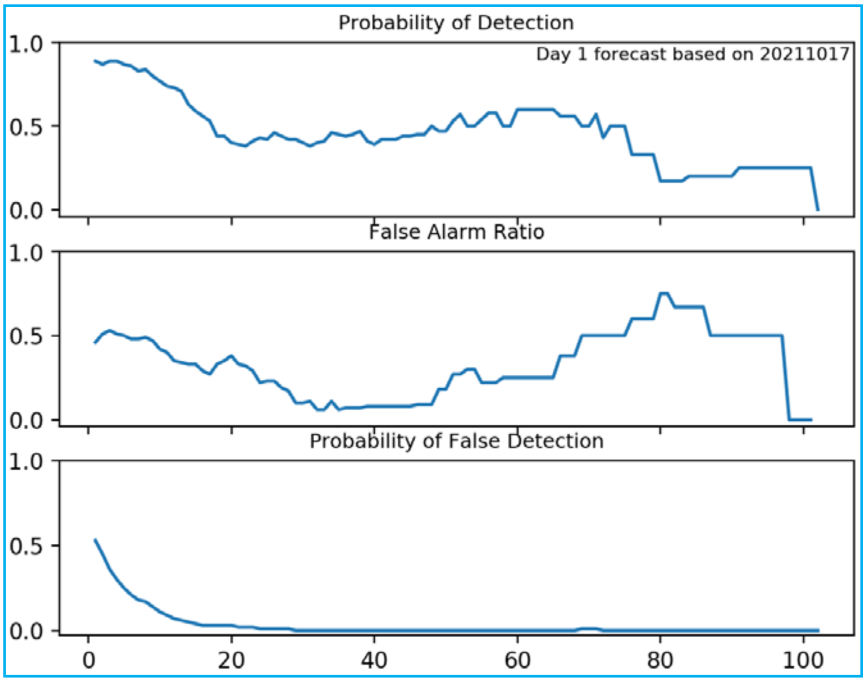

Fig. 8.15. POD (top), FAR (middle) and POFD (bottom) skill scores in Day 1 MME rainfall forecast valid for 18 October 2021

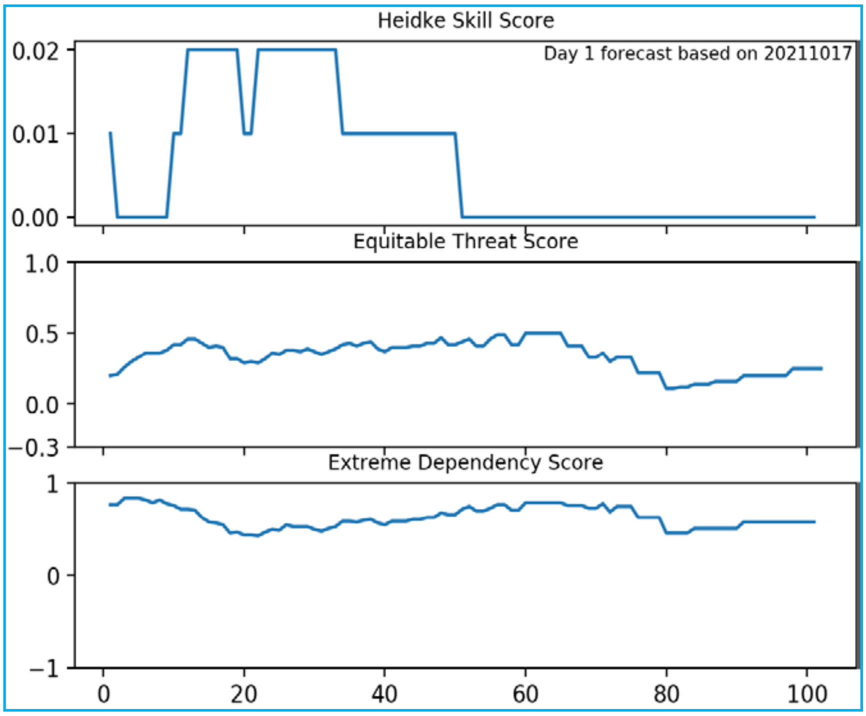

Fig. 8.16. HSS (top), ETS (middle) and EDS (bottom) skill scores in Day 1 MME rainfall forecast valid for 18 October 2021

8.5. Summary

This report describes about the development of MME based forecast for Indian city, districts, coastal and meteorological sub-divisions. These forecasts are made available in IMD's website for decision support for the forecasters. The verification of MME forecast shows that MME has a potential of predicting weather events in medium range. The correlation coefficient between observed rainfall and day 1, day 2, day 3, day 4 and day 5 forecast during July to October 2021 for Indian districts are 0.65, 0.61, 0.56, 0.51 and 0.47 respectively. Different forecast skill score are also presented in this report. The MME based forecast at different spatial scales like city level, district level, coastal region and met subdivision level for providing weather forecast and warning services will be helpful for various sectors.

Acknowledgement

Authors are thankful to the NCMRWF, NCEP and JMA for their valuable data.

References

Chakraborty, A., Krishnamurti, T. N., and Gnanaseelan, C., (2007) Prediction of the diurnal cycle using a multimodel superensemble. Part II: Clouds, *Mon. Wea. Rev*., **135**, 4097–4116.

Chandler, R. E. (2013) Exploiting strength, discounting weakness: combining information from multiple climate simulators, Phil. Trans. R. Soc. A, 371, 20120388, doi:10.1098/rsta.2012.0388.

Christensen, J. H., Kjellström, E., Giorgi, F., Lenderink, G., and Rummukainen, M., (2010) Weight assignment in regional climate models, **44**, 179–194, doi:10.3354/cr00916.

Christiansen, B. (2018) Ensemble averaging and the curse of dimensionality. *J. Climate*, **31**, 1587–1596, https://doi.org/10.1175/JCLI-D-17-0197.1.

Christiansen, B. (2019) Analysis of ensemble mean forecasts: The blessings of high dimensionality. *Mon. Wea. Rev*., **147**, 1699–1712, https://doi.org/10.1175/MWR-D-18-0211.1.

Déqué, M. and Somot, S., (2010) Weighted frequency distributions express modelling uncertainties in the ENSEMBLES regional climate experiments, *Clim. Res*., **44**, 195–209, doi:10.3354/cr00866.

Deshpande M., Johny C. J., Kanase R., Tirkey S., Sarkar S. Goswami, T., Roy K., Ganai M., Krishna R. P. M., Prasad V. S., Mukhopadhyay P., Durai V. R., Nanjundiah R. S. And Rajeevan, M., (2020), Implementation of Global Ensemble Forecast System (GEFS) at 12 km Resolution. ISSN 0252-1075, IITM Technical Report No.TR-06, ESSO/IITM/MM/ TR/02(2020)/200.

JMA, (2019) Joint WMO technical progress report on the global data processing and forecasting system and numerical weather prediction research activities for 2019, http://www.jma.go.jp/jma/jma-eng/jma-center/nwp/report/2019_Japan.pdf.

Johnson, C. and Swinbank, R., (2009) Medium-range multimodel ensemble combination and calibration, *Q. J. Roy. Meteorol. Soc*., **135**, 777–794.

Johny, C.J. and Prasad, V.S., (2020) Application of hind cast in identifying extreme events over India,*J. Earth Syst. Sci*.,**129**, 163. https://doi.org/10.1007/s12040-020-01435-8.

Knutti, R., Furrer, R., Tebaldi, C., Cermak, J., and Meehl, G. A., (2010) Challenges in combining projections from multiple climate models, *J. Climate*, **23**, 2739–2758, doi:10.1175/2009JCLI3361.1.

Kotal, S. D. and Roy Bhowmik, S. K., (2011) A Multimodel Ensemble (MME) Technique for Cyclone Track Prediction over the North Indian Sea, *Geofizika*, **28**, 275–291.

Krishnamurti, T. N., Kishtawal, C. M., LaRow, T. E., Bachiochi, D. R., Zhang, Z., Williford, C. E., Gadgil, S. and Surendran, S., (1999) Improved weather and seasonal climate forecasts from multi-model super ensemble, *Science*, **285**, 1548–1550.

Krishnamurti, T. N., Kishtawal, C. M., Zhang, Z., LaRow, T. E., Bachiochi, D. R., Williford, C. E., Gadgil, S. and Surendran, S., (2000b) Improving tropical precipitation forecasts from a multi analysis super ensemble, *J. Climate*, **13**, 4217–4227.

Krishnamurti, T. N., Kishtawal, C. M., Zhang, Z., LaRow, T., Bachiochi, D., Williford, E., Gadgil, S. and Surendran, S., (2000a) Multimodel Ensemble Forecasts for Weather and Seasonal Climate, *J. Climate*, **13**, 4196–4216, doi:10.1175/1520- 0442(2000)0132.0.CO;2.

Krishnamurti, T. N., Mishra, A. K., Chakraborty, A., and Rajeevan, M., (2009) Improving Global Model Precipitation Forecasts over India Using Downscaling and the FSU Superensemble, Part I: 1–5-Day Forecasts, *Mon. Wea. Rev*., **137**, 2713–2735.

Krishnamurti, T. N., Sanjay, J., Mitra, A. K., and Vijaya Kumar, T. S. V., (2004) Determination of Forecast Errors Arising from Different Components of Model Physics and Dynamics, *Mon. Wea. Rev*., **132**, 2570–2594, doi:10.1175/MWR2785.1.

Kumar, A., Mitra, A. K., Bohra, A. K., Iyengar, G. R., and Durai, V. R., (2012) Multi-model ensemble (MME) prediction of rainfall using neural networks during monsoon season in India, *Meteorol. Appl*., **19**, 161–169.

Lenartz, F., Mourre, B., Barth, A., Beckers, J.-M., Vandenbulcke, L., and Rixen, M., (2010) Enhanced ocean temperature forecast skills through 3-D super-ensemble multi-model fusion, *Geophys. Res. Lett*., **37**, L19606, doi:10.1029/2010GL044591.

Lorenz, E. N. (1965) A study of the predictability of 28-variable atmosphere model, *Tellus*, **17**(3), 321-333.

Mitra, A. K., Iyengar, G. R., Durai, V. R., Sanjay, J., Krishnamurti, T. N., Mishra, A., and Sikka, D. R., (2011) Experimental Real-Time Multi-Model Ensemble (MME) Prediction of Rainfall During Monsoon 2008: Large-Scale Medium-Range Aspects, *J. Earth Syst. Sci*., **120**, 27–52.

Palmer, T. N., R. Buizza, R. Hagedorn, A. Lorenze, M. Leutbecher, and S. Lenny, (2006) Ensemble prediction: A pedagogical perspective. *ECMWF Newsletter*, No. 106, ECMWF, Reading, United Kingdom, 10–17, https://www.ecmwf.int/sites/default/files/elibrary/2006/18024-ensemble-prediction-pedagogical-perspective.pdf.

Roy Bhowmik S. K. , Durai V.R., (2008) Multi-model ensemble forecasting of rainfall over Indian monsoon region. *Atmosfera*,**21**(3), 225–239.

Roy Bhowmik S. K., Durai V.R., (2010) Application of multi-model ensemble techniques for real time district level rainfall forecasts in short range time scale over Indian region. *Meteorology and Atmospheric Physics*, **106**(1–2), 19–35.

Saulo, A. C., Seluchi, M., Campetella, C., and Ferreira, L., (2001) Error evaluation of NCEP and LAHM regional model daily forecasts over southern South America, *Weather Forecast*, **16**, 697–712.

Silva Dias, P. L., Moreira, D. S., and Neto, G. D., (2006) The MASTER Model Ensemble System (MSMES). Preprints, Eighth Int. Conf. on Southern Hemisphere Meteorology and Oceanography, Foz do Iguaçu, Brazil, *Amer. Meteor. Soc*., 4pp.

Sumit K., Bushair, M.T., Jangid, B.P., Lodh, A., Sharma, P., George, G., Rani, S.I., George, J.P., Jayakumar, A., Mohandas, S., Sushant, K., (2020). NCUM Global NWP System: Version 6, NCMRWF Technical Report. https://www.ncmrwf.gov.in/Reports-eng/New_NCUMImplementation_Report.pdf.

Tebaldi, C., Mearns, L. O., Nychka, D. and Smith, R. L. (2004) Regional probabilities of precipitation change: A bayesian analysis of multimodel simulations, *Geophys. Res. Lett*., **31**, L24213, doi:10.1029/2004GL021276.

Thompson, P. (1957) Uncertainty of initial state as a factor in predictability of large-scale atmospheric flow patterns, *Tellus*, **9**, 275–295.

Van Lier-Walqui, M., T. Vukicevic, and D. J., Posselt, (2012) Quantification of cloud microphysical parameterization uncertainty using radar reflectivity. *Mon. Wea. Rev.*, **140**, 3442-3466, doi:10.1175/MWR-D-11-00216.1.

Weigel, A. P., Knutti, R., Liniger, M. A. and Appenzeller, C. (2010) Risks of model weighting in multimodel climate projections, *J. Climate*, **23**, 4175–4191, doi:10.1175/2010JCLI3594.1.

Yun, W.T., Stefanova, L. and Krishnamurti, T. N., (2003) Improvement of the multimodel super ensemble technique for seasonal forecasts, *J. Climate*, **16**, 3834–3840.

CHAPTER 9

Customized New NWP Ensemble Products for Weather Forecasting and Warning Services

T. ARULALAN, D. R. PATTANAIK and PRADEEP MISHRA

9.1. Introduction

The World Meteorological Organization (WMO) provided guidelines on "Ensemble Prediction Systems and Forecasting" to the world weather forecasting institutes. WMO (2012), "The Ensemble Prediction Systems (EPS) are numerical weather prediction (NWP) systems that allow us to estimate the uncertainty in a weather forecast as well as the most likely outcome. Instead of running the NWP model once (a deterministic forecast), the model is run many times from very slightly different initial conditions. Often the model physics is also slightly perturbed, and some ensembles use more than one model within the ensemble (multi-model EPS) or the same model but with different combinations of physical parameterization schemes (multi-physics EPS). The EPS normally includes a control forecast that uses the ensemble resolution model but without any perturbations to the analysis or model. The individual NWP solutions that make up the ensemble are often referred to as the ensemble members. The range of different solutions in the forecast allows us to assess the uncertainty in the forecast, and how confident we should be in a deterministic forecast. The uncertainty in a weather forecast can vary widely from day to day according to the synoptic situation, and the EPS approach provides an estimate of this day-to-day uncertainty. The EPS is designed to sample the probability distribution function (pdf), mean, spread of the forecast, and is often used to produce probability forecasts – to assess the probability that certain outcomes will occur".

Why is EPS needed? : The NWP forecasts the weather by starting the model from an analysis of the state of the atmosphere based on the latest observations that are taken all around the world. The model then calculates how the atmosphere will change and evolve from this initial analysis state over the coming days. The NWP global deterministic (also known as control) forecast model is able to predict many weather parameters including precipitation, temperature, wind, cloud, and much more, which are most useful to the common people. WMO (2012), "NWP is well known that forecasts from even the very best models can often go badly wrong. This is most obvious in forecasts several days ahead and is due to the chaotic nature of the atmosphere. Chaos theory means that the way the atmosphere evolves is very sensitive to small errors in that initial analysis, so that a tiny error (often too small for the forecaster to even notice) can become a large error in the forecast. Even with the best observations we can never make a perfect analysis, so we cannot make perfect forecasts. This is why we run EPS (ensembles). In an ensemble forecast we make very small changes (perturbations) to the analysis, and then re-run the model from these slightly perturbed starting conditions. If the different forecasts in the ensemble are all very similar to each other then we can be confident of our forecast, but if they all develop differently, and for example some develop a major storm while others develop a much weaker depression, then we will be much less confident. However, by looking at the proportion of the ensemble members that predict a storm, we can make an estimate of how likely the storm is, in 10-15 days advance (Medium range) forecasts. When we look at shorter-range forecasts of 1 or 2 days ahead, the general pattern of the weather is usually much more predictable, but we can still find important differences between ensemble members when we look at the local detail of the weather which may be important to many forecast users. Also, occasionally the larger-scale evolution can be uncertain even at short range – this is most likely to happen during the development of major storms, so it is important to take account of the EPS even in short-range forecasts".

Usage of EPS in Extreme Events Predictions : The severe weather events or extreme weather events are most vulnerable to the public, economic, livelihood, etc., which are most common in the world by heavy rainfall, cyclonic storms, extreme temperature (heatwaves, oldwaves). The prediction of extreme events in advance is essential, also how much probability to occur such an extreme event is questionable by the forecasters. To answer such a question, EPS is the only solution. For example, by using EPS, NWP can guide the forecasters by telling what is the probability of occurrence (confidence) of greater than 10 cm rainfall (or heatwave) over any particular region, in 5 days' advance. So this will help the government and other organizations to plan during the extreme events, such as evacuation during severe cyclones and heat action plan during summer, etc. By using a single control (deterministic) NWP model, one can not draw the chance of any particular events, not only extremes. Ensembles are most useful in NWP which provide confidence of occurrence, but it requires much more computing power compared to a single control model forecast.

EPS in IMD : The India Meteorological Department (IMD), Numerical Weather Prediction (NWP) division runs the **IMDGFS** as a deterministic global forecasting model and **IMDGEFS** as ensemble global forecasting model with 20 members at both 00 UTC and 12 UTC cycles, with 0.12°x0.12° horizontal resolution, operationally for every day since June 2018 (high resolution ensembles). In the global, only IMD produces a very high resolution (0.12°x0.12°) ensemble global model forecasts (1 control + 20 members) from June 2018 to till date (January 2022).

EPS in Other WMO Institutes : Not only in IMD, there are more than 12 global WMO institutes that are making ensemble global numerical weather predictions on a daily basis, operationally. Some of them are producing every 6 hourly or 12 hourly cycles for next 10 (or more than that) days forecasts over the globe. The WMO countries are sharing their ensemble global model forecasts among them, also to the public for free of cost. This data shared among global modeling NWP groups, will make grand global ensemble forecasts which is useful to overcome bias from particular models (overestimate, underestimate, etc) by making global grand ensemble mean and other statistics outputs. The WMO initiated a project named as "THORPEX Interactive Grand Global Ensemble" (TIGGE) for global ensemble model outputs data sharing from all over the world Institutes (NWP model prediction centers) to the public for free of cost, discussed in section 9.2.

Applications of EPS forecasts : There are numerous most useful applications available from the ensemble forecasts. The NWP division of IMD developed a few new products using EPS model forecasts outputs, which are discussed in this chapter-9, sections 9.3 to 9.7. The wind speed probabilities at threshold ≥ 28 Knots, ≥ 34 Knots, ≥ 50 Knots, and ≥ 64 Knots using IMD's GEFS, and NCMRWF's Unified Model - NEPS ensemble model forecasts are produced daily operationally, which are discussed in section 9.3. The Multi Model Ensemble Tropical Cyclone Tracker outputs are shown for a recent cyclonic storm (Dec 2021) as a case study with verification are discussed in section 9.4. The Weather Pattern Forecasts using IMDGEFS model are shown in section 9.5. The Madden–Julian Oscillation (MJO) Monitoring and Real-time Verification using IMDGEFS are shown and discussed in section 9.6. The state level spatial rainfall forecasts and its verification against the observed gridded rainfall is discussed in 9.7. Finally, summaries of this chapter mentioned in section 9.8.

9.2. Grand Global Ensemble Models (TIGGE)

The THORPEX Interactive Grand Global Ensemble (TIGGE, Philippe Bougeault *et al.* 2010) is an implementation of ensemble forecasting for global weather forecasting and is part of THORPEX, an international research programme established in 2003 by the World Meteorological Organization (WMO) to accelerate improvements in the utility and accuracy of weather forecasts up to two weeks ahead. In the TIGGE project, the more than ten International Institutes are contributing their global numerical weather prediction model ensemble outputs daily initial condition at 00Z, and 12Z (and/or 06Z and 18Z) forecasts lead time upto ≥ 240 hours at 6 hourly intervals, and at various horizontal grid resolutions. The Bureau of Meteorology, Australia (BoM), Environment and Climate Change Canada (ECCC), European Centre for Medium-Range Weather Forecasts (ECMWF), India Meteorological Department (IMD), Japan Meteorological Agency (JMA), Korea Meteorological Administration (KMA), Met Office - UK (UKMO), and National Centers for Environmental Prediction, USA (NCEP), and National Centre for Medium Range Weather Forecasting (NCMRWF) are nine International Institutes model outputs (contributing to the TIGGE) are chosen based on availability at the ECMWF-TIGGE web data portal https://apps.ecmwf.int/datasets/data/tigge/levtype=sfc/type=cf/ as on December 2021. All these model outputs are being released to the public in the ECMWF web domain under open data license - creative commons 4.0, for free of cost but at 2-3 days lag access. These 2-3 days lag time is taken in account of data acquisition from different Institutes to a central place at ECMWF data web portal.

9.3. Wind speed probabilities

Mohapatra (2021) briefed the standard operating procedures (SOP) of the cyclonic warning in India, as follows that a "Cyclonic Storm or a Cyclone is an intense vortex or a whirl in the atmosphere with very strong winds circulating around it in anti-clockwise direction in the Northern Hemisphere and in clockwise direction in the Southern Hemisphere. The word Cyclone is derived from the Greek word Cyclos meaning the coil of a snake. To Henri Piddington, the tropical storms in the Bay of Bengal and in the Arabian Sea appeared like the coiled serpents of the Sea and he named these storms as 'Cyclones'. Tropical cyclones are also referred to as 'Hurricanes' over Atlantic Ocean, 'Typhoons' over Pacific Ocean, 'Willy-Willies' over Australian Seas and simply as 'Cyclones' over north Indian Ocean (NIO)". The following 8 categories defined the name of cyclone categories along with its associated surface wind speed.

1. Low Pressure Area Not exceeding 17 knots (<31 kmph)
2. Depression 17 to 27 knots (31-49 kmph)
3. Deep Depression 28 to 33 Knots (50-61 kmph)
4. Cyclonic Storm 34 to 47 Knots (62-88 kmph)
5. Severe Cyclonic Storm 48 to 63 Knots (89-117 kmph)
6. Very Severe Cyclonic Storm 64 to 90 Knots (118-167 kmph)
7. Extremely Severe Cyclonic Storm 91 to119 Knots (168-221 kmph)
8. Super Cyclonic Storm 120 Knots and above (≥222 kmph)

The Numerical Weather Prediction (NWP) division of the India Meteorological Department (IMD) runs the IMDGFS and IMDGEFS (20+1 members) global weather prediction models at 0.12°x0.12° horizontal resolution, operationally. The National Centre for Medium Range Weather Forecasting (NCMRWF) runs the NCUM and NEPS (22+1 members) global weather prediction models at 0.12°x0.18° horizontal resolution, operationally. The Wind speed is one of the major parameters to identify the intensity of the cyclonic circulation. The IMD-NWP division developed and implemented to monitor the surface (10meter height) wind speed probabilities exceeding particular 4 different thresholds which can explain the intensity of the cyclonic circulations using IMDGEFS (21 members) and NEPS (23 members) ensemble models. The four operational wind speed thresholds are ≥ 28 knots (14.4 m/s), ≥ 34 knots (17.5 m/s), ≥ 50 knots (25.7 m/s), ≥ 64 knots (32.9 m/s) and its associated categories are such as Deep Depression, Cyclonic Storm, Severe Cyclonic Storm, and Very Severe Cyclonic Storm, respectively. This wind speed forecast probabilities monitor figures are produced at every 6 hourly intervals up to 240 hours. The screenshots of operationalized wind speed probabilities plots using IMDGEFS and NEPS of the IMD-NWP website are shown in screenshot figure 9.3.1.

Operational Web Link : Go to https://nwp.imd.gov.in -> MEDIUM RANGE FORECASTS -> GEFS (T-1534) -> WIND SPEED PROBABILITIES

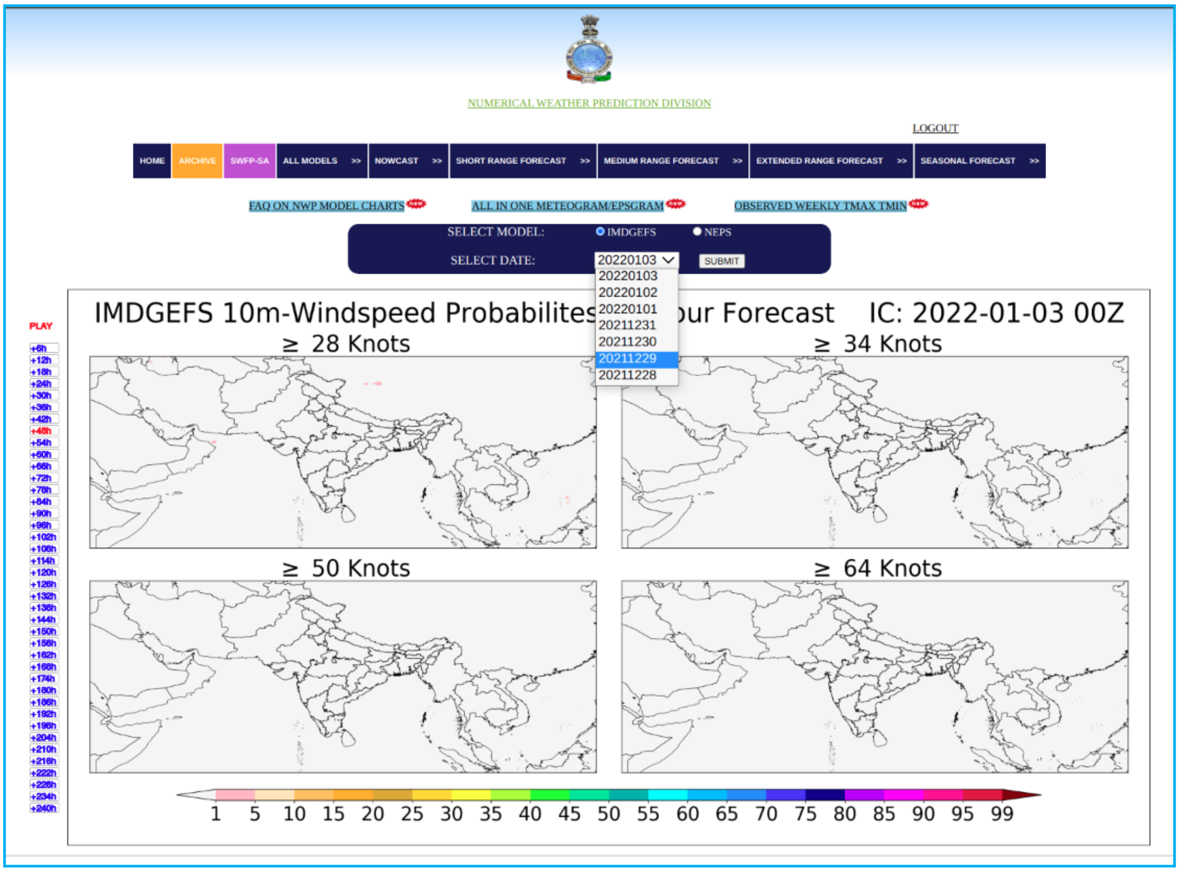

Fig. 9.3.1. Screenshot of wind speed probability product at IMD-NWP website, also shown the user select date (i.e., initial condition date) and also shown that left side of figure contains 6-hourly forecast hours where user can mouse overlay on any forecast lead hours (numbers) to view that particular forecast hour's wind speed probabilities plot. Also, users can click on the play button which will start to animate continuously from 6 to 240 hours forecasts

A cyclonic storm occurred during 2021-12-02 to 2021-12-04 and is named as 'JAWAD'. Figures 9.3.2 to 9.3.6 show the different forecast lead time of wind-speed probabilities using IMDGEFS model outputs, based on initial condition as on 2021-11-30-00Z, which tells that four different wind-speed thresholds from 24 to 120 hours forecast lead time. The 72-hour forecast of IMDGEFS (figure 9.3.4) shows that the chances of occurrence (maximum probabilities) of the Deep Depression, Cyclonic Storm, Severe Cyclonic Storm, and Very Severe Cyclonic Storm are greater than 95%, 90%, 45%, 35% respectively over the Bay of Bengal. Similarly, figures 9.3.7 to 9.3.11 are showing results of NEPS model outputs. The 72-hour forecast of NEPS (figure 9.3.9) shows that the maximum probabilities of the Deep Depression, Cyclonic Storm, are greater than 50%, 15% respectively, and there is no significant probability of the Severe Cyclonic Storm, and Very Severe Cyclonic Storm. This wind speed probabilities of both the IMDGEFS and NEPS model outputs are being generated operationally at every day. In upcoming days, the NWP division planned to extend this work for making dynamic zoomed in areas throughout the north Indian Ocean and entire tropical ocean regions by adding multi global ensemble models. Also, this wind speed probabilities monitor is a quick glance of cyclonic circulation. The actual tropical cyclonic circulation tracker using multi model forecast outputs has been implemented and it's more details can be seen at section 9.4 for the same duration.

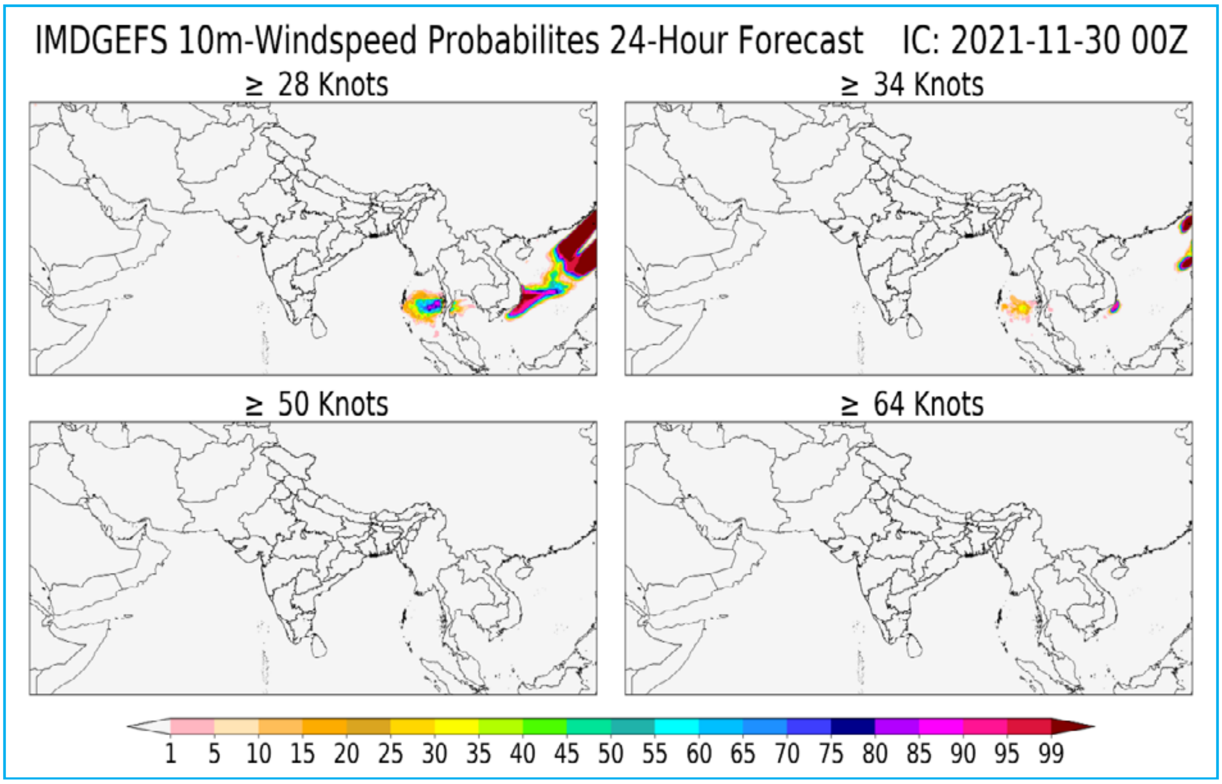

Fig. 9.3.2. 10-meter wind speed probability at threshold ≥ 28 Knots, ≥ 34 Knots, ≥ 50 Knots, and ≥ 64 Knots using IMDGEFS (20 ensemble members + 1 Control run) based on initial condition as on 2021-11-30-00Z valid for 24th hour forecast

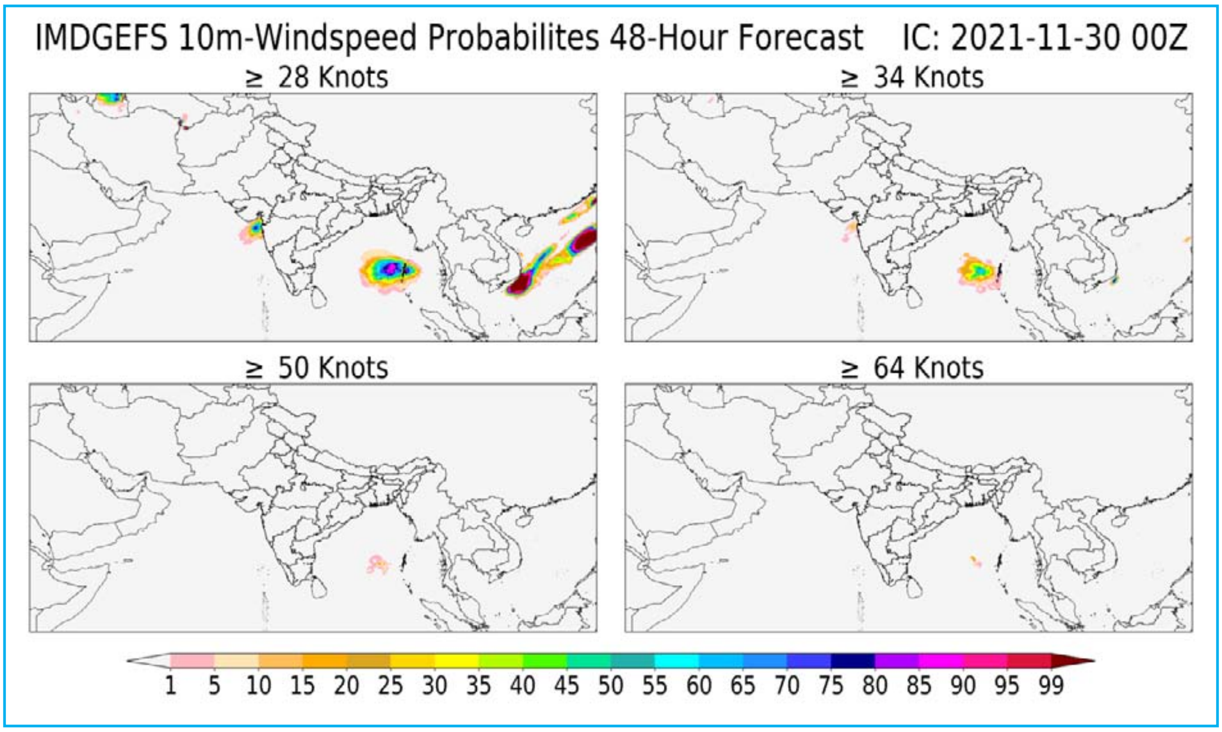

Fig. 9.3.3. Same as figure 9.3.2 but valid for 48th hour forecast

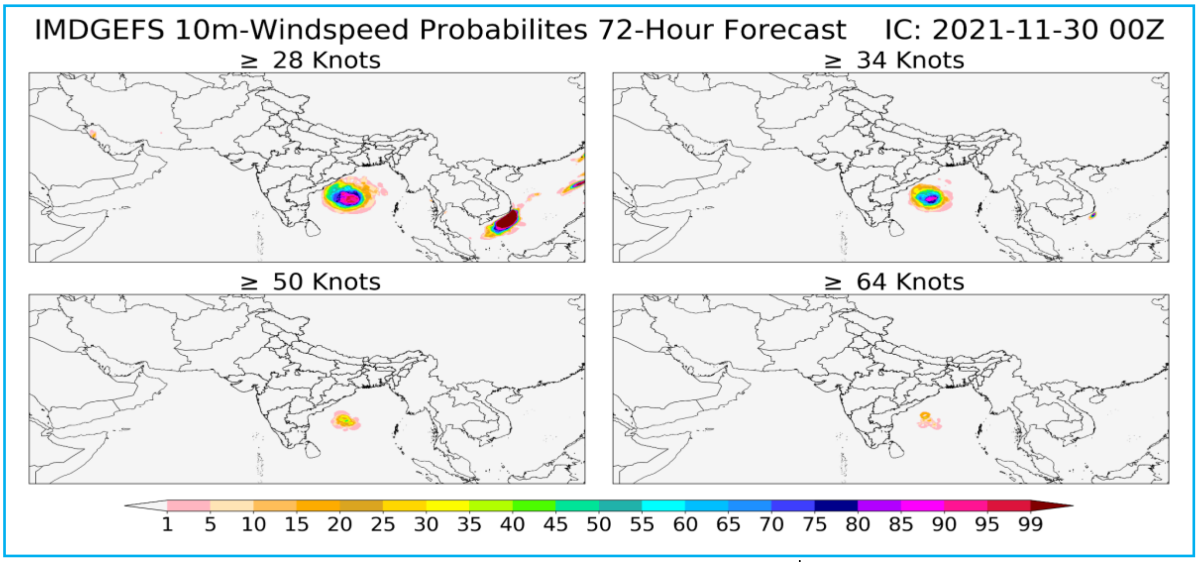

Fig. 9.3.4. Same as figure 9.3.2 but valid for 72nd hour forecast

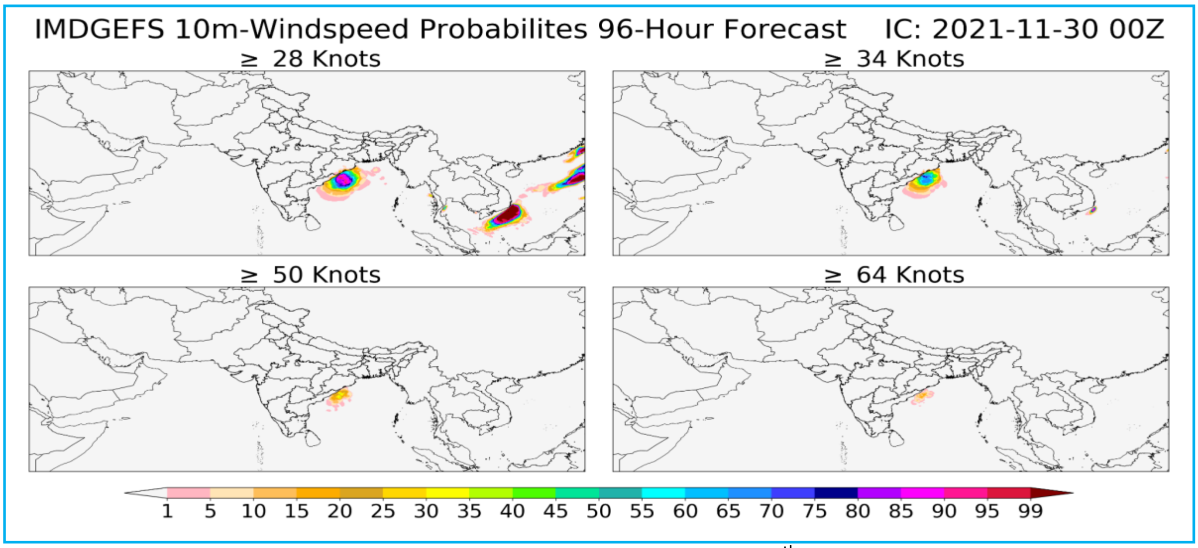

Fig. 9.3.5. Same as figure 9.3.2 but valid for 96th hour forecast

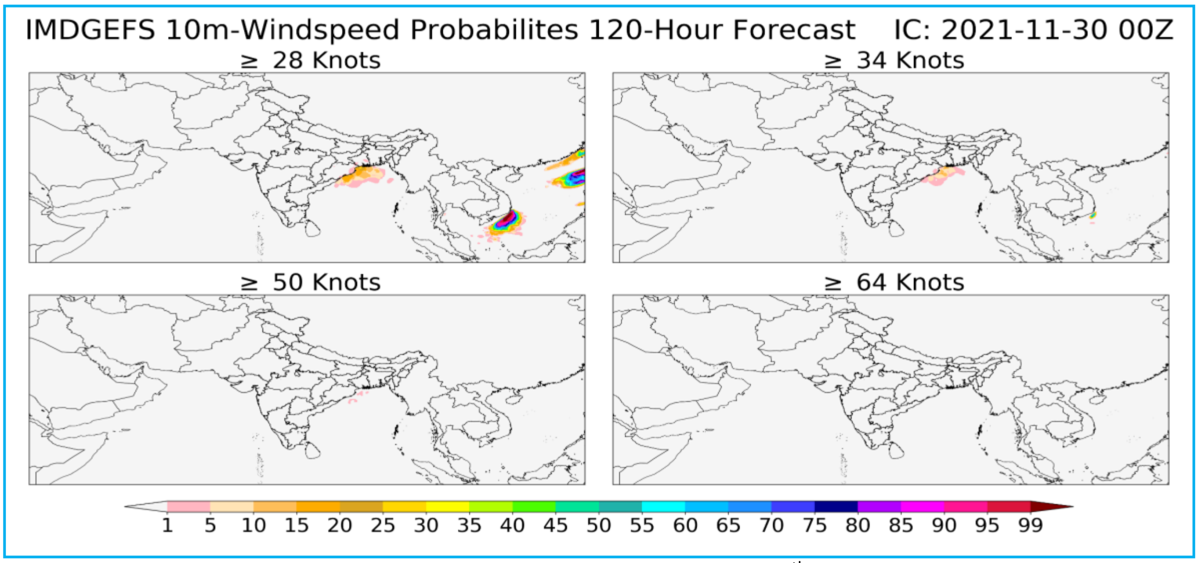

Fig. 9.3.6. Same as figure 9.3.2 but valid for 120th hour forecast

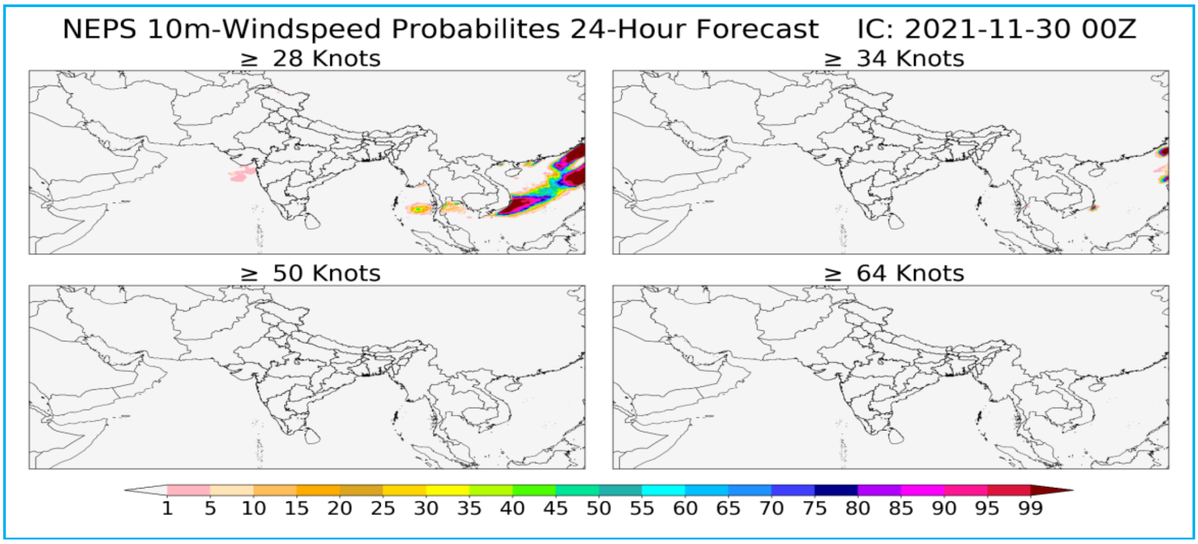

Fig. 9.3.7. 10-meter wind speed probability at threshold ≥ 28 Knots, ≥ 34 Knots, ≥ 50 Knots, and ≥ 64 Knots using NEFS (22 ensemble members + 1 Control run) based on initial condition as on 2021-11-30-00Z valid for 24th hour forecast

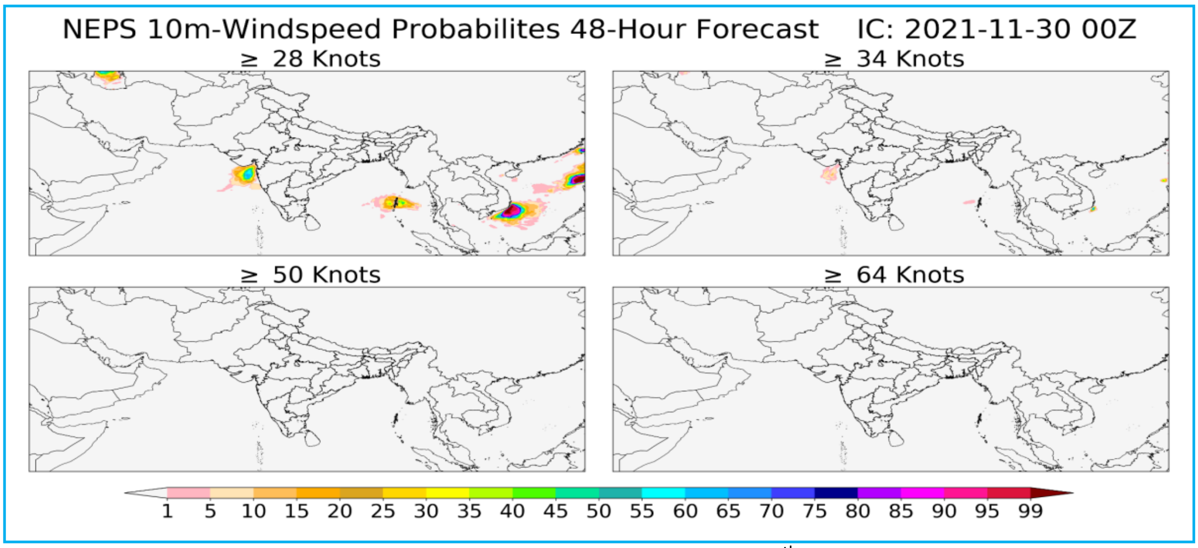

Fig. 9.3.8. Same as figure 9.3.7 but valid for 48th hour forecast

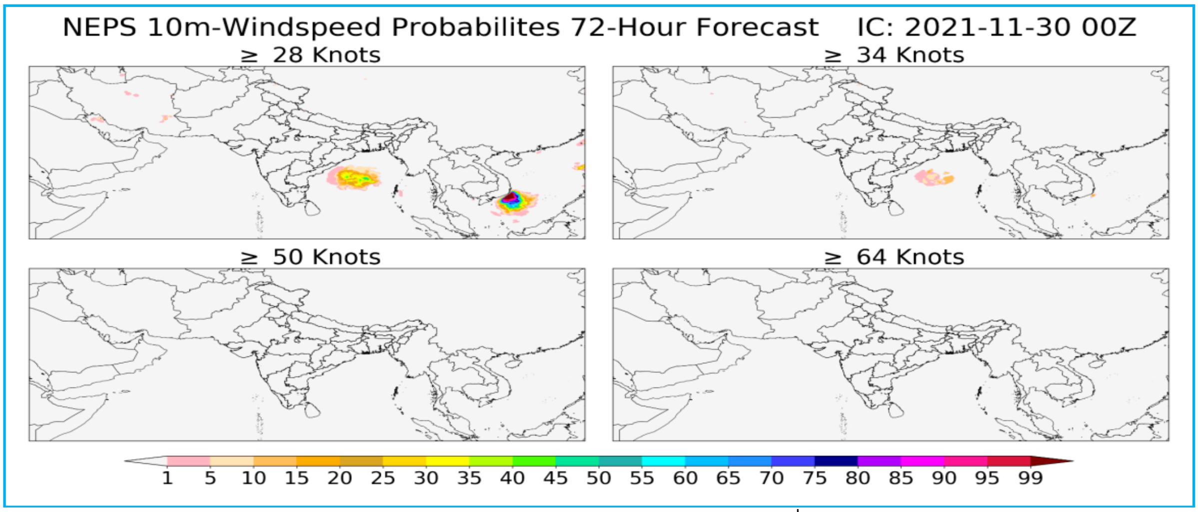

Fig. 9.3.9. Same as figure 9.3.7 but valid for 72nd hour forecast

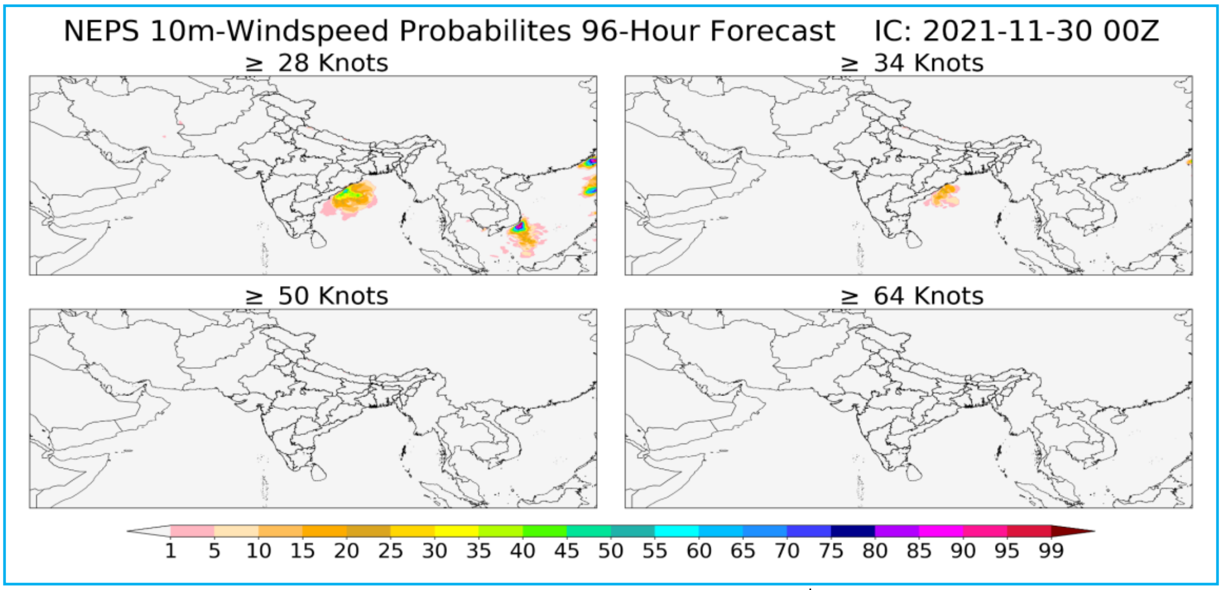

Fig. 9.3.10. Same as figure 9.3.7 but valid for 96th hour forecast

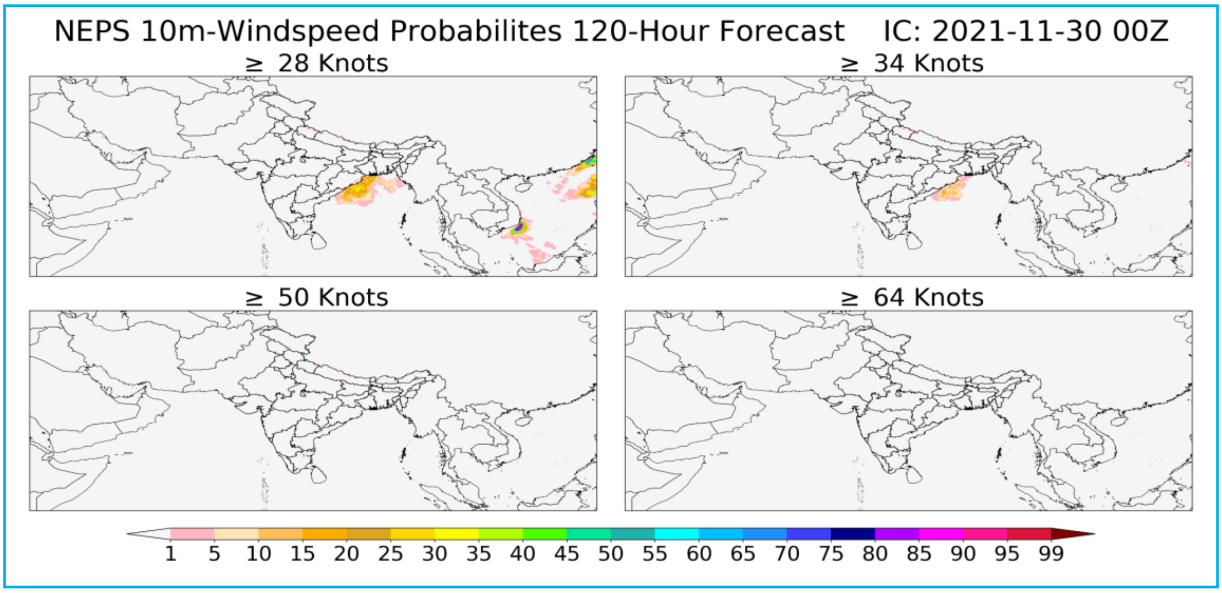

Fig. 9.3.11. Same as figure 9.3.7 but valid for 120th hour forecast

9.4. Multi model ensemble tropical cyclone tracker

ECMWF IFS TC Tracker: The European Centre for Medium-Range Weather Forecasts (ECMWF) developed the Integrated Forecasting System (IFS) model for the global numerical weather prediction at medium range timescale and also developed Tropical Cyclone tracker (TC-Tracker). Hereafter called as IFS-TC-Tracker in this section 2. For the Tropical Cyclones (TC), ECMWF uses the same tracker for all timescales based on Vitart *et al.* (1997) and van der Grijn *et al.* (2005), described in Vitart *et al.* (2012). The main three steps of ECMWF's TC tracker are illustrated in Figure 9.4.0. In Step 1, the warm-core TCs are identified using 6-hourly fields of vorticity, temperature, and mean sea level pressure (MSLP) fields at a low resolution (TL159, about 100 km). The use of low-resolution data is motivated by a reduction of the computing cost and the need to filter small-scale vorticity fields. Further details on the algorithm can be seen in the technical memo of ECMWF (2021).

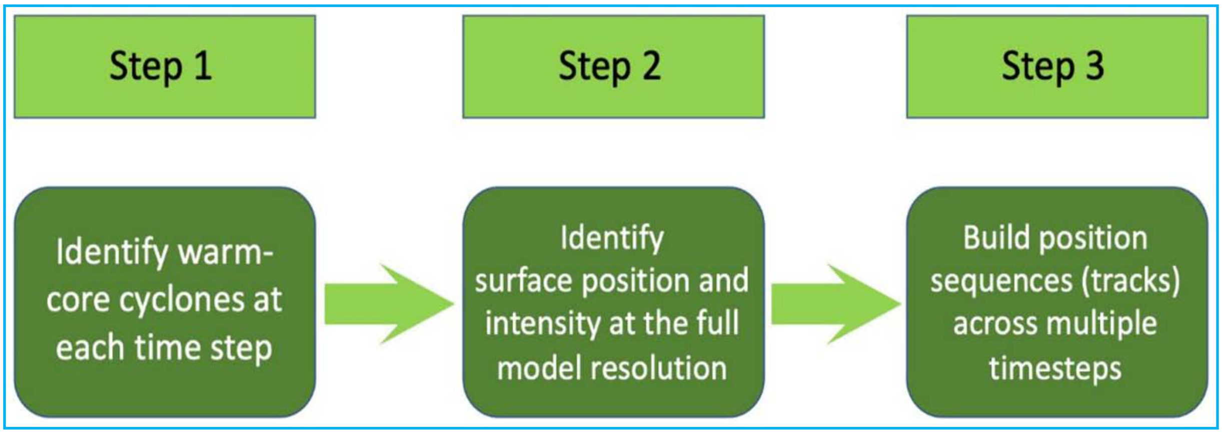

Fig. 9.4.0. The main three steps of the ECMWF IFS-TC- tracker. This schematic figure taken from ECMWF (2021) technical memo for the reference

The ECMWF IFS-TC-Tracker source code has been modified by the NWP division of IMD, to feed in multi-model global forecasts outputs and made the individual model TC-tracker lines plot along with multi-model-mean, displayed and described in sections 9.4.1 to 9.4.5. Using the TIGGE nine global model outputs (listed in section) are fed into the IFS-TC-Tracker to generate the tropical cyclone tracker and followed by multi-model-mean of TC-tracker. Based on availability of TIGGE model outputs on real-time access and on near-real-time access (on 2 days delayed lag mode), generated TC-Tracker plots are discussed in the section 9.4.1 and 9.4.2. In section 9.4.2, the multi model mean of Tc-Tracker, and followed by the verifications of Tc-Tracker both the visual, and statistical outputs are discussed.

9.4.1. *Real-time Multi Model Mean (5 models from TIGGE) of Tropical Cyclone Tracker using IFS-TC-Tracker*

As of December 2021, IMD has collaborated with other International numerical weather prediction Institutes such as ECMWF, NCEP, UKMO and NCMRWF to receive their global model forecast outputs in real-time upon mutual understanding. By using these 5 global model outputs including IMDGFS, the IFS-TC-Tracker outputs have been made over north Indian Ocean, operationally at NWP, IMD. All model outputs are being interpolated to T159 Gaussian Grid horizontal resolution before running the IFS-TC-Tracker. For the case study, the recent cyclonic storm named as 'JAWAD' during 2021-12-02-00Z to 2021-12-04-00Z over the Bay of Bengal (BoB) has been explored.

Figures 9.4.1.1 to 9.4.1.5 shows the Tropical Cyclone Tracker over BoB for the different initial conditions from 2021-11-30-00Z to 2021-12-04-00Z with 5 different global deterministic models and its multi-model mean (MMMean). Similarly, TC Tracker outputs based on 12Z initial conditions are also being prepared operationally but not shown in this report. These 5 models and MMMean TC Tracker outputs and plots are much helpful to the forecasters while making hard decisions such as intensity, landfall location, re-curvature, windspeed, etc., and declaring the same accordingly.

The NWP, IMD is planning to communicate with other TIGGE contributing modeling Institutes for getting their model outputs in real-time for increasing the ensemble size to compute the multi-model-mean which improves over the number of models and will give confidence/uncertainty by its standard deviation. Also working on making the weightage of all the TIGGE models by studying its performance for past case study events and the same weightage will be applied on real time during any future cyclonic storm event.

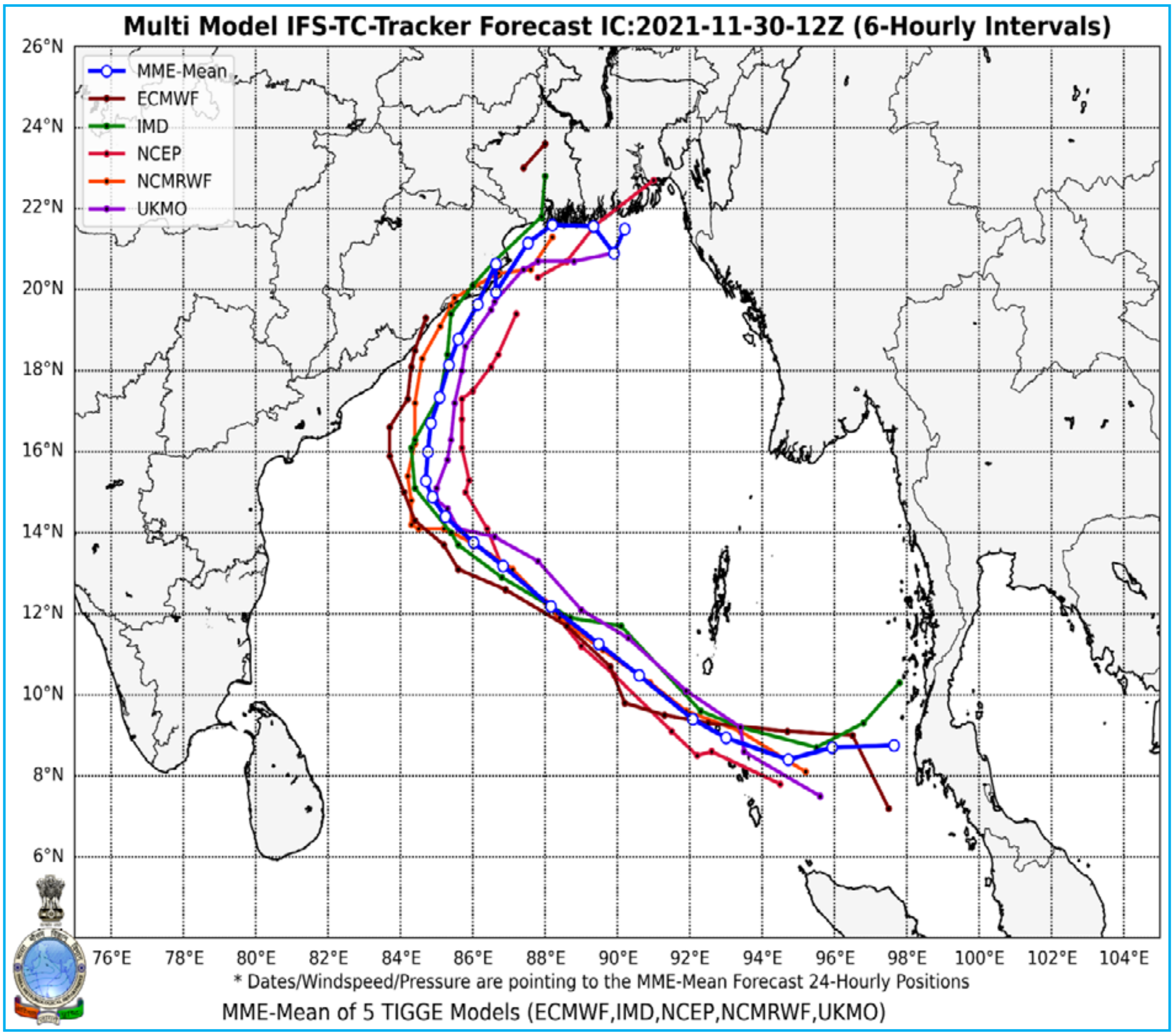

Fig. 9.4.1.1. Real-time production of tropical cyclone tracker outputs ('JAWAD' cyclone storm) using ECMWF's IFS-TC-Tracker based on initial condition as on 2021-11-30-12Z by feeding-in the five global deterministic model outputs which are produced by the WMO International Institutes namely ECMWF, IMD, NCEP, NCMRWF and UKMO. The Multi Model Mean is shown in dark blue line and it is produced by the mean track from the above listed 5 model tracker outputs, which are shown in different line colours mentioned in the legend. The TC tracker outputs are at 6-hourly intervals which are marked in black colour dots over individual model-coloured lines and white colour hollow circles over the MMMean blue line. The number of different models used to compute the Multi Model Mean cyclone track details are mentioned in the bottom of figure

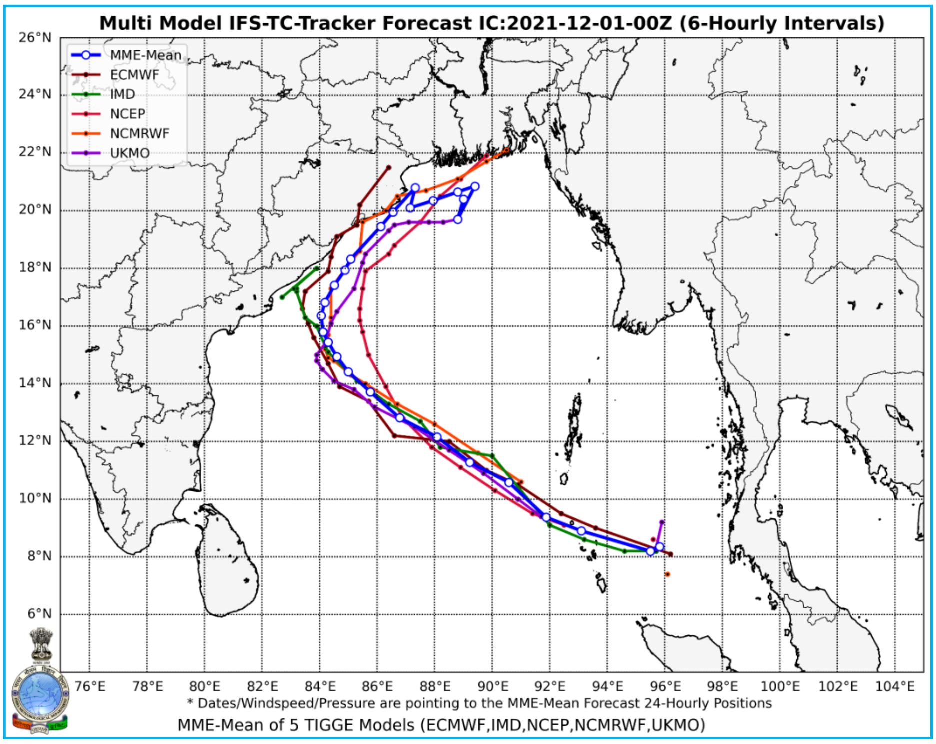

Fig. 9.4.1.2. Same as figure 9.4.1.1 but for initial conditions as on 2021-12-01-00Z

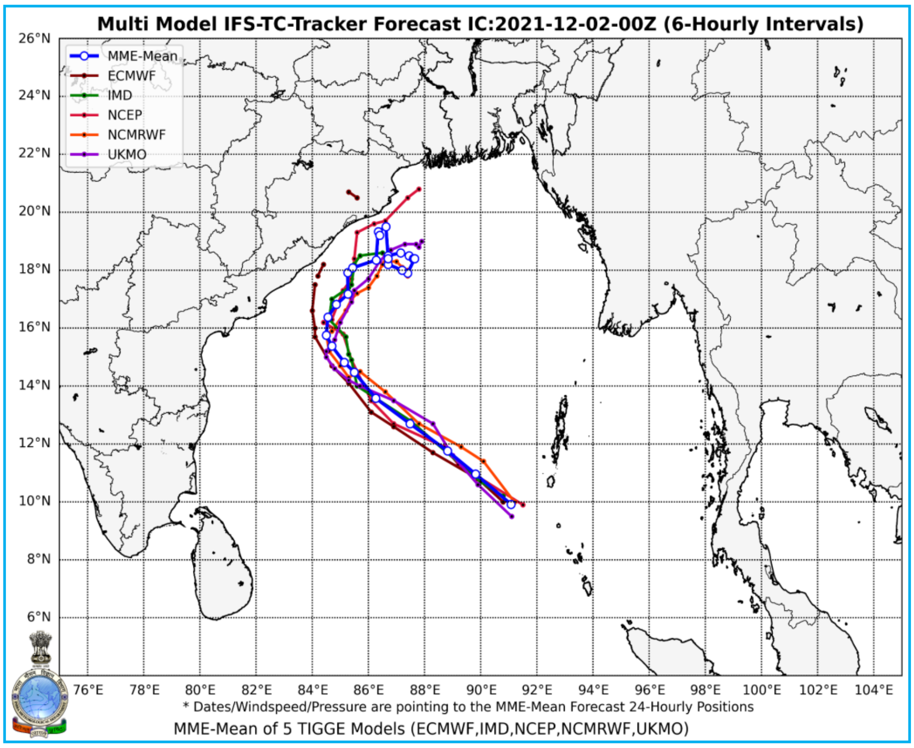

Fig. 9.4.1.3. Same as figure 9.4.1.1 but for initial conditions as on 2021-12-02-00Z

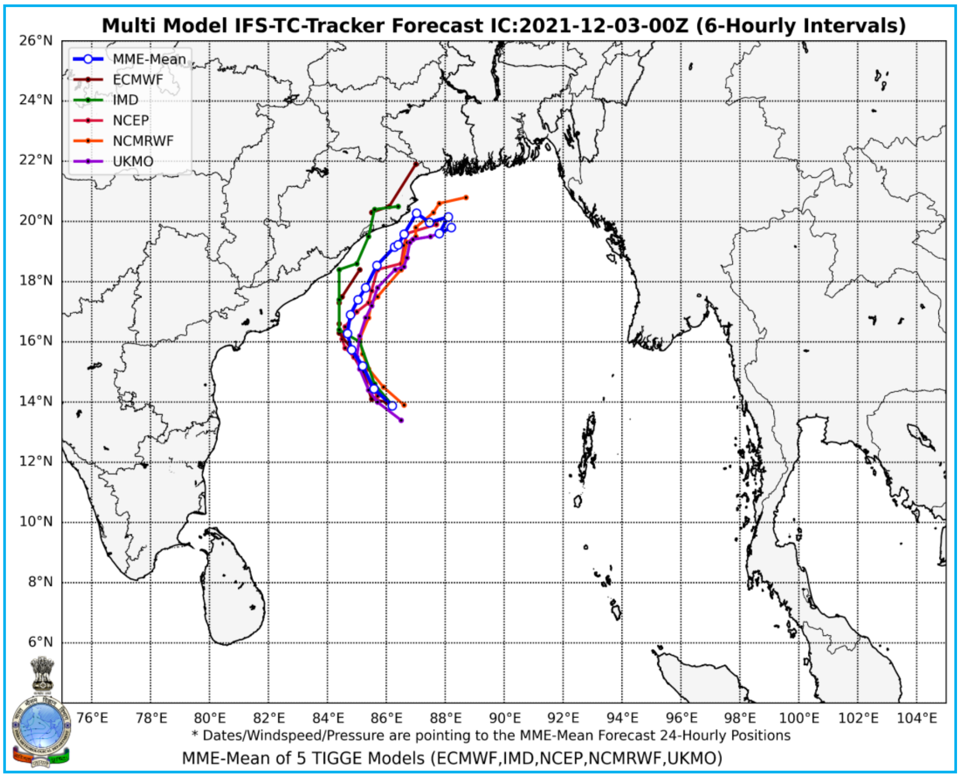

Fig. 9.4.1.4. Same as figure 9.4.1.1 but for initial conditions as on 2021-12-03-00Z

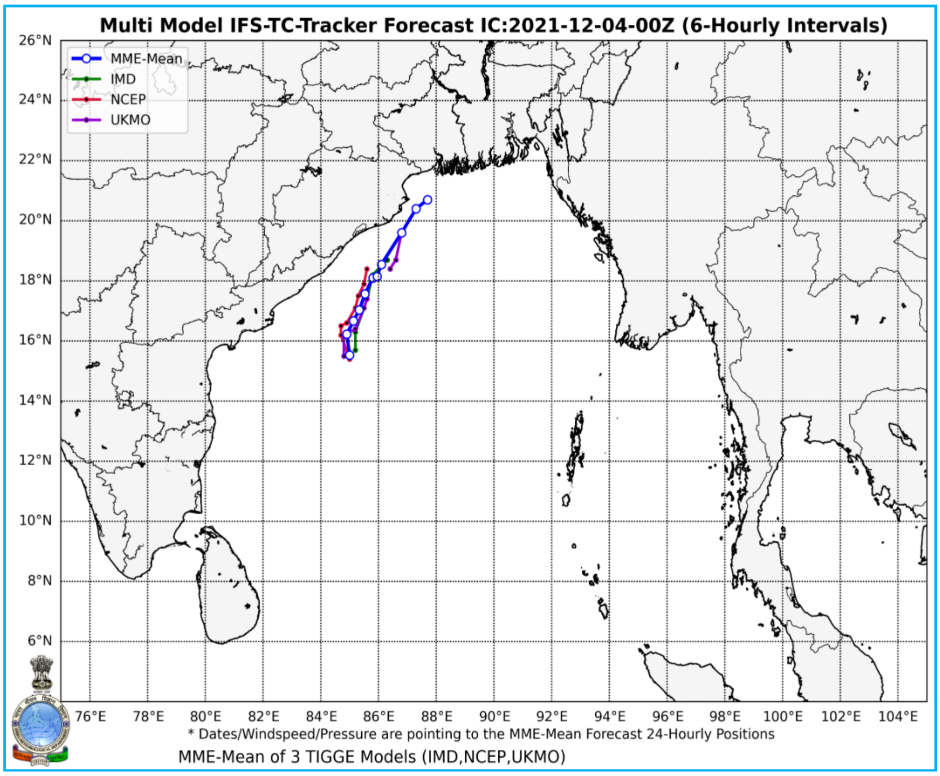

Fig. 9.4.1.5. Same as figure 9.4.1.1 but for initial conditions as on 2021-12-04-00Z

9.4.2. *Near Real-time (2-days lag) Multi Model Mean (9 models from TIGGE) of Tropical Cyclone Tracker using IFS-TC-Tracker and verification*

As of December 2021, IMD has collaborated with WMO-TIGGE project since July 2020 onwards and is able to download the numerical weather prediction model outputs of the nine International Institutes such as BOM, ECCC, ECMWF, JMA, KMA, NCEP, NCMRWF and UKMO. There are 9 global deterministic models (including IMDGFS) outputs are made available at 2 days lag time and fed into the IFS-TC-Tracker. All model outputs are being interpolated to T159 Gaussian Grid horizontal resolution before running the IFS-TC-Tracker. By using these 9 global model outputs including IMDGFS, the IFS-TC-Tracker outputs have been made over north Indian Ocean, operationally at NWP, IMD.

For the case study, the recent cyclonic storm named as 'JAWAD' during 2021-12-02-00Z to 2021-12-04-00Z over the Bay of Bengal (BoB) has been explored. In figure 9.4.2.1, shows the Tropical Cyclone Tracker over BoB for the different initial conditions from 2021-11-30-12Z (similar to figure 9.4.1.1) with 9 different global deterministic models and its multi-model mean (MMMean). The multi model mean is the simplest average from different model outputs, it gives the average forecast from all models. This simple average gives good confidence in the mean state of the forecasts. In figures 9.4.2.2 shown the multi-model-mean forecast alone which mean is computed from average of 9 different global deterministic TC-tracker outputs, along with its values of date-time, position such as latitude, longitude, windspeed (knots), lowest mean sea level pressure (hPa) in table format (right side of the figure), which is much useful to the forecaster to read clearly and finer visible out of crowded lines. Figures 9.4.2.1 showed the visual verification of all 9 global model TC-Tracker outputs and its multi model mean at different initial conditions by plotting against the observed best track.

Similarly, the TC Tracker outputs based on 00Z and 12Z with different initial conditions are also being prepared operationally but not shown in this report. These 9 models and MMMean TC Tracker outputs and plots are much helpful to the forecasters while making hard decisions such as intensity, landfall location, recurvature, windspeed, etc., and declaring the same accordingly. The NWP, IMD is planning to extend the operational forecast area over the entire tropical oceanic region by utilizing the TIGGE models, which will be beneficiary to the WMO-tropical working countries. The statistical verification cannot be done in near real-time at least during any ongoing cyclonic storm events. But the visual (Eyeball) verification can be done in near real time during the ongoing cyclonic storm event itself, which supports the forecasters to make decisions on to omit any particular model's forecasts (track, landfall, intensity, etc.,), which is shown in figure 9.4.2.1. The statistical verification of cyclonic storm 'JAWAD' using 9 different models and multi-model mean outputs fed into the IFS-TC-Tracker at different forecast lead times (upto 132 hours by 6 hourly intervals). In figure 9.4.2.3 shows the distance position error (DPE) of the IFS-TC-Tracker outputs of the nine TIGGE models and MMMean, during different initial conditions from 2021-11-30-00Z and 2021-12-04-12Z at both 00 and 12 UTC, and upto 240 hours forecast lead time. Three models track errors are within 150 km for lead time upto 30 hours, 6 models track errors are within 200 km for lead time upto 120 hours. Both ECCC and JMA model errors are more than 200 km from 48-, 60-hours forecast lead time onwards, respectively. The IMD GFS model track error went beyond 200 km from 90-hours forecast lead time onwards. The Multi Model Mean Track error is consistently below 100 km, 150 km upto 72-, 132-hours forecast lead time, respectively. Figure 9.4.2.4 showed the same DPE but during the initial conditions from 2021-12-02-12Z to 2021-12-04-12Z at both 00 and 12 UTC, and upto 240 hours forecast lead time. Due to reduction of the number of samples of forecast lead hours in the figure 9.4.2.4, the overall DPE gets reduced compared to the figure 9.4.2.3. Notably, IMD GFS track error got reduced below 150 km upto 72-hours forecast lead time. Similarly, JMA track error has reduced below 250 km, except the ECCC.

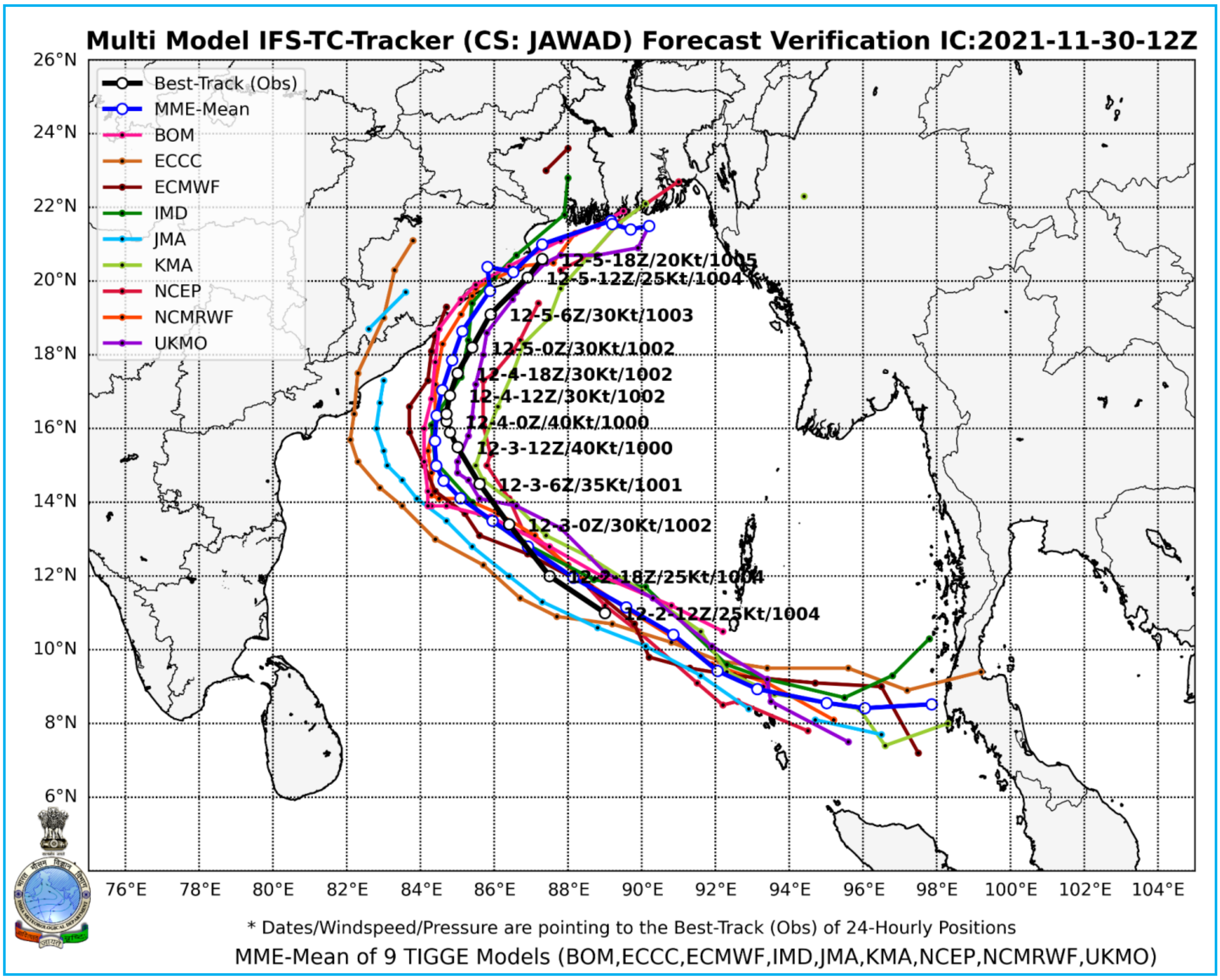

Fig. 9.4.2.1. Near Real-time production of tropical cyclone tracker outputs ('JAWAD' cyclone storm) using ECMWF's IFS-TC-Tracker based on initial condition as on 2021-11-30-12Z by feeding-in the nine global deterministic model outputs which are produced by the WMO International Institutes namely BOM, ECCC, ECMWF, IMD, JMA, KMA, NCEP, NCMRWF and UKMO. The Multi Model Mean is shown in dark blue line and it is produced by the mean track from the above listed 9 model tracker outputs, which are shown in different line colours mentioned in the legend. The TC tracker outputs are at 6-hourly intervals which are marked in black colour dots over individual model-coloured lines and white colour hollow circles over the MMMean blue line. The verification is plotted with the observed best track marked in black coloured line. The values of 'JAWAD' cyclone storm track date-time/windspeed/mslp are marked at every 24-hourly of observed best track positions

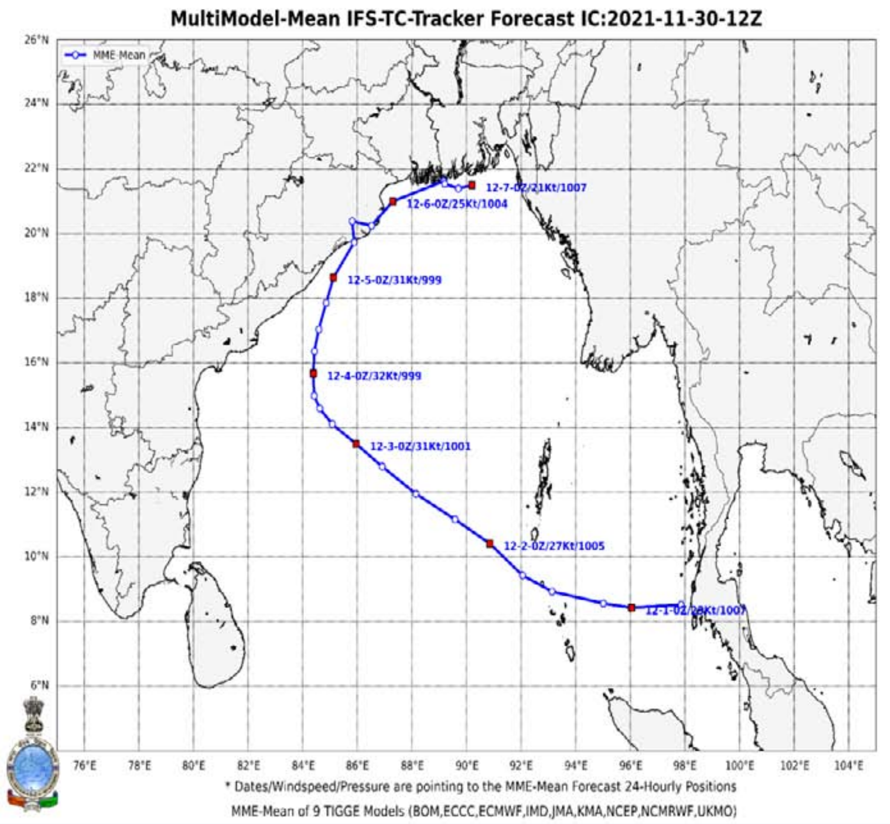

MME-MEAN

DATE	LAT	LON	WS (Kt)	MSLP (hPa)
2021-11-30-18Z	8.52	97.86	22.0	1007.6
2021-12-01-00Z	8.42	96.05	24.67	1006.67
2021-12-01-06Z	8.56	95.01	26.29	1005.86
2021-12-01-12Z	8.93	93.13	25.56	1005.33
2021-12-01-18Z	9.43	92.05	25.88	1006.0
2021-12-02-00Z	10.41	90.86	26.89	1005.0
2021-12-02-06Z	11.16	89.58	27.44	1005.11
2021-12-02-12Z	11.96	88.14	27.44	1003.22
2021-12-02-18Z	12.8	86.91	29.33	1003.44
2021-12-03-00Z	13.5	85.96	31.44	1000.89
2021-12-03-06Z	14.11	85.08	31.33	1000.56
2021-12-03-12Z	14.59	84.62	31.78	999.33
2021-12-03-18Z	14.99	84.42	31.56	1000.33
2021-12-04-00Z	15.67	84.39	32.22	998.67
2021-12-04-06Z	16.36	84.43	34.22	998.78
2021-12-04-12Z	17.04	84.59	33.56	997.56
2021-12-04-18Z	17.86	84.86	33.56	999.44
2021-12-05-00Z	18.64	85.13	30.78	999.33
2021-12-05-06Z	19.74	85.89	30.88	1001.12
2021-12-05-12Z	20.39	85.81	25.71	1002.43
2021-12-05-18Z	20.25	86.52	25.17	1003.83
2021-12-06-00Z	21.0	87.3	25.2	1004.0
2021-12-06-06Z	21.63	89.17	23.33	1006.0
2021-12-06-12Z	21.55	89.2	25.5	1005.0
2021-12-06-18Z	21.4	89.7	23.5	1006.0
2021-12-07-00Z	21.5	90.2	21.0	1007.0

Windspeed >= 34 Knots are marked in red color

Fig. 9.4.2.2. The Multi Model Mean alone showed in this figure, which is the same as in figure 9.4.2.1 based on initial condition as on 2021-11-30-12Z. Every 24-hour interval is marked in red filled square boxes and every 06Z, 12Z and 18Z are marked in white hollow circles. In the right side of the figure, the table contains values of cyclone positions as latitude and longitude, windspeed (knots), and low sea level pressure (hPa) for every 6 hours. The 9 TIGGE models MMMean of TC Tracker date-time/wind-speed/ mslp values are marked at every 24-hour interval next to red filled squares

This section 9.4.2 describes the new product implemented by the NWP, IMD during December 2021 operationally and one cannot draw a solid conclusion based on a single TC case study. The NWP team is planning to study for many TC case studies from 2017-2021 over north India and followed by other tropical cyclogenesis regions. Also most importantly, TIGGE models are providing their ensemble members and which will be utilized to make uncertainty of individual model's TC track predictions and overall multi model grand ensemble members statistical confidence (cone of uncertainty). Also, by studying the tropical cyclone cases during past years (2017-2021) by using all available TIGGE model, will be able to identify the weightage of individual model and its ensemble mean, which can be applied to the real-time available of multi-model (5 model from TIGGE) tropical cyclone track outputs at NWP, IMD.

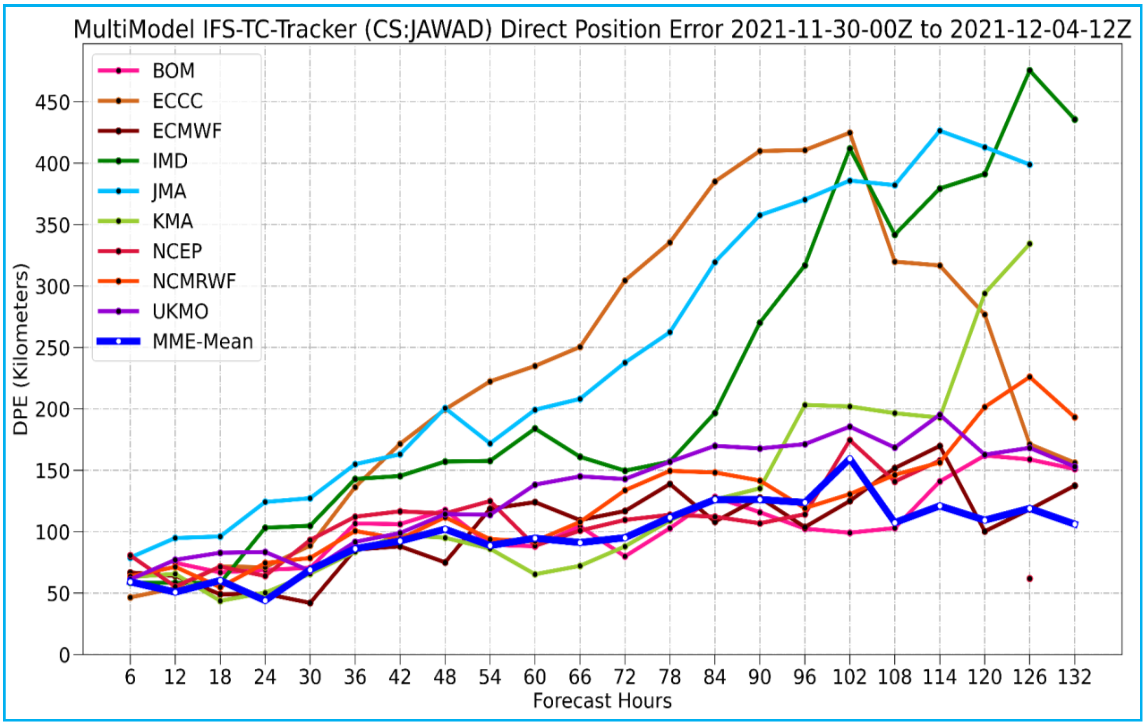

Fig. 9.4.2.3. Verification of JAWAD cyclone storm predicted by the ECMWF IFS-TC-Tracker using 9 TIGGE multi model outputs (shown in multiple-coloured lines) and MMMean (shown in thick blue line) during 2021-11-30-00Z to 2021-12-04-12Z. X-axis shows forecast lead hours and Y-axis shows Distance Position Error (DPE) in Kilometers

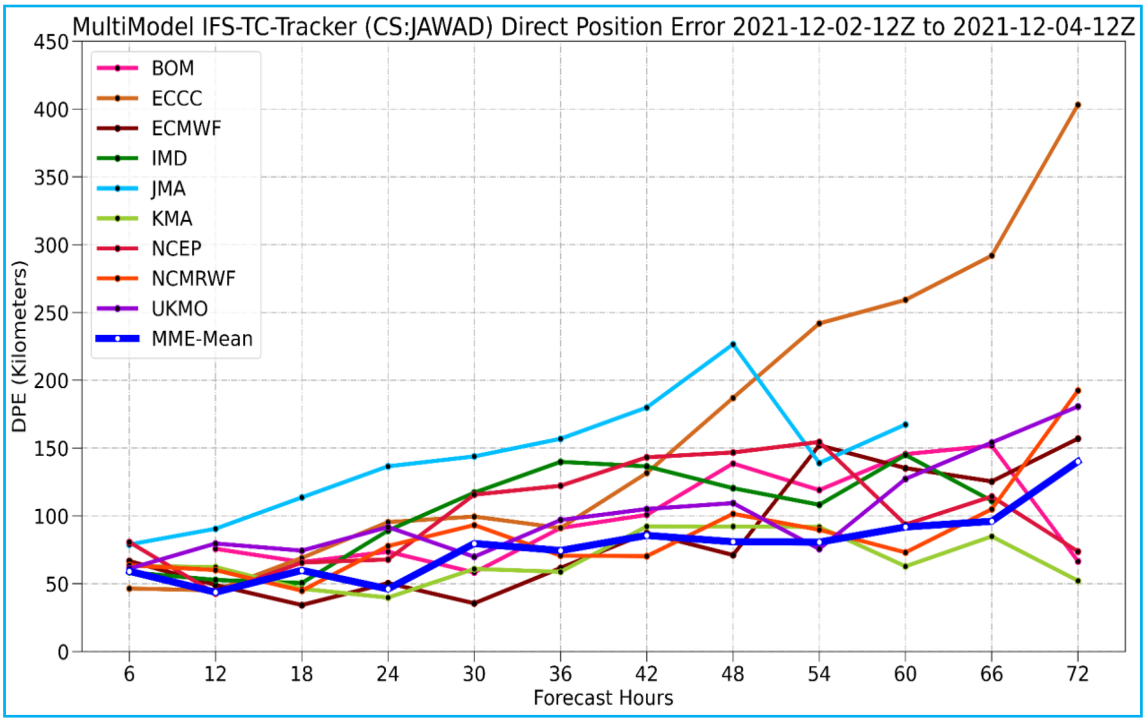

Fig. 9.4.2.4. Same as figure 9.4.2.4 but during 2021-12-02-12Z to 2021-12-04-12Z

9.5. Weather pattern forecasts

Neal. R *et al.*, 2020 has derived 30 different Indian weather patterns at climate time scale using 850-hPa winds from 1979-2016 using ERA5 reanalysis and IMD Observed rainfall pattern to match with the same 30 weather patterns. These 30 weather patterns are categorized into the following 7 types such as 'Monsoon Onset', 'Active Monsoon / Southwest Monsoon', 'Break Monsoon', 'pre/post Monsoon', 'Retreating Monsoon/Northeast Monsoon', 'Western Disturbances', and 'Winter Dry Period', which is much useful to the forecasters to identify the weather pattern and situation.

Neal. R *et al.*, (2020), developed a web interface to match a real-time numerical weather prediction ensemble model with predefined 30 Indian weather patterns, and tells the confidence (probability to occur) in terms of percentage for next 10 days forecast. Under WCSSP phase 4, Met. Office, UK has shared their source code for finding and matching the current weather into the predefined 30 Indian Climate Weather Pattern, and NWP, IMD has customized it for using IMD-GEFS ensemble model. Ensemble members are objectively assigned to their closest matching weather pattern definition, using a set of 30 predefined weather patterns (Figure 9.5.1). In Figure 4.2 shown, the weather pattern monthly and annual historical frequency occurrences of IMDAA regional reanalysis over Indian Region (1979 to 2020) for different 30 predefined weather patterns as shown in figure 9.5.1. The assignment is achieved by finding the ensemble member and weather pattern pairing with the smallest area-weighted sum of squared differences between their corresponding *u*- and *v*-component winds at 850-hPa – this metric is commonly referred to as "distance". The set of tables are being prepared operationally at both 00Z and 12Z using IMDGEFS ensemble model. Figures from 9.5.3 to 9.5.7 are shown screenshots of web interface tables produced as on 2021-10-27-00Z. Also, similar figures are being prepared daily, operationally at NWP, IMD.

Weather Pattern Forecast Probabilities : The forecast probabilities (as shown in the table Figure 9.5.3) are then based on the total number of ensemble members assigned to each weather pattern. Click on the "Pattern" links in the first column to view weather pattern definition wind fields at 850-hPa as well as their rainfall climatology. One can click on the "Historical frequency occurrences" (shown in Figure 9.5.2) links in the last three columns to view a full breakdown for all months in the year. Table cells are colour-coded according to their probability to assist with identifying the most likely weather pattern transitions.

Cumulative Probabilities for each Weather Pattern Category : The probabilities are aggregated for weather patterns with the same descriptions in the table (Figure 9.5.4). For example, probabilities for all weather patterns described as "active monsoon" will be aggregated. This helps identify transitions in the large-scale circulation and is especially useful when there is a lot of ensembles spread across the set of 30 weather patterns.

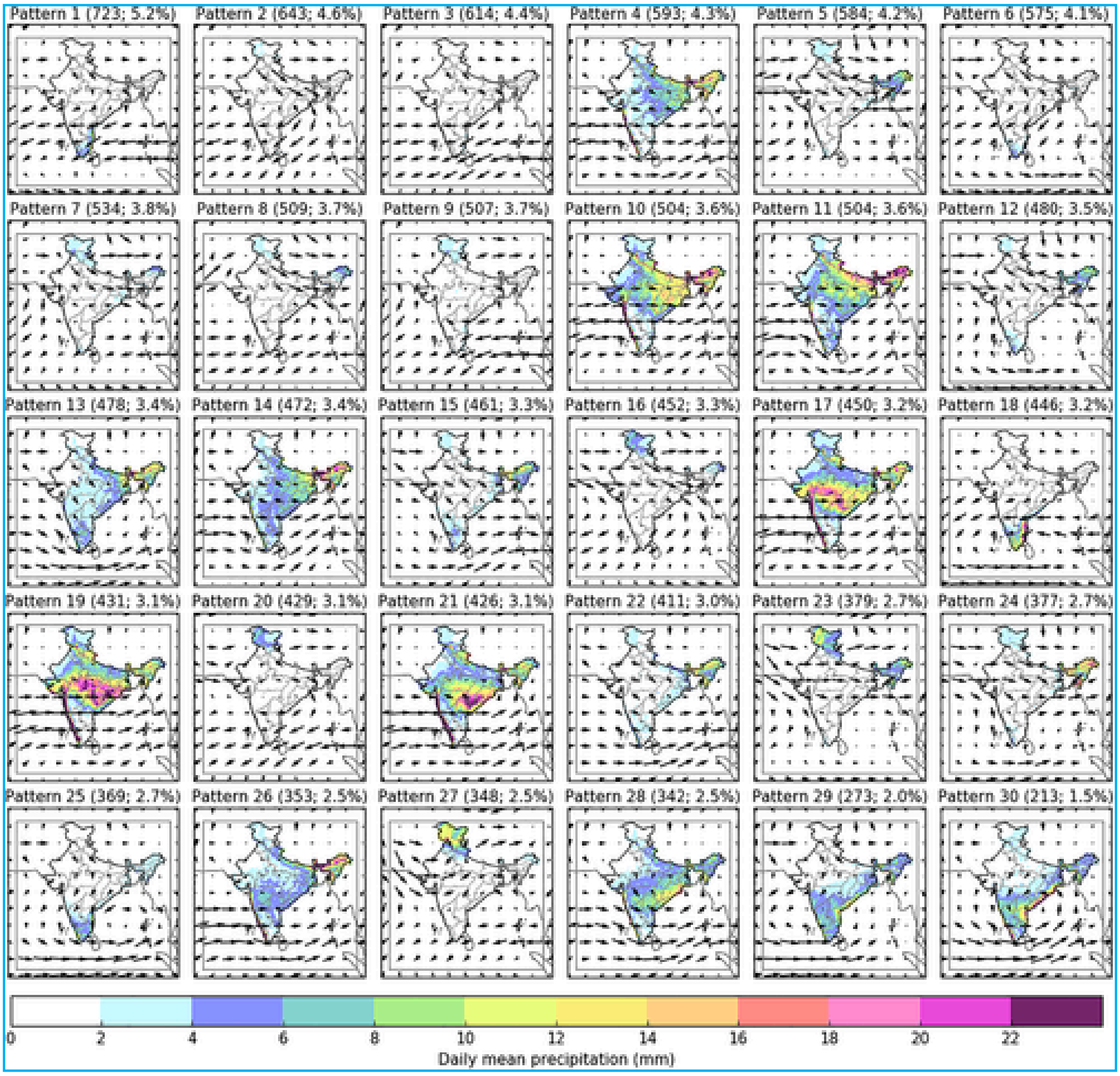

Fig. 9.5.1. Weather pattern definition maps for the preferred set of weather patterns. Arrows represent wind speed and direction at 850-hPa from ERA-interim. Coloured contours show daily mean rainfall from IMD's 0.25° resolution gridded observation dataset–data is plotted at grid resolution with no neighborhood post-processing. The inner box shows the area used in the clustering. Numbers in brackets give the sample size followed by mean annual occurrence for each weather pattern. All data is valid for the period 1979 to 2016 (Figure4, from Neal R, 2020)

Circulation Trend Indicator Tables : Weather patterns have been classified according to their dominant circulation characteristics during four broad seasons: (1) summer monsoon, (2) summer to retreating monsoon - Figure 9.5.5, (3) winter dry period and (4) pre-monsoon to monsoon onset. Circulation trends indicator tables are shown in figure 9.5.5 for both the latest and most recent forecasts with daily validity times aligned. This allows for a rapid assessment of forecast consistency over consecutive model runs. In addition, these tables are useful for identifying key transitions in the large-scale circulation. Tables for seasons (1), (3), and (4) are not shown here.

	Jan	Feb	Mar	Apr	May	Jun	Jul	Aug	Sep	Oct	Nov	Dec	Pattern Category	Annual
Pattern 1	3.1%	1.2%	0.8%	0.2%	0.1%					8.4%	29.5%	20.9%	Retreating Monsoon	5.36%
Pattern 2	17.8%	11.0%	4.8%	0.5%						0.2%	2.8%	14.1%	Winter Dry Period	4.24%
Pattern 3	17.9%	10.0%	4.4%	0.4%						0.7%	5.4%	22.2%	Winter Dry Period	5.08%
Pattern 4					2.1%	19.9%	14.1%	13.0%	2.9%				Break Monsoon	4.35%
Pattern 5	0.1%	3.0%	13.7%	31.5%	5.8%				0.1%	0.2%			Western Disturbances	4.52%
Pattern 6	3.3%	0.8%	0.8%	1.2%	0.7%				1.0%	19.4%	23.8%	6.8%	Retreating Monsoon	4.82%
Pattern 7	9.9%	14.8%	11.5%	7.5%	0.5%				0.1%	0.7%	1.5%	3.9%	Winter Dry Period	4.15%
Pattern 8	3.9%	12.8%	19.8%	4.8%	0.1%					0.1%		0.5%	Winter Dry Period	3.45%
Pattern 9	21.5%	10.8%	3.7%	0.4%						0.8%	3.7%	12.6%	Winter Dry Period	4.44%
Pattern 10					0.1%	6.5%	12.3%	10.9%	1.0%				Break Monsoon	2.59%
Pattern 11					0.7%	4.4%	19.7%	14.4%	2.9%				Break Monsoon	3.56%
Pattern 12	0.2%	0.9%	6.1%	21.8%	12.7%	0.1%		0.2%	1.2%	1.2%	0.4%	0.2%	Pre/Post-Monsoon	3.76%
Pattern 13				1.6%	12.3%	4.8%	1.1%	3.0%	16.3%	4.8%	0.2%	0.1%	Pre/Post-Monsoon	3.68%
Pattern 14					1.7%	6.3%	2.6%	9.3%	12.8%	0.2%			Pre/Post-Monsoon	2.74%
Pattern 15			0.2%	1.3%	19.0%	3.2%		0.2%	9.1%	4.8%	0.6%	0.2%	Pre/Post-Monsoon	3.24%
Pattern 16	5.0%	9.4%	13.1%	2.0%	0.1%					0.1%	0.5%	0.9%	Winter Dry Period	2.56%
Pattern 17						4.9%	10.3%	11.8%	7.1%	0.3%			Active Monsoon	2.88%
Pattern 18	0.3%		0.1%	0.2%	0.6%				0.6%	11.0%	18.5%	8.4%	Retreating Monsoon	3.31%
Pattern 19						6.9%	18.4%	13.0%	0.5%				Active Monsoon	3.27%
Pattern 20	10.1%	11.3%	6.6%	1.7%	0.2%					0.1%	0.4%	3.4%	Winter Dry Period	2.76%
Pattern 21						9.7%	13.4%	14.1%	2.9%				Active Monsoon	3.37%
Pattern 22				0.2%	16.4%	7.1%	0.5%	1.2%	4.6%	1.5%		0.1%	Pre/Post-Monsoon	2.64%
Pattern 23	0.6%	2.9%	7.7%	9.8%	2.8%				0.2%	0.6%		0.2%	Western Disturbances	2.06%
Pattern 24		0.1%	0.8%	11.0%	13.6%	0.2%	0.1%		0.3%	0.1%		0.2%	Western Disturbances	2.19%
Pattern 25			0.1%	2.1%	2.1%				3.0%	18.0%	8.9%	2.5%	Retreating Monsoon	3.07%
Pattern 26					2.7%	21.3%	6.9%	3.8%	1.4%				Monsoon Onset	3.01%
Pattern 27	6.1%	11.0%	5.7%	1.8%	0.3%				0.2%	0.2%	0.1%	2.5%	Western Disturbances	2.27%
Pattern 28					2.0%	2.4%	0.6%	4.8%	21.2%	3.8%			Retreating Monsoon	2.89%
Pattern 29	0.2%		0.2%		1.6%	1.5%		0.2%	5.7%	12.2%	2.9%	0.3%	Retreating Monsoon	2.07%
Pattern 30					1.9%	0.8%		0.2%	5.0%	10.6%	1.0%	0.2%	Retreating Monsoon	1.64%

Fig. 9.5.2. Weather pattern monthly and annual historical frequency occurrences of IMDAA regional reanalysis over Indian Region (1979 to 2020)

Weather Regime Stacked Probabilities : In Figure 9.5.7 shown, the weather pattern probabilities are aggregated according to their common regime group and presented as stacked probabilities. Regime bars are colour-coded based on their dominant circulation characteristics. Here, orange indicates winter types, light blue indicates pre- and post-monsoon / monsoon onset types, dark blue indicates the main summer monsoon types (active / break) and green indicates the retreating monsoon type. Hatching is used to distinguish between sub-types within a given colour. The regime ordering always remains the same to allow for an easy comparison with forecasts from previous runs and from different models. These plots complement the circulation trend indicator tables by enabling a quick assessment of any large-scale circulation changes and can be compared with previous runs to interpret forecast consistency. Regime descriptions in the plot are for guidance only; please refer to the top-level weather pattern forecasts for more detail.

Forecast Confidence Index : In Figure 9.5.6 shown, the forecast confidence index plot allows for an objective assessment of ensemble spread across the set of 30 weather patterns, by comparing the forecast confidence index from the latest run to that from a number of historical runs (as defined in the plot title). A score of 0 means that all members are equally distributed across all weather patterns, whereas a score of 1 means that all members are assigned to the same weather pattern. Green shading highlights days where ensemble spread is less than normal and red shading highlights days where ensemble spread is more than normal. Note that the forecast confidence index is not a measure of forecast skill.

NWP IMD Operational Web Link :

https://nwp.imd.gov.in/gefs/wpf/imdgefs_all_forecasts_summary_30patterns_62W_98E_2S_37N_850hPaWind.html

	Wed 27 Oct	Thu 28 Oct	Fri 29 Oct	Sat 30 Oct	Sun 31 Oct	Mon 1 Nov	Tue 2 Nov	Wed 3 Nov	Thu 4 Nov	Fri 5 Nov	Pattern Category	Historical frequency occurrences (September)	Historical frequency occurrences (October)	Historical frequency occurrences (November)
Pattern 1			10%								Retreating Monsoon	0.0%	8.4%	29.5%
Pattern 2											Autumn Dry Period	0.0%	0.2%	2.8%
Pattern 3											Autumn Dry Period	0.0%	0.7%	5.4%
Pattern 4											Break Monsoon	2.9%	0.0%	0.0%
Pattern 5											Western Disturbances	0.1%	0.2%	0.0%
Pattern 6					5%				38%	33%	Retreating Monsoon	1.0%	19.4%	23.8%
Pattern 7											Autumn Dry Period	0.1%	0.7%	1.5%
Pattern 8											Autumn Dry Period	0.0%	0.1%	0.0%
Pattern 9											Autumn Dry Period	0.0%	0.8%	3.7%
Pattern 10											Active Monsoon	1.0%	0.0%	0.0%
Pattern 11											Break Monsoon	2.9%	0.0%	0.0%
Pattern 12											Post-Monsoon	1.2%	1.2%	0.4%
Pattern 13											Post-Monsoon	16.3%	4.8%	0.2%
Pattern 14											Pre/Post-Monsoon	12.8%	0.2%	0.0%
Pattern 15											Post-Monsoon	9.1%	4.8%	0.6%
Pattern 16											Autumn Dry Period	0.0%	0.1%	0.5%
Pattern 17											Active Monsoon	7.1%	0.3%	0.0%
Pattern 18	100%	100%	90%	100%	95%	95%	81%	57%	24%	10%	Retreating Monsoon	0.6%	11.0%	18.5%
Pattern 19											Active Monsoon	0.5%	0.0%	0.0%
Pattern 20											Autumn Dry Period	0.0%	0.1%	0.4%
Pattern 21											Active Monsoon	2.9%	0.0%	0.0%
Pattern 22											Post-Monsoon	4.6%	1.5%	0.0%
Pattern 23											Western Disturbances	0.2%	0.6%	0.0%
Pattern 24											Western Disturbances	0.3%	0.1%	0.0%
Pattern 25											Retreating Monsoon	3.0%	18.0%	8.9%
Pattern 26											Monsoon Onset	1.4%	0.0%	0.0%
Pattern 27											Western Disturbances	0.2%	0.2%	0.1%
Pattern 28											Retreating Monsoon	21.2%	3.8%	0.0%
Pattern 29						5%	19%	43%	38%	57%	Retreating Monsoon	5.7%	12.2%	2.9%
Pattern 30											Retreating Monsoon	5.0%	10.6%	1.0%

Fig. 9.5.3. Weather pattern forecast probabilities as on 2021-10-27-00Z

	Wed 27 Oct	Thu 28 Oct	Fri 29 Oct	Sat 30 Oct	Sun 31 Oct	Mon 1 Nov	Tue 2 Nov	Wed 3 Nov	Thu 4 Nov	Fri 5 Nov
Pre/Post-Monsoon										
Active Monsoon										
Western Disturbances										
Monsoon Onset										
Post-Monsoon										
Autumn Dry Period										
Break Monsoon										
Retreating Monsoon	100%	100%	100%	100%	100%	100%	100%	100%	100%	100%

Fig. 9.5.4. Cumulative probabilities for each weather pattern category

	Wed 27 Oct	Thu 28 Oct	Fri 29 Oct	Sat 30 Oct	Sun 31 Oct	Mon 1 Nov	Tue 2 Nov	Wed 3 Nov	Thu 4 Nov	Fri 5 Nov
Latest model run (27/00 UTC)	100%	100%	100%	100%	100%	100%	100%	100%	100%	100%
Previous model run (run -1)										
Previous model run (run -2)										
Previous model run (run -3)										
Previous model run (run -4)										
Previous model run (run -5)										
Previous model run (run -6)										
Previous model run (run -7)										
Previous model run (run -8)										
Previous model run (run -9)										

Weather patterns typically associated with **summer monsoon** tendencies over India are most likely
Weather patterns 12, 13, 15, 15 and 22 (pre/post summer monsoon); 26 (onset); 10, 17, 19 and 21 (active); 4 and 11 (break)

Weather patterns typically associated with **no summer or retreating monsoon** tendencies over India are most likely
Weather patterns not listed above and below

Weather patterns typically associated with **retreating monsoon** tendencies over India are most likely
Weather patterns 1, 6, 18, 25, 28, 29 and 30 (retreating)

Fig. 9.5.5. Circulation trend indicator table - Summer to retreating monsoon circulation trend

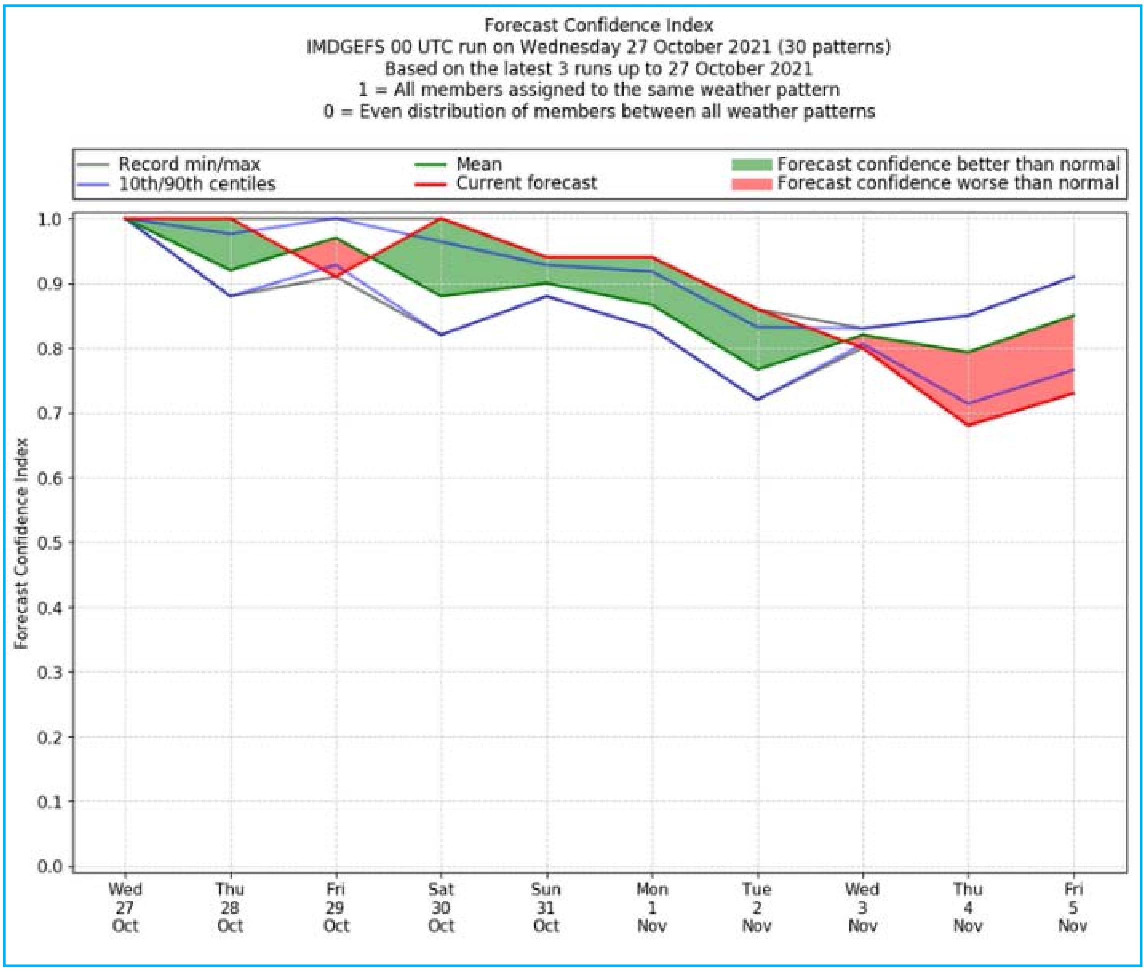

Fig. 9.5.6. Forecast Confidence Index

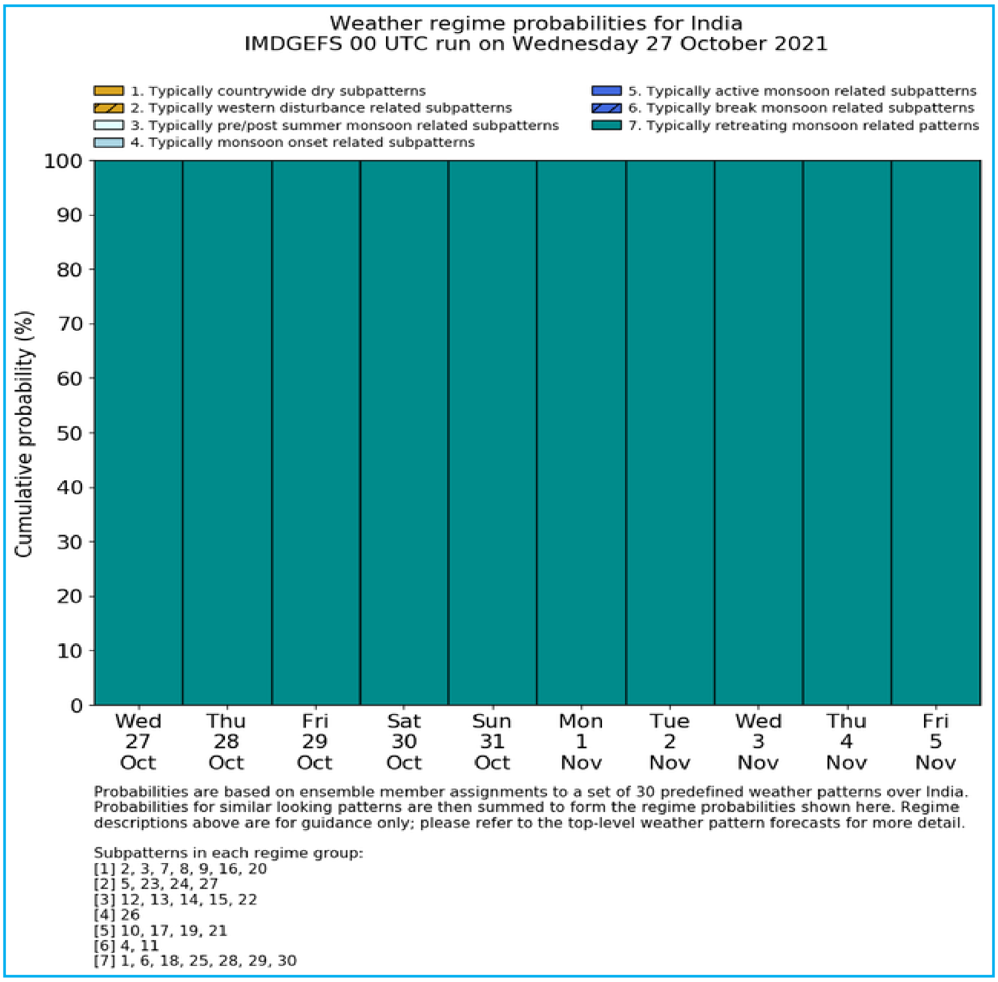

Fig. 9.5.7. Weather regime stacked probabilities

9.6. Madden-Julian Oscillation (MJO) Monitoring and Real-time Verification

The Madden–Julian Oscillation (MJO) is the largest element of the intra-seasonal (30- to 90-day) variability in the tropical atmosphere. It was discovered in 1971 by Roland Madden and Paul Julian of the American National Center for Atmospheric Research (NCAR). It is a large-scale coupling between atmospheric circulation and tropical deep atmospheric convection. Unlike a standing pattern like the El Niño–Southern Oscillation (ENSO), the Madden–Julian oscillation is a travelling pattern that propagates eastward, at approximately 4 to 8 m/s , through the atmosphere above the warm parts of the Indian and Pacific oceans. This overall circulation pattern manifests itself most clearly as anomalous rainfall.

The Madden-Julian oscillation is characterized by an eastward progression of large regions of both enhanced and suppressed tropical rainfall, observed mainly over the Indian and Pacific Ocean. The anomalous rainfall is usually first evident over the western Indian Ocean, and remains evident as it propagates over the very warm ocean waters of the western and central tropical Pacific. This pattern of tropical rainfall generally becomes nondescript as it moves over the primarily cooler ocean waters of the eastern Pacific, but reappears when passing over the warmer waters over the Pacific Coast of Central America. The pattern may also occasionally reappear at low amplitude over the tropical Atlantic and higher amplitude over the Indian Ocean. The wet phase of enhanced convection and precipitation is followed by a dry phase where thunderstorm activity is suppressed. Each cycle lasts approximately 30–60 days. Because of this pattern, the Madden-Julian oscillation is also known as the 30- to 60-day oscillation, or intra-seasonal oscillation.

Figures 9.6.1 and 9.6.2 are displaying the NWP, IMD operational version of the Wheeler and Hendon (2004) daily MJO index for both the past 40, and 90days analysis. The methodology followed at NWP, IMD is nearly identical to that outlined in the above reference and operationally displayed at the Australia Bureau of Meteorology Research Centre (BMRC). Slight differences may occur at times due to subtle deviations in input data and methodology and mainly occur during weak MJO periods.

IMDGFS analysis u-wind at 850 hPa and 200 hPa and near-real time (with 2 days lag time) observed NCEP-NOAA satellite derived Outgoing Longwave Radiation (OLR) Level-1 have been used to compute the past 90 days and 40 days Real-time Multivariate MJO Index (RMM-1 & RMM-2). The NWP, IMD developed a python script to plot RMM1 and RMM2 similar in Wheeler and Hendon (2004) phase plots. Figures 9.6.1 and 9.6.2 are showing the last 90 days, 40 days observed + analysis MJO Index monitoring along with next 10 days forecasts based on initial condition as on 2021-11-23-00Z. The MJO forecast ensemble (IMDGEFS) indices are at phase 3, 4, 5, and 6, and its consequences as expected for the much activity over Bay of Bengal, and it happened as a Cyclonic Storm (JAWAD) during 2021-12-02-00Z to 2021-12-04-00Z. Also, the NWP developed a real-time verification of MJO Index with observed (OLR) + IMD GFS analysis (u-winds) by 11 days lag time, which is shown in Figure 9.6.3 (forecasts based on initial condition as on 2021-11-23-00Z). This figure shows that IMDGEFS ensemble forecasts are matched with observed+analysis MJO index up to 7 days lead time and beyond it not matched perfectly. It happens whenever there is amplitude of MJO less than unity, i.e., Model unable to predict the correct phase and amplitude during low amplitude. At the same time, the model predicts very well the strongest mode (when amplitudes are >1) of MJO index in 10 days well advanced.

Operational Web Link : Go to https://nwp.imd.gov.in -> MEDIUM RANGE FORECASTS -> GEFS (T-1534) ->MJO MONITORING, FORECAST & VERIFICATION

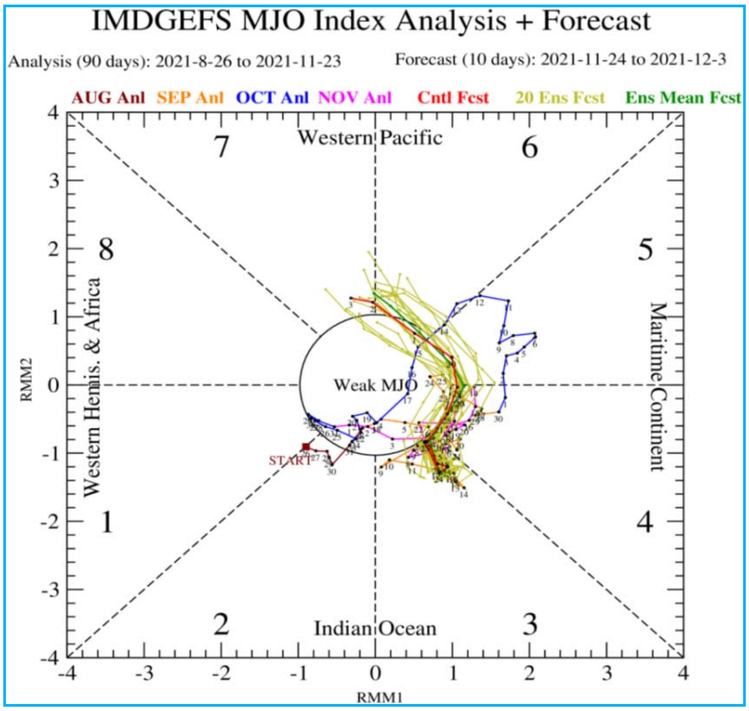

Fig. 9.6.1. MJO Monitoring for past 90 days(2021-08-26 to 2021-11-23) as on 2021-11-23-00Z using IMDGFS analysis u-winds (850 hPa and 200 hPa) and observed OLR (NOAA) along with IMDGEFS - 10 days ensemble forecasts based on initial conditions as on 2021-11-23-00Z. In this figure August, September, October, November 2021 months MJO monitor is plotted in brown, orange, blue, pink coloured lines, respectively. IMDGFS deterministic model 10 days MJO forecast is plotted in red line, 20 ensemble forecasts are plotted in light green lines and ensemble mean line is plotted in dark green line

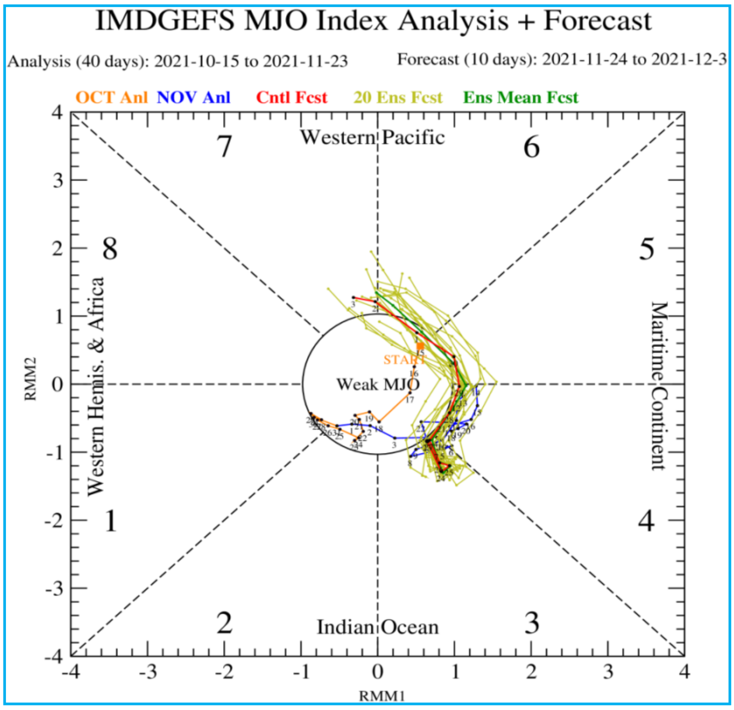

Fig. 9.6.2. MJO Monitoring for past 40 days as on 2021-11-23-00Z using IMDGFS analysis u-winds (850 hPa and 200 hPa) and observed OLR (NOAA) along with IMDGEFS - 10 days ensemble forecasts based on initial conditions as on 2021-11-23-00Z. Orange colour represents October 2021, blue colour represents November 2021 month MJO index. IMDGFS deterministic model 10 days MJO forecast is plotted in red line, 20 ensemble forecasts are plotted in light green lines and ensemble mean line is plotted in dark green line

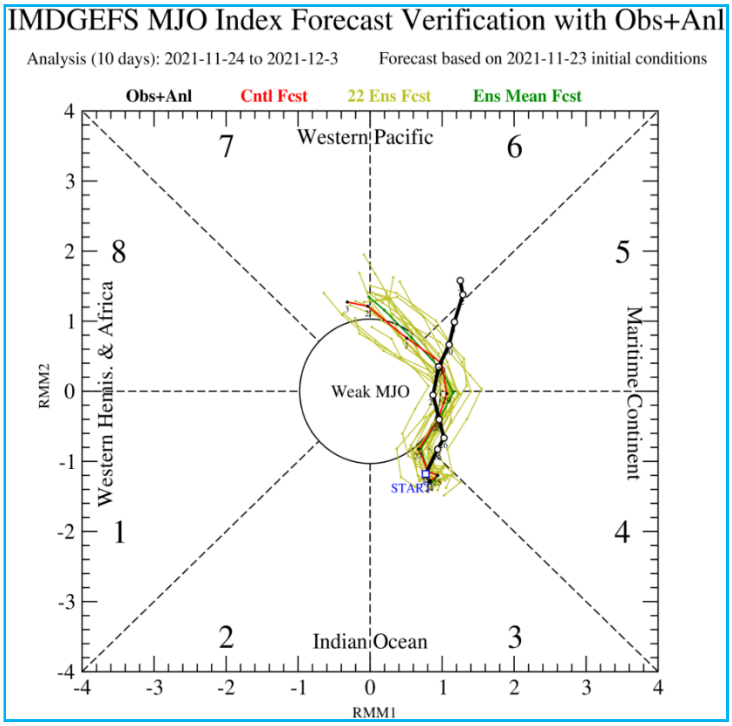

Fig. 9.6.3. Verification of IMDGEFS MJO index ensemble 10 days forecast based on initial condition as on 2021-11-23-00Z.Forecast index is verified against the IMDGFS analysis u-winds (850, 200 hPa) and observed OLR (NOAA) which is shown in black thick line. The forecast lines are the same as shown in figure 9.6.1 and figure 9.6.2

9.7. State level spatial rainfall forecasts and verification

The NWP division of IMD, developed and operationalized all Indian states level spatial region figures where neighborhood regions are masked other than particular state boundaries, to view more focused daily accumulated rainfall (03-03UTC) with multi model predictions. In Figure 9.7.1, shows the daily rainfall over the Andhra Pradesh State using IMDGFS (0.12°x0.12°), IMDGEFS-Mean (0.12°x0.12°), NCUM (0.12°x0.18°), NEPS-Mean (0.12°x0.18°), NCEP (0.25°x0.25°), JMA (0.25°x0.25°) and Multi-Model-Mean (0.125°x0.125°) valid on 2021-11-18-03Z which is Day-1 forecast based on initial condition as on 2021-11-17-03Z. It's verification against the observed IMD gridded (0.25°x0.25°) rainfall is also shown in figure 9.7.3. Similarly, a Day-1 forecast over the same state and its verification also shown in figure 9.7.2 and 9.7.4, respectively valid on 2021-11-18-03Z. This kind of state level figures with multi model forecasts and the multi-model mean forecasts guide the forecasters in more focused manner. All the Indian state level region figures for rainfall are being produced daily, operationally at NWP, IMD. Also, NWP-IMD plans to extend the same work for maximum and minimum surface temperature forecasts and its verification. Currently, NWP team is working on making a web interactive map interface to select the particular state with colour coded warning out of next 10 days forecasts.

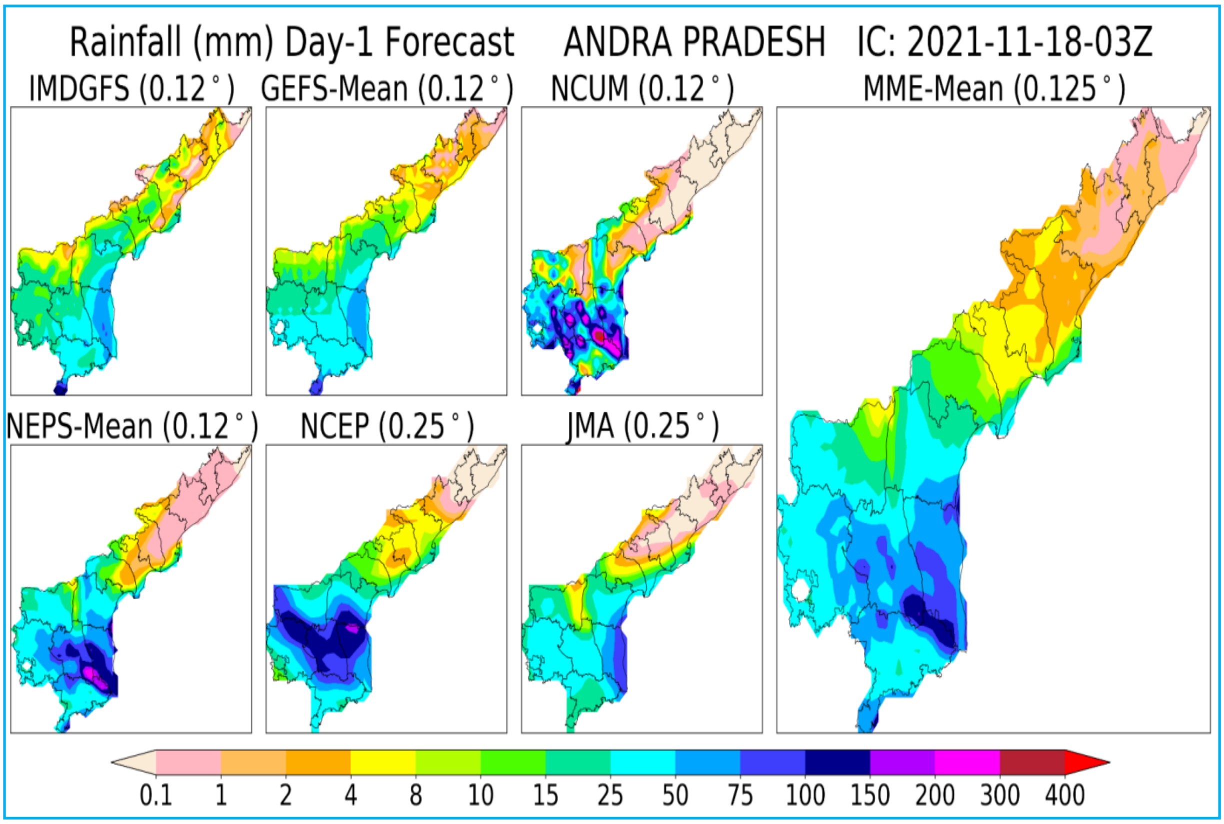

Fig. 9.7.1. Daily rainfall (03-03Z) over the Andhra Pradesh State using IMDGFS (0.12°x0.12°), IMDGEFS-Mean (0.12°x0.12°), NCUM (0.12°x0.18°), NEPS-Mean (0.12°x0.18°), NCEP (0.25°x0.25°), JMA (0.25°x0.25°) and Multi-Model-Mean (0.125°x0.125°) valid on 2021-11-19-03Z which is Day-1 forecast based on initial condition as on 2021-11-18-03Z

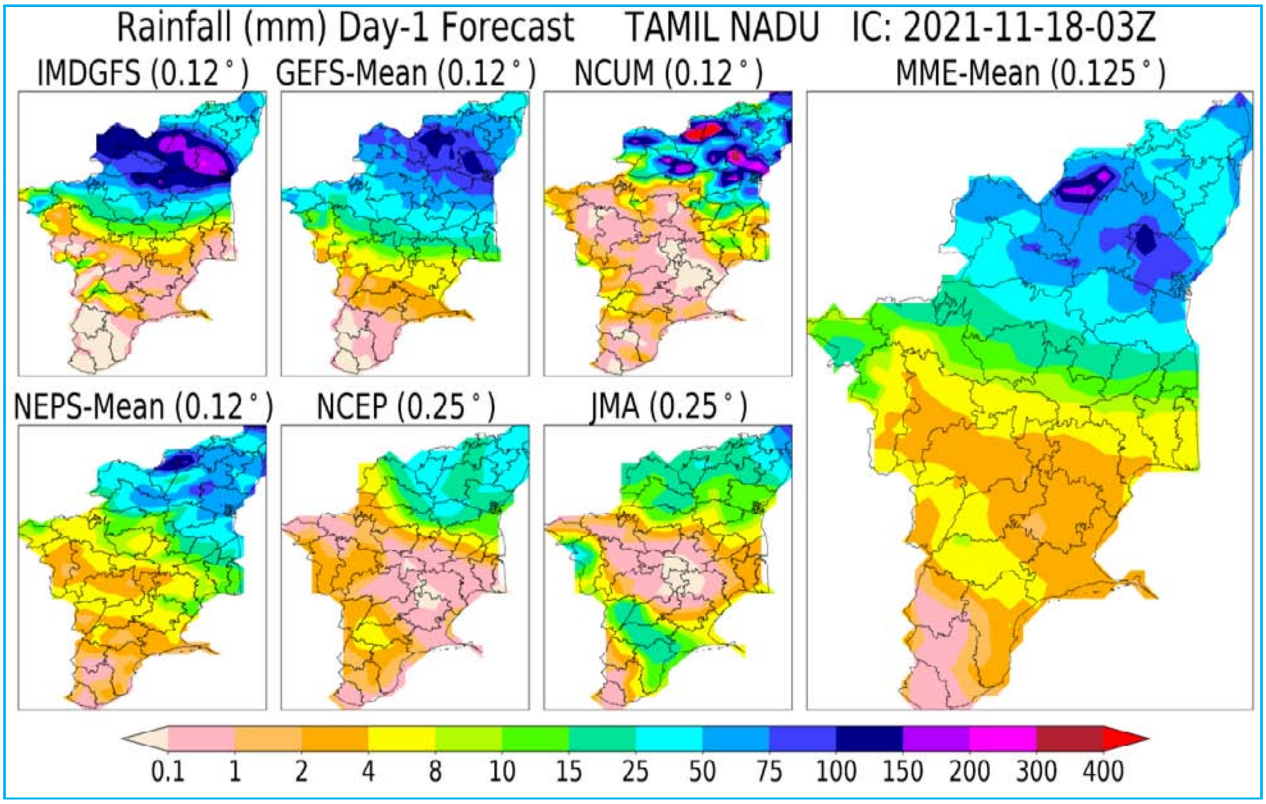

Fig. 9.7.2. Same as figure 9.7.1 but for Tamil Nadu State

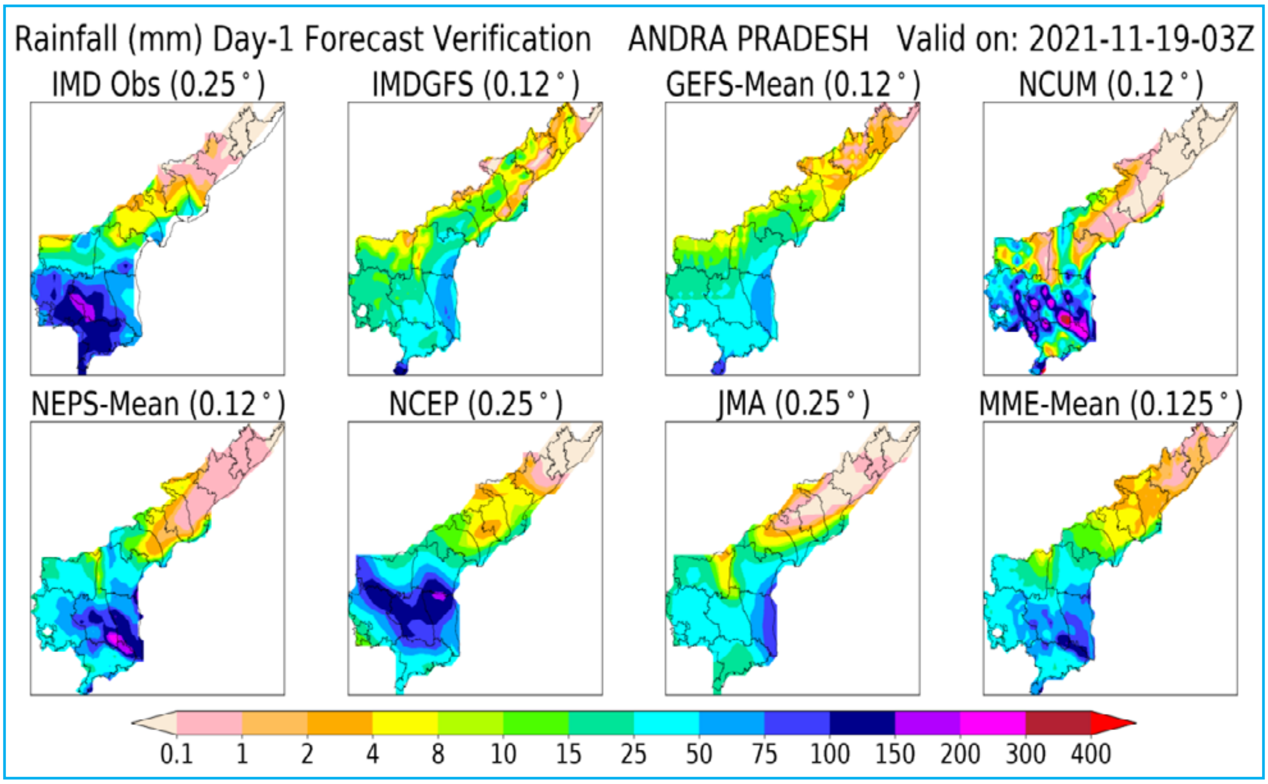

Fig. 9.7.3. Verification of daily rainfall over Andhra Pradesh State using IMDGFS (0.12°x0.12°), IMDGEFS-Mean (0.12°x0.12°), NCUM (0.12°x0.18°), NEPS-Mean (0.12°x0.18°), NCEP (0.25°x0.25°), JMA (0.25°x0.25°) and Multi-Model-Mean (0.125°x0.125°) models Day-1 forecast based on initial condition as on 2021-11-18-03Z, against the IMD Observation (0.25°x0.25°) on 2021-11-19-03Z

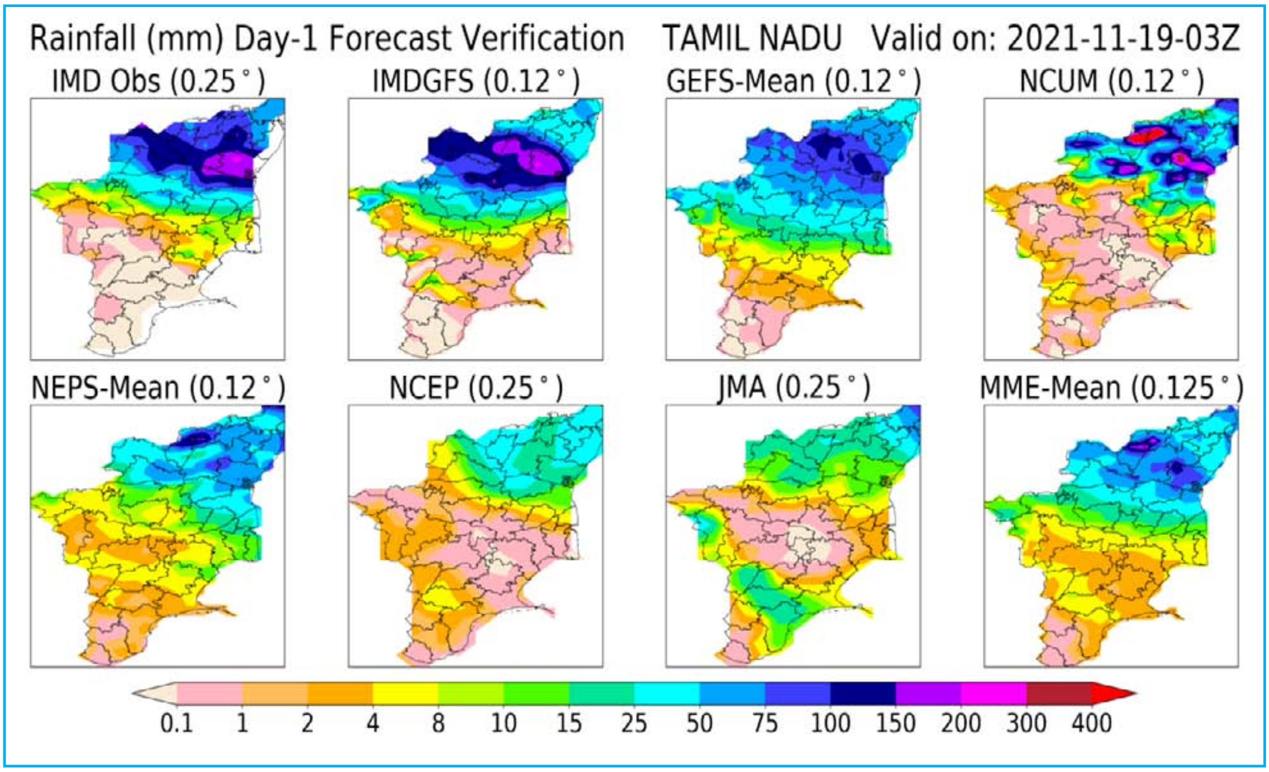

Fig. 9.7.4. Same as figure 9.7.2 but for Tamil Nadu State

9.8. Summary

As discussed in this chapter-9, with sections from 9.1 to 9.7, it brings out the conclusion that the ensemble forecast is most essential one in the numerical weather predictions and also it estimating the forecast uncertainty (or in other words confidence, chance of occurrences, etc.,), which is more useful to the forecasters especially during severe weather events. In section 9.3, discussed the wind speed probabilities at four different thresholds ≥ 28 Knots, ≥ 34 Knots, ≥ 50 Knots, and ≥ 64 Knots using IMDGEFS, and NEPS ensemble model forecasts, which are produced daily operationally. It gives a foreseen warning for the cyclonic storm, by 10-days advance. The Multi Model Ensemble Tropical Cyclone Tracker outputs are discussed for a recent cyclonic storm ('JAWAD' Dec 2021) as a case study with verification in section 9.4. The multi model mean and its verification gives robust result for this JAWAD case. The Weather Pattern Forecasts using IMDGEFS model are discussed in section 9.5, which is much useful to the forecasters by giving the probabilities of occurrence for climatic-weather patterns with respect to the current seasons. The Madden–Julian Oscillation (MJO) Monitoring and Real-time Verification using IMDGEFS are shown and discussed in section 9.6, which also supports the decision makers during oceanic activities (cyclones) over Bay of Bengal and Arabian Sea. The state level spatial rainfall forecasts and its verification against the observed gridded rainfall is discussed in 9.7, which is much more useful to the forecasters and state government authorities to take detailed decisions. In the sections from 9.3 to 9.7 are the new products developed by this chapter author, and by collaborating with scientists from ECMWF (IFS-TC-Tracker, 9.4), UKMO (Weather Pattern Forecasts, section 9.5), and BoM (MJO, section 9.6) institutes.

Acknowledgement

The authors are grateful to Dr. M. Mohapatra, the Director General of Meteorology, India Meteorological Department for his encouragement, constant support and providing all facilities to make these new ensemble NWP products at IMD. Also, thank the ECMWF authorities and point of contact Dr. Richard Mladek and Dr. Emma Pidduck for sharingthe IFS-TC-Tracker source code. And thanks to Dr. Matthew Wheeler (BoM) for guidance on making MJO Index real-time monitor. The authors would like to thank Dr. Robert Neal (UKMO) who provided the source code of weather pattern forecasts. Finally, thank WMO partner institutes who are all providing their global ensemble model outputs to the TIGGE project archives. The authors acknowledge the use of best-track data of tropical cyclone 2021 from the Regional Specialized Meteorological Centre (RSMC) in New Delhi.

References

Neal, R, Robbins, J, Dankers, R, *et al.* (2020) Deriving optimal weather pattern definitions for the representation of precipitation variability over India. *Int. J. Climatol.*, 2020; **40**, 342–360. https://doi.org/10.1002/joc.6215.

Van der Grijn, G., Paulsen, J. E., Lalaurette, F., Leutbecher, M. (2005). Early medium-range forecasts of tropical cyclones. ECMWFNewsletter102.

https://www.ecmwf.int/sites/default/files/elibrary/2004/14623-newsletter-no102-winter-200405.pdf.

Vitart, F., Anderson, J. L., Stern, W. F. (1997). Simulation of Interannual Variability of Tropical Storm Frequency in an Ensemble of GCM Integrations, *Journal of Climate*, **10**(4), 745-760.https://doi.org/10.1175/1520-0442(1997)010<0745:SOIVOT>2.0.CO;2.

Vitart, F., Prates, F., Bonet, A., Sahin, C. (2012). New tropical cyclone products on the web. ECMWF Newsletter 130, https://doi.org/10.21957/TI1191E2.

Wheeler, M. C. and Hendon, H. H. (2004). An All-Season Real-Time Multivariate MJO Index: Development of an Index for Monitoring and Prediction. *Monthly Weather Review*,**132**, 8, 1917-1932. https://doi.org/10.1175/1520-0493(2004)132<1917:AARMMI>2.0.CO;2.

WMO (2012), Guidelines on Ensemble Prediction Systems and Forecasting, No. 1091.https://library.wmo.int/doc_num.php?explnum_id=7773.

Philippe Bougeault; *et al.* (August 2010). The THORPEX Interactive Grand Global Ensemble. *Bulletin of the American Meteorological Society*,*91* (8): 1059–1072.https://doi:10.1175/2010BAMS2853.1.

M. Mohapatra (March 2021), "Cyclone Warning In India Standard Operation Procedure", India Meteorological Department, Ministry Of Earth Sciences, Government Of India.https://mausam.imd.gov.in/imd_latest/contents/pdf/cyclone_sop.pdf.

ECMWF (October 2021), Tropical cyclone activities at ECMWF, *Technical Memorandum* No.888. https://www.ecmwf.int/sites/default/files/elibrary/2021/20228-tropical-cyclone-activities-ecmwf.pdf

CHAPTER 10

Development of Numerical Weather Prediction Products for Marine Services

AMIT BHARDWAJ, M. T. BUSHAIR, D. R. PATTANAIK, ANANDA K. DAS and ANSHUL CHAUHAN

10.1. Introduction

Marine weather forecasts contribute to safety at sea by providing vital information and warning (WMO-2018; Finnis *et al.* 2019). Forecast and warning services for high seas are coordinated by Marine Services Division of India meteorological Department (IMD) Delhi with Contribution from ACWC Kolkata for Bay of Bengal and ACWC Mumbai for Arabian Sea. This Division issues Global maritime Distress Safety System (GMDSS) Bulletin for the Area VIII (N), Sea Area and Fleet forecast for Indian Ocean covering the domain range between 45°N-10°S and Longitude 30°E-110°E. This division also issue Fishermen warning for coastal as well as deep sea areas. It is important to mention that the role and the area of operations of the India Navy has significantly increased over the past years in tune with the nations core interests. Considering this, an additional increased sea area was proposed by Indian Navy for naval operations and information regarding weather in sea areas for critical planning and safe conduct of operations.

With the advancement of the technology, numerical weather prediction (NWP) has incredible growth in development various weather-related application with higher accuracy by providing higher resolution operational global/Regional models forecast. IMD has made progress in operationalization of different NWP models to cater to variety of needs specified by the forecasters. With the commissioning of High-Performance Computing system (HPCS) Aditya, Bhaskara, Mihir and Pratyush HPCS by Ministry of Earth Science (MoES), IMD enabled to operationalize the model at finer resolution. NWP division of the India Meteorological Department (IMD) was given the responsibility for development and upgradation the Marine Weather Forecasting products based on the currently available state of art operational numerical prediction models.

10.2. Operational Numerical weather prediction Global models

NWP division of IMD is currently running various regional and Global models like GFS, GEFS, WRF and ERF models. The brief detail of the operational global models used in the development of marine services products are given in the following sub-sections.

10.2.1. *Operational IMD-GFS version 14.1.0*

The IMD-Global forecast System (GFS) is adopted from NCEP-GFS and run with more accurate assimilation of observations for the Indian regions (Prasad *et al.* 2021). IMD-GFS runs at T1534L64 (~12km) with 3072x1536 gaussian grid points horizontally and vertical resolution of 64-hybrid sigma pressure levels. (Kanamitsu, 1989; Kalnay *et al.*, 1990; Kanamitsu *et al.*, 1991; Moorthi *et al.*, 2001; Durai *et al.*, 2010; Saha *et al.*, 2010). The atmospheric forecast model used in the GFS is a global spectral model (GSM) with spherical harmonics basis functions. It provides 10 days of forecasts daily for (00 and 12 UTC) and 5 days (06 and 18 UTC) with up to 36 hours 1-hourly forecast and beyond 36 hours 3-hourly forecast. We currently utilize 5-days daily forecast data from the IMD GFS for the NWP products for the Marine services.

10.2.2. *Operational IMD-GEFS T1534/64 version 14.1.0*

The Global Ensemble forecast system (GEFS) is a semi-implicit, semi-lagrangian linear grid global spectral model with horizontal resolution of ~12km and vertical resolution of 64 hybrid sigma pressure levels (Deshpande *et al.*, 2020). IMD-GEFS provides the total of 21 (20 perturbed +1 control forecast). Each of these ensemble members are generated with the Ensemble Kalman Filter (EnKF) method. IMD-GEFS runs two times a day at (00 and 12 UTC) for 10 days in 3-hourly intervals.

10.2.3. *Operational JMA High-resolution GSM Model*

The Japan Meteorological Agency's Global Spectrum model (GSM) is a global model with a resolution of 0.1875 degrees (~20km). Although the operational data provided by JMA is at a resolution of 0.25 degrees for surface layers). JMA provide data up to 132 hours four times a day with initial time of 00, 06, 12 and 18 UTC) with four hours of initial time.

10.2.4. *Operational NCEP-GFS Model*

The National Centers for Environmental Prediction (NCEP) GFS model at the resolution 0.25 degrees.GFS is a global model with a base horizontal resolution of ~28km between grid points. The temporal resolution is up to 16 days. Horizontal resolution of NCEP GFS models drop to 70km for forecasts between one week and two weeks.

10.2.5. *Operational NCMRWF Unified Model (NCUM) version 10.8*

The National Centre for Medium Range Weather Forecasting (NCMRWF) runs the NCUM. The NCUM system is based on the Unified Model (UM) developed Met Office UK, UK, BoM/CSIRO, Australia, KMA, South Korea, NIWA, New Zealand and MoES/NCMRWF, India. The horizontal resolution of the model is ~12km. The NCUM model utilize hybrid 4D-var method for data assimilation.

Table 10.1

Summarizing the models in the below table

S.No.	Operational Global Models	Resolution
1.	IMD-GFS	~12km
2.	IMD-GEFS	~12km
3.	JMA	~25km
4.	NCEP-GFS	~25km
5.	NCUM (NCMRWF)	~12km

We used data from five models as listed in Table 10.1 for the operational short to medium range forecast and developments of the Marine products for the three domains as described in the below.

10.3. Marine Weather Forecasting having three modules

10.3.1. *Global Maritime Distress Safety System (GMDSS) Domain*

India has been designated one of the 16 services in the world as an issuing authority under the Global Maritime Distress Safety System (GMDSS) program for Meteorological Area VIII (N). The domain area covered is shown in the Fig. 10.1. The GMDSS domain is divided in four regions two in Arabian Sea as (ARB-A1 & ARB-A2) and two in Bay of Bengal (BoB-A3 & BoB-A4). The IMD is principal government agency in the country in all matters relating to meteorology and allied subjects.

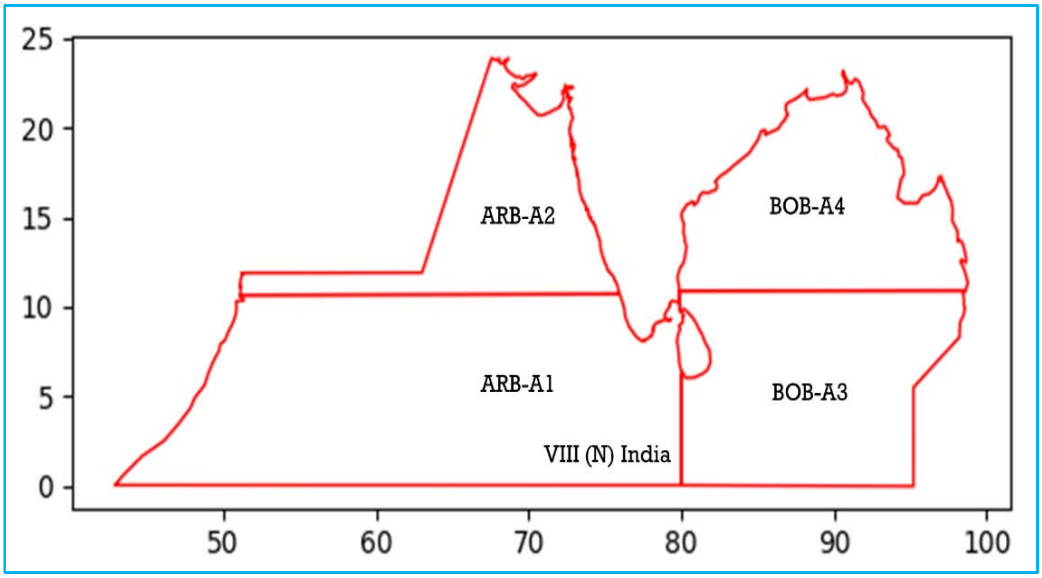

Fig. 10.1. MET AREA VIII (N) India has four subdivisions ARB-A1, ARB-A2, BOB-A3 and BOB-A4

10.3.2. *Sea Area Domain*

The sea area domain is covering the region of Arabian Sea, Bay of Bengal (BoB) of the India Ocean. The area is further divided into north, central, and South section of east and west side of the India including Lakshadweep (LAK) and Maldives area (MAL). The labels are marked for the regions and are shown in the sea area Fig. 10.2.

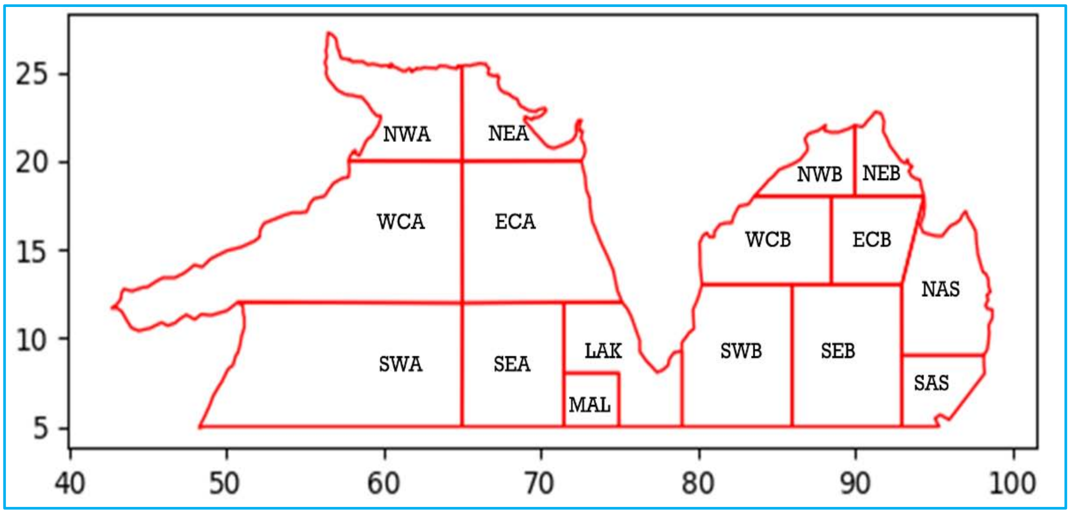

Fig. 10.2. Sea Area regions and labels for Arabian sea and Bay of Bengal

10.3.3. *Updated Indian Navy (Fleet Forecast) Domain*

It is pertinent to mention that the role and the area of operations of the India Navy have significantly increased over the past years in tune with the nation's core interests. Therefore, the additional areas mention in the Fig. 10.3 are considered vital for naval operations and information regarding weather in these areas is critical for planning and safe conduct of operations. In view of the above, an additional area as mentioned in the Fig.10.3 is included in the Fleet forecast.

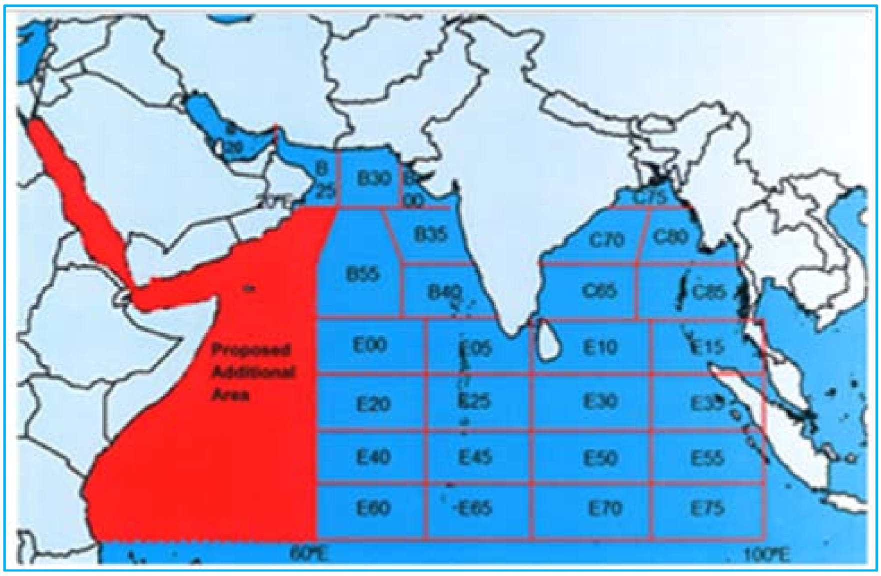

Fig. 10.3. Additional proposed Area (Red) of responsibility of IMD included for fleet forecast

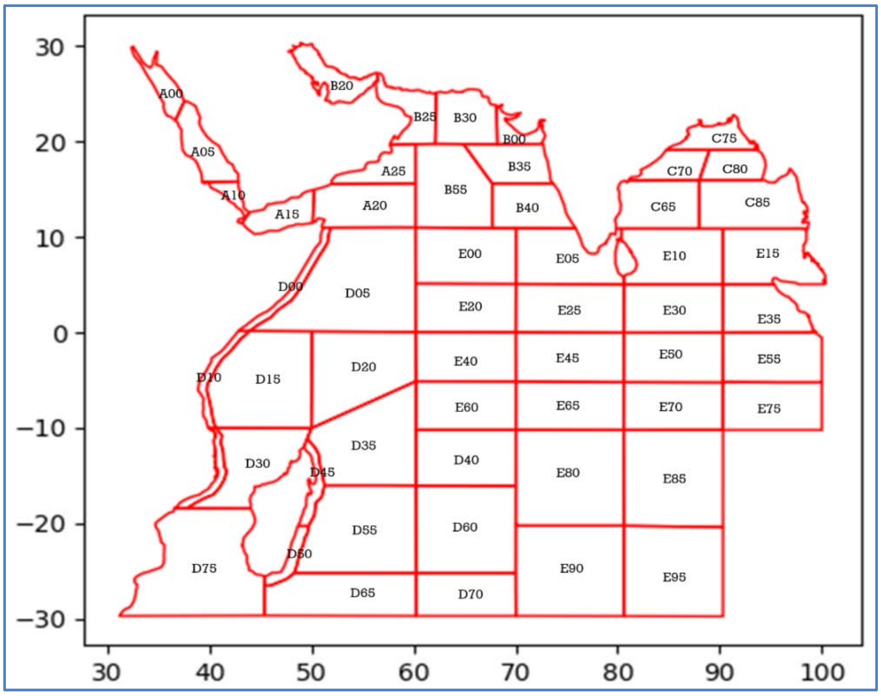

Fig. 10.4. Additional proposed Area included for fleet forecast updated with the label of the regions

The red portion of the area is updated as per Fig. 10.4. We prepared the python based automated scripts for computation of the variables from the five models (IMD-GFS, IMD-GEFS, JMA, NCEP and NCUM) for the 5-day forecast.

10.4. Development of Numerical Weather prediction products

We used data from above the five global operational model's forecasts daily up to five days. The development of the products for the Marine required computation surface wind, visibility, weather, state of sea information. Therefore, seven variables are computed as written in the Table 10.2.

Table 10.2.

Numerical Weather Prediction Operational Global Models

S.No.	Operational Global Models	Variables
1.	IMD-GFS	Wind speed, wind direction, Rainfall Intensity, Rainfall Distribution, Significant Wave Height, Visibility, Heavy Rainfall Distribution
2.	IMD-GEFS	Wind speed, wind direction, Rainfall Intensity, Rainfall Distribution, Significant Wave Height, Visibility, Heavy Rainfall Distribution
3.	JMA	Wind speed, wind direction, Rainfall Intensity, Rainfall Distribution, Significant Wave Height, Visibility, Heavy Rainfall Distribution
4.	NCEP-GFS	Wind speed, wind direction, Rainfall Intensity, Rainfall Distribution, Significant Wave Height, Visibility, Heavy Rainfall Distribution
5.	NCUM (NCMRWF)	Wind speed, wind direction, Rainfall Intensity, Rainfall Distribution, Significant Wave Height, Visibility, Heavy Rainfall Distribution

10.4.1. *Rainfall Intensity*

It is the average rainfall amount over the shape regions of the domain. One example average valued for the Sea Area and for the MME of all the five models is shown in the Table 10.3. This table provides single value for each layer or the sub-region of the Sea Area.

The values are thus computed for all the variables and automatized python scripts prepared which are operationalized to generate.

Table 10.3.

Sea Area MME data for five days forecast is listed in the below table

Id	layer	20211202	20211203	20211204	20211205	20211206
101	NWA	0	0	0	0	0
102	NEA	5.9	0	0	0	0
104	ECA	22.4	0.8	0.4	0.3	0.1
103	WCA	0.3	0.5	0.7	0.4	0.1
105	SWA	1.6	0.5	0.6	1	1.6
106	SEA	3.9	1	1.2	1.4	1.3
108	MAL	5.7	4.4	3.1	6.6	1.7
107	LAK	8.7	1.8	1.8	3.1	2
109	SWB	3.1	5.8	1.8	2.7	2.9
111	WCB	2.2	44.2	24.2	8.6	2.4
113	NWB	0	3.4	24.2	22.9	11.5
114	NEB	0	0.1	5.7	7.4	9.4
112	ECB	4.5	18.3	15.4	11.3	5.3
110	SEB	29.4	14.4	3.2	5	4.4
115	SAS	19.3	20.9	17.8	8.4	11.5
116	NAS	10.4	14.3	6.7	1.5	0.2

Computation/estimation of the variables for the GMDSS, Sea Area and Fleet Forecast are described below:

10.4.2. *Rainfall distribution*

It is defined as the percentage rainfall over the grid points exceeds the 2.5 mm rainfall over the shape of the regions. And the rainfall distribution is categorised based on the Table 10.4.

Table 10.4.

Categories of the rainfall distribution based on percentage of grid points exceed 2.5 mm rainfall

Spatial Distribution of Rainfall	Descriptive term used	Criteria for observed
Dry	Dry	No stations/grid points reported/expected rainfall
Isolated	One or two places	<25% of stations/grid points to get rainfall
Scattered	At a few places	(26-50)% of stations/grid points to get rainfall
Fairly Widespread	At many places	(51-75) % of stations/grid points to get rainfall
Widespread	At most place	(76-100) % of stations/grid points to get rainfall

Note:Only daily rainfall over a grid point/station of at least 2.5 mm is taken into consideration

10.4.3. *Horizontal visibility*

Model based products are not reliable for the visibility under bad weather conditions these it is estimated based on the Rainfall distribution as Table 10.5. The range of estimated Visibility is given in Nautical Miles.

Table 10.5.

Horizontal Visibility estimation from Rainfall distribution

Spatial distribution of rainfall/Intensity of rainfall	Estimated Visibility (Nautical Miles)	Values available in CSV file
Fair	8-10	10
Isolated	6-8	8
Scattered	4-6	6
Fairly widespread	3-4	4
Widespread	2-3	3
Fairly widespread/ widespread with heavy rainfall	<2	2

10.4.4. *Wind Driven Significant Wave Height*

Some important terminology used in the bulletin pertain to description of sea Conditions, amount/intensity of heavy rainfall, distribution of rainfall etc. These are presented in the following Table 10.6.

Table 10.6.

Estimation of Significant wave height and terminology used in thebulletins

S. No.	Significant wave height	Descriptive term	Height Meters	Wind speed Knots(kmph)	Beaufort Scale
1.	0	Calm (Glassy)	0	0	0
2.	0.1	Calm (Rippled)	0-0.1	1-3 (2-6)	1
3.	0.5	Smooth (Waveless)	0.1-0.5	4.10 (7-19)	2-3
4.	1.25	Slight	0.5-1.25	11-16 (20-30)	4
5.	2.5	Moderate	1.25-2.5	17-21 (31-39)	5
6.	4	Rough	2.5-4.0	22-27 (41-50)	6
7.	6	Very Rough	4.0-6.0	28-33 (52-61)	7
8.	9	High	6.0-9.0	34-40 (63-74)	8
9.	14	Very High	9.0-14.0	41-63 (76-117)	9-11
10.	20	Phenomenal	Over 14	64 or above (119 or above)	12

10.4.5. *Wind Speed and Direction*

Wind speed is the average values over the region and their average instant direction.

10.4.6. *Heavy Rainfall Distribution*

This is based on the rainfall intensity (> maximum values as listed in the Table 10.7).

Table 10.7.

Heavy Rainfall intensity categories

S. No.	Rainfall	Rain amount (mm)
1.	Very Light to light Rainfall	0.1-15.5
2.	Moderate Rainfall	15.6-64.4
3.	Heavy Rainfall	64.5-115.5
4.	Very Heavy Rainfall	115.6-204.4
5.	Extremely Heavy Rainfall	>=204.5

10.5. Final Products graphics

Individual models and their simple Multi-Model Ensemble (MME) are generated. Some example products based on MME are prepared and included below for the GMDSS, Sea Area, Fleet.

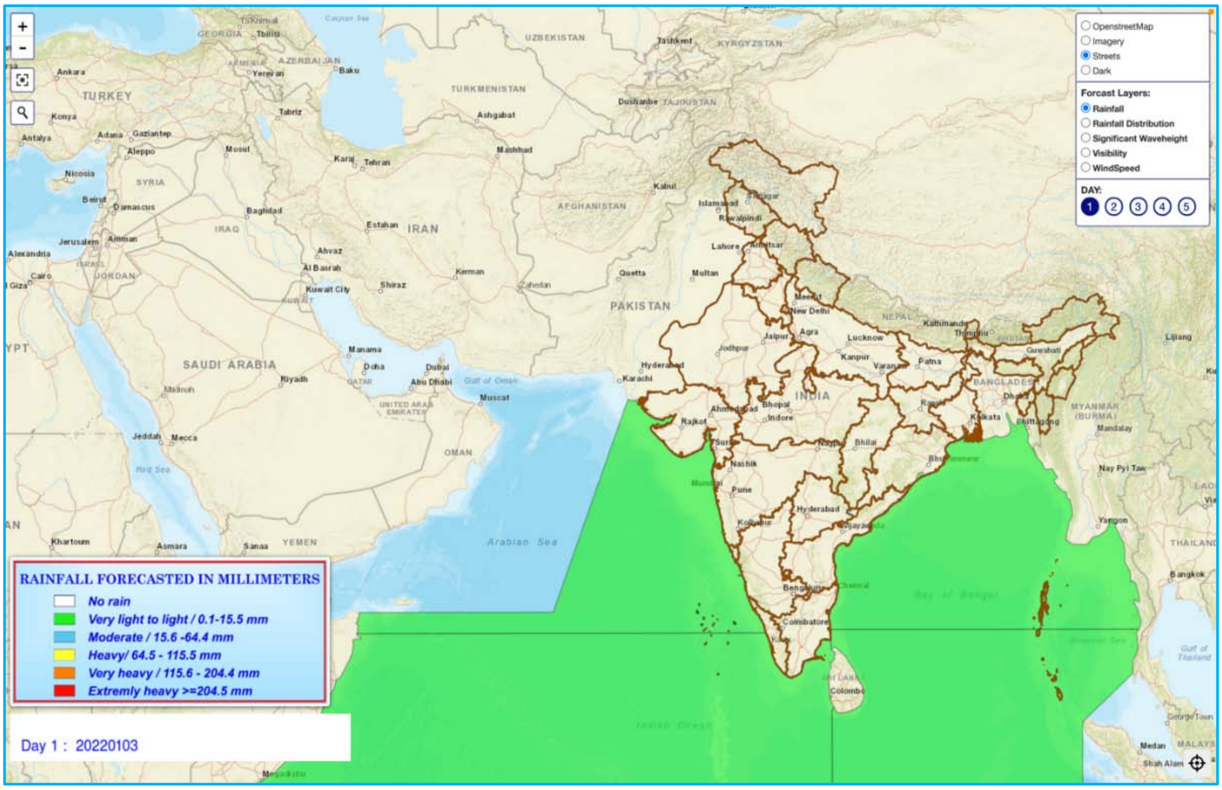

Fig. 10.5. Rainfall Intensity for GMDSS

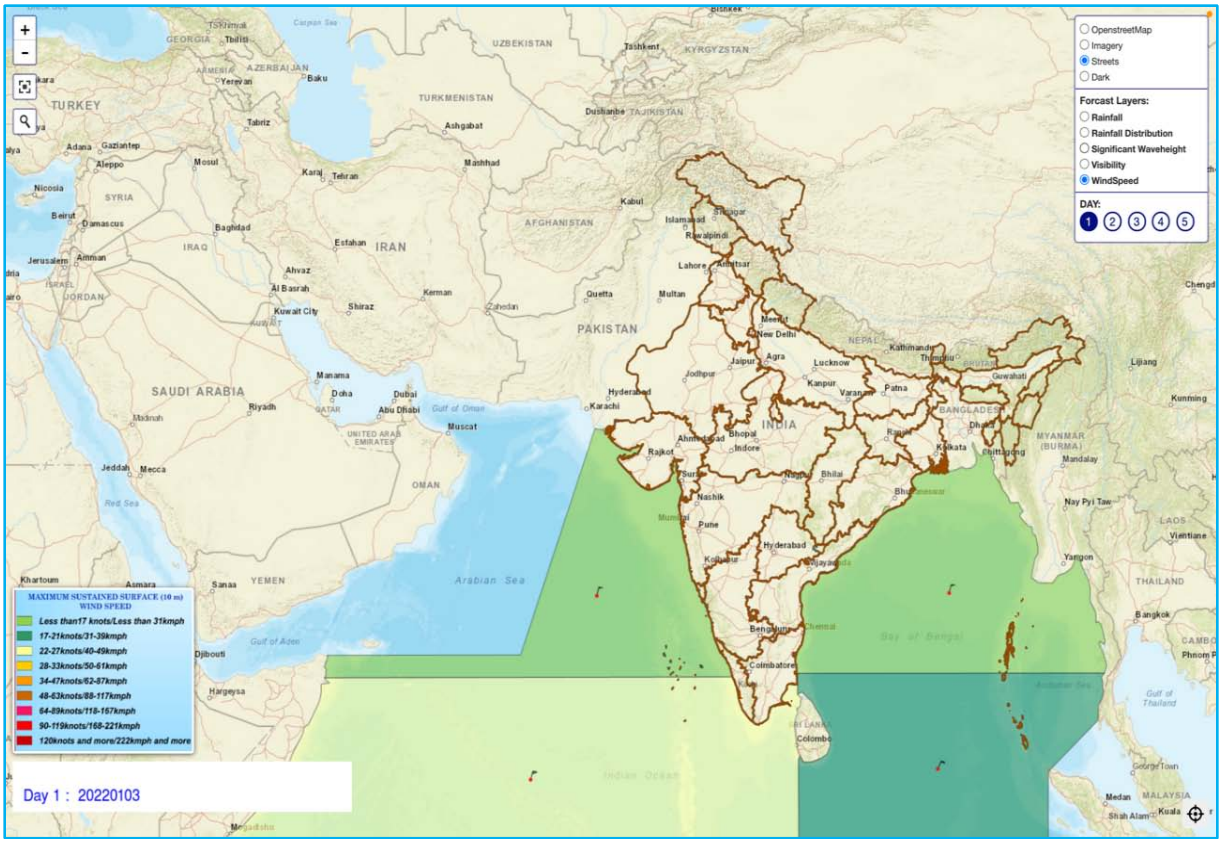

Fig. 10.6. GMDSS Interactive map for Wind speed and direction

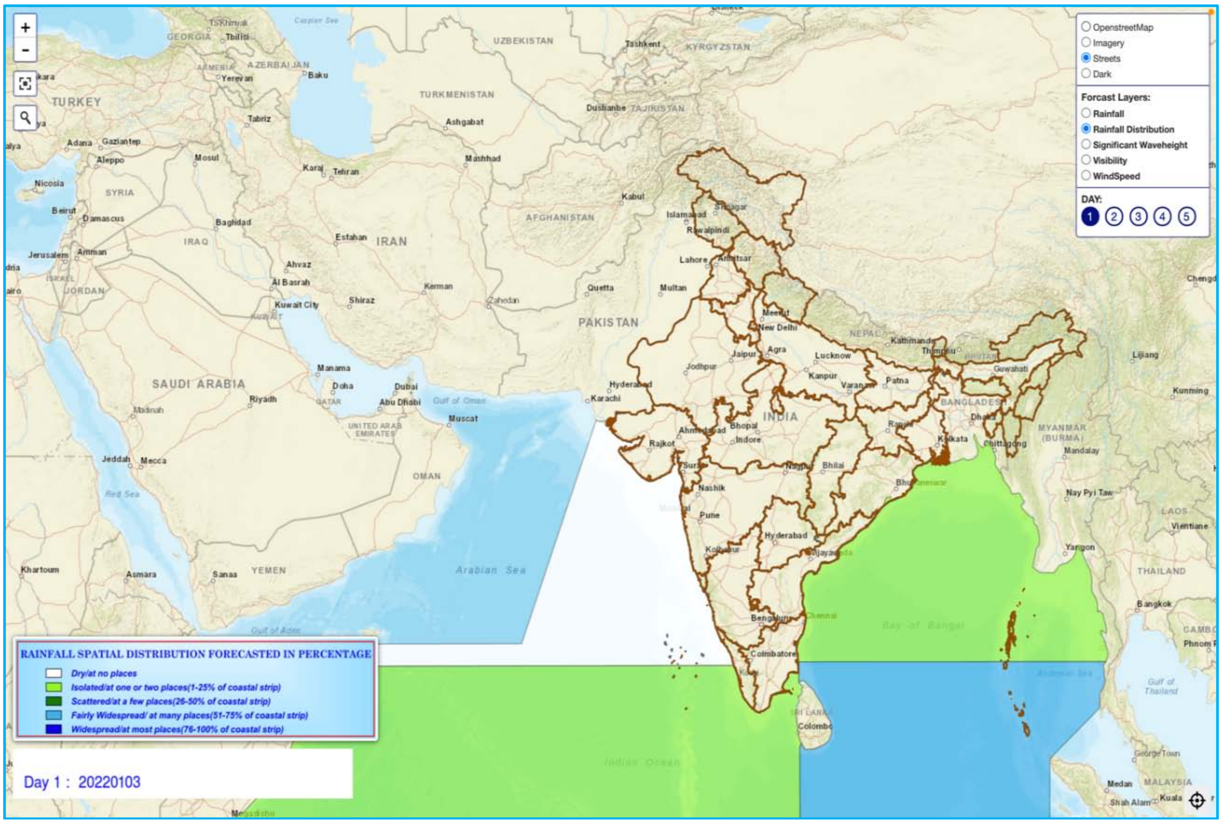

Fig. 10.7. Rainfall Distribution for GMDSS

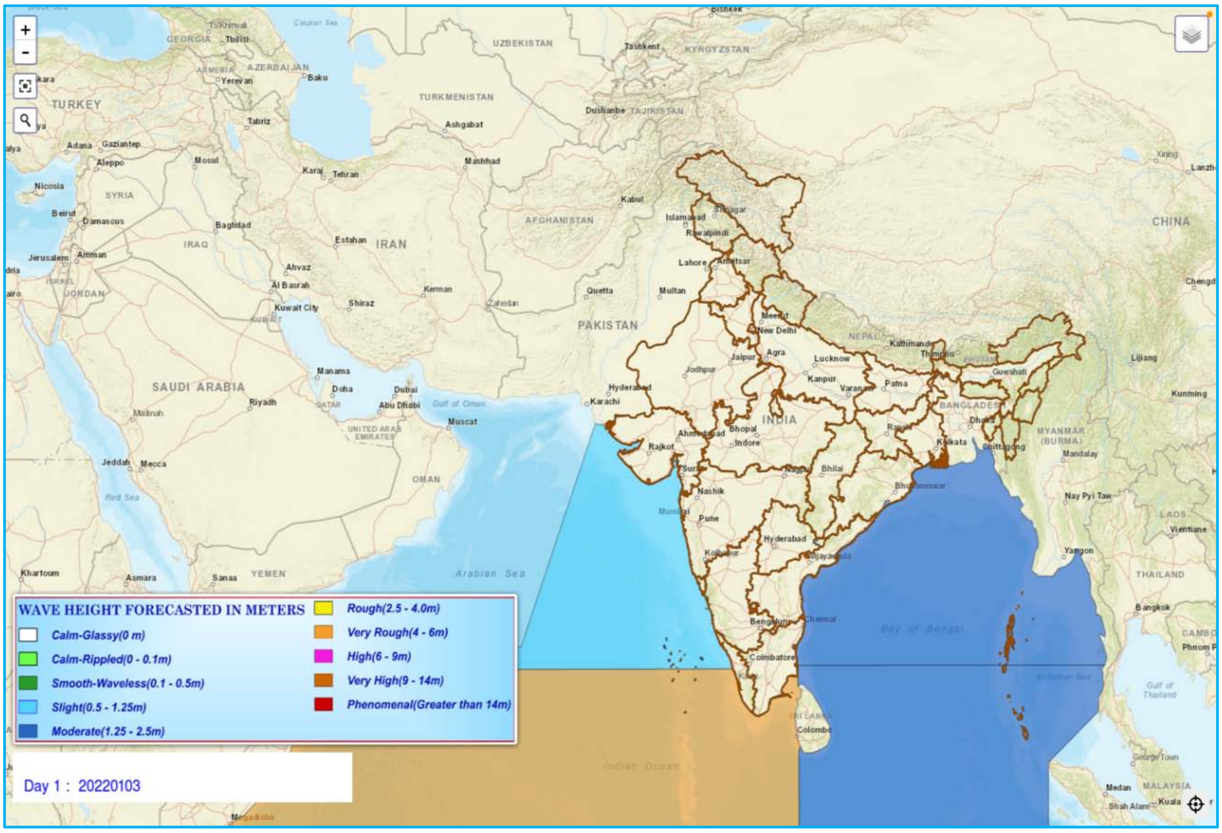

Fig. 10.8. Significant wind generated wave height

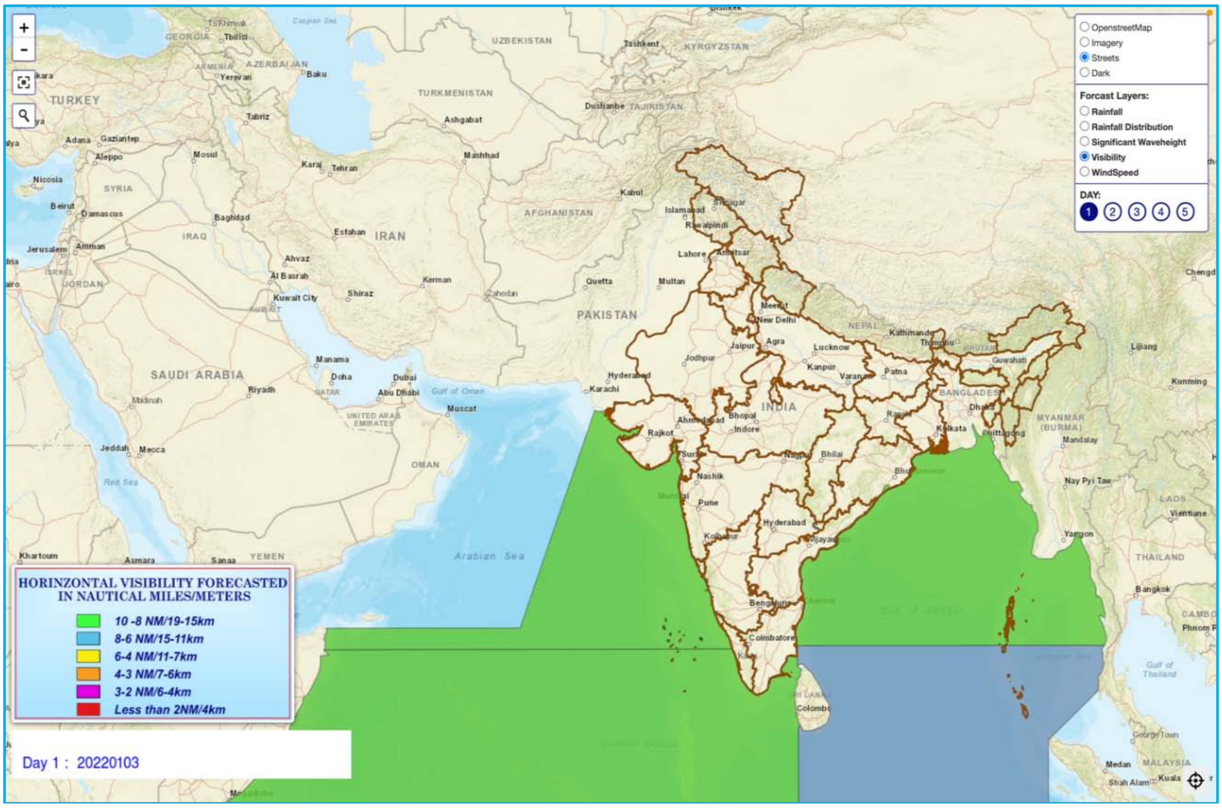

Fig. 10.9. Horizontal Visibility for GMDSS

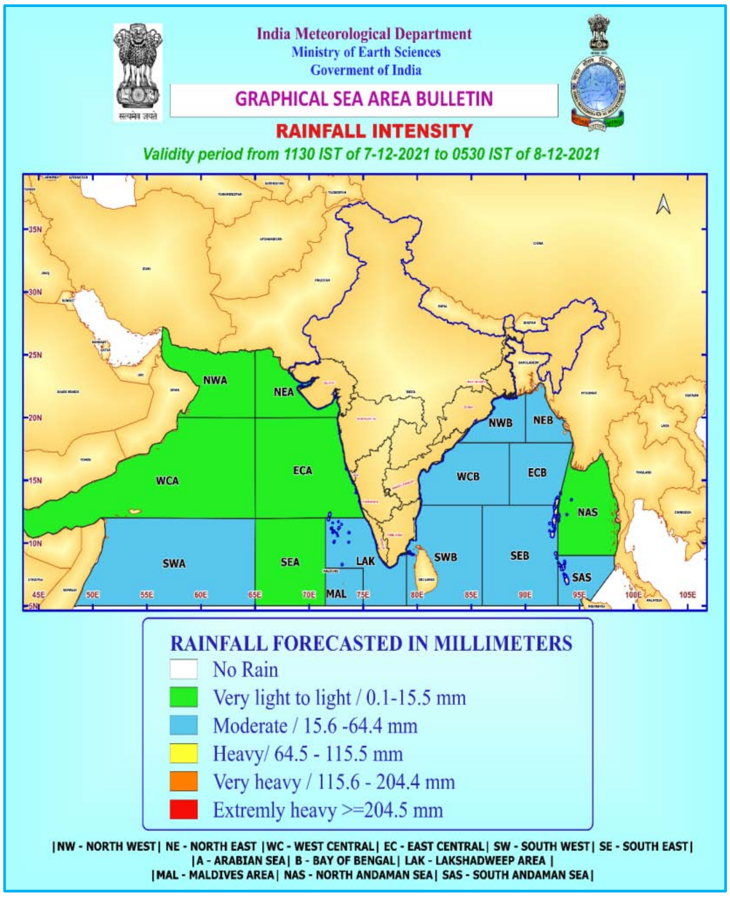

Fig. 10.10. Sea Area for the Rainfall Intensity

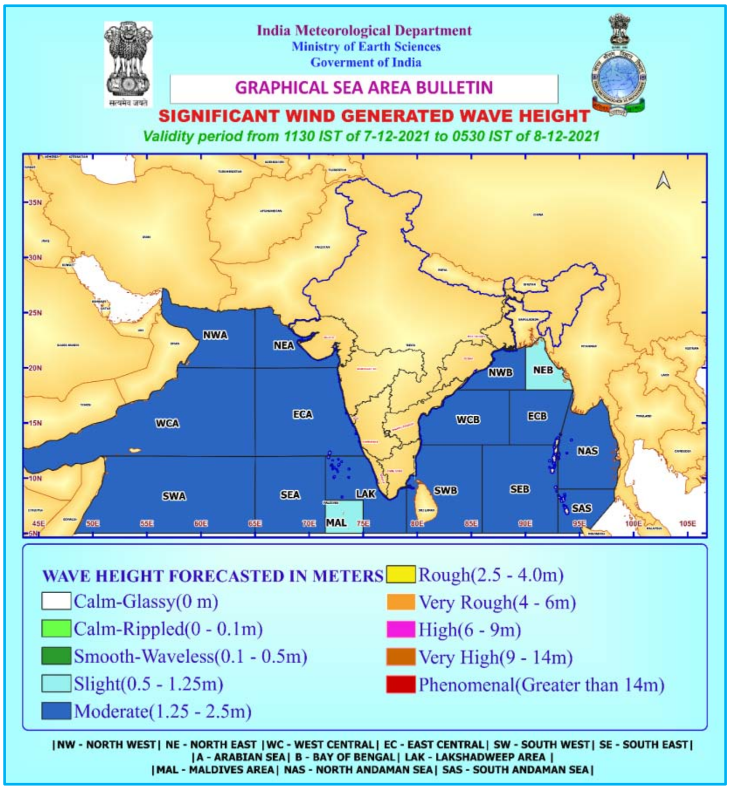

Fig. 10.11. Significant wind generated wave height

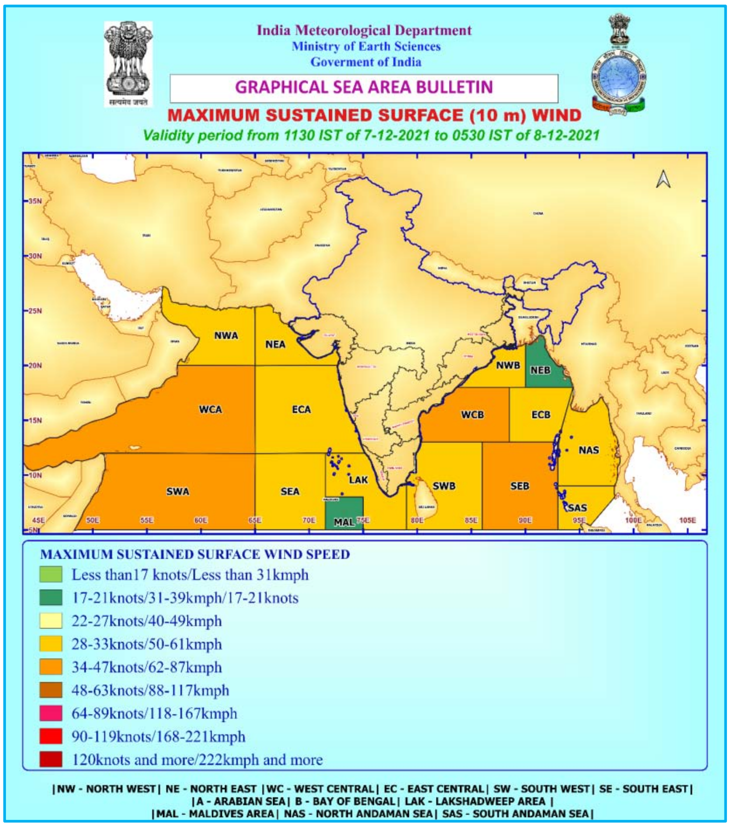

Fig. 10.12. Maximum sustained surface wind (10m)

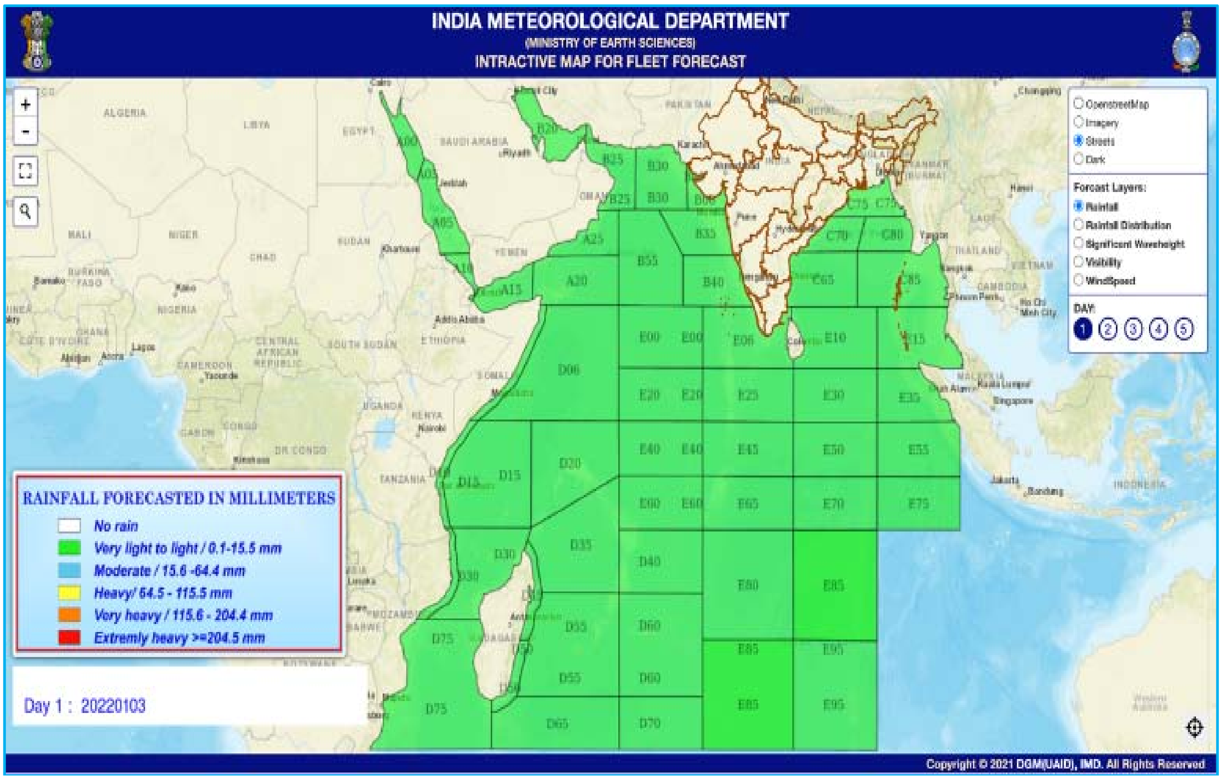

Fig. 10.13. Rainfall Intensity

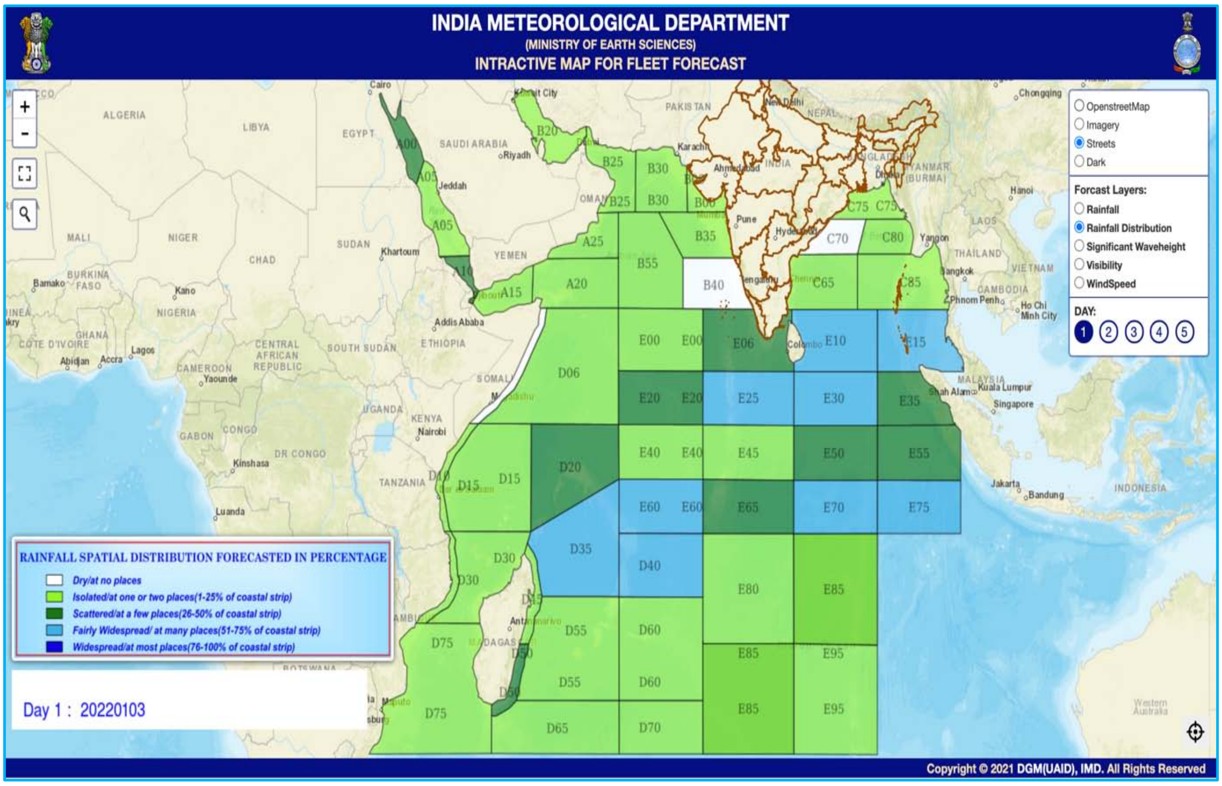

Fig. 10.14. Rainfall Distribution

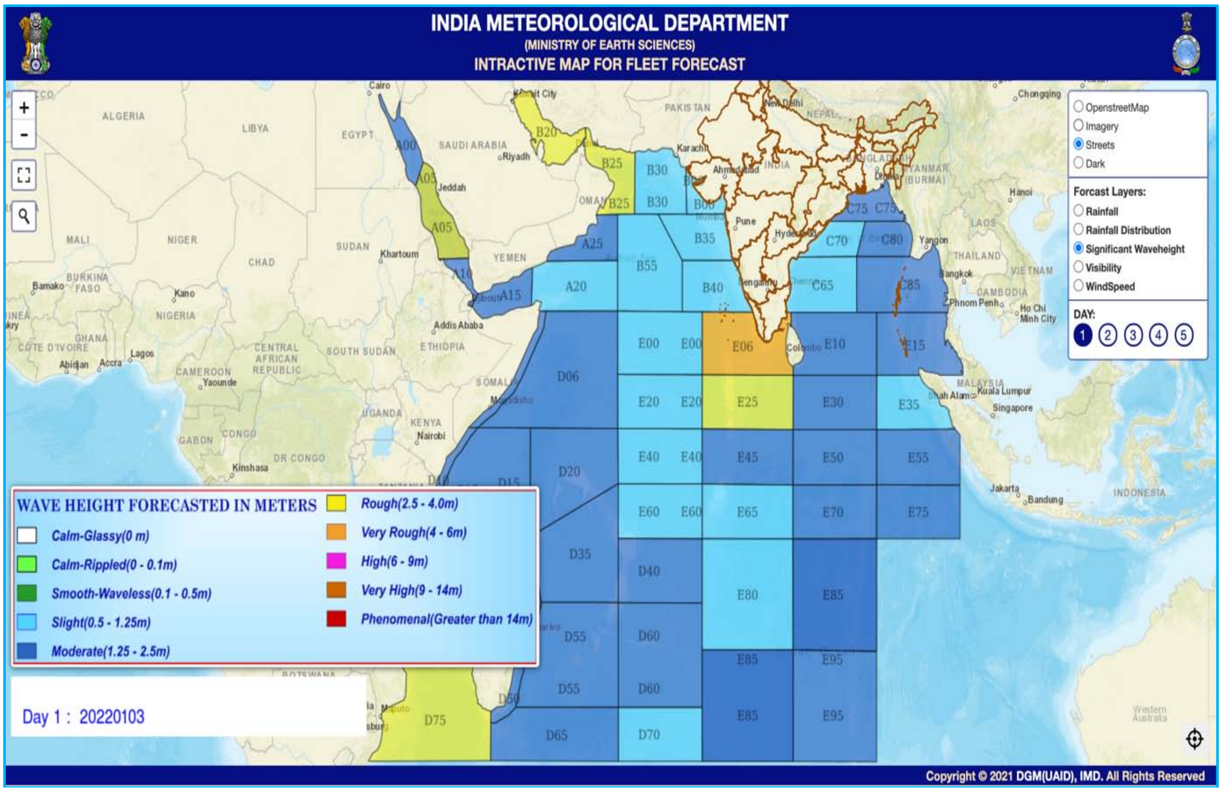

Fig. 10.15. Significant wind generated Wave Height

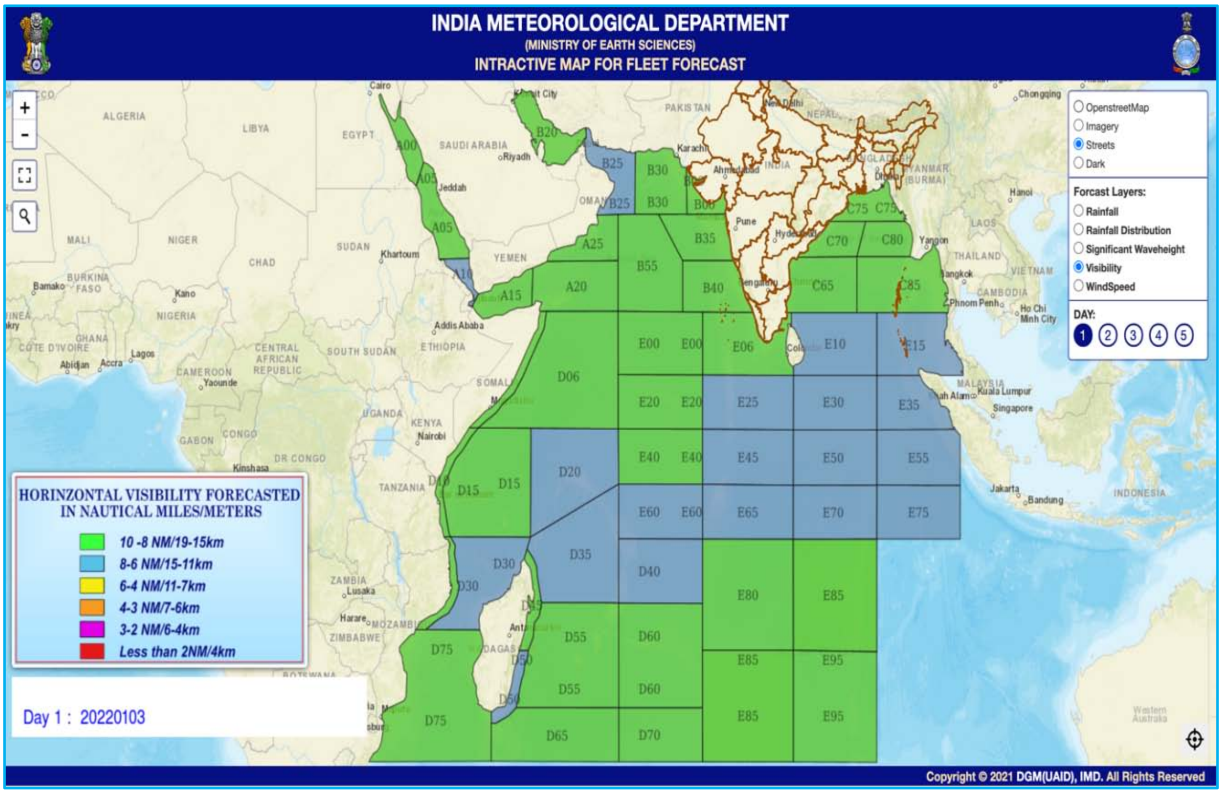

Fig. 10.16. Visibility

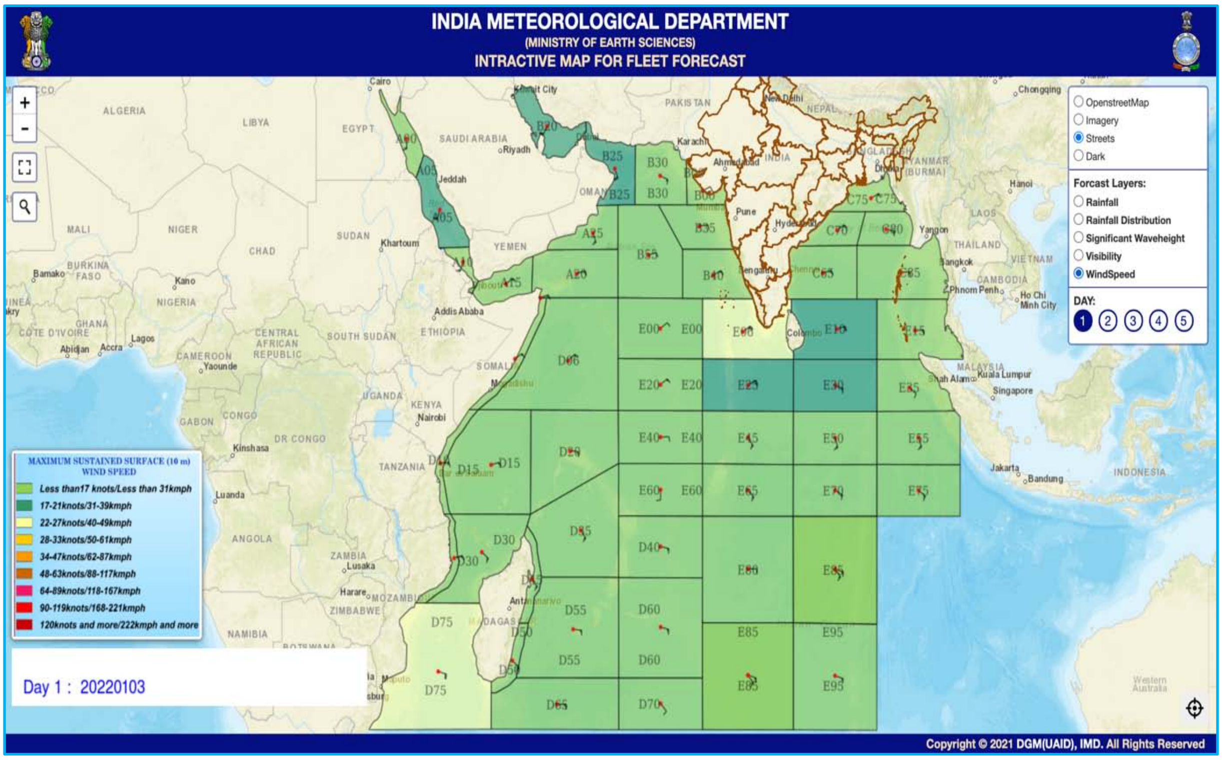

Fig. 10.17. Wind Speed and direction

References

Deshpande M., Johny C.J., Kanase R., Tirkey S., Sarkar S. Goswami, T., Roy K., Ganai M., Krishna R. P. M., Prasad V. S., Mukhopadhyay P., Durai V. R., Nanjundiah R. S. and Rajeevan, M., (2020) Implementation of Global Ensemble Forecast System (GEFS) at 12 km Resolution, ISSN 0252-1075, IITM Technical Report No. TR-06, ESSO/IITM/MM/ TR/02(2020)/200.

Durai, V. R., Roy Bhowmik, S. K. and Mukhopadhaya, B. (2010) Performance Evaluation of precipitation Prediction skill of NCEP Global Forecasting System (GFS) over Indian region during summer Monsoon 2008, *Mausam*, **61**, 139–154.

Johny C.J. and Prasad V.S., (2020) Application of hind cast in identifying extreme events over India. *J. Earth Syst. Sci*., **129**,163.https://doi.org/10.1007/s12040-020-01435-8.

Kalnay, E., Kanamitsu, M. and Baker, W. E. (1990) Global numerical weather prediction at the National Meteorological Center, *Bull. Amer. Meteor. Soc.*, **71**, 1410–1428,DOI: 10.1175/1520-0477(1990)071<1410:GNWPAT>2.0.CO;2.

Kanamitsu, M. (1989) Description of the NMC global data assimilation and forecast system, *Weather Forecast*, **4**, 335–342, DOI: 10.1175/15200434(1989)004<0335:DOTNGD>2.0.CO;2.

Kanamitsu, M., Alpert, J. C., Campana, K. A., Caplan, P. M., Deaven, D. G., Iredell, M., Katz, B.,Pan, H.L., Sela, J. and White, G. H. (1991) Recent changes implemented into the global for cast system at NMC, *Weather Forecast*, **6**, 425–435, DOI: 10.1175/1520-0434(1991)006<0425:RCIITG>2.0.CO;2.

Moorthi, S., Pan, H. L. and Caplan, P. (2001) Changes to the 2001 NCEP operational MRF/AVNglobal analysis/forecast system, *NWS Technical Procedures Bulletin*, **484**, pp 14, available athttp://www.nws.noaa.gov/om/tpb/484.htm.

Saha, S., Moorthi, S., Pan, H.-L., Wu, X., Wang, J., Nadiga, S., Tripp, P., Kistler, R., Woollen, J., Behringer, D., Liu, X., Stokes, D., Grumbine, R., Gayno, G., Wang, J., Hou, Y.T., Chuang, H.-Y., Juang, H.M. H., Sela, J., Iredell, M., Treadon, R., Kleist, D., Van Delst, P., Keyser, D., Derber, J., Ek, M., Meng, J., Wei, H., Yang, R., Lord, S., van den Dool, H., Kumar, A., Wang, W., Long, C., Chelliah, M., Xue, Y., Huang, B., Schemm, J.-K.,Ebisuzaki, W., Lin, R., Xie, P., Chen, M., Zhou, S., Higgins, W., Zou, C.Z., Liu, Q., Chen, Y., Han, Y., Cucurull, L., Reynolds, R. W., Rutledge, R. and Goldberg, M. (2010): The NCEP climate forecast system reanalysis, *Bull. Amer. Meteor. Soc.*, **91**, 1015–1057, DOI: 10.1175/2010BAMS3001.1.

V.S. Prasad, V.S., Suryakanti Dutta, Sujata Pattanayak, C. J. Johny, John P. George, Sumit Kumar and S. Indira Rani (2021), Assimilation of satellite and other data for the forecasting of tropical cyclones over NIO, *MAUSAM*, Vol. **72**, No. 1.

CHAPTER 11

NWP support for Severe Weather Forecasting Project – SouthAsia (SWFP-SA)

D. R. PATTANAIK and PRADEEP MISHRA
NWP Division, IMD, New Delhi – 110 003

1. Introduction

The basic goals of the Severe Weather Forecasting Project (SWFP) of WMO are to :

- Improve Severe Weather Forecasting
- Improve lead-time of Warnings
- Improve interaction of NMHSs with users: media, disaster management, civil protection authorities, public

The Global NWP Centres, Regional centres and NMCs have different role to play under SWFPs implementation as mentioned below.

- **Global NWP centres** to provide available NWP/EPS and sat-based products, including in the form of probabilities, cut to the project window frame;

- **Regional centres** to interpret information received from global centres, prepare daily guidance products (out to day-5) for NMCs, run limited-area model to refine products, maintain RSMC Web site, liaise with the participating NMCs;

- **NMCs** to issue alerts, advisories, severe weather warnings; to liaise with user communities, and to contribute feedback and evaluation of the project; NMCs have access to all products, and maintained responsibility and authority over national warnings and services.

RSMC New Delhi is functioning as Regional Centre for the countries viz., *Afghanistan, Bangladesh, Bhutan, India, Maldives, Myanmar, Nepal, Pakistan, Sri Lanka and Thailand* covering the domain 45E – 110E ; 10S – 45N. IMD Numerical Weather Prediction Division, NCMRWF, IITM & INCOIS provide the NWP/EPS products for use by RSMC for preparing the guidance products for NMCs.

2. How to access SWFP-SA webpage to get all NWP/EPS products:

NWP division has developed a dedicated page hosting all NWP and Ensemble products for use by forecasters., which can be directly visited through following webpage

(i) http://www.rsmcnewdelhi.imd.gov.in/ and select SWFP-SOUTH ASIA
or go directly

(ii) https://nwp.imd.gov.in/mme/fdp-bob/login.php

username :swfdp-bob
password :imd

3. All products in SWFP-SA webpage including NWP/EPS products

3.1. Graphical guidance products for 5 days for severe weather (Rainfall, strong winds, high wave and Storm surge)

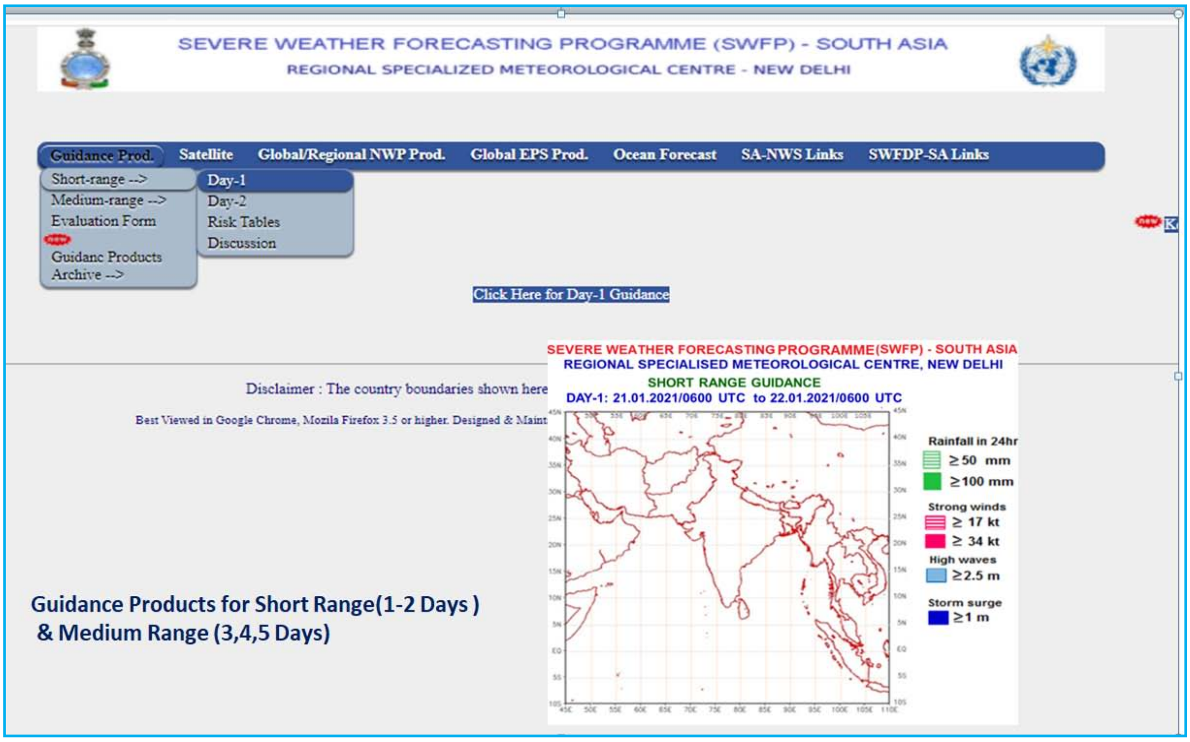

Guidance products archive for graphics available from 1st January 2020 for five day forecast and guidance products archive for Risk Tables, Prob. Tables & Discussions available from 1st January 2020 for five day forecast.

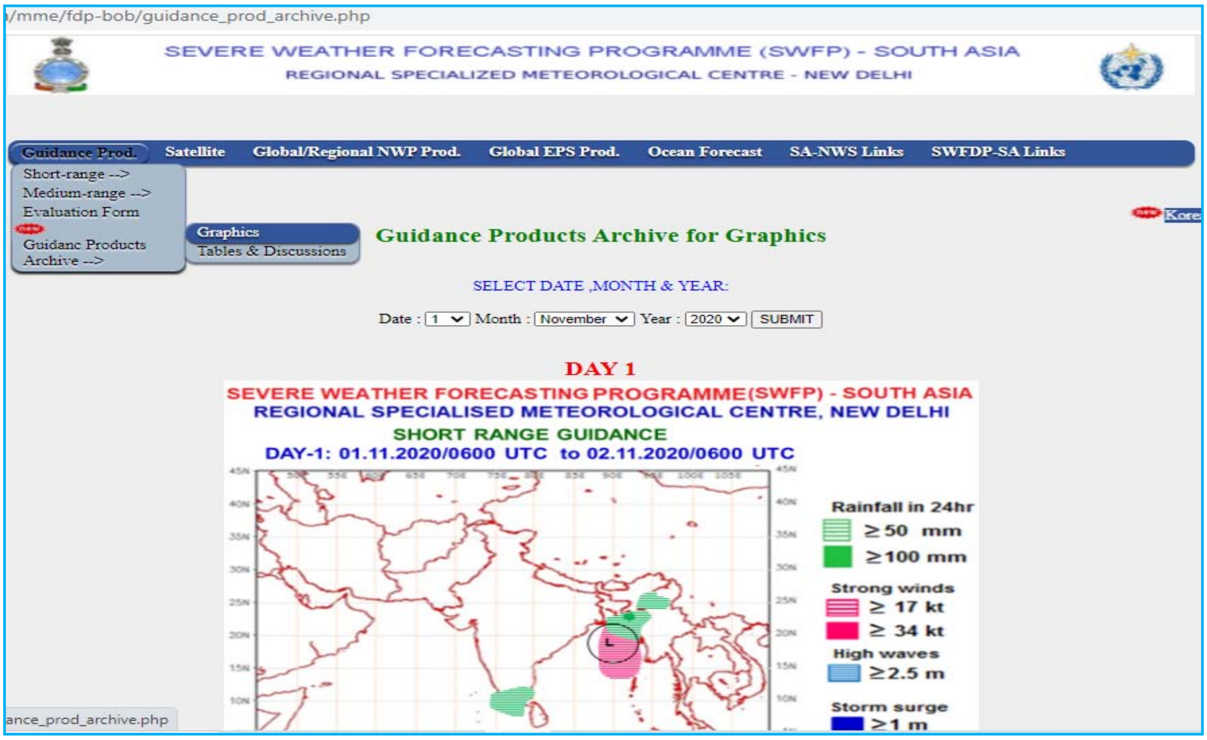

3.2. *Satellite products (RAPID utility from INSAT)*

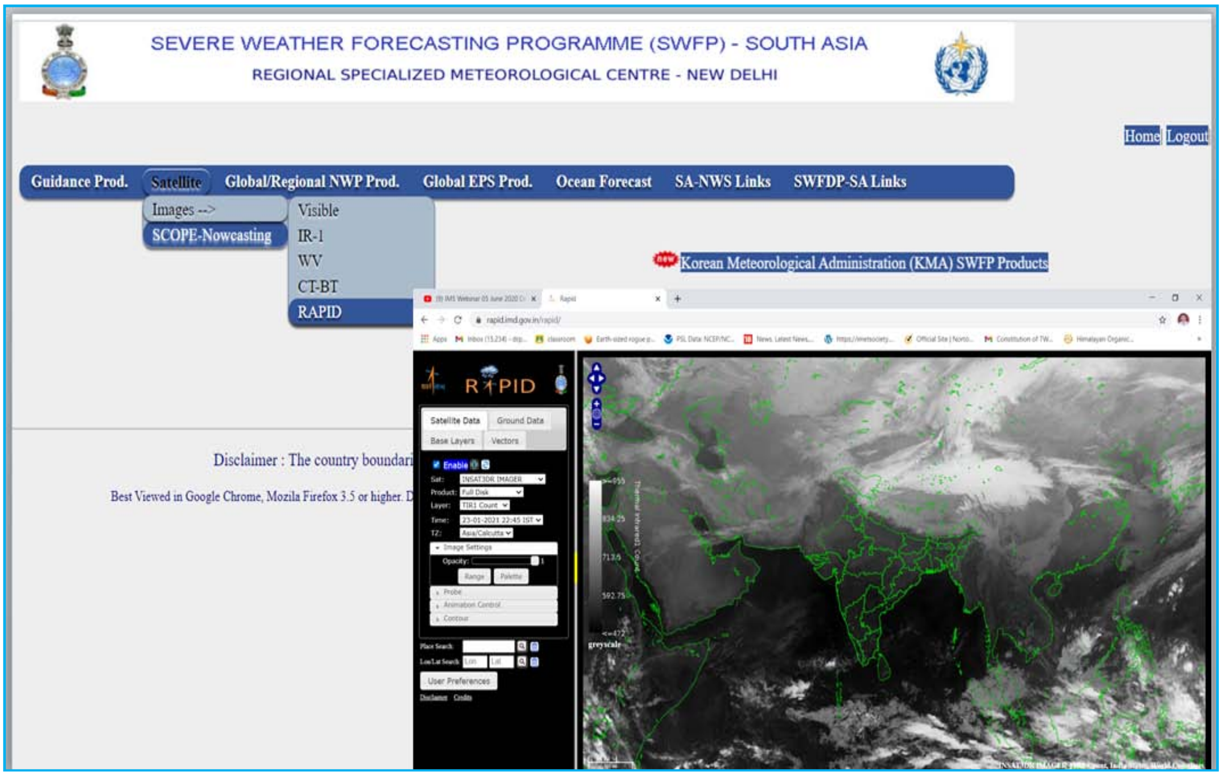

3.3. *Other NWP/EPS Products (Short Range to Extended Range)*

(Extended Range Severe Weather Products)

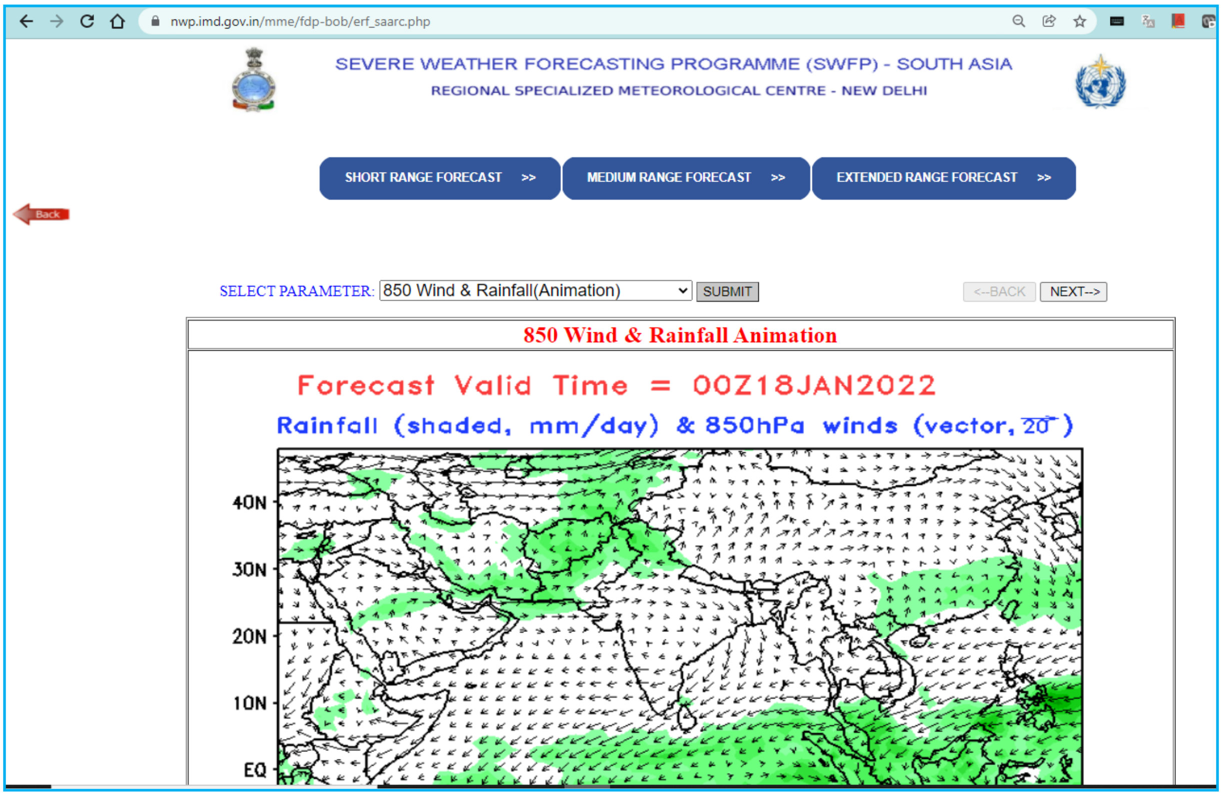

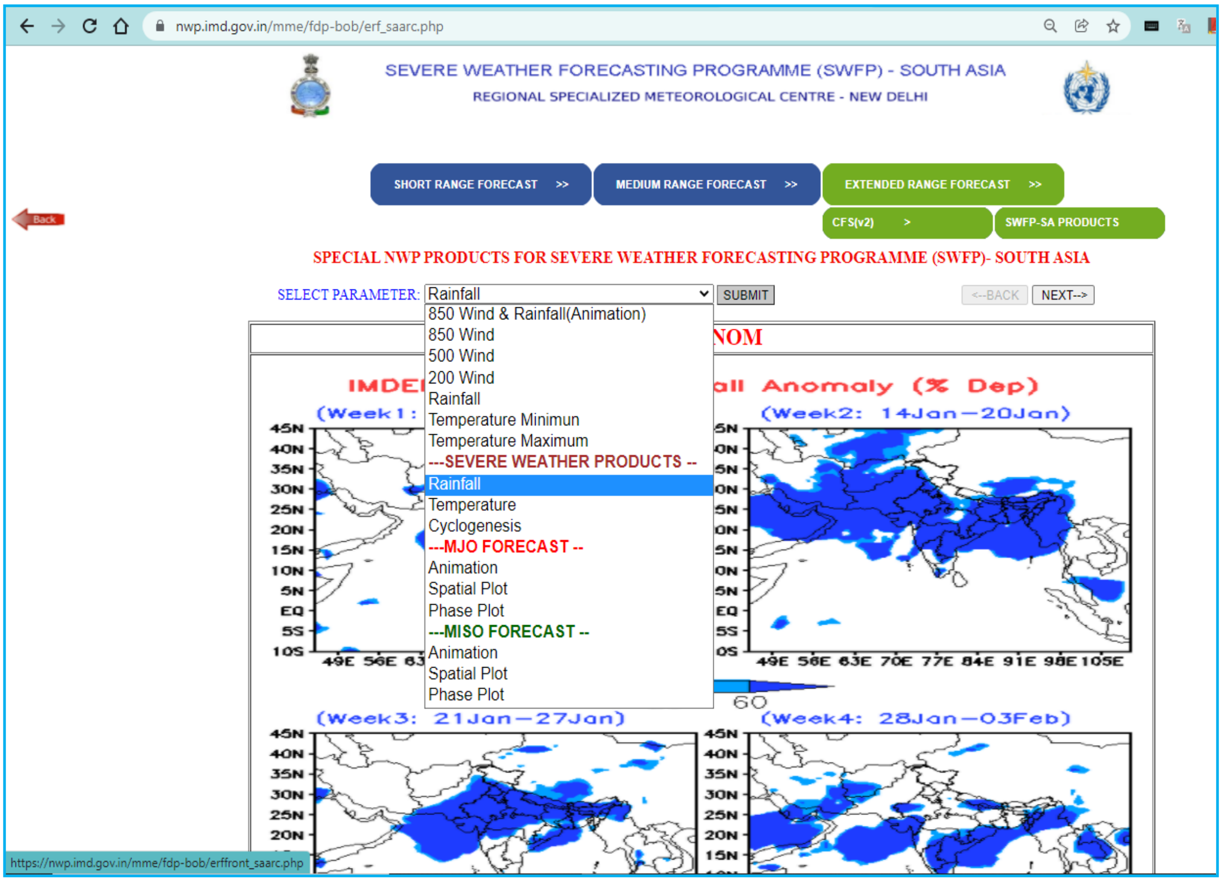

Meteograms from IMD GFS & IMD WRF models

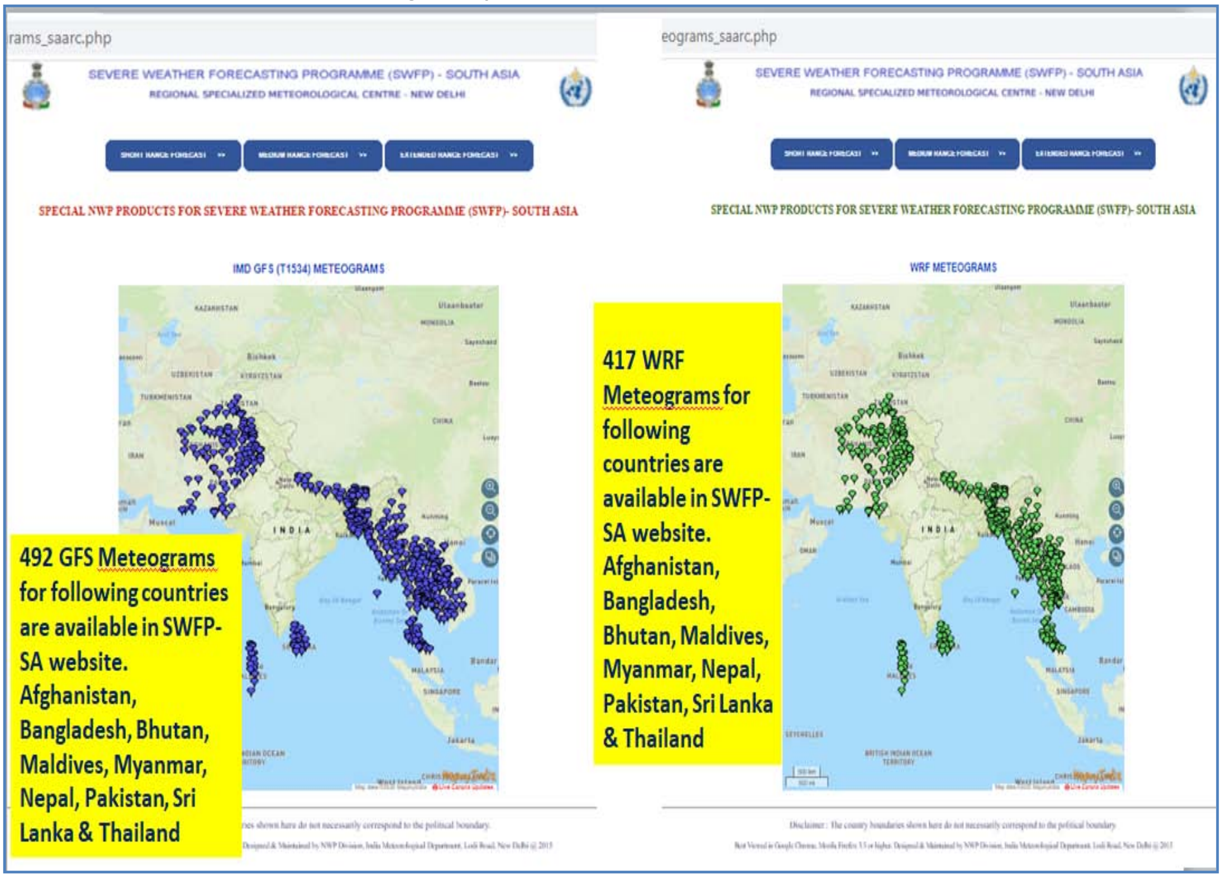

JMA Products, ECMWF, UKMO(EPSgrams) at 4 times a day are available along with EPS products from IITM, Pune (GEFS model) and NCMRWF (NEPS model). The ECMWF products are accessed through separate login credentials provided to each country.

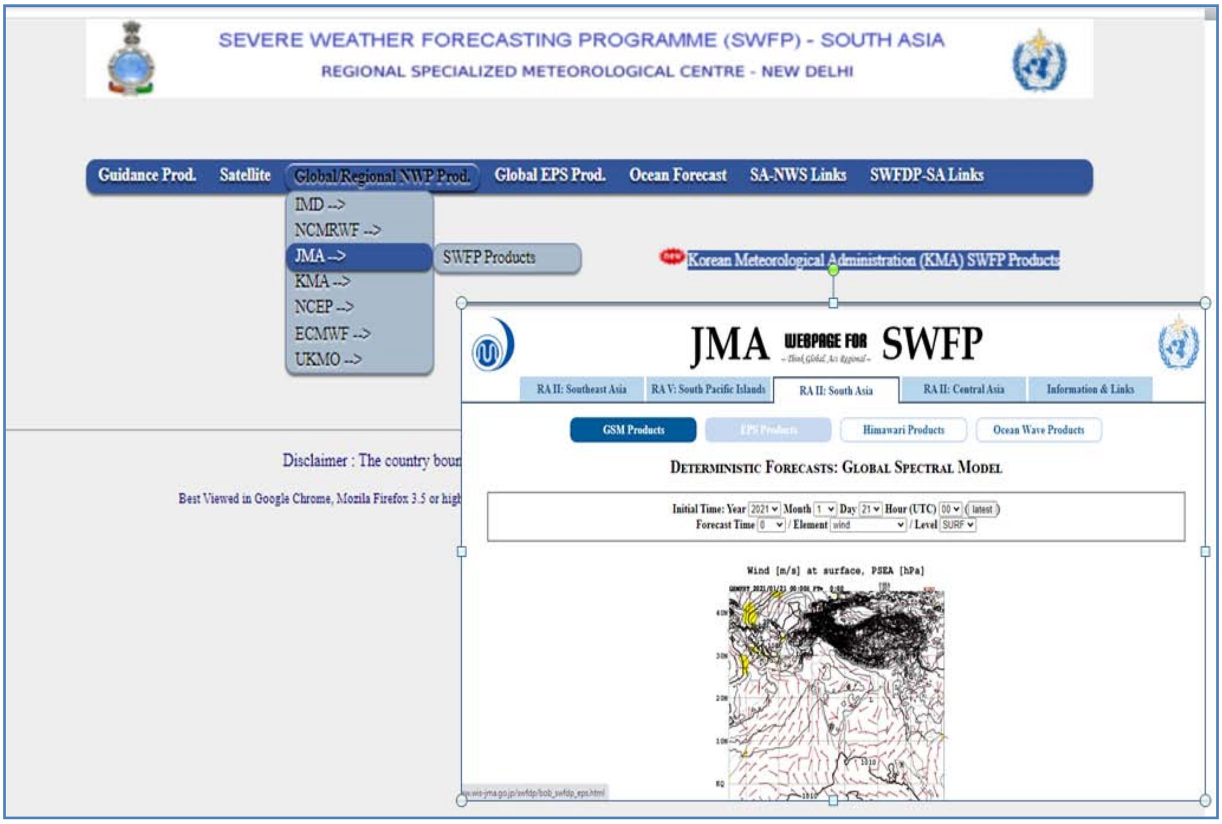

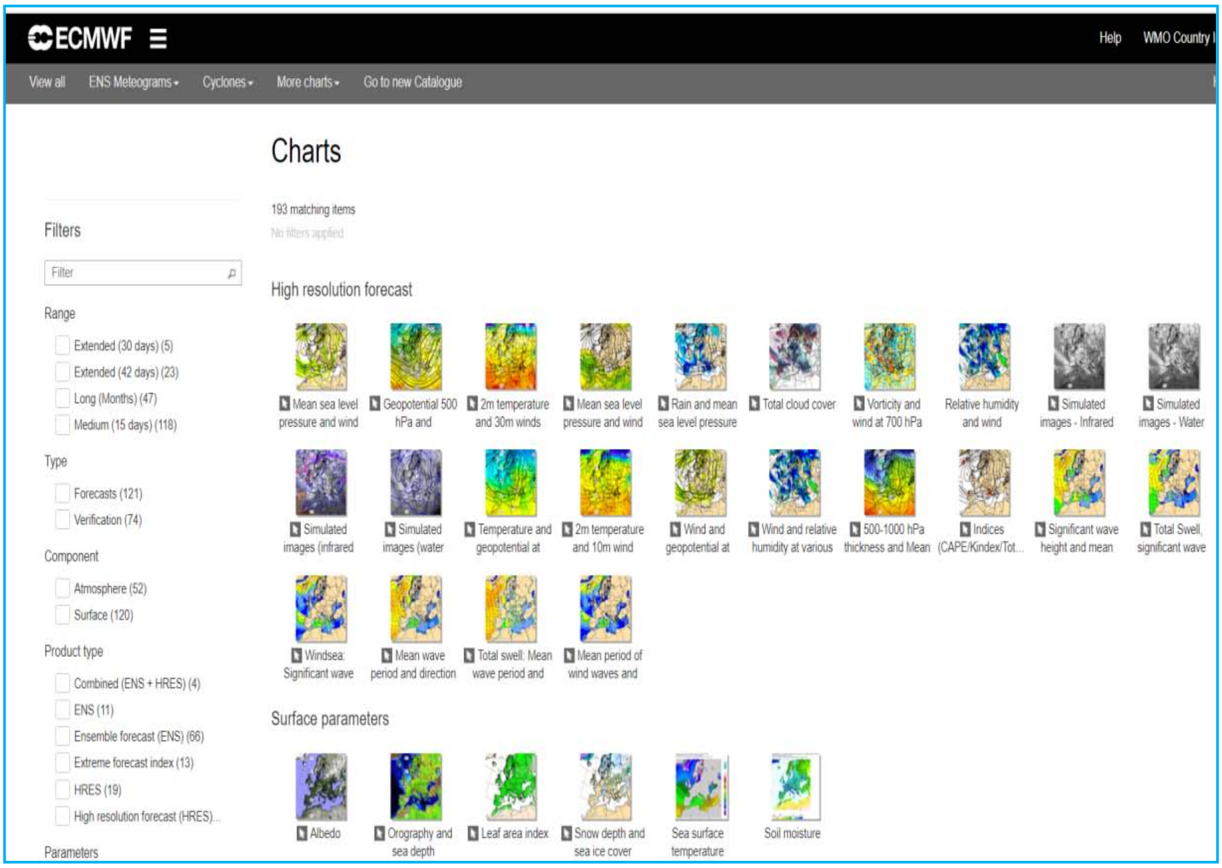

UKMO meteograms

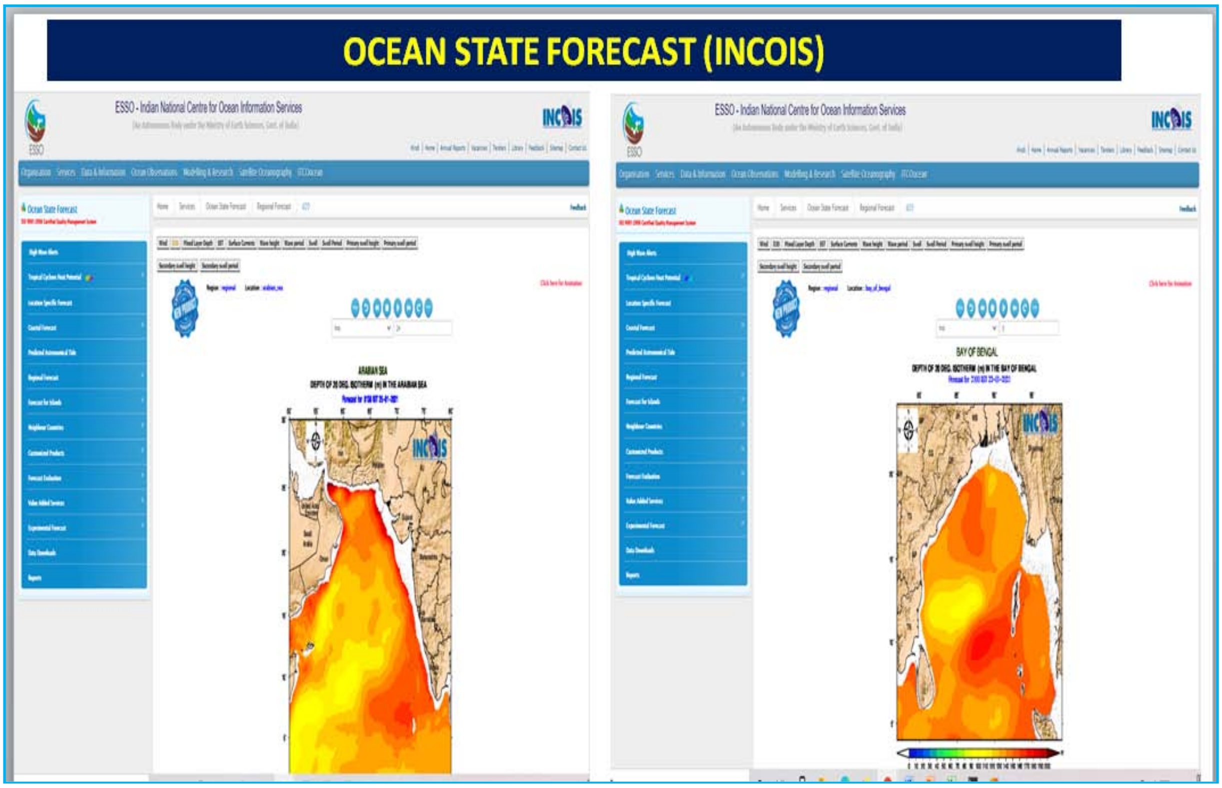

Finally, all the website addresses of NMCs are also provided.

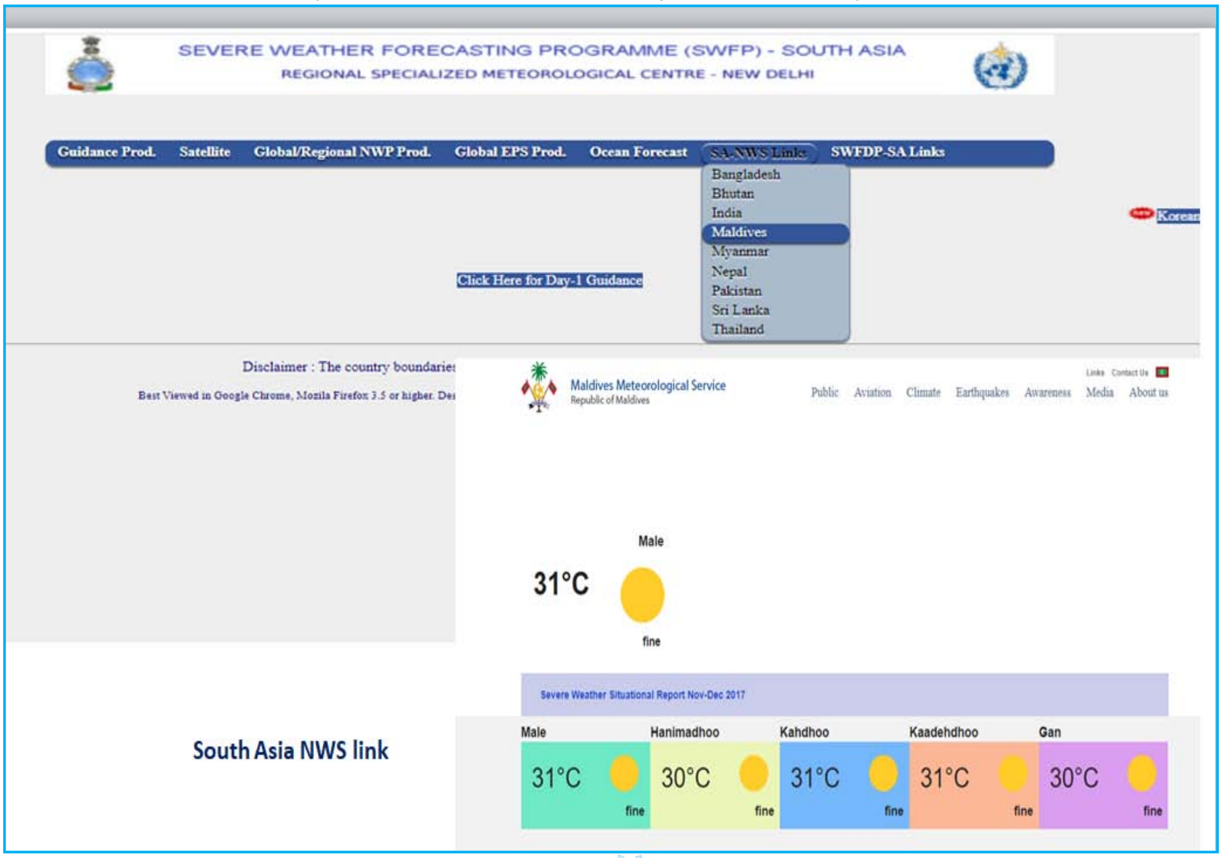

CHAPTER 12

Numerical Weather Prediction (NWP) Model Forecast Data Supply

SATENDRA KUMAR

IMD NWP division is regularly supplying model forecast data to various institutes and also the disaster management centres for operational use and also for collaborative study. In last one decade there have been increases in number of models that are running operationally in IMD. At present high resolution (About 12 km) global model like GFS & high resolution (About 12 km) Global Ensemble Model like GEFS forecasts for medium range; regional model like Weather Research Forecast (WRF) model at 3 km resolution for short range forecast; and Climate Forecast System (CFS) coupled model for the extended range forecast up to 4 weeks. The NWP division is uninterruptedly supplying NWP model forecasts data daily available in various format on operational basis to many institutes as given below :

1. Indian Air Force (IAF)
2. Central Water Commission (CWC)
3. The Regional Integrated Multi-Hazard Early Warning System (RIMES)
4. Flood Management Information System Cell (FMISC) in Bihar & Uttar Pradesh
5. Geohazard Research & Management (GHRM) Centre, Kolkata
6. Centre for Development of Advanced Computing (CDAC)
7. The Energy and Resource Institute(TERI)
8. Jhelum and Tawi Flood Recovery Project(J&TFRP)
9. 50 HERTZ ENERGY PRIVATE LIMITED (MANIKARAN)
10. Extended Hydrological Prediction under National Hydrology Project (CWC-EHP)
11. Watershed Organization Trust (WOTR)
12. Geological Survey of India (GSI)
13. National Disaster Management Authorities (NDMA)
14. SDMA in Kerala, Andhra Pradesh, Odisha, Telangana.
15. Power System Operation Corporation Limited (POSCO)
16. Uttar Pradesh Power Corporation Limited, UPPCL, Lucknow
17. The Bhakra-Nangal Dam
18. Indian Institute of Remote Sensing (IIRS), Dehradun
19. Water Resource Department (WRD), Punjab
20. Center for Snow and Avalanche Study Establishment (SASE)
21. Polar Met Services (PMS)
22. The National Highways Authority of India (NHAI)

In addition NWP data for R&D Purposes is provided to : DRDO, TERI, NRSC, IGCAR, IIT's (Delhi, IIT Bhubaneswar and IIT Gandhinagar, etc).

These NWP model data and product is of different types, which include direct model outputs, derived graphics, time series data etc as given below.

- Direct Model Outputs
- Model Derived Graphics Plot & Data

- Processed data
- Aviation Products
- District Level Forecast
- Time Series Data
- Meteograms
- Amarnath, Chardham Yatra Forecast
- National Highway Forecast
- Antarctica Forecast
- Aviation Products
- Block Level Gridded Data:

There have been increase in the number of departments and institutes those who are taking data for operational basis. Also the volume of data have been increased in last 7 years with 56.26 TB of data in 2015 to 87.68 data in 2021 (Fig. 12.1).

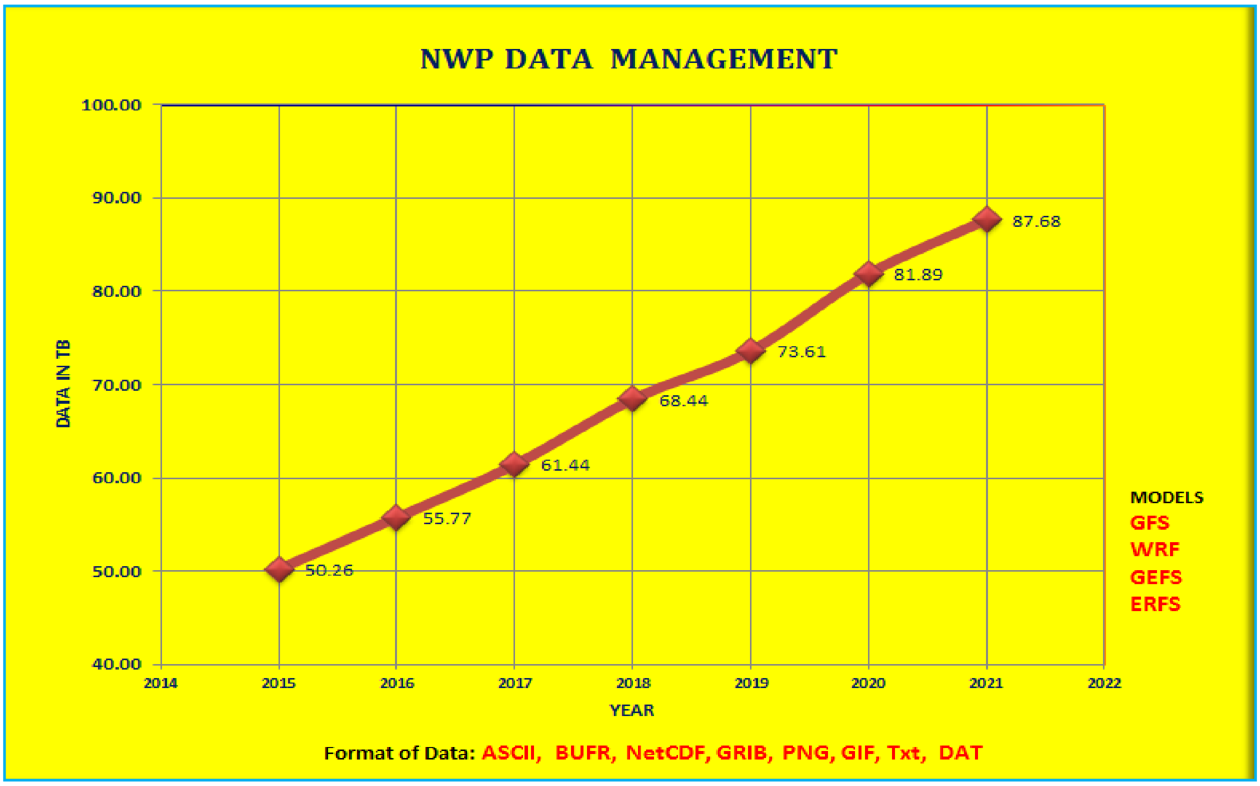

Fig. 12.1. Increase of NWP model data supply to various users in last 7 years

CHAPTER 13

Development of New Webpages for NWP Products Dissemination

PRADEEP MISHRA

- District wise MME Rainfall forecast for 05 days.
- River Basin MME Rainfall forecast for 05 days.
- Wind speed Probability Plots for 10 Days for IMDGEFS & NCEP Models.
- IMDGEFS MJO monitoring, forecast and verification.
- Delhi NCR - Urban Weather & Air Quality Forecast for Mausam Website.
- Addition of HRRR products for South Peninsular India domain.
- Rainfall Intensity & Distribution tables of 05 Models (GFS, JMA, NCUM, NCEP, GEFS) for 05 Days forecast.
- Addition of SILAM Dust Forecast Maps.
- SSL Certificate updated on NWP Website to increase security.
- Web based past 07 Days Archive of WRF & GFS Model Plots for various parameters.
- Panel Plot of Multi Models (GFS, NCEP, JMA, NEPS, GEFS, NCUM, WRF, NCUM-R, ECMWF) for current and past 07 days.
- Rainfall Intensity & Rainfall Distribution csv files for ISSD Division.
- New ERF SAARC webpage without Password.
- Observed Weekly TMax and TMin Products.
- Special NWP Products for Severe Weather Forecasting Programme (SWFP)- South Asia, comprising Short, Medium & Extended Range Products.
- Addition of MJO & MISO plots in ERF webpage for South Asia.
- ERF South Asia Products without Password.
- 04 weeks State wise ERF forecast plots TMax, TMin & Rainfall & anomaly for use by MCs/RMCs.
- 04 weeks ERF District Level forecast for Minimum, Maximum temperature (Bias Corrected) & anomaly & Rainfall.
- ERF Sub-Division wise Maximum & Minimum Temperature Time series (Experimental).
- ERF Land Surface Products for weekly observed conditions, Daily forecast variable, Weekly forecast cumulative, anticipated weekly changes, SRI & SSI on NWP website.

Following new webpages have been created for the use of forecasters on NWP & SWFP-SA Website.

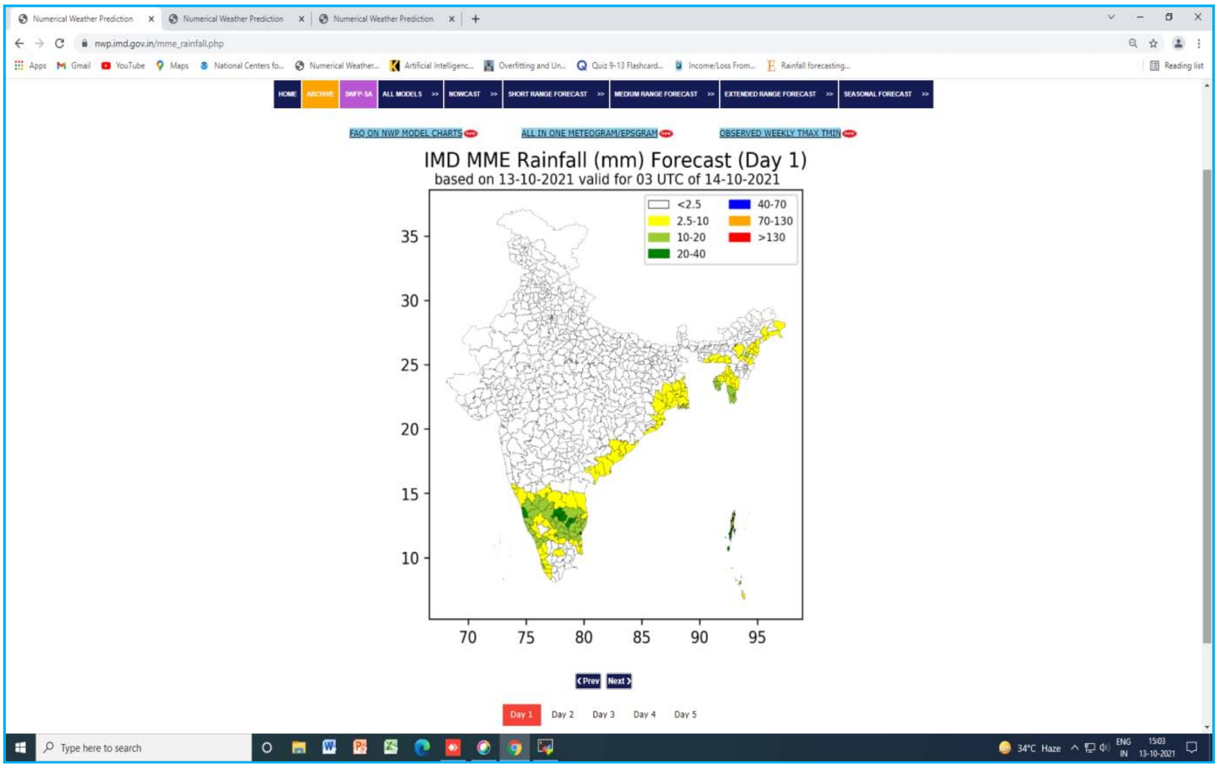

District wise MME Rainfall forecast for 05 days

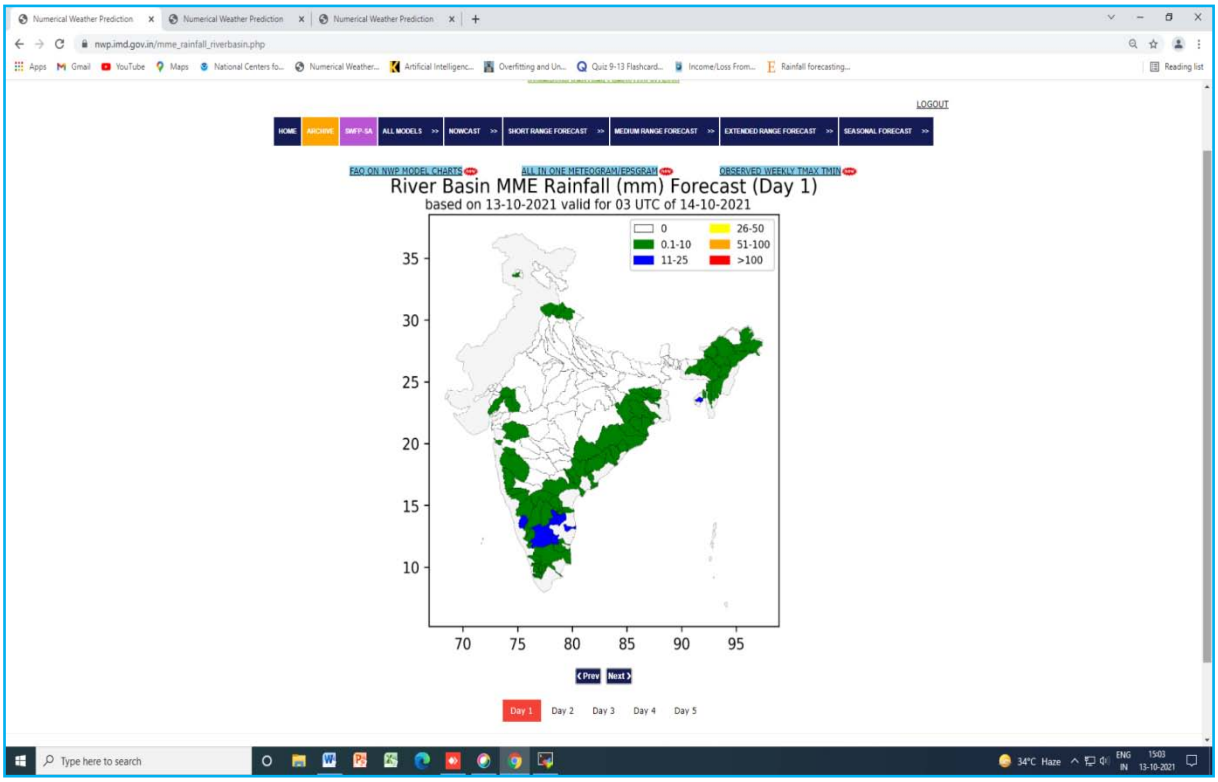

River Basin MME Rainfall forecast for 05 days

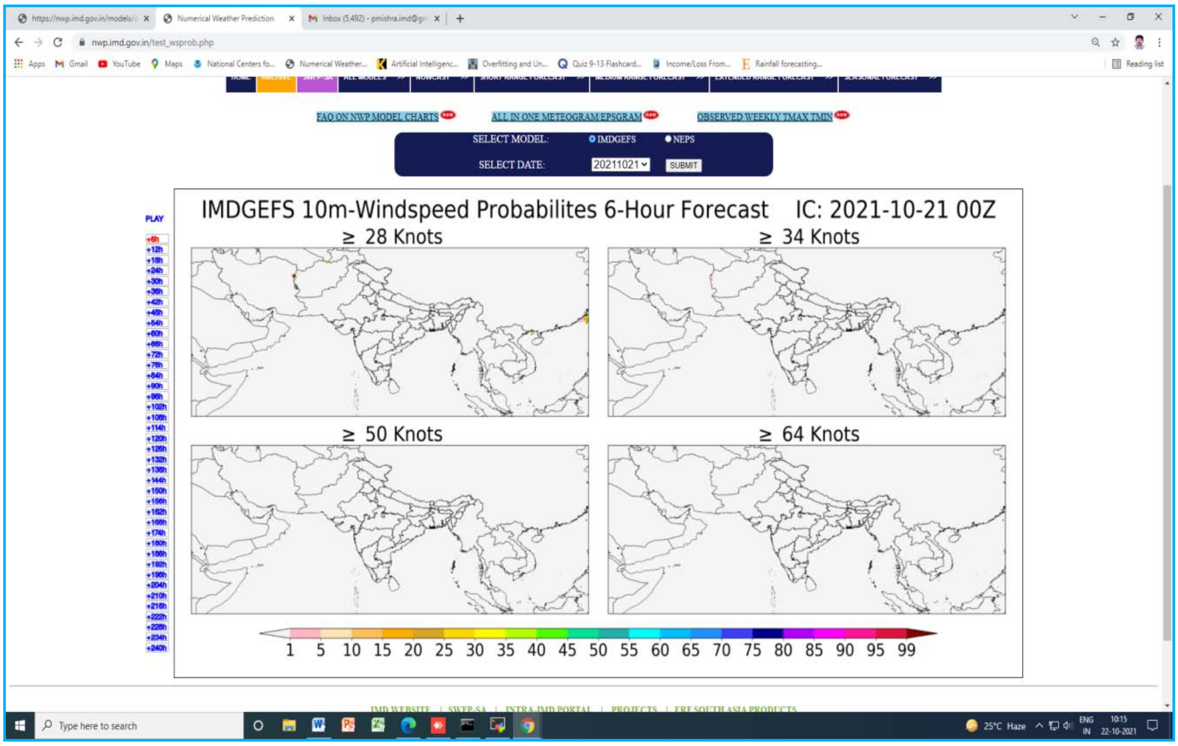

Wind speed Probability Plots for 10 Days for IMDGEFS & NCEP Models

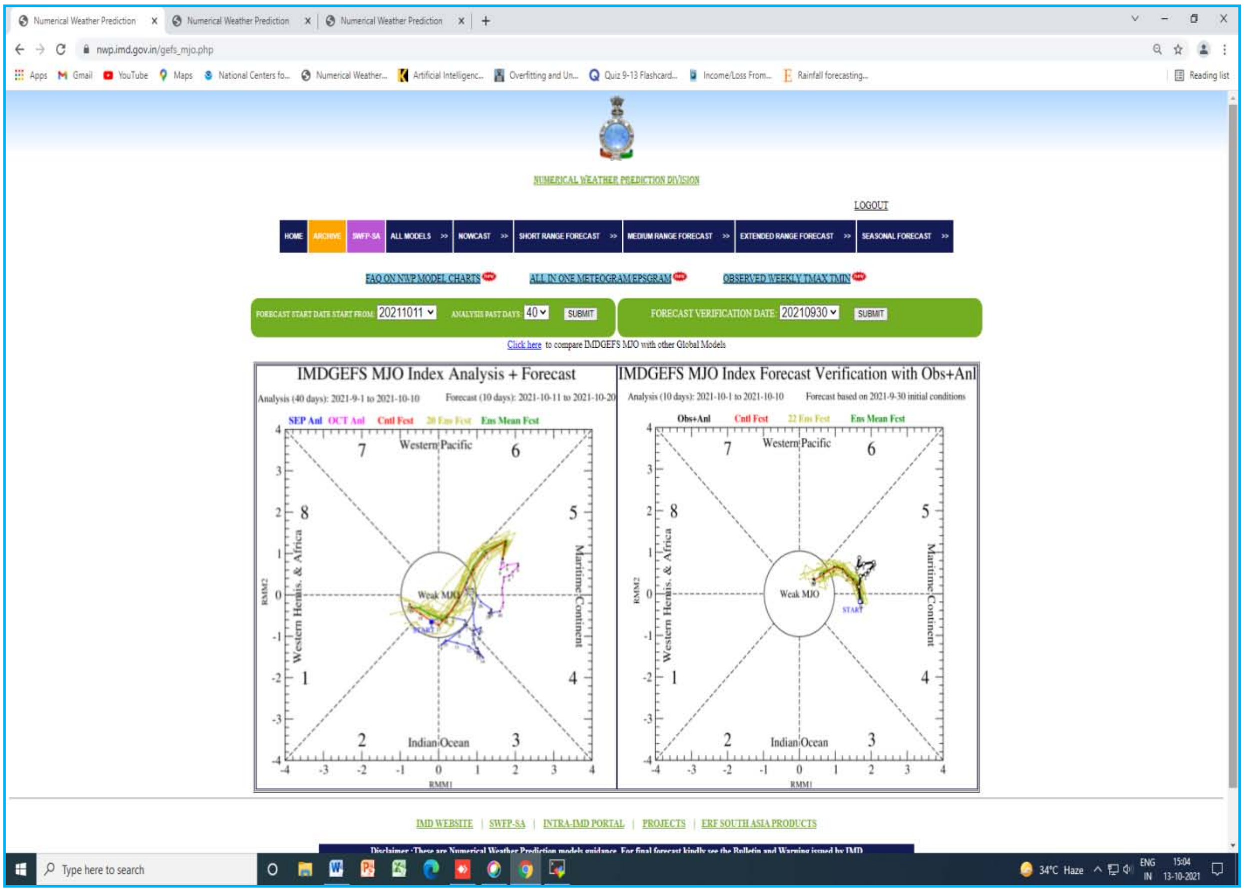

IMDGEFS MJO monitoring, forecast and verification

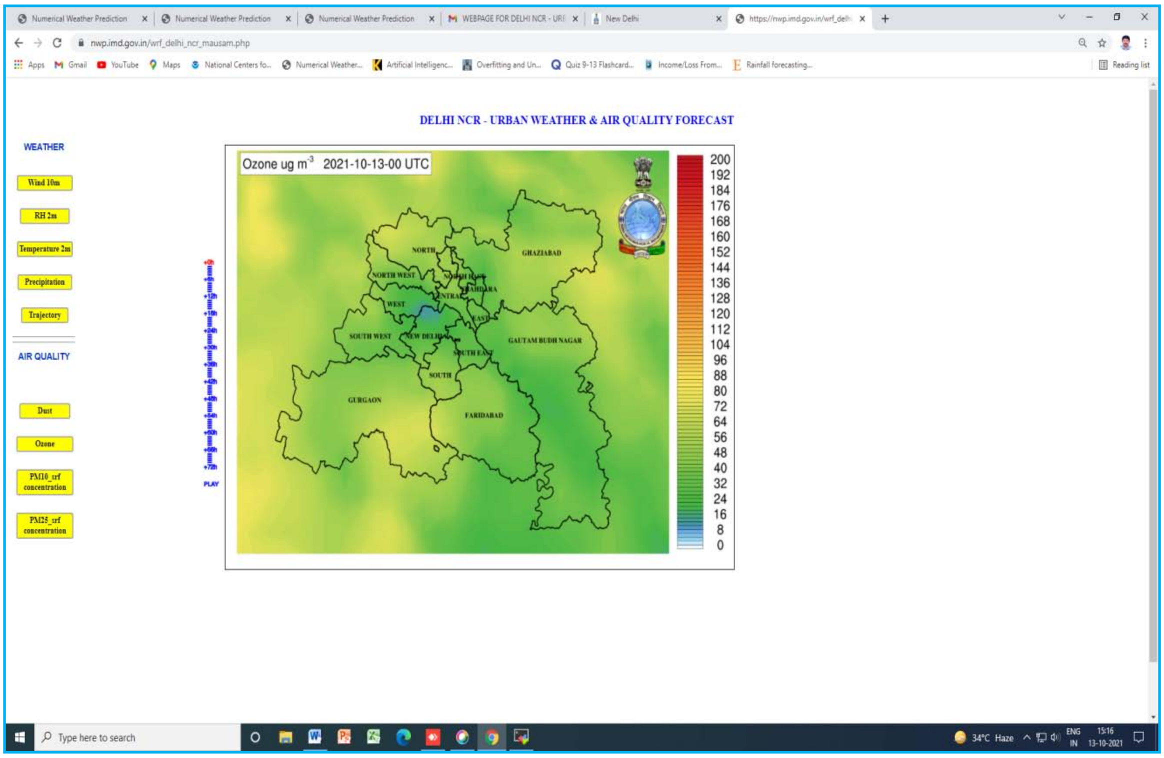

Delhi NCR - Urban Weather & Air Quality Forecast for Mausam Website

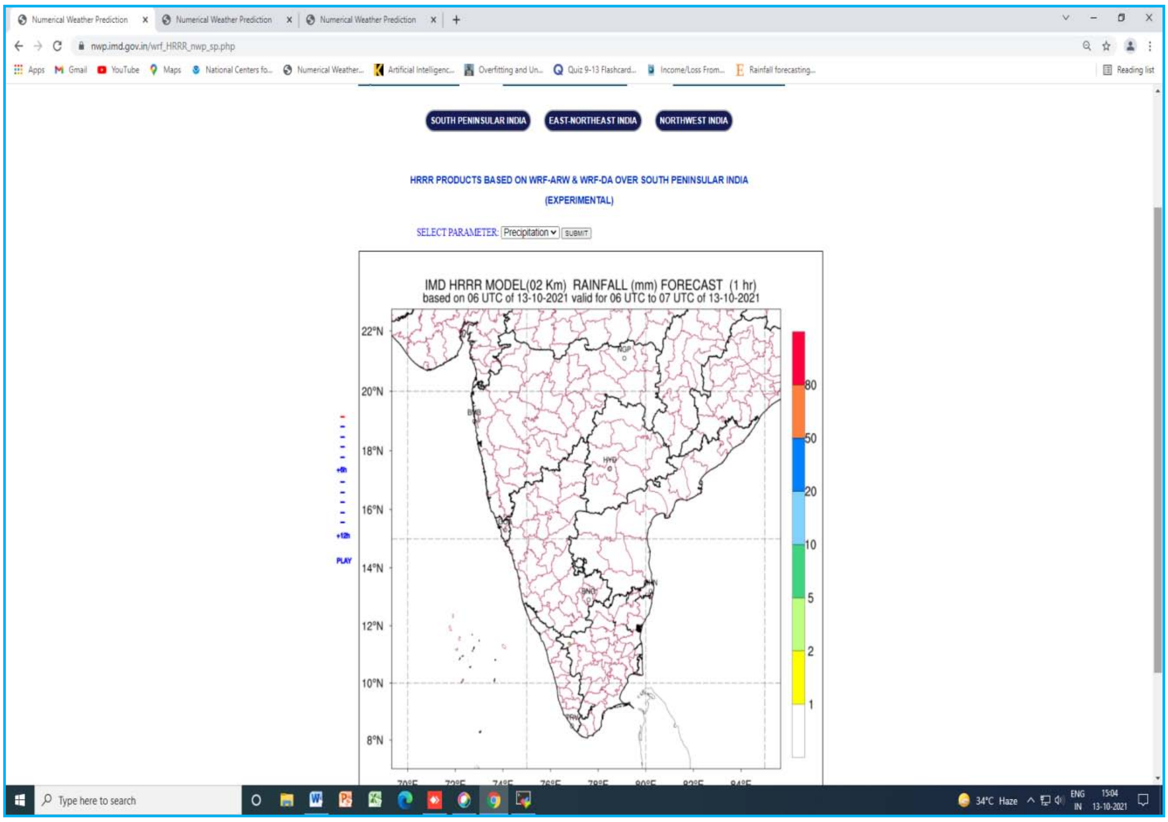

Addition of HRRR products for South Peninsular India domain

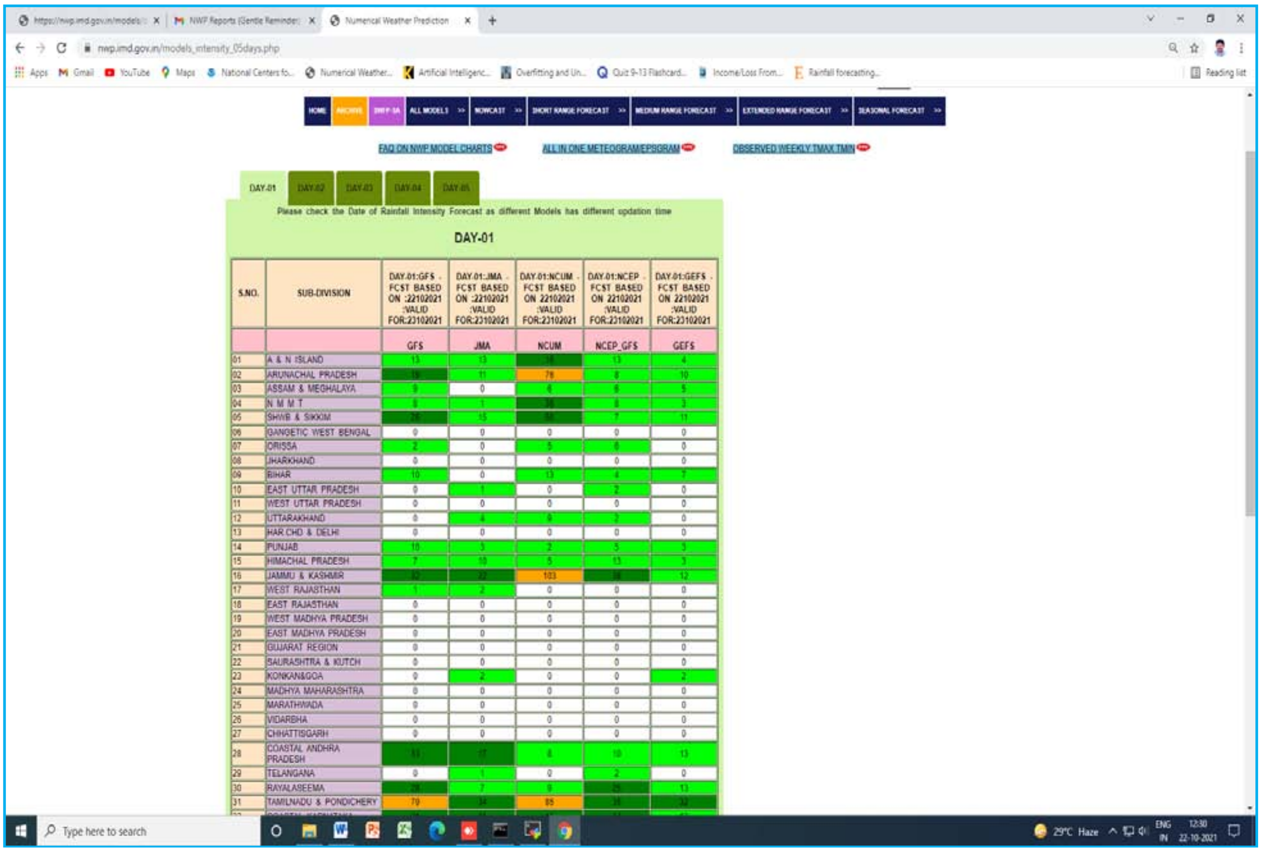

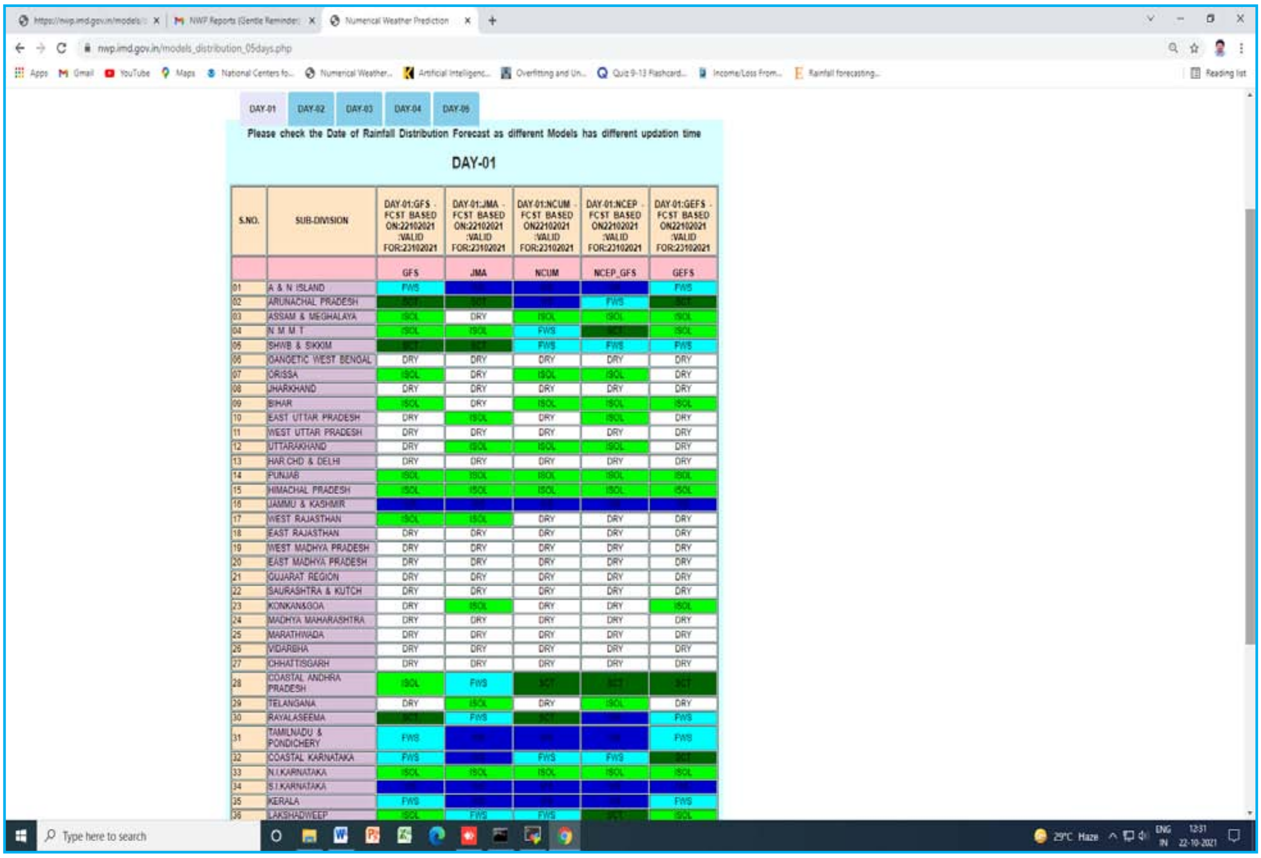

Rainfall Intensity & Distribution tables of 05 Models (GFS, JMA, NCUM, NCEP, GEFS) for 05 Days forecast

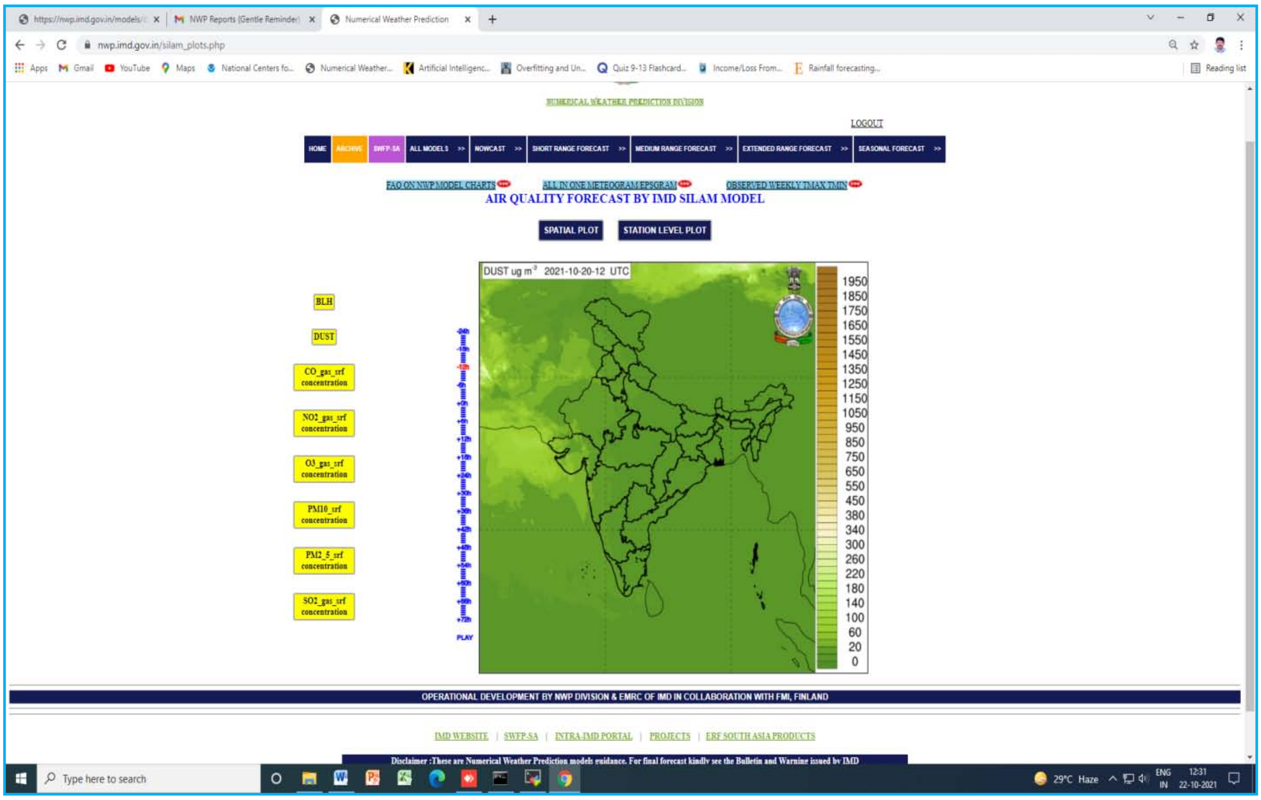

Addition of SILAM Dust Forecast Maps

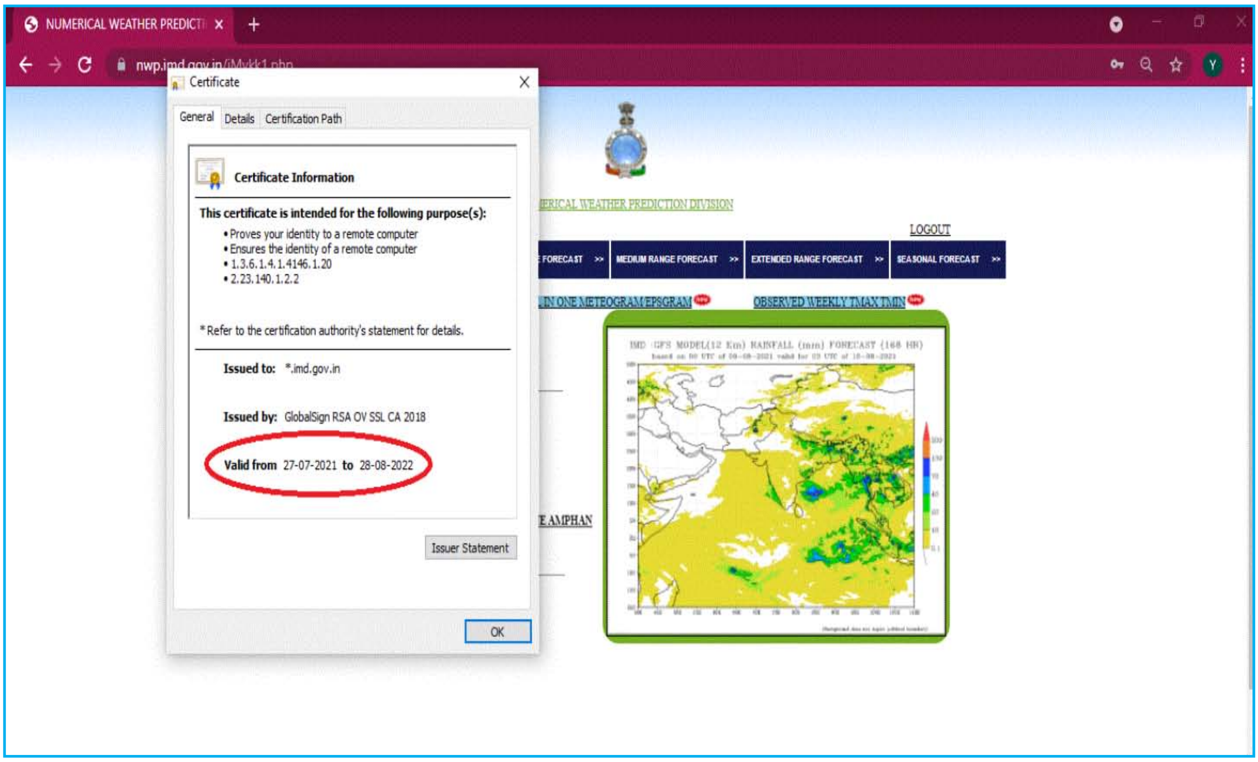

SSL Certificate updated on NWP Website to increase security

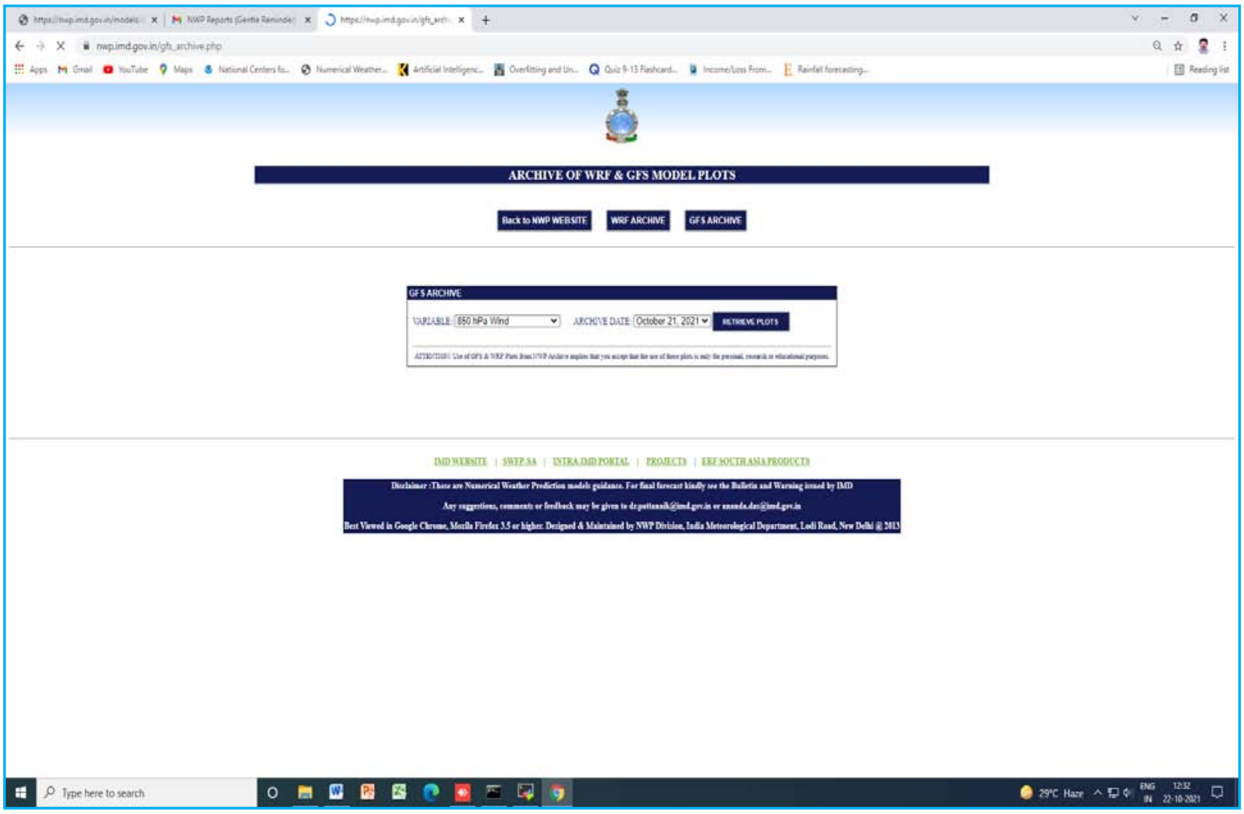

Web based past 07 Days Archive of WRF & GFS Model Plots for various parameters

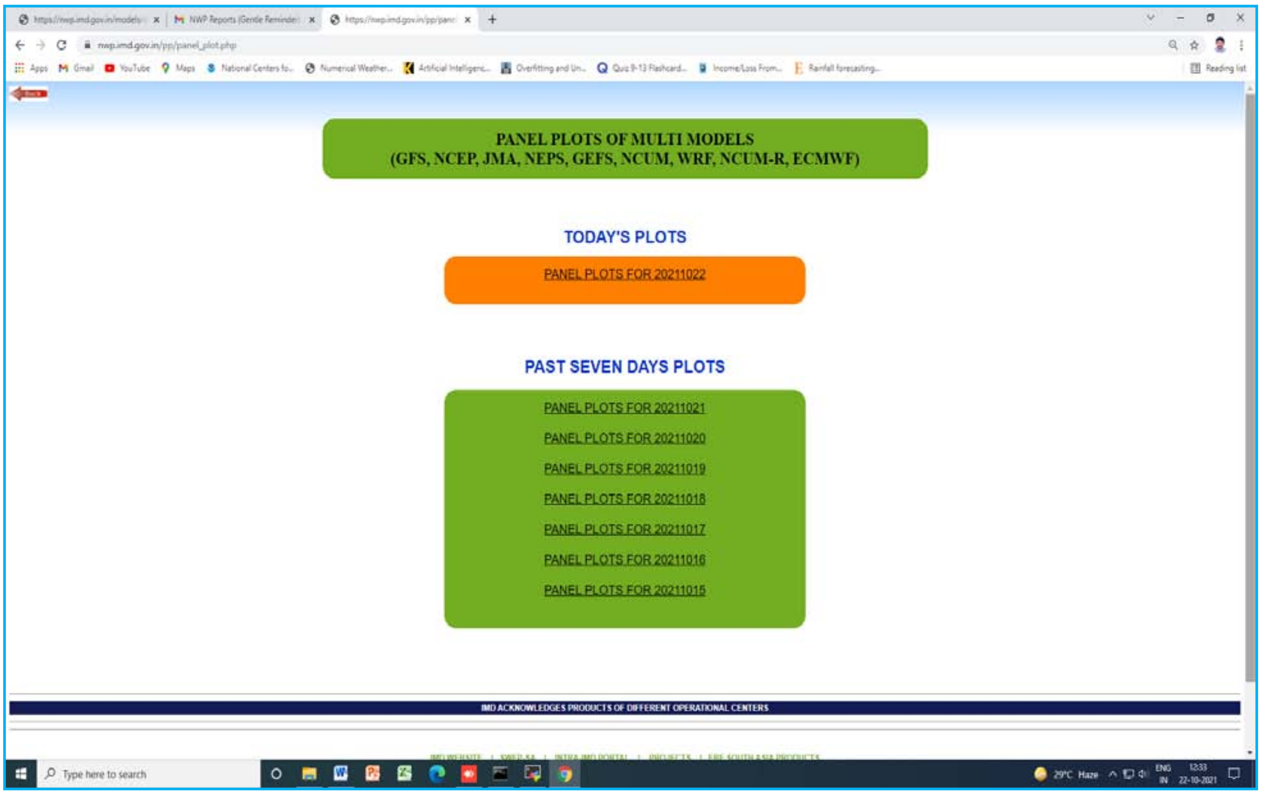

Panel Plot of Multi Models (GFS, NCEP, JMA, NEPS, GEFS, NCUM, WRF, NCUM-R, ECMWF) for current and past 07 days

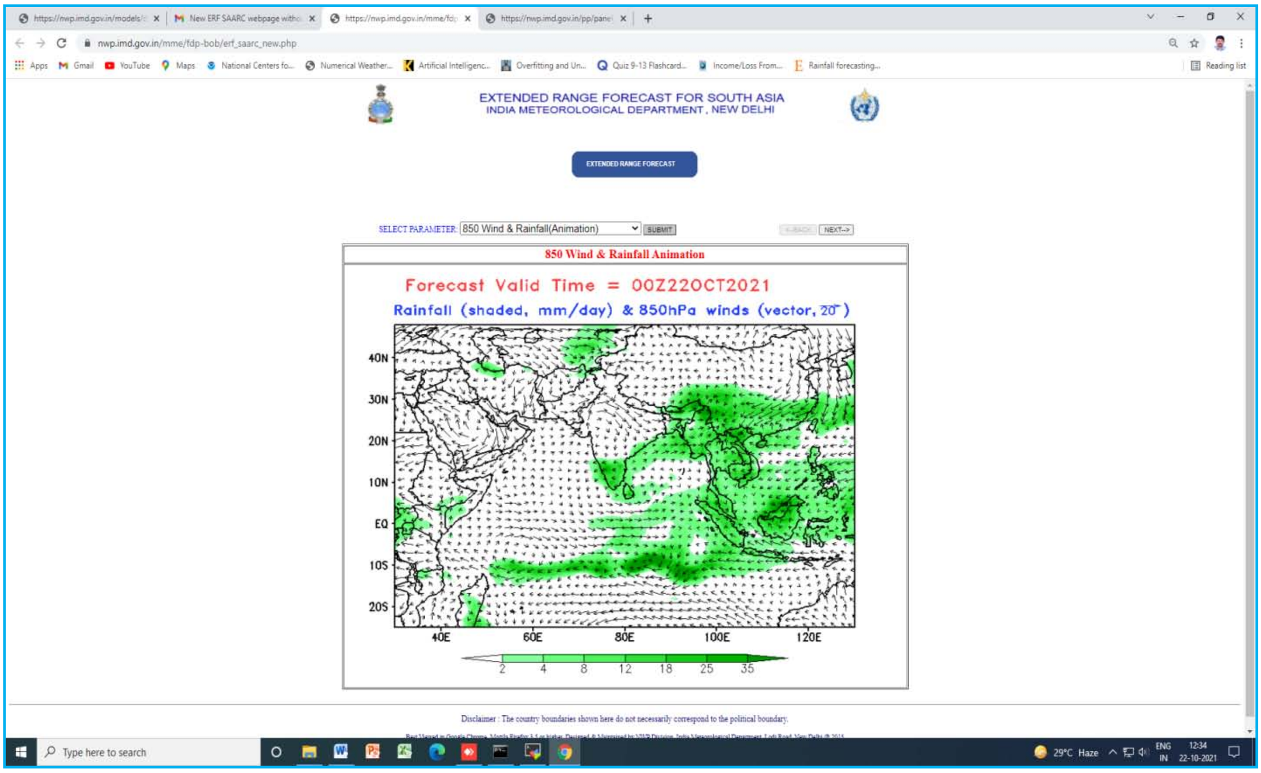

New ERF SAARC webpage without Password

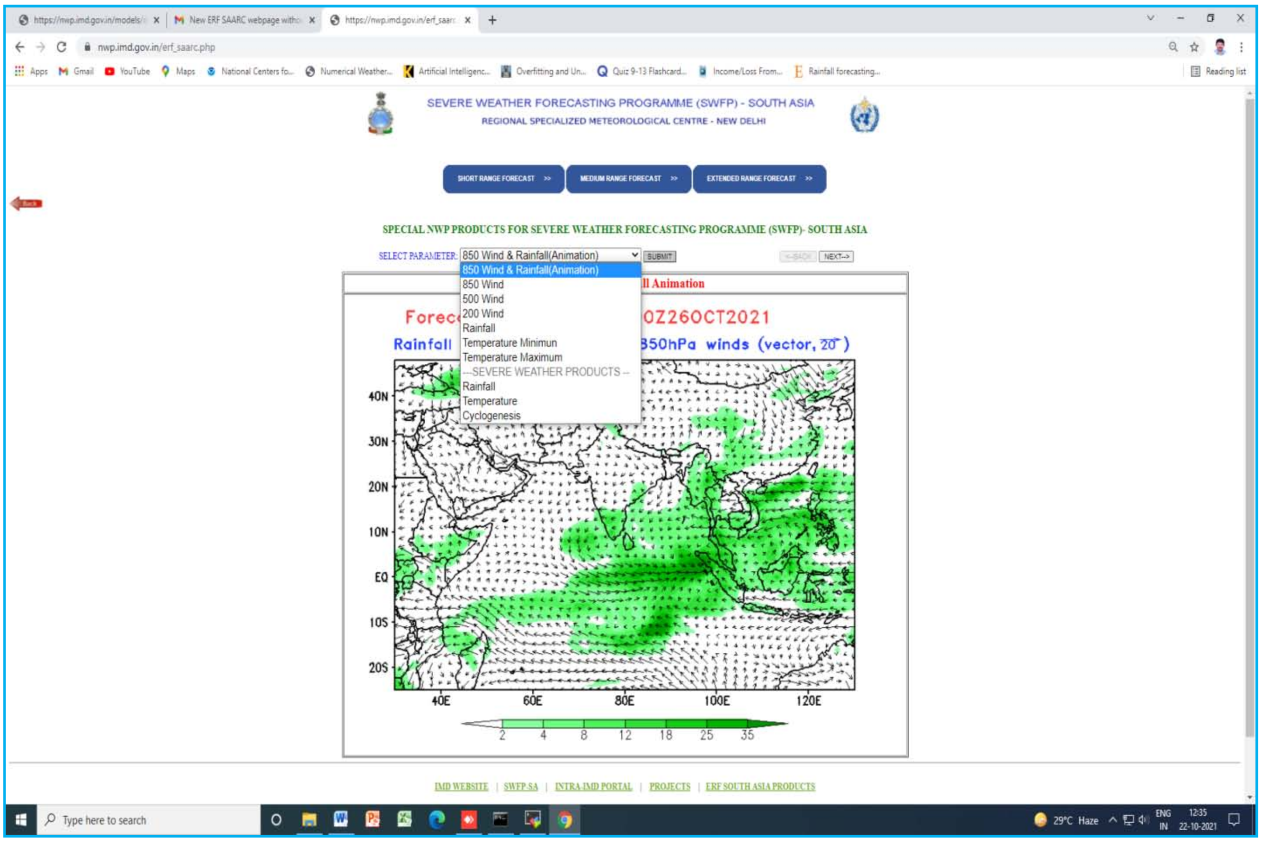

Special NWP Products for Severe Weather Forecasting Programme (SWFP)- South Asia, comprising Short, Medium & Extended Range Products

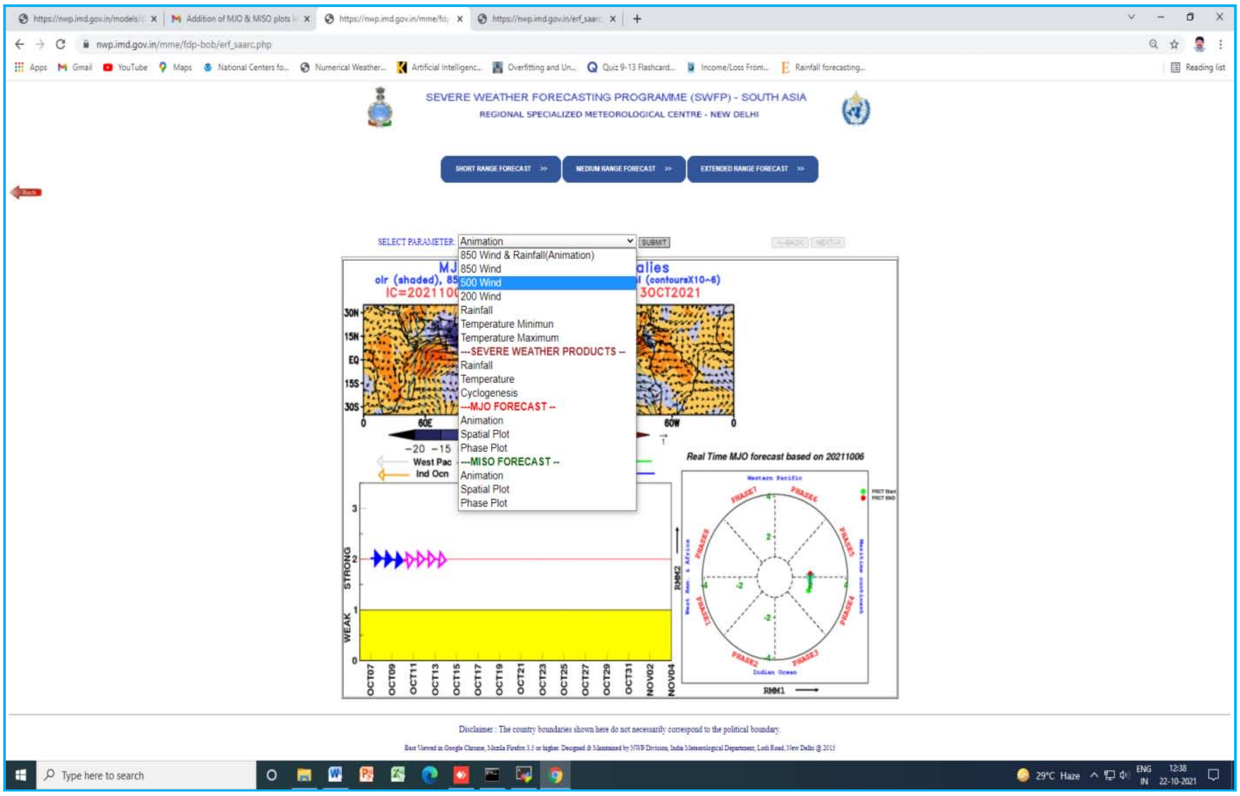

Addition of MJO & MISO plots in ERF webpage for South Asia

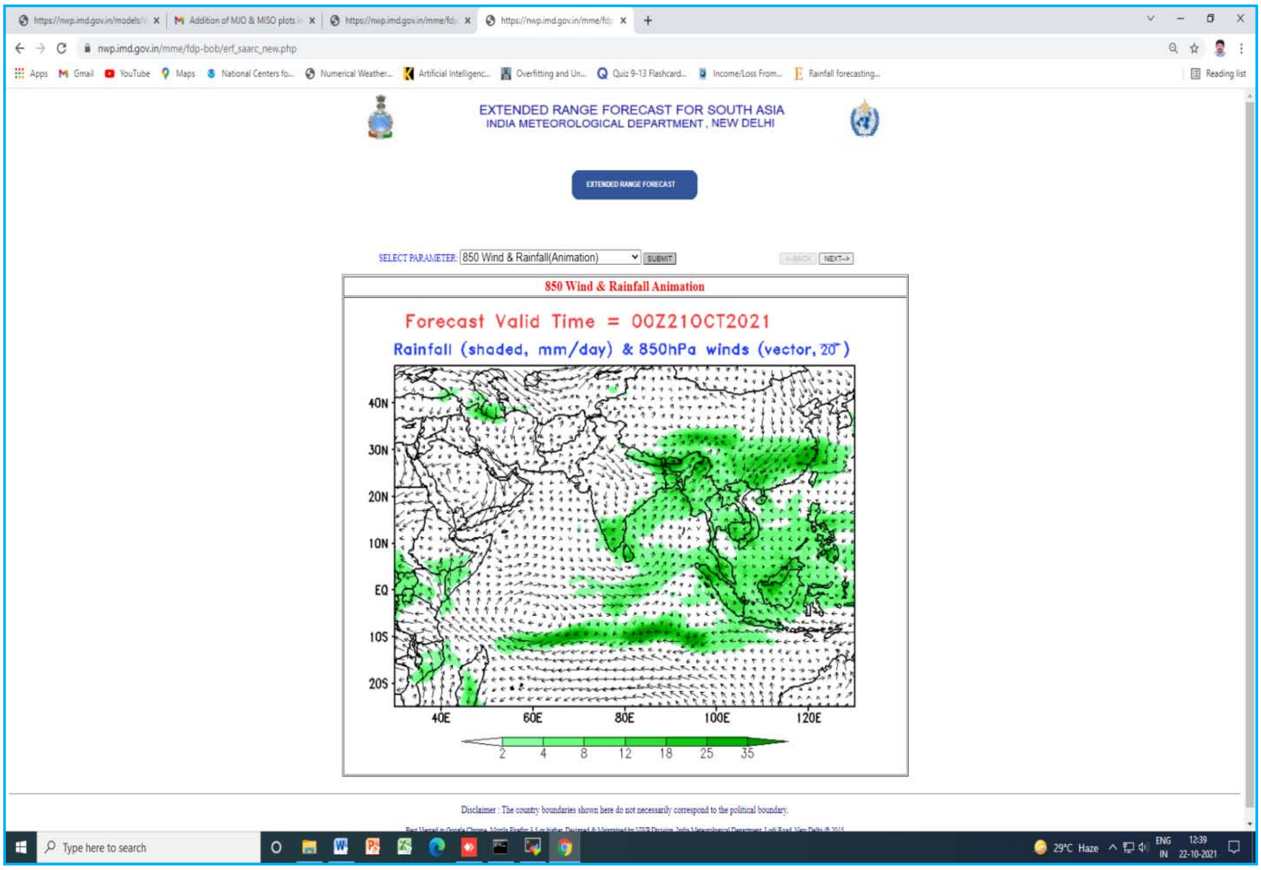

ERF South Asia Products without Password

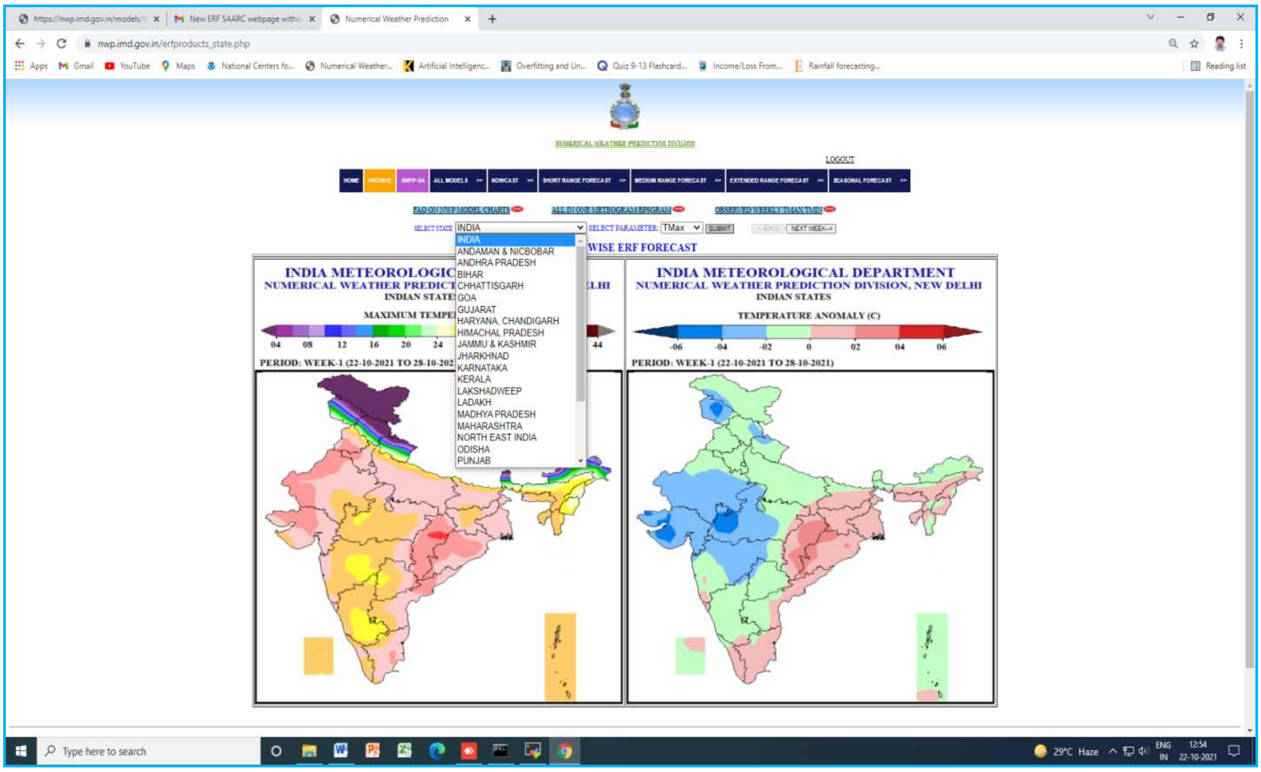

04 weeks State wise ERF forecast plots TMax, TMin & Rainfall & anomaly for use by MCs/RMCs

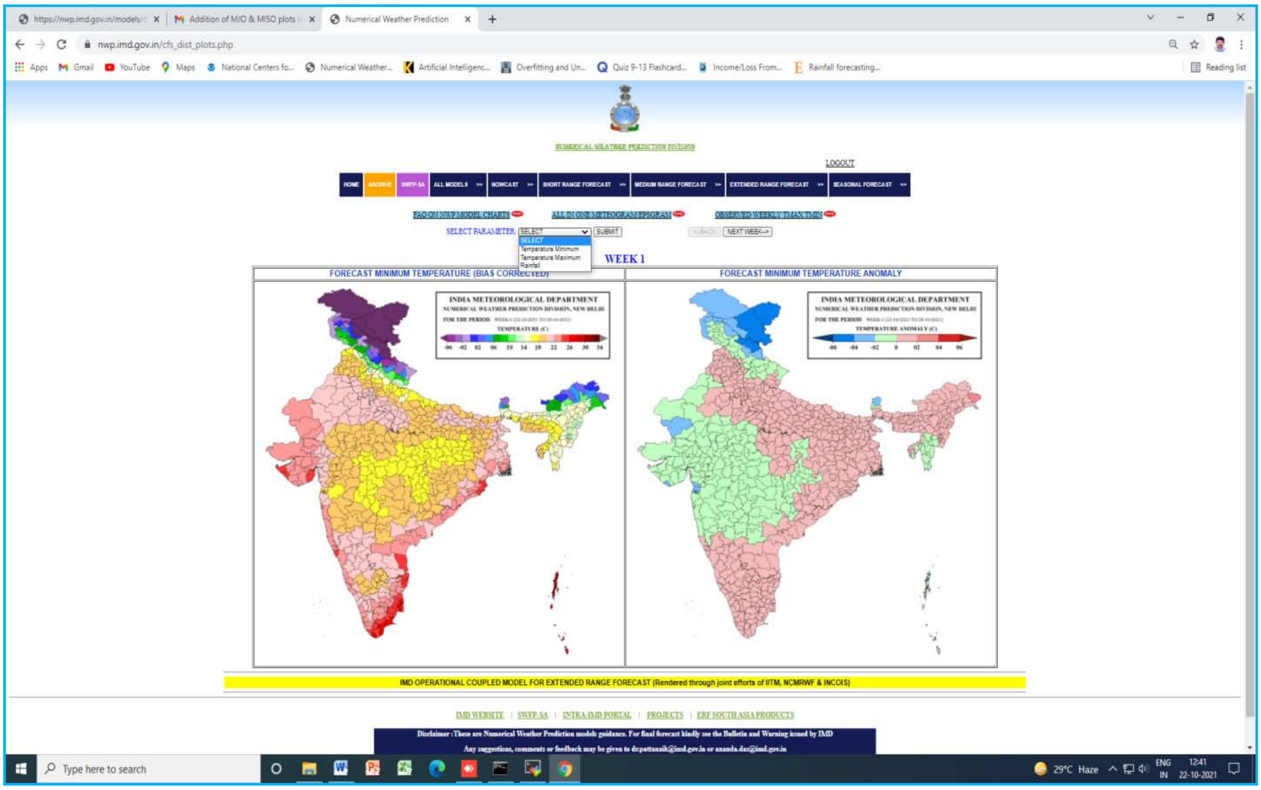

04 weeks ERF District Level forecast for Minimum, Maximum temperature (Bias Corrected) & anomaly & Rainfall

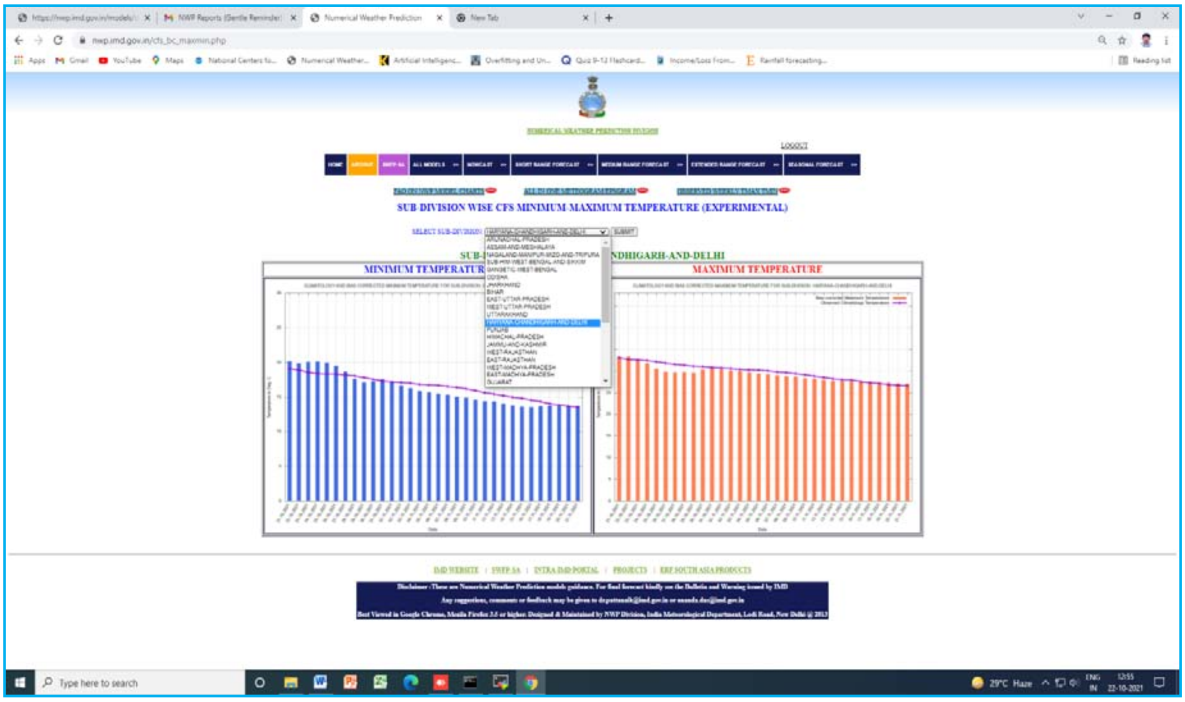

ERF Sub-Division wise Maximum & Minimum Temperature Time series (Experimental)

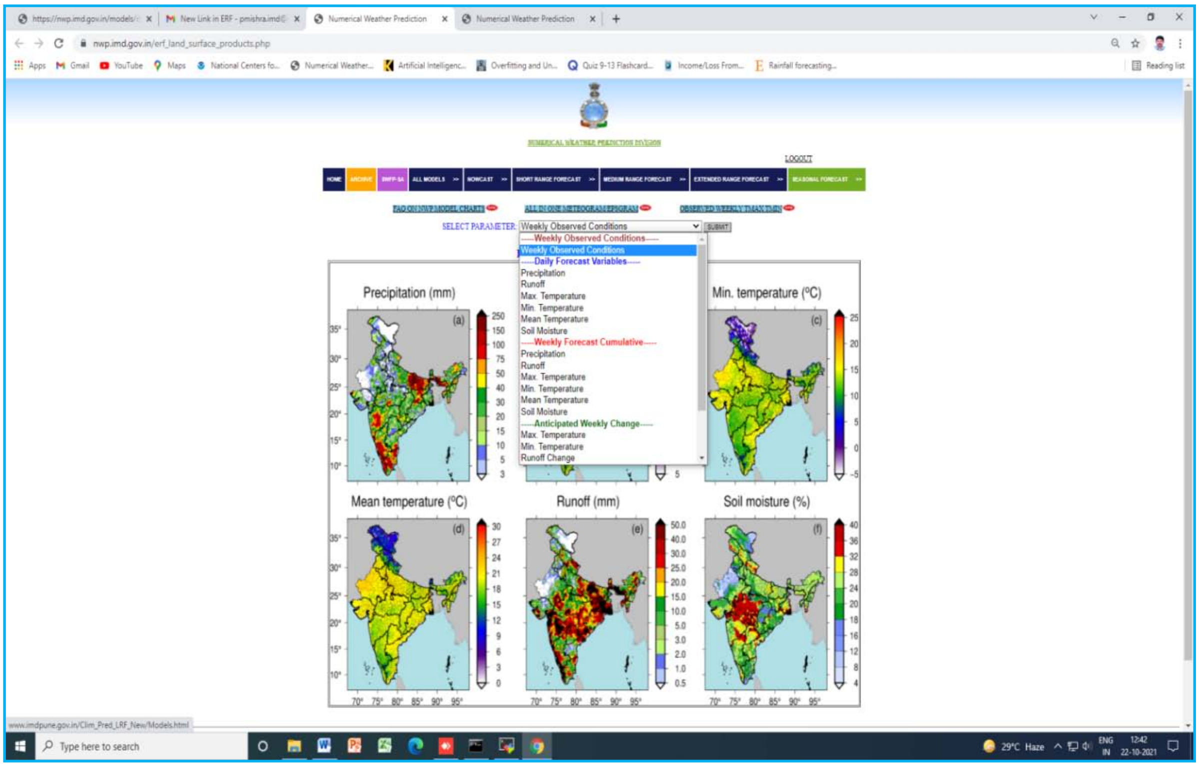

ERF Land Surface Products for weekly observed conditions, Daily forecast variable, Weekly forecast cumulative, anticipated weekly changes, SRI & SSI on NWP website

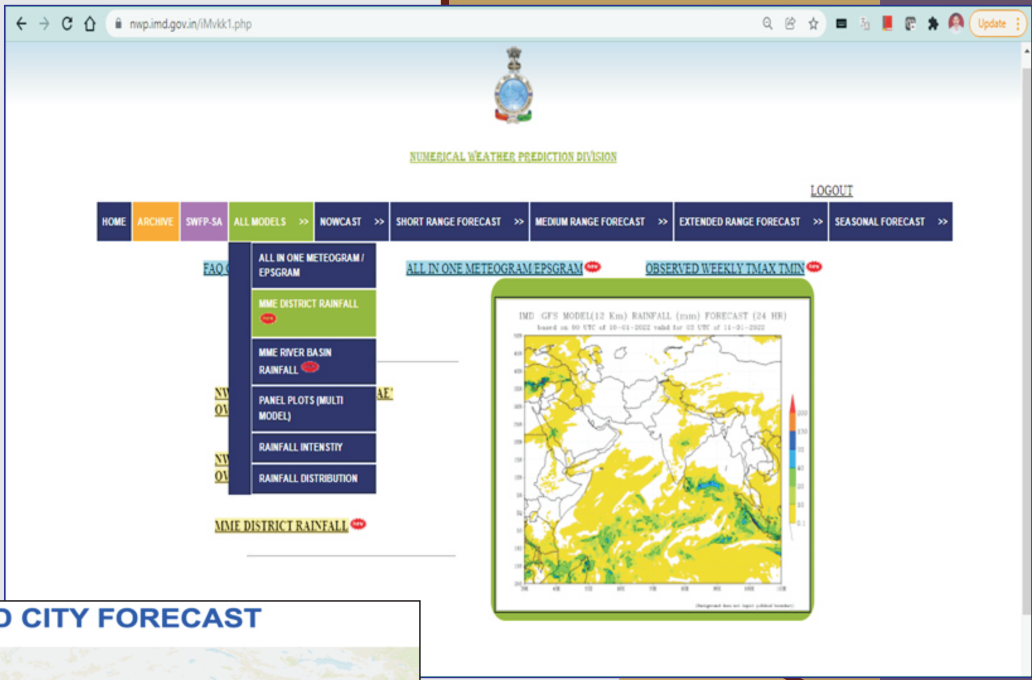

MME BASED CITY FORECAST

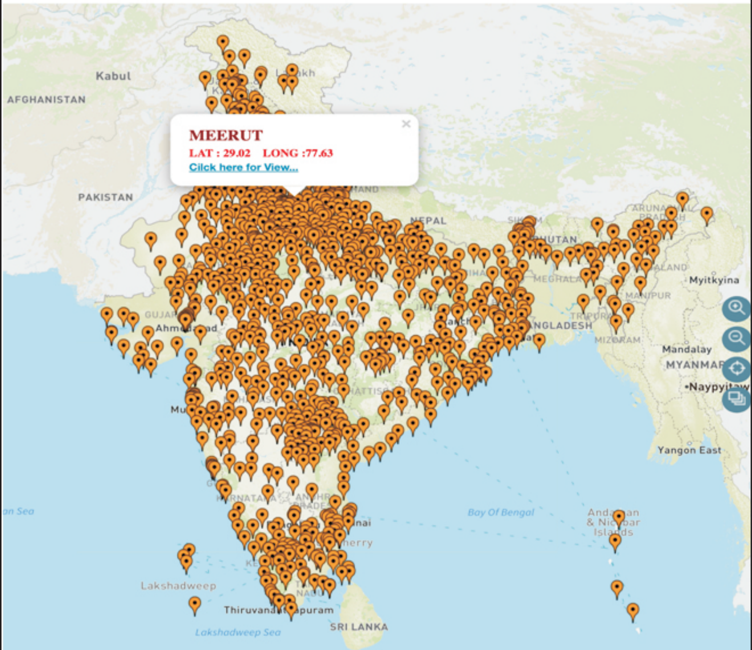

https://nwp.imd.gov.in/models/input/JAIPUR.php - Google Chrome

https://nwp.imd.gov.in/models/input/JAIPUR.php

MME BASED CITY FORECAST FOR :JAIPUR

MAXIMUM TEMPERATURE (DEG. C)BASED ON 20220102

MODEL	DAY1	DAY2	DAY3	DAY4	DAY5	DAY6	DAY7
GFS	22.7	23.3	15.5	17.6	22.1	20.1	21.4
GEFS	22.0	22.5	16.1	17.9	20.1	21.7	22.2
NCEP	21.6	22.9	21.6	21.9	23.9	23.3	23.1
NCUM	18.7	20.2	20.0	19.0	17.3	17.2	17.8
JMA	21.9	23.2	21.4	18.7	18.2	17.1	18.6
MME	21.4	22.4	18.9	19.0	20.3	19.9	20.6

MINIMUM TEMPERATURE (DEG. C) BASED ON 20220102

MODEL	DAY1	DAY2	DAY3	DAY4	DAY5	DAY6	DAY7
GFS	15.0	16.5	15.0	12.3	13.1	15.9	15.2
GEFS	14.9	15.9	14.1	13.3	13.5	14.7	15.4
NCEP	10.9	12.5	15.8	13.5	14.0	14.7	14.6
NCUM	8.1	9.0	12.2	11.3	13.0	12.6	13.3
JMA	8.9	9.9	15.8	13.2	14.2	14.7	13.4
MME	11.6	12.8	14.6	12.7	13.6	14.5	14.4

RAINFALL (mm) BASED ON 20220102

MODEL	DAY1	DAY2	DAY3	DAY4	DAY5	DAY6	DAY7
GFS	0.0	0.0	2.94	6.31	0.0	11.25	10.12
GEFS	0.0	0.0	4.5	8.6	1.9	6.1	9.3
NCEP	0.0	0.0	0.0	0.88	0.75	3.0	5.62
NCUM	0.0	0.0	0.06	7.97	2.91	11.09	2.03
JMA	0.0	0.0	0.06	4.19	0.12	3.25	8.5
MME	0.0	0.0	1.5	5.6	1.1	6.9	7.1

RELATIVE HUMIDITY (%) BASED ON 20220102

MODEL	DAY1	DAY2	DAY3	DAY4	DAY5	DAY6	DAY7
GFS	36.7	28.6	38.3	32.1	61.8	67.0	83.1
GEFS	69.7	89.6	67.1	89.1	72.2	76.4	50.0
NCEP	32.8	27.1	36.7	34.4	65.0	77.1	87.6
NCUM	73.5	88.6	64.2	86.6	62.0	83.6	54.5
JMA	42.9	38.0	44.6	38.5	45.3	45.3	69.3
MME	61.7	79.1	58.4	94.0	76.6	76.5	55.6

WIND DIRECTION (360 Of Compass) BASED ON 20220102

MODEL	DAY1	DAY2	DAY3	DAY4	DAY5	DAY6	DAY7
GFS	54.8	83.7	77.6	89.7	69.8	128.5	112.6
GEFS	59.7	98.0	88.8	105.5	85.1	91.1	74.7
NCEP	68.4	88.1	35.9	71.8	62.2	141.3	328.6
NCUM	45.0	45.0	45.0	45.0	45.0	45.0	45.0
JMA	19.5	18.3	73.2	100.8	78.2	110.9	97.8
MME	48.3	68.2	64.4	76.9	64.1	109.0	66.8

WIND SPEED (m/sec) BASED ON 20220102

MODEL	DAY1	DAY2	DAY3	DAY4	DAY5	DAY6	DAY7
GFS	1.0	0.8	2.7	3.8	4.1	6.0	1.6
GEFS	1.5	1.2	3.3	2.3	3.1	3.5	1.8
NCEP	1.0	1.7	2.3	4.4	3.3	3.5	0.2
NCUM	1.7	1.8	3.0	4.4	7.1	3.6	4.4
JMA	1.0	0.9	2.2	1.8	2.6	3.6	0.9
MME	1.2	1.1	2.5	3.1	3.9	3.4	1.5

CLOUD COVER (%) BASED ON 20220102

MODEL	DAY1	DAY2	DAY3	DAY4	DAY5	DAY6	DAY7
GFS	1.0	0.0	100.0	2.0	0.0	100.0	4.0
GEFS	0.0	4.0	100.0	90.0	48.0	47.0	68.0
NCEP	100.0	42.7	100.0	97.5	50.2	24.3	91.5
NCUM	0.0	0.0	0.0	13.38	13.56	84.12	80.38
JMA	33.98	50.63	96.44	56.1	60.94	99.95	56.4
MME	33.7	24.3	99.1	61.4	39.8	67.8	55.0

FOR FURTHER DETAILS, WRITE TO US OR VISIT

EMAIL: - NWP-DIVISION@IMD.GOV.IN

WEBSITE: - HTTPS://NWP.IMD.GOV.IN